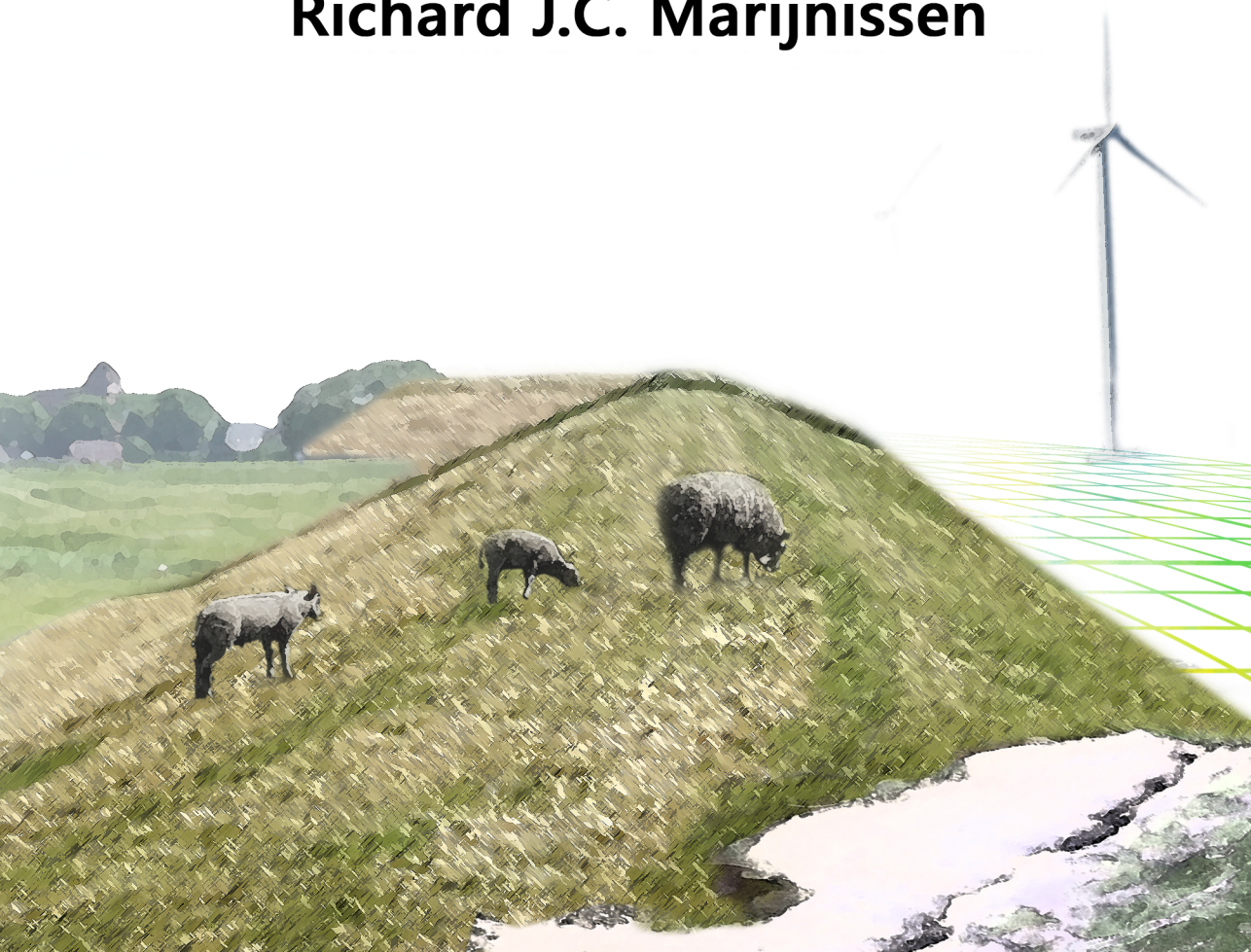


# **Shared-use of Flood Defences**

**Richard J.C. Marijnissen**



## Propositions

1. With every new dike reinforcement the prospects for multifunctional use of flood defences increase.  
(this thesis)
2. Contrary to current practise, multifunctional use is an opportunity to improve flood protection rather than an additional risk.  
(this thesis)
3. Risk, of any kind, is both a matter of perspective and objective truth.
4. Knowledge about uncertainties is the most undervalued aspect of science.
5. The greatest thing about online meetings is that one can join more meetings, while actually spending less time in them.
6. COVID-19 is both a health and a risk communication crisis.

Propositions belonging to the thesis, entitled

Shared-Use of Flood Defences

Richard Johannes Cornelis Marijnissen  
Wageningen, 6 October 2021

# Shared-use of Flood Defences

**Richard J.C. Marijnissen**

## **Thesis committee**

### **Promoters:**

Prof. Dr C. Kroeze

Professor of Water Systems and Global Change

Wageningen University & Research

Prof. Dr M. Kok

Professor of Flood Risk at the department of Hydraulic Engineering

Delft University of Technology

### **Co-promotor:**

Dr J.M. van Loon-Steensma

Assistant professor, Water Systems and Global Change Group

Wageningen University & Research

### **Other Members:**

Prof. Dr A.J.F. Hoitink, Wageningen University & Research

Prof. Dr S.N. Jonkman, Delft University of Technology

Prof. Dr S. Temmerman, University of Antwerp, Belgium

Dr B.G. van Vuren, Rijkswaterstaat, Netherlands

*This research was conducted under the auspices of the Graduate School for Socio-Economic and Natural Sciences of the environment (SENSE)*

# Shared-use of Flood Defences

**Richard J.C. Marijnissen**

## **Thesis**

submitted in fulfilment of the requirements for the degree of doctor at  
Wageningen University  
by the authority of the Rector Magnificus  
Prof. Dr A.P.J. Mol,  
in the presence of the  
Thesis Committee appointed by the Academic Board  
to be defended in public on  
Wednesday 6 October 2021  
at 4:00 p.m. in the Aula

Richard J.C. Marijnissen

Shared-use of Flood Defences, 251 pages.

PhD thesis, Wageningen University, Wageningen, the Netherlands (2021)

With references, with summary in English

ISBN: 978-94-6395-891-2

DOI: <https://doi.org/10.18174/549897>

## Summary

Many regions face an increasing flood risk as a result of sea-level rise, climate change, and a growing population in flood prone deltas. Flood protection infrastructure like dikes, levees, and barriers is essential in reducing the threat of flooding. As areas are redeveloped for the construction or reinforcement of flood protection, often the question arises whether other developments like housing, recreational facilities or nature restoration, can be combined with the flood protection infrastructure as well. When adapting to higher extreme water levels and storm events in the future, the types of uses that can be maintained on or nearby flood defences are intrinsically linked to the flood protection measures implemented. While combining other activities with flood protection can have many benefits in principle, in practise there are some obstacles remaining preventing the construction of such multifunctional flood defences. One of those obstacles is a lack of knowledge on the safety provided by multifunctional flood protection measures due to the uncertainties introduced. This PhD research addresses this obstacle by developing a framework to assess the safety of multifunctional flood protection measures.

When flood protection infrastructure is combined with other uses, it must be demonstrated that the flood defences comply with minimum safety standards. This involves identifying the modes of failure of the flood defence, modelling the processes causing the failure, and assessing the probability of the failure by extreme events. A multifunctional flood defence will only be constructed if the assessed probability of failure is acceptably small. Regulations, manuals, and guidelines exist to evaluate the safety of flood defences, yet these provide little guidance on assessing the large variety of multifunctional flood defences. As of yet, constructing multifunctional flood protection either requires highly specialised time-consuming studies, must comply to strict conservative standards, or the

implementation of multifunctional flood protection is discouraged entirely.

A probabilistic risk-based approach, as introduced in the Netherlands, allows for methods to quantify risks and benefits of multifunctional use in dike safety assessments. Therefore, the aim of this thesis is: *to investigate how combining different activities on or near flood defences affects the safety provided by flood defences assessed with a risk-based approach*. To this end, four research questions are addressed in case studies:

- *How can a dike assessment framework be adapted to probabilistically evaluate multifunctional use of a flood defence?* (Chapter 2)
- *How can additional defences constructed for multifunctional use of the flood protection zone be incorporated and evaluated within a probabilistic evaluation framework?* (Chapter 3)
- *How can a probabilistic framework account for long-term climate adaption benefits of multifunctional use within a flood protection zone?* (Chapter 4, 5)

How much a conservative approach to multifunctional use can affect the perception of the safety of a multifunctional flood defence was explored in Chapter 2. A scenario-based approach was introduced into the assessment framework to quantify both risks and benefits for flood protection. As the analysis shows, the current conservative approach can lead to a significant overestimation of the probability of failure, up to several orders of magnitude. This is most notable when the dominant failure mechanism is directly affected by the multifunctional use. Furthermore, the influence of multifunctional use on safety is proportional to the size and protection level of the flood defence itself. The safety of large flood defences will thus be impacted less by multifunctional use than conventional assessments would suggest, but flood protection benefits of multifunctional use will also be limited.

Other uses of the flood protection zone can also be accommodated by introducing additional flood defences in a double dike system. The area in between the defences can be flooded, e.g. through a culvert, and used for other uses like clay mining, nature creation, and aquaculture. Chapter 3 concludes not all double dike configurations may improve flood protection however. When the size of the seaward defence is much larger than the landward defence, the bulk of the safety is provided by the seaward defence while a culvert introduces a new mechanism for flooding the hinterland. To evaluate benefits of double dikes, Chapter 3 proposes to treat the seaward defences as transmitting loads to the final seaward defence in the assessment framework. This way, different configurations of dike heights and culvert sizes can be explored, while the development of failures across the parallel defences during storm events remains accounted for.

Long-term benefits are often not included in risk assessments. The Wide Green Dike case explored in Chapters 4 and 5 is an exception by incorporating the sediment dynamics on the foreshore in its design and construction. The results indicate extracting clay from pits on the salt-marsh foreshore is feasible to obtain sufficient material for future dike reinforcements, provided a salt marsh can persist under sea-level rise. Still, uncertainty in marsh accretion due to compaction of the foreshore (e.g. by grazing) or the reduction of available sediment directly affects the need for future dike heightening, up to several additional millimetres each year. Results stress the importance of management of the foreshore in future dike reinforcements against sea-level rise.

Chapter 6 compiles the lessons from the other chapters and shows that multifunctional use can be facilitated by four design components: 1) the foreshore 2) the geometry of the flood defence system, 3) the (state of) materials used for flood protection elements, and 4) objects in, on or near the flood protection zone. Changes in dike composition and geometry can already be accounted for in the assessment procedure. Foreshores need to

be evaluated by the transmission of hydraulic loads. Objects introduced for multifunctional use are the most complicated to incorporate as these may directly affect hydraulic loads and the dike's resistance as well as introduce additional uncertainty. A scenario-based approach as introduced in Chapter 2 is needed to quantify the effect on flood protection across different potential states of the object during an extreme event.

The thesis shows that the safety of flood defences shared with other uses can be assessed using a risk-based approach. This includes common features (Chapter 2), additional defences to enable other uses (Chapter 3), as well as climate adaptation designs (Chapters 4, 5) through analysing the ramifications of four design components (Chapter 6). For a full risk-based analysis the use of advanced hydrological, geotechnical, statistical and morphological models is required. Still, the developed framework can be improved by including the effects of other uses on reducing the vulnerability or exposure of the hinterland. With a growing need for integrated flood protection solutions due to climate change and urbanisation, the shared-use of flood defences is only expected to increase. This research is a starting point for developing new integrated flood protection solutions within a probabilistic risk-based approach.

## Samenvatting

Veel delta's op aarde worden kwetsbaarder voor overstromingen door zeespiegelstijging, klimaatverandering, en bevolkingsgroei. Waterkeringen zoals dijken zijn essentieel om de kans op een overstroming te beperken. Wanneer er een dijkversterkingsopgave ligt vraagt men zich vaak af of andere ontwikkelingen in het gebied meegekoppeld kunnen worden zoals woningen, recreatie faciliteiten of nieuwe natuur. Bij het anticiperen op hogere waterstanden en extremere stormen zijn de mogelijke vormen van medegebruik bij waterkeringen direct afhankelijk van de voorziene versterkingsopgave. Alhoewel er veel voordelen kunnen zijn bij het combineren van andere gebiedsfuncties binnen een versterkingsopgave, blijkt in de praktijk dat er barrières zijn voor het implementeren van multifunctionele waterkeringen. Één van deze barrières is het gebrek aan kennis om de veiligheid van multifunctionele keringen en de inherente onzekerheden van multifunctioneel gebruik te kwantificeren. In dit promotieonderzoek wordt de kennisbarrière verkleind door een beoordelingskader voor multifunctionele waterveiligheidsconcepten te ontwikkelen.

Wanneer een waterkering wordt gecombineerd met andere gebiedsfuncties moet worden aangetoond dat de waterkering nog steeds voldoet aan de veiligheidsnormen. Hiertoe moeten de faalmechanismen van de kering worden geïdentificeerd, de faalprocessen worden gemodelleerd, en de kans op falen door extreme condities als een storm worden berekend. Alleen als de kans op falen van de kering voldoende klein wordt ingeschat zal deze gebouwd mogen worden. Normen, ontwerpmethodieken en leidraden zijn beschikbaar om de veiligheid van waterkeringen te kunnen inschatten. Toch blijken deze weinig handvaten te bieden voor het omgaan met de grote variatie aan multifunctioneel gebruik die rond een kering kan plaatsvinden. Op dit moment vergt de implementatie van een multifunctionele kering geavanceerde en

tijdrovende studies, moet de kering voldoen aan strenge conservatieve veiligheidseisen ten aanzien van de functies rond de kering, of wordt multifunctioneel gebruik in zijn geheel ontmoedigd.

Een probabilistische risicobenadering zoals onlangs in Nederland is geïntroduceerd biedt de mogelijkheid om zowel de risico's als voordelen van multifunctioneel gebruik in het veiligheidsoordeel te betrekken. Dit proefschrift heeft dan ook als doel om: *te onderzoeken hoe het combineren van verschillende functies op of bij de waterkering het veiligheidsoordeel van de waterkering beïnvloedt binnen de risicobenadering*. Zodoende zijn vier onderzoeksvragen opgesteld:

- *Hoe kan een beoordelingskader voor dijken aangepast worden voor het probabilistisch evalueren van multifunctioneel gebruik van de kering?* (Hoofdstuk 2)
- *Hoe kunnen extra dijken aangelegd voor medegebruik van de waterveiligheidszone worden betrokken en geëvalueerd binnen een probabilistisch beoordelingskader?* (Hoofdstuk 3)
- *Hoe kan een probabilistisch beoordelingskader rekening houden met klimaatadaptatievoordelen van multifunctioneel gebruik van de waterveiligheidszone op de lange termijn?* (Hoofdstuk 4, 5)

Hoeveel een conservatieve benadering het veiligheidsoordeel van een multifunctionele kering kan beïnvloeden is onderzocht in hoofdstuk 2. Een scenario-aanpak wordt geïntroduceerd binnen het beoordelingskader om zowel voor- als nadelen voor waterveiligheid te kwantificeren. Volgens de analyses kan een conservatieve benadering leiden tot een significante overschatting van de faalkans, tot meerdere ordes van grootte. Dit komt vooral tot uiting wanneer het dominante faalmechanisme direct beïnvloed kan worden door het medegebruik. Verder is het effect van medegebruik op de waterveiligheid proportioneel aan de sterkte en faalkans van de dijk zelf. De veiligheid van een zware veilige kering zal minder beïnvloedt worden door medegebruik dan de

huidige conservatieve aanpak doet vermoeden. Anderzijds zullen voordelen van medegebruik voor waterveiligheid in deze gevallen beperkt zijn.

Medegebruik van de beschermingszone kan ook mogelijk gemaakt worden door het aanbrengen van extra keringen in een dubbele dijk systeem. Het tussengebied kan overstromen, b.v. via een duiker, en gebruikt worden voor het winnen van klei, het creëren van nieuwe natuur, of voor aquacultuur. Hoofdstuk 3 concludeert dat niet alle configuraties met dubbele dijken de veiligheid bevorderen. Wanneer de buitenliggende kering veel groter is dan de binnenliggende kering zal het merendeel van de veiligheid door de buitenliggende kering worden geleverd, terwijl een duiker een nieuw faalmechanisme voor overstroming kan introduceren. Om de veiligheid van dubbele dijksystemen te kwantificeren stelt hoofdstuk 3 voor om de buitenliggende kering te beschouwen als een (beperkt) doorlatend element voor hydraulische belastingen op weg naar de binnenliggende kering. Op deze manier kunnen verschillende configuraties van dijkhoogtes en duikerdimensies worden onderzocht, terwijl de effecten van faalmechanismen aan de buitenliggende kering tijdens een storm verdisconteerd worden.

Voordelen van medegebruik op de lange termijn blijven vaak buiten het vizier van veiligheidsbeoordelingen. Het Brede Groene Dijk concept dat is onderzocht in hoofdstukken 4 en 5 vormt daarop een uitzondering door de dynamiek van sediment op het voorland in het ontwerp te betrekken. De resultaten laten zien dat het winnen van klei uit putten op het voorland een realistische strategie is voor het verkrijgen van voldoende materiaal voor toekomstige versterkingen. Een voorwaarde daarbij is dat de kwelder op het voorland zichzelf in stand kan houden bij de verwachte zeespiegelstijging. Desalniettemin hebben onzekerheden rond het opslibben van de kwelder, denk aan compactie als gevolg van beweiding en de toevoer van sediment, een directe invloed op de

benodigde dijkversterking in de toekomst. Per jaar bespaart de kwelder enkele millimeters aan benodigde dijkverhoging met zeespiegelstijging.

Hoofdstuk 6 brengt de lessen van de voorgaande hoofdstukken samen en identificeert vier elementen in het ontwerp waarop multifunctioneel gebruik voor veiligheid getoetst wordt: 1) de vooroever, 2) geometrie van de kering, 3) de (staat van de) gebruikte materialen, en 4) de objecten in, op, of bij de waterveiligheidszone. Veranderingen in materiaalcompositie en geometrie zijn in veel gevallen al onderdeel van de beoordeling. Vooroevers kunnen beoordeeld worden op basis van de invloed op hydraulische belastingen. Objecten voor medegebruik zijn moeilijker te beoordelen omdat deze direct kunnen acteren op de hydraulische belastingen, de stevigheid van de dijk, en extra onzekerheden introduceren. Een scenario aanpak zoals voorgesteld in hoofdstuk 2 is nodig om de effecten op waterveiligheid bij verschillende mogelijke situaties van het object tijdens een hoogwater te beoordelen.

Het proefschrift laat zien dat de veiligheid van waterkeringen met multifunctioneel gebruik beoordeeld kunnen worden met een risicobenadering. Dit omvat veelvoorkomende functies (hoofdstuk 2), extra keringen voor medegebruik (hoofdstuk 3), en klimaat adaptieve elementen (hoofdstukken 4 en 5) door het analyseren van vier ontwerpelement (hoofdstuk 6). Voor een volledige risicobenadering zijn geavanceerde hydrologische, geotechnische, statistische en morfologische modellen nodig. Het ontwikkelde beoordelingskader kan verder worden verbeterd door rekening te houden met de effecten van medegebruik op de kwetsbaarheid van het achterland. Zeker nu er voor het aanpassen aan klimaatverandering en bevolkingsgroei integrale oplossingen worden gezocht, zal het medegebruik van waterkeringen steeds vaker worden overwogen. Dit onderzoek is een startpunt voor het ontwikkelen van nieuwe integrale waterveiligheidsconcepten door middel van een probabilistische risicobenadering.

# Contents

Summary .....	i
Samenvatting .....	v
Contents.....	ix
1. Introduction .....	1
1.1. Background .....	2
1.2. Knowledge gaps and research objectives .....	13
1.3. Research approach .....	13
1.4. Thesis outline.....	18
2. Re-evaluating safety risks of multifunctional dikes with a probabilistic risk framework .....	21
2.1. Introduction .....	23
2.2. Formulating a framework for MFFD assessment.....	26
2.3. Application of the risk frameworks.....	30
2.4. Results.....	36
2.5. Discussion .....	40
2.6. Conclusions.....	42
3. Flood risk reduction by parallel flood defences – case-study of a coastal multifunctional flood protection zone .....	45
3.1. Introduction .....	47
3.2. Assessment of double dike systems .....	52
3.3. Application to Ems-Dollard double dike.....	56
3.4. Results.....	66
3.5. Discussion .....	71
3.6. Conclusions.....	77
4. How natural processes contribute to flood protection - A sustainable adaptation scheme for a wide green dike.....	79

4.1.	Introduction .....	81
4.2.	The study area .....	83
4.3.	Methods.....	86
4.4.	Trust in the model system.....	94
4.5.	Results.....	98
4.6.	Discussion .....	104
4.7.	Conclusions.....	108
5.	The Sensitivity of a Dike-Marsh System to Sea-Level Rise—A Model-Based Exploration .....	111
5.1.	Introduction .....	113
5.2.	Marsh processes and flood protection .....	114
5.3.	Methods.....	118
5.4.	Results.....	124
5.5.	Discussion .....	127
5.6.	Conclusions.....	130
6.	General framework.....	133
6.1.	Introduction .....	134
6.2.	Reflection on the case-studies .....	136
6.3.	General framework for multifunctional dike design.....	140
6.4.	Discussion .....	146
6.5.	Conclusions.....	148
7.	Synthesis.....	151
7.1.	Introduction .....	152
7.2.	Key findings and novelties for multifunctional flood defences 152	
7.3.	Strengths and weaknesses .....	157
7.4.	Outlook.....	165
7.5.	Implications for the Dutch Flood Protection Program .....	170

Bibliography .....	175
Appendices .....	199
Appendix A: Appendices belonging to Chapter 2 .....	200
Appendix B: Appendices belonging to Chapter 3 .....	209
Appendix C: Appendices belonging to Chapter 4 .....	216
Appendix D: Appendices belonging to Chapter 5 .....	225
Acknowledgements .....	229
About the author .....	231
SENSE training and education diploma .....	233



# 1

# Introduction

R.J.C. Marijnissen



## **1.1. Background**

### **1.1.1. Multifunctional flood defences**

For over millennia humans have depended on natural recourses within deltas like fresh water, fertile floodplains, and abundance in marine resources, to fuel urban development (Day, Gunn, Folan, Yáñez-Arancibia, & Horton, 2007). Over time settlements have developed into large urban centres and transportation hubs providing a myriad of additional functions to the region. Aside from direct economic value, deltas harbour a variety of unique habitats providing important ecosystem services (Barbier, 2017). Deltas are also the most densely populated areas in the world with over 300 million people living there (Edmonds *et al.*, 2017), roughly 270 million of whom can expect flooding at least once per century (Jongman, Ward, & Aerts, 2012). The exposure to flooding is reduced by the construction of flood defences. Still, any flood defence will inevitably affect other uses present either directly or indirectly (Adams, Adger, & Nicholls, 2018; van Wesenbeeck *et al.*, 2014).

Accelerating sea-level rise as a result of climate change is further increasing flood risk, with annual global flood costs expected to reach up to US\$ 210 billion by 2100 without new or reinforced flood defences (Hinkel, van Vuuren, Nicholls, & Klein, 2013). If new coastal flood defences were to be constructed and existing defences were maintained economically, globally the population at risk of flooding is estimated to reduce by as much as a factor of 500 and annual flood costs would reduce by a factor of 5 by 2100 compared to business as usual (Hinkel *et al.*, 2013). When improving flood protection, it is often considered whether the flood protection zone could also be combined with other needs and services for the area like nature, recreation, or urban development. As of yet, there is little guidance on how such activities will affect the safety provided by the flood protection measures.

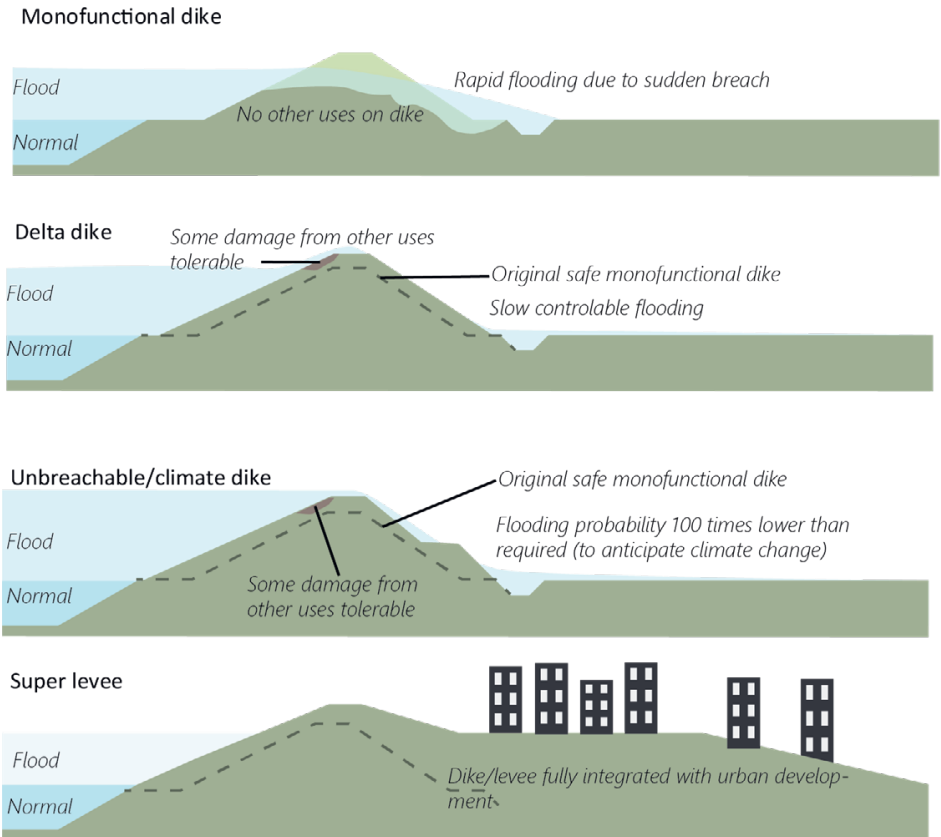
Multifunctional use can exploit synergies between uses, for example when excess heat from industry is used to heat houses (Weinberger, Amiri, & Moshfegh, 2017). Other times combining uses concentrates adverse effects so these are more easily managed or mitigated, for example when bundling line infrastructure like highways, rail lines, pipelines, and power lines, to concentrate noise pollution and nuisance during maintenance. Similar beneficial combinations of uses for flood

protection could improve flood protection while addressing the demand for other uses. Therefore, options have been, and still are, explored to combine other uses with flood protection in so-called *multifunctional flood defences* (MFFDs). In this thesis a multifunctional flood defence is defined as *any flood protection structure sharing physical space with a use not tied to retaining water*.

While many flood defences may have accumulated different uses over time, e.g. the presence of a road, buildings, trees, etc., examples of flood defences designed for multifunctional use in literature are still rare. Prominent examples are given by Voorendt (2017) such as flood retention walls within houses in Dordrecht and a parking garage inside a dune at Katwijk. Another example is the super levee in Tokyo where a city block is integrated with the flood defence (Nakamura, 2016). Rather than employing synergies to reduce the size of flood defences, in practise multifunctional flood defences are often over-dimensioned, i.e. safer than strictly necessary to meet the flood protection norm. This results in a “robust” dike (van Loon-Steensma & Vellinga, 2014) which is more resilient to damage or additional loads by multifunctional use. Examples of robust dike concepts designed to be safer than the safety norm are: the Delta dike (Knoeff & Ellen, 2011), the climate dike (de Moel *et al.*, 2010), and the so-called “unbreachable” dike which is technically still breachable (Silva & van Velzen, 2008) (**Figure 1.1, Table 1.1**).

Multifunctional use is not limited to robust dike concepts. According to van Veelen, Voorendt, and van der Zwet (2015) there are different degrees of multifunctionality:

- Shared-use: A flood defence is (temporarily) used by another function without adapting the design of the dike to the function.
- Spatial optimisation: The design of the flood defence is altered to accommodate another function, but remains technically separate from the other function.
- Structural integration: A non-water retaining object (NWO) is built on, in or under the flood defence. This type includes the over-dimensioned dike concepts discussed before.
- Functional integration: Elements built in the dike for other uses double as water-retaining elements. These are often called hybrid defences.



**Figure 1.1** A monofunctional dike and different "robust" reinforcement concepts suitable for shared-use, spatial optimisation, and/or structural integration

**Table 1.1** Multifunctional dike concepts classified by type and scale of multifunctionality

Dike scale				Flood defence system scale
Shared-use	Spatial optimisation	Structural integration	Functional integration	
Robust dike		Super levee	Hybrid defence	Eco-engineering, natural foreshores
				Parallel dikes

Expanding the scope from a single flood defence to a larger flood defence zone, other multifunctional options like parallel dikes and eco-engineering solutions can be explored (van Loon-Steensma *et al.*, 2014b). Parallel flood defences are systems with two or more dikes, where both contribute to mitigating flood risk. The space between the dikes can be used for agriculture, aquaculture, and nature development (Kwakernaak *et al.*, 2015). Recent literature advocates for incorporating potential synergies of natural elements like salt marshes, mangroves, and reefs, with flood protection (Borsje *et al.*, 2011; Möller *et al.*, 2014; Scheres & Schüttrumpf, 2019). A major benefit of eco-engineering is that the adaptive capacity of ecosystems (e.g. sediment accumulation, soil stabilization, etc.) is utilised to reinforce flood defences over time, while preserving other ecosystem services for the region. Apart from flood storage measures like the Dutch “Room for the River” or the flood retention areas of the “Sigmaplan” in Belgium, considering elements beside the flood defence itself for flood protection is not yet common practise. As a result, there is little guidance available to assess how uses within the flood protection zone might affect safety now, let alone in the future.

### 1.1.2. Assessment of flood protection

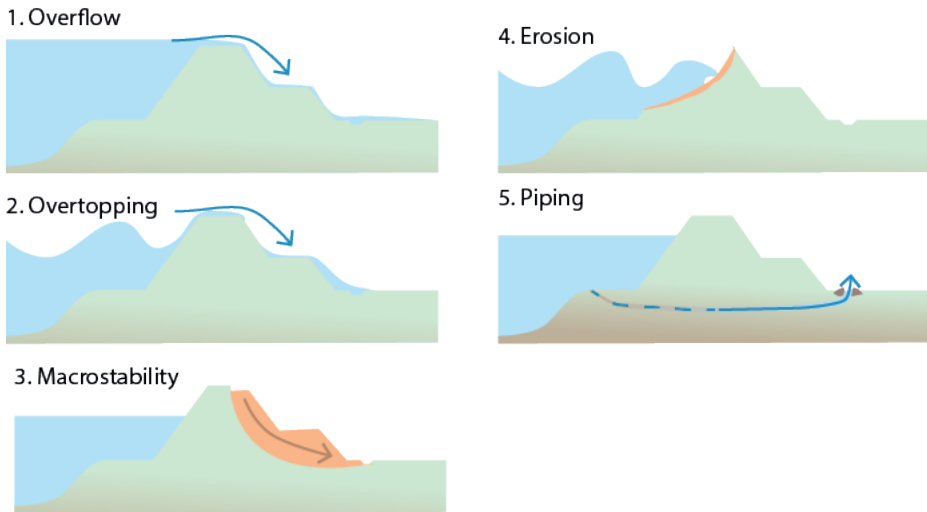
There are many options for multifunctional use in flood protection. However, before multifunctional elements can be incorporated, it is important to know how flood defences are usually assessed.

The methods to assess flood protection are rooted in reliability theory. The goal of a reliability analysis is to determine the probability of failure of a system or component. Interpreting “failure” as a flood and the “component” as a physical process to allow water into the hinterland, it becomes clear that quantifying flood risk is a specialised application of reliability theory. Concepts of reliability theory can be expressed in failure mechanisms, limit states, and fault trees when applied for assessing flood protection measures (Bakker & Vrijling, 1980; Vrijling, 1987, 2001).

A sequence of events that can result in a flood is known as a *failure mechanism*. The most common dike failure mechanisms (Figure 1.2) for a dike are:

- overtopping & overflow: water flowing over the crest of the dike inundating the hinterland and/or eroding the landward slope of the dike

- macrostability: loss of stability of the soil at the landward side due to water pressure
  - erosion: erosion of the dike by wave action on the outer slope
  - piping: water flowing beneath the dike eroding the subsoil
- 



**Figure 1.2** The most common failure mechanisms of a dike

---

The vast majority of dike breaches can be attributed to these failure mechanisms (Danka & Zhang, 2015; Özer, van Damme, & Jonkman, 2020). For each mechanism methods are available to compute the flow, force balance, or erosion given the hydraulic boundary conditions like water level and wave action. A critical flow, erosion or force threshold (i.e. a *limit state*) is defined such that, when exceeded, will result in failure. The probability of a failure mechanism is thus defined as the probability the limit state is exceeded by a (combination of) hydraulic load(s). The different parallel and sequential events needed to initiate a failure mechanism are structured in a *fault tree*. Each stage of the fault tree is evaluated to evaluate the probability of failure for any (combination of) mechanisms.

Probabilistic calculations can be performed at varying degrees of complexity. In a level I analysis the dike resistance ( $R$ ) and hydraulic loads ( $S$ ) are multiplied by partial safety factors that represent the uncertainty (Jongejan, Diermanse,

Kanning, & Bottema, 2020). These factors need to be calibrated by more complex probabilistic techniques. In a more complex level II analysis the probability of failure is obtained by approximating the limit-state surface around the design point (Der Kiureghian & Dakessian, 1998). In a level III analysis neither the probability distributions nor the limit state are approximated. Computationally intensive algorithms like Monte-Carlo sampling or numerical integration are required for to this level of analysis.

Since the 2000's the probabilistic approach from reliability theory has seen wide spread adoption in flood risk assessments with varying approaches to stochastic hydraulic boundary conditions, statistical algorithms, and limit state definitions (Apel, Thieken, Merz, & Blöschl, 2006; Jonkman, Kok, Van Ledden, & Vrijling, 2009; Neal, Keef, Bates, Beven, & Leedal, 2013; Purvis, Bates, & Hayes, 2008). This approach has also been adopted nationally in the Netherlands (see section 1.1.4). The probabilistic method allows for uncertainties in the design of a flood defence to be accounted for explicitly, as well as give a better estimation of the true probability of flooding. The downside is the complexity of estimating the necessary probability distributions and the large number of model runs required to estimate probabilities in level II or III algorithms. While the application of the probabilistic approach for regular flood defences is well established, very few studies so far have attempted to incorporate multifunctional use of the flood defence in the assessment (see next section).

### 1.1.3. Advances in the probabilistic assessment of multifunctional flood defences

While there are many different concepts and ideas surrounding multifunctionality of flood defences, there is no clear framework for how these multifunctional aspects can be accounted for in flood risk assessments. For objects commonly found at flood defences guidelines to deal with safety risks are already present. A simple method to assess flood defences with non-water retaining objects (NWOs), e.g. trees, pipes, and small structures, is already part of Dutch safety regulations (Rijkswaterstaat, 2016c). In this conservative approach a MFFD is safe if the NWOs cannot interfere with the profile designed to the required flood

protection level. As a result, MFFDs are required to be larger than monofunctional flood defences. For pipelines an exception is made if the pipeline itself is already designed to meet the NEN-norm for pipelines near important public works (NEN, 2012), ensuring it has an insignificantly low probability of failure.

During the writing of this thesis additional studies have been conducted to advise the Dutch Flood Protection Program (abbreviated as *HWBP* in Dutch) on common issues. These explorations across projects (*projectoversteigende verkenningen* or *POVs* in Dutch) have identified two options for evaluating multifunctional use. The first option is to evaluate a fault tree of scenarios with different states of the object. The second option considers failure of a multifunctional element as an additional failure mechanism in the assessments. “POV cables and pipelines” (Schelfhout, Nurmohamed, Janssen, & de Koning, 2020) considers both approaches acceptable, but prefers the second option for pipelines to avoid major changes to the current assessment of failure mechanisms. “POV foreshores” (Roode, Maaskant, & Boon, 2019) suggests the first option for objects on foreshores.

Scientific studies have already been conducted to device more advanced safety assessments of multifunctional elements in MFFDs (Table 1.2). Multifunctional flood defences can include a wide range of implemented multifunctional elements, each interacting in a variety of complex ways with the flood defence depending on the context. As a result, studies so far have focussed primarily on assessing the effects of a specific multifunctional element on a specific failure mechanism, usually for a specific case-study. As a result, the approaches do not lend themselves for a wider implementation. Overall, MFFDs are safer than conventional assessments often suggest because positive interactions can be incorporated while the risk of negative interactions is quantified, e.g. (Aguilar-López, Warmink, Schielen, & Hulscher, 2018b; Vuik, van Vuren, Borsje, van Wesenbeeck, & Jonkman, 2018b). The approaches of previous studies are discussed in detail below.

Ways of probabilistically assessing specific types of multifunctional flood defences were explored by Aguilar-López (2016). The effect of two multifunctional uses (a pipeline and a road) were assessed for two failure mechanisms (piping and overtopping). The strategy employed by Aguilar-López (2016) follows a similar

scheme for each use: 1) collect field data of the failure mechanism affected by a use, 2) reproduce the results with a high-detail model (e.g. Finite Element Model or Computational Fluid Dynamics simulation, etc.), 3) emulate the advanced model with a faster model to reduce computation time, 4) fit probability density functions and correlation models to site data, 5) use Monte-Carlo Sampling to assess failure for thousands of parameter combinations, 6) estimate the probability of failure from the samples, 7) update the existing formulas to better represent the case results. The use of experimental data and advanced models allows Aguilar-López (2016) to thoroughly test the validity of commonly applied models of failure mechanisms like the piping formula of Sellmeijer, de la Cruz, van Beek, and Knoeff (2011) when new uses are present. The major downside of the approach is the extensive data collection and modelling needed to update design formulas of failure mechanisms whenever a new use on a flood defence is considered.

As Vuik *et al.* (2018b) demonstrated for natural foreshores, additional uses not necessarily require updating models of failure mechanisms. Instead, the reduction in hydraulic loads (wave height) by the presence of natural features is explicitly modelled prior to modelling the failure mechanism itself. Lanzafame (2017) accomplished assessing the effects of woody vegetation on the macrostability of dikes by updating soil parameters (cohesion and friction angle) with results from a root growth model, rather than adding steps to the description of the failure mechanism itself. Halter (2015) approached wind turbines near flood defences as a risk of falling components damaging the defence and considered this a new failure mechanism. Finally, Chen, Jonkman, Pasterkamp, Suzuki, and Altomare (2017) approached safety from the perspective of the new use, i.e. a building. To do so, they considered the collapse of the building as a new failure mechanism and derived a new sequence of design formulas to assess its probability. Apart from these studies, the probabilistic assessment of multifunctional elements has remained largely unexplored in scientific literature.

**Table 1.2** Overview of scientific literature probabilistically assessing the influence of multifunctional elements on flood defences

Multifunctional element	Studied failure mechanism(s)	Failure model	Probabilistic method	Study
Wind turbine	- Damage by falling blade or mast	- Fall impact model (of debris)	Scenarios (Level I)	Halter (2015)
Building	- Collapse of buildings due to overtopping	- Empirical wave peak loads - Design formulas	Scenarios (Level I)	Chen <i>et al.</i> (2017)
Tree	- Macro stability	- Empirical root biomass model - Finite-element ground water flow model - Design formulas	First Order Reliability Method (Level II)	Lanzafame (2017)
Road	- Overtopping	- Computational fluid dynamics (CFD) - Artificial neural network emulator	Monte-Carlo (Level III)	Aguilar-López, Warmink, Bomers, Schielen, and Hulscher (2018a)
Sewer pipe	- Piping	- Finite-element ground water flow model - Artificial neural network emulator	Monte-Carlo (Level III)	Aguilar-López <i>et al.</i> (2018b)
Salt-marsh	- Overtopping - Revetment erosion	- Numerical wave model - Design formulas	First Order Reliability Method (Level II)	Vuik <i>et al.</i> (2018b)

### 1.1.4. The Dutch case

About 60% of the Netherlands is prone to flooding from the sea or rivers (Kok, Jongejan, Nieuwjaar, & Tanczos, 2017; Slomp, 2012). Flood protection has therefore always been a priority. However it was only after the large flood in 1953 that a large national plan was prepared to ensure national flood safety. The first Delta Committee was established to advise the government in policies for flood risk management. The Delta Committee advised an acceptable yearly design water level exceedance probability of 1/10,000 for the west of the Netherlands, with higher acceptable flood probabilities for rural areas in the north and south of the Netherlands, based on the extrapolation of observed water-levels and storm surges, and an economic optimisation of damages in case of a flood (Maris *et al.*, 1961). This advice has been the basis of Dutch flood risk policy ever since, cemented in legislation such as the Water Act.

The Flood Protection Program (*Hoogwaterbeschermingsprogramma in Dutch, or HWBP*) is part of the larger Delta program initiated by the Delta Committee. It consists of all 21 waterboards of the Netherlands and the national water authority Rijkswaterstaat. This alliance is tasked with maintaining and reinforcing the flood defences up to the safety standards across the Netherlands. From a total of 3,750 kilometres of primary flood defences in the Netherlands, 1,640 kilometres of flood defences have been in need of reinforcement since 2006. By 2020 the HWBP has already reinforced 354 kilometres of flood defences (HWBP, 2020). In order for all remaining primary flood defences to meet the safety standards by 2050, roughly 1 kilometre of flood defence must be reinforced weekly (HWBP, 2020). Among these flood defences many feature multifunctional elements. Thus, to meet the target of all flood defences being up to standard by 2050, an effective strategy for incorporating multifunctional use must be developed.

Recently (2017) the Water Act has been changed from (storm) exceedance based norms to flood probability based norms. That is, it is no longer sufficient to demonstrate a flood defence can survive a design storm or water level of a specified exceedance frequency, but instead all uncertainties in the hydraulic loads and the dike should be incorporated to determine the probability of a flood. To determine whether a flood defence complies with these new standards, the legal assessment tools “WBI2017” (*Wettelijk Beoordelings Instrumentarium 2017* in Dutch) have been

developed. These tools are largely adapted from previous design guidelines like VTV2006 (Ministerie van Verkeer en Waterstaat, 2007), as well as the large amount of grey literature on the strength of dikes accumulated over many years. The WBI consists of three types of assessment: 1) basic assessments, 2) detailed assessments, and 3) advanced assessments (Rijkswaterstaat, 2016a; Slomp, Knoeff, Bizzarri, Bottema, & de Vries, 2016). Basic assessments consist of simple but conservative rules and are intended to quickly approve dike sections on failure mechanisms that are highly unlikely to be relevant. The advanced assessments on the other hand allow for highly detailed, highly location-specific models to be employed for evaluating a failure mechanism on a particular dike section and are intended for evaluating unusual circumstances. The detailed assessments are most commonly employed for assessing flood defences.

In a detailed probabilistic assessment, the first step consists of retrieving and hydraulic load distributions (e.g. water level, wave height, etc.) for the relevant dike section from the official hydraulic databases. Tools like Hydra-NL (Duits & Kuijper, 2018) have been made available for this purpose. The second step is schematising a representative dike cross-section for the failure mechanisms to be assessed. Schematisation guides for each mechanism have been made available online ([www.helpdeskwater.nl](http://www.helpdeskwater.nl)) to guide the development of cross-sections and the uncertainties to include. Finally, failure of the cross-section by the relevant failure mechanisms is assessed according to the methods outlined in Rijkswaterstaat (2016c). Versions of these models and probabilistic routines for assessing failure probabilities have been made available directly in the assessment tools like Riskeer (Deltares, 2021), but may also be evaluated manually as in this thesis. In the WBI, a section is safe if the combined probability of failure from all failure mechanisms remains below the safety norm set for the dike section.

The shift to a full probabilistic approach allows for optimisation of dike designs as knowledge and uncertainties of local conditions and uses can be incorporated directly in the safety assessment. However, there is little experience how to apply the probabilistic approach in cases of multifunctional use. Still, by 2050 all primary flood defences, including those with multifunctional elements, must conform to the new safety standards in the Water Act.

## 1.2. Knowledge gaps and research objectives

Based on the available literature the following knowledge gaps regarding the reliability of multifunctional flood defences can be formulated:

1. There are no clear guidelines of how multifunctional elements can be included in a risk-based approach for flood defences.
2. The effects of different activities near flood defences and their implementation within a reliability framework are unclear and often omitted.
3. Multifunctional flood defences are generally considered as long-term climate adaptation measures, yet changes to the flood protection system over time as a result of multifunctional use are absent from the reliability framework.

Therefore, the main objective of this PhD thesis is: *to investigate how combining different activities on or near flood defences affects the safety provided by flood defences assessed using a risk-based approach*. To this end, I will develop a framework for assessing and designing flood defences in which effects of multifunctional use within the flood protection zone on safety can be quantified. To do so, the following research questions are addressed in this thesis.

RQ1: How can a dike assessment framework be adapted to probabilistically evaluate multifunctional use of a flood defence?

RQ2: How can additional defences constructed for multifunctional use of the flood protection zone be incorporated and evaluated within a probabilistic evaluation framework?

RQ3: How can a probabilistic framework account for long-term climate adaption benefits of multifunctional use within a flood protection zone?

## 1.3. Research approach

### 1.3.1. General approach

Multifunctional use of flood defences covers a wide range of functions and the implementation is highly context specific. As a result, formulating a generic

framework for assessing multifunctional use is complicated. In general, studying changes in flood risk requires (any combination of) three types of analyses:

1. An analysis of the frequency of (extreme) hydrological events
2. An analysis of the stability or strength of flood defences
3. An analysis of the damages or consequences of a flood

The first type of analysis can consist of a statistical analysis of long-term observations. The observed variability in hydraulic loads in the system can be schematised by (a set of) probability distributions, i.e. mathematical functions describing the range of values a system variable can reach and the associated likelihood of each value (Bernardara, Schertzer, Sauquet, Tchiguirinskaia, & Lang, 2008). If there is reason to believe the distribution of extreme events will change, models are required to quantify these changes. A prime example for this type of analysis is assessing the effects of climate change. Results from large scale climate models have been utilised to predict changes in river discharge (Bastola, Murphy, & Sweeney, 2011), the frequency of storm events (Salathé *et al.*, 2014) and the likelihood of hurricanes (Marsooli, Lin, Emanuel, & Feng, 2019), which will in turn affect the frequency of hydraulic load conditions. Hydraulic load distributions may also shift due to changes in land-use (Schilling *et al.*, 2014), the loss of natural features like marshes and coral reefs (Ferrario *et al.*, 2014; Möller, Spencer, French, Leggett, & Dixon, 2001), and man-made structures like dams (Lee, Heo, Lee, & Kim, 2017). Some additional uses on or near a flood defence may similarly result in a shift in hydraulic loads in which case computer models are required to quantify the change in hydraulic loads from the specific use.

The second type of analysis is concerned with determining the capacity of flood protection infrastructure to prevent flooding or designing sufficiently strong flood defences. As described in Section 1.1.2, the probability of failure of a flood defence is determined by modelling the different failure mechanisms of the flood defence within a reliability framework. The hydraulic conditions determined in the first type of analysis are used as design criteria the flood defence is required to retain up to an acceptable level. A vast amount of literature has explored various effects and design options for flood defences by assessing the probability of failure of the flood defence through modelling (Bischiniotis, Kanning, Jonkman, & Kok, 2018; van Loon-Steensma & Schelfhout, 2017). The effect of additional features

such as pipelines and asphalt roads (Aguilar-López *et al.*, 2018a; Aguilar-López *et al.*, 2018b), and different types of foreshores (Oosterlo *et al.*, 2018a; Vuik *et al.*, 2018b) were all assessed by different models for predicting dike failure. Calculating the probability of failure by incorporating effects of multifunctional use in dike failure models is therefore a promising approach to quantify the effects of multifunctional use on flood protection in this research.

The third type of analysis involves determining and/or mitigating the consequences of a flood. Many studies have been conducted to estimate the vulnerability of areas across the world to flooding. Such studies explore options to minimise consequences of floods, e.g. through regional policies (Koks, Jongman, Husby, & Botzen, 2015), or use these metrics to determine an economically optimal protection level (Jonkman *et al.*, 2009). This research is mainly concerned with the effects of multifunctional use in reducing or increasing the risk flooding. Therefore, no such analyses are conducted for this research.

The implementation of additional functions within a flood defence is highly context specific. As a result studies on multifunctional use so far have analysed case-studies to study multifunctional elements of interest (Aguilar-López *et al.*, 2018a; Aguilar-López *et al.*, 2018b; Chen *et al.*, 2017; van Loon-Steensma & Vellinga, 2014; Vuik, Borsje, Willemsen, & Jonkman, 2019; Vuik *et al.*, 2018b; Yang, Shi, Bouma, Ysebaert, & Luo, 2012) (**Table 1.2**). Similarly, to ensure multifunctional use is understood within the relevant context, a suitable case-study from the Dutch Flood Protection Program (HWBP) is selected to answer each research question in this thesis as well.

To effectively study the effects of multifunctional use on flood risk, it is not necessary to redevelop all three types of flood risk analyses for each case-study. As discussed in sections 1.1.2 and 1.1.3, there are already developments in the probabilistic assessment of flood defences. It is therefore more efficient to adapt an existing probabilistic framework for assessing flood risk, rather than developing a new one. This thesis adapts the Dutch legal assessment tools (*abbreviated as WBI in Dutch*) and design guidelines (*abbreviated as OI in Dutch*). This probabilistic framework is implemented since 2017 (Slomp *et al.*, 2016) and specifies methods for the analyses discussed above of 1) deriving hydraulic loads (Rijkswaterstaat, 2016b), 2) models for failure mechanisms (Rijkswaterstaat, 2016c), and 3) prescribes

the appropriate safety level for dike sections given expected damages and casualties in the hinterland (Rijkswaterstaat, 2016a). This approach ensures the research can focus on areas in the framework affected by multifunctional use and the reliability framework developed throughout the thesis remains consistent with current practises while allowing insights of the thesis to be more easily adopted in dike assessments and designs.

### 1.3.2. Approach per research question

This thesis explores three research questions to develop a framework for assessing the effects of multifunctional use of flood defences on flood risk. Starting with the WBI framework introduced in the Netherlands in 2017 (Slomp *et al.*, 2016), each research question will be used to adapt the framework in some aspect.

The first research question asks *how a dike assessment framework can be adapted to probabilistically evaluate multifunctional use of a flood defence?* As explained in Section 1.1.3, some multifunctional uses like trees and pipelines are common along river dikes and do have procedures to ensure a safe design. Examining these procedures of the WBI framework within the context of a case-study is the first step in identifying how multifunctional elements can be accounted for in a dike design. To this end a multifunctional dike is schematised according to the current safety framework and its relevant failure mechanisms are evaluated by models already used in practise (e.g. (Sellmeijer *et al.*, 2011; van der Meer *et al.*, 2016)). The safety level is assessed with a level II probabilistic algorithm. An improved probabilistic schematisation for multifunctional use is suggested and the effect on the safety level is again assessed using the same models and probabilistic routine. The case-study selected is the Grebbedijk in Wageningen, the Netherlands. While the Grebbedijk was used as a starting point, the multifunctional elements explored (buildings, trees) are common enough that the approach is easily generalised to other river dikes with such elements.

The second research question asks *can additional defences constructed for multifunctional use of the flood protection zone be incorporated and evaluated within a probabilistic evaluation framework.* While aspects of multifunctional use of a single flood defence have been incorporated within the WBI framework to some degree

as examined in the previous question, multifunctional use of a flood protection system can also be achieved by the construction of additional defences in the flood protection zone. A prime example is the construction of additional defences and inlets for restoring wetlands in polders while improving flood protection, e.g. (Cox *et al.*, 2006). At the time this research was conducted the framework needed to probabilistically evaluate this type of flood protection is extensively discussed. The question is explored by analysing the case of the Double Dike between Eemshaven and Delfzijl, the Netherlands. Based on the Double Dike case, changes to the WBI framework are explored to evaluate the effect of the additional dike on flood protection. Similar to the approach of the previous question, the relevant failure mechanisms for the case are identified, modelled, and evaluated with a probabilistic algorithm. The applied failure models (wave impact and overtopping) are rooted in the models applied and developed for the WBI, with additions made for the case-study area. The approach is generalised such that it can be applied to similar multifunctional flood protection concepts where additional flood defences are constructed.

The third research question asks how *a probabilistic framework can account for long-term climate adaption benefits of multifunctional use within a flood protection zone?* Multifunctional use of flood defences is not only considered for immediate benefits, but also for potential long-term benefits. This is the case for the Wide Green Dike case-study in the Ems estuary, the Netherlands. Previous studies have suggested aligning the dike design with the nearby marshes is a promising long-term climate adaptation strategy (van Loon-Steensma & Schelfhout, 2017). Nevertheless, it is not yet explored how such benefits can be represented in a probabilistic flood risk framework. Changes to the WBI framework are explored in order to quantify these benefits. As climate change, in particular sea-level rise, presents a change in the hydraulic system, hydro-morphological models are used to identify changes in the frequency of extreme hydraulic loads on flood defences. In addition, the multifunctional design of the dike will again be evaluated probabilistically by modelling the relevant failure mechanisms within a probabilistic calculation.

## **1.4. Thesis outline**

The thesis is divided into 7 chapters (Figure 1.3). Chapter 1 presents the background, the research objectives, a description of the research approach, and the structure of the thesis.

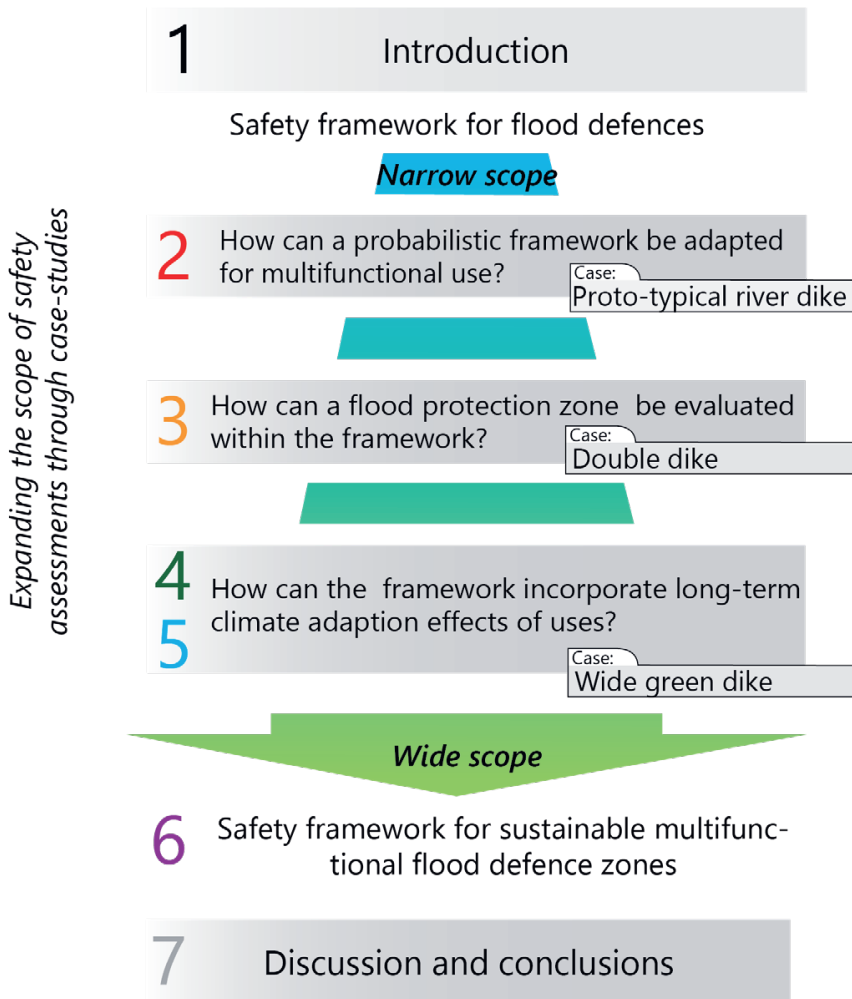
Chapter 2 addresses the first research question: *“How can a dike assessment framework be adapted to probabilistically evaluate multifunctional use of a flood defence?”* by evaluating a typical river dike with common multifunctional elements. The current practise for common multifunctional elements is described and compared to an alternative assessment methods with scenarios for the state of each multifunctional element.

Chapter 3 addresses the second research question: *“How can additional defences constructed for multifunctional use of the flood protection zone be incorporated and evaluated within a probabilistic evaluation framework?”* by studying the Double Dike near Delfzijl, the Netherlands. A new framework is proposed to propagate hydraulic loads through multiple flood defence elements and demonstrated for the relevant failure mechanism of the Double dike (i.e. revetment erosion and overtopping).

Chapters 4 and 5 relate to the research question: *“How can a probabilistic framework account for long-term climate adaption benefits of multifunctional use within a flood protection zone?”* and explore it with the Wide Green Dike case-study in the Ems-Dollard estuary. Chapter 4 evaluates the feasibility of sediment capture by man-made pits to reinforce dikes against sea-level rise while chapter 5 explores how sedimentation on a natural foreshore can already reduce the need for future reinforcements.

Chapter 6 presents the main result of the thesis: *“a framework for assessing and designing flood defences in which effects of multifunctional use within the flood protection zone on safety can be quantified”* by combining the lessons learned in the previous chapters into one framework for assessing multifunctional flood defences and provides insights how other uses influence the design of flood defences.

Finally, Chapter 7 provides a discussion of the results of the thesis, discusses the weaknesses of the approach and how these can be addressed, and provides an outlook for the implementation of multifunctional flood defences in the future.



**Figure 1.3** Overview of the thesis chapters with the research questions and case-studies. Each step the scope of the multifunctional use is expanded in space (from a single flood defence to a flood protection zone), and in time (from short-term effects on flood protection to long-term climate adaptation effects on flood protection)



# 2

## Re-evaluating safety risks of multifunctional dikes with a probabilistic risk framework

R.J.C. Marijnissen, M. Kok, C. Kroeze, J.M. van Loon-Steensma

This chapter was published as:

Marijnissen, R.J.C., Kok, M., Kroeze, C., & van Loon-Steensma, J.M. (2019). Re-evaluating safety risks of multifunctional dikes with a probabilistic risk framework. *Natural Hazards and Earth System Sciences*, 19(4), 737-756. <https://doi.org/10.5194/nhess-19-737-2019>



The background of the page is a photograph of a flooded landscape. In the foreground, there is a body of water reflecting the sky. In the middle ground, a dike or embankment runs across the frame, with trees and vegetation on top. The sky is overcast and grey. The overall tone is somewhat somber and naturalistic.

## Abstract

It is not uncommon for a flood defence to be combined with other societal uses as a multifunctional flood defence, from housing in urban areas to nature conservation in rural areas. The assessment of the safety of multifunctional flood defences is often done using conservative estimates. This study synthesizes new probabilistic approaches to evaluate the safety of multifunctional flood defences employed in the Netherlands and explores the results of these approaches. In this chapter a case representing a typical Dutch river dike combining a flood safety function with a nature and housing function is assessed by its probability of failure for multiple reinforcement strategies considering multiple relevant failure mechanisms. Results show how the conservative estimates of multifunctional flood defences lead to a systematic underestimation of the reliability of these dikes. Furthermore, in a probabilistic assessment uncertainties introduced by multifunctional elements affect the level of safety of the dike proportional to the reliability of the dike itself. Hence, dikes with higher protection levels are more suitable to be combined with potentially harmful uses for safety, whereas dikes with low protection levels can benefit most from uses that contribute to safety.

## 2.1. Introduction

### 2.1.1. Evolution of the flood risk approach

With rising sea level and an expected rise in extreme rainfall events due to climate change, many regions in the world are faced with increasing flood risk (Bouwer, Bubeck, & Aerts, 2010; Hirabayashi *et al.*, 2013). Risk-based approaches towards flood protection have been applied all over the world to inform decision makers on effective flood risk measures in spite of the large (Hall *et al.*, 2003; Jonkman *et al.*, 2009; Kheradmand, Seidou, Konte, Batoure, & Bohari, 2018). Nevertheless, a better understanding of the fragility of flood protection measures, including innovative ones like natural flood defences (Temmerman *et al.*, 2013), is instrumental to properly evaluate the flood risk in the future.

The Netherlands in particular is vulnerable to rising flood risks as about 60 % of its area is prone to flooding from the sea or rivers (Kok *et al.*, 2017). After the large flood of 1953 a design water level with an acceptably small exceedance probability was set based on an economic optimization between investment costs and obtained risk reduction (Maris *et al.*, 1961). Many studies have argued for a comprehensive probabilistic approach towards assessing the protection level provided by flood defences (Apel *et al.*, 2006; Hall *et al.*, 2003; Vrijling, 2001). As of January 2017 the water-level exceedance-based national risk standards were replaced by a more complex full probabilistic approach to more effectively adapt to social and economic developments and climate change (Kok *et al.*, 2017). The Dutch Water Act is the first to require the implementation of these principles on a nationwide scale. While these approaches were developed for dikes that serve as flood protection only, in practice many dikes have features serving other functions than flood protection. It is still unclear how such multifunctional aspects of a flood defence must be included in probabilistic safety assessments.

### 2.1.2. Multifunctional flood defences

Multifunctional flood defences (MFFDs) are engineered structures designed for the purpose of flood protection while simultaneously enabling other uses (Voorendt, 2017). Combining dikes with other functions is fairly common. Dikes can have roads on top, cables and/or pipelines running through them, or structures

on them or are part of a historic landscape. In the Netherlands alone, the majority of dike reinforcement projects already face the presence of more than one function. Usually, enabling multiple functions requires strengthening of the dike beyond the minimal requirements for a traditional dike to account for uncertainties related to those functions (van Loon-Steensma, Schelfhout, & Vellinga, 2014c). Multifunctional use of the flood defence does not need to decrease safety. For example, the development of green foreshores for flood protection services is an attractive option for future climate adaption (van Loon-Steensma *et al.*, 2014c) as such flood defences can reduce the risk of flooding through natural processes (van Loon-Steensma, Hu, & Slim, 2016; van Loon-Steensma & Kok, 2016).

Flood defences can strengthen other values when functions are properly integrated (Lenders, Huijbregts, Aarts, & van Turnhout, 1999; van Loon-Steensma *et al.*, 2014c). In urban areas where space is limited, there is continuous pressure to build on or integrate structures with the flood defence (Stalenberg, 2013). In rural areas, nature-based solutions have gained interest because they combine beneficial properties of natural systems for flood protection (e.g. wave attenuation by vegetation on foreshores) with conservation or development of important natural values (Pontee, Narayan, Beck, & Hosking, 2016; Temmerman *et al.*, 2013). In the Netherlands these developments favour the implementation of a multifunctional flood defence due to the limited space and government policy to consider other uses (e.g. natural, historical, and economical)(van Loon-Steensma & Vellinga, 2014).

Despite the large number of multifunctional dikes and incentives, the tools to assess the safety of MFFDs have still been limited to rules of thumb and in-depth tailor-made studies. Unless the multifunctionality is a key feature, assessments are often limited to proving multifunctional use does not significantly diminish the safety of the flood defence, ignoring potential positive contributions to safety. Using such a conservative approach for dike assessments does ensure safe dikes from a flood risk perspective but may result in requiring larger and more expensive dikes.

### 2.1.3. Aim

There is a need for improved flood defences due to climate change (rising sea levels, higher river discharges) and socio-economic developments. The number of people exposed to a high risk of flooding is expected to increase from 271 million in 2010 to 345 million in 2050 due to socio-economic growth alone (Jongman *et al.*, 2012). By 2100, 168 million people per year will experience floods due to sea-level rise. By reinforcing dikes this number can already be reduced by a factor of 461 (Hinkel *et al.*, 2013). While reinforcing dike systems, there is plenty of opportunity to enable multifunctional use of the flood defence.

However, the means to determine the safety provided by multifunctional flood defences remain limited to conservative approaches in which multifunctional elements can only be shown to have no significant negative influence. Spurred on by the threat of increasing flood risks by climate change and the revised legislation on flood standards in the Netherlands, a new probabilistic framework to assess multifunctional flood defences is emerging that can be used for a wider context. The aim of this chapter is to synthesize the new approaches to evaluate the safety of MFFDs employed in the Netherlands into a single coherent framework and evaluate how this new probabilistic approach towards MFFDs can change the assessed safety compared to the commonly applied conservative approach towards MFFDs.

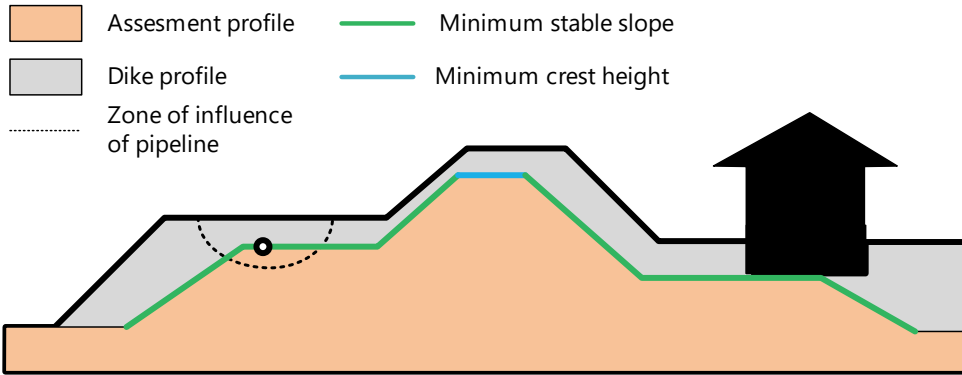
To this end, first the existing official framework for assessing multifunctional dikes in the Netherlands is analysed and alternative frameworks in both scientific and grey literature for a probabilistic risk-based approach towards assessing MFFDs as required by the new Water Act are explored. These are synthesized in an adapted framework (Sect. 2.2). Secondly the methods used to calculate the probability of failure of several dikes are explained using the synthesized probabilistic approach and the traditional conservative approach (Sect. 2.3) to show the differences in assessed safety level (Sect. 2.4). Finally the implications and results are discussed (Sects. 2.5 and 2.6). By illustrating how a probabilistic approach towards multifunctional use can affect the assessed level of safety, new types of integrated solutions can be more fairly compared to monofunctional dikes, both in the Netherlands and beyond.

## **2.2. Formulating a framework for MFFD assessment**

### **2.2.1. Official Dutch guidelines for MFFD dike assessments and design**

The methods to assess flood defences in compliance with the official Dutch safety standard are documented in official guidelines (Ministerie van Infrastructuur en Milieu, 2016; Ministerie van Verkeer en Waterstaat, 2007). The assessment can be performed on different levels: basic, detailed, and tailored. Basic assessments are a quick scan with simple rules to approve flood defences with an insignificantly low failure probability. Detailed assessments consist of design formulas and models taken or adapted from Dutch design manuals and are commonly applied for (initial) designs and assessments. These are suitable for predicting the failure of dikes when general descriptions of dike failures can be applied. Such generalizations are not always suitable for MFFDs. Tailored assessments allow for the use of advanced models and experiments outside the guidelines to assess the probability of failure as accurately as possible. These assessments require a large amount of information for a specific location and are generally expensive to perform. The dike needs to pass at least one of these assessments to be considered safe and a proper design ensures the dike will pass the assessments for its entire designed lifespan.

In the official Dutch framework, multifunctional use of the dike is considered either directly as objects on the dike, by the materials used, or indirectly by the geometry of the dike. When only the geometry of the dike is affected or a different material is used (e.g. to integrate with the surrounding landscape) the official framework can still be applied (Slomp *et al.*, 2016). However, if multifunctional use of the dike is facilitated by a non-water retaining object (NWO), e.g. a house or pipeline, an additional assessment must be made for the NWO. For a few multifunctional elements, a basic safety assessment is described in guidelines (structures, vegetation, and traffic) (Ministerie van Infrastructuur en Milieu, 2016; STOWA, 2000, 2010; TAW, 1985, 1994; van Houwelingen, 2012). Only for pipelines is a more detailed assessment available following the Eurocode (NEN, 2012), which ensures the pipeline itself has an acceptably small probability of failure. If a dike cannot be approved by a basic assessment and no suitable detailed assessment is available, a tailored assessment for that specific dike section with NWOs must be made.



**Figure 2.1** Assessment profile for a dike with NWOs (pipeline and house with basement). Adapted from Fig. A4 of the current Dutch guidelines (Rijkswaterstaat, 2016).

2

The philosophy of a basic assessment is to rule out the possibility of the NWO affecting the dike significantly. Hence, the dike is considered safe only if the dike is dimensioned such that the zone of influence of the NWO does not extend into the minimum dike profile needed to meet the safety standard (see **Figure 2.1**). As a result, in basic assessments the NWO is always assumed to be in its most critical state during design conditions (e.g. uprooting of a tree). This is the conservative approach to assess the influence of multifunctional elements on safety because the actual probability of multifunctional elements being in a critical state is not considered. The ambition of the Dutch Water Act is to consider the actual probability of flooding which necessitates a risk-based approach to these elements.

### 2.2.2. Synthesizing a risk-based approach to MFFD design

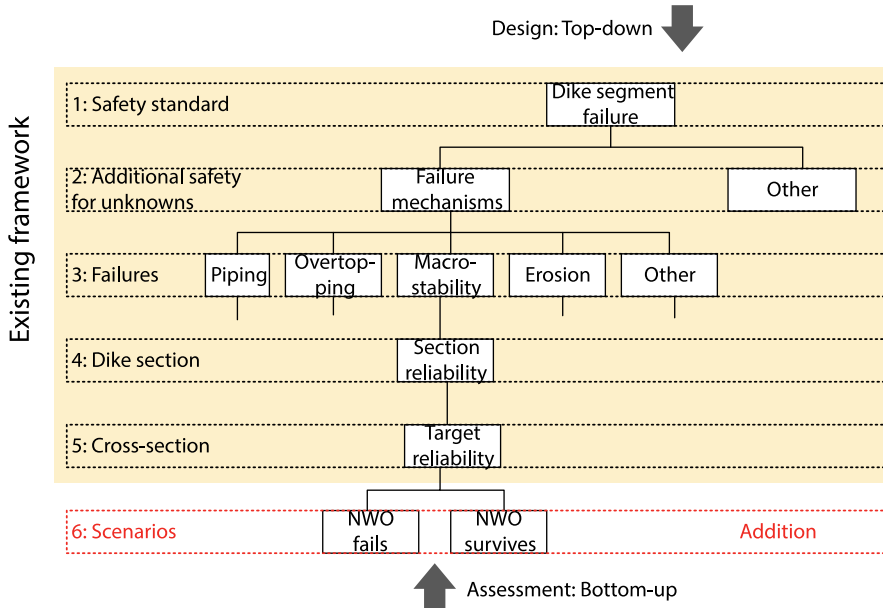
The scientific basis for the risk-based framework adopted in the Netherlands was presented by Vrijling (2001). The risk of a flood is decomposed into a fault tree of failure mechanisms, each of which can be described with a mathematical limit state function and evaluated probabilistically. Limit states are common for designing structures in civil engineering and define when a structure collapses resulting in damages and casualties (ultimate limit state) or can no longer perform its intended use (serviceability limit state) (Gulvanessian, 2009). Vrijling's approach of structuring the ultimate limit states of flood defences into a fault tree for risk analyses has been incorporated into many frameworks of flood defences (Apel, Thieken, Merz, & Blöschl, 2004; Steenbergen, Lassing, Vrouwenvelder, & Waarts,

2004; van Gelder *et al.*, 2008; Vorogushyn, Merz, Lindenschmidt, & Apel, 2010) and has already been applied on a large scale to evaluate the Dutch flood defences (Jongejan *et al.*, 2013). However, the framework was developed for monofunctional flood defences.

Studies on MFFDs specifically are available. However, the developed frameworks address different aspects, like the identification of the degree of spatial and structural integration (Ellen *et al.*, 2011b; van Veelen *et al.*, 2015; Voorendt, 2017), the identification of costs and benefits (Anvarifar, Oderkerk, van der Horst, & Zevenbergen, 2013), the identification of the threats and opportunities (Anvarifar, Voorendt, Zevenbergen, & Thissen, 2017), and the identification and evaluation of flexibility for MFFDs (Anvarifar, Zevenbergen, Thissen, & Islam, 2016). Other studies on MFFDs tend to only focus on the effects of a specific multifunctional element or failure mechanism (Bomers, Aguilar-López, Warmink, & Hulscher, 2018; Chen *et al.*, 2017; Zanetti, Vennetier, Mériaux, Royet, & Provansal, 2011). Only recently was an assessment framework specifically for hybrid nature-based flood defences put forward, accounting for multiple failures by putting vegetation-specific equations directly into the assessment procedure (Vuik *et al.*, 2018b).

Pending an official framework, practitioners in the Netherlands have used approaches to integrate multifunctional dike elements. One such approach was put forward for trees through the use of scenarios such as uprooting (van Houwelingen, 2012). An approach for assessing NWOs as indirect failure mechanisms with scenarios is being suggested in these cases (Knoeff, 2017). This approach will be explored further in this chapter.

Formulating a practical framework for the assessments of MFFDs is challenging due to the large variety of possible configurations and range of multifunctional elements. Multifunctional elements can be evaluated in different scenarios with simple or complex models in literature while preserving the established structure of the existing Dutch framework. Scenarios in this context are different possible states of a multifunctional element with a probability of occurrence in which the element affects the flood defence. By assessing each scenario and weighing up the probability of failure in each scenario by the probability of the scenario, the probability of failure of the flood defence is calculated accounting for the



**Figure 2.2** A framework for a detailed assessment and design of a dike with multifunctional elements. The yellow section is the existing framework, while the last step in red denotes the addition of scenarios (e.g. a failed NWO and functioning NWO) to conform to a risk-based approach.

uncertainty in the state of the multifunctional element. Therefore the steps for MFFD assessments in the Netherlands are synthesized as follows (also see **Figure 2.2**):

- *Step 1.* Establish the required safety level of the dike segment.
- *Step 2.* Assign a portion of the required safety level to unknown/unquantifiable risks.
- *Step 3.* Distribute the remaining failure budget across the known failure mechanisms.
- *Step 4.* Divide the dike into (close to) homogeneous sections.
- *Step 5.* Determine a representative cross section and safety level, taking variations along the dike section into account (length effect).
- *Step 6 (addition).* Determine the scenarios, i.e. states, in which the NWO affects the flood defence differently, assess the probability of these scenarios, and combine them based on their probability of occurrence.

The difference between a basic assessment and a probabilistic one is the addition of Step 6. In a basic assessment, i.e. a detailed assessment without NWOs followed by a basic NWO assessment to exclude significant potential negative influences, first a dike cross section would be designed with the criteria found in Step 1 to 5 and then adapted such that the influence of the intended NWO is outside the designed profile. In the risk-based probabilistic assessment the effects of NWOs are calculated directly with the scenarios in Step 6 and combined with their probability of occurrence to arrive at a safe cross section.

### 2.3. Application of the risk frameworks

#### 2.3.1. Comparing the basic assessment with the expanded probabilistic assessment

To answer how a probabilistic approach towards multifunctional dikes can affect the evaluated safety compared to a monofunctional dike, a set of MFFDs is assessed with the new probabilistic approach and the traditional conservative approach (see **Table 2.1** for values per scenario, see Appendix A.1 for all values). The calculations are performed on a cross-sectional level. The reliability of a cross section is calculated for the most common dike failure mechanisms by probabilistically evaluating the models describing failure for the different scenarios. The failure probabilities per scenario and failure mechanism are combined to arrive at the probability of failure.

#### 2.3.2. Failure mechanisms

To assess the risk of a flood, it is important to know the mechanisms by which the flood defence could fail. Though many failure mechanisms are possible (Kok *et al.*, 2017), the vast majority of documented dike failures worldwide are the result of three dominant mechanisms: overtopping (resulting in erosion of the inner slope), internal erosion (also referred to as piping), and inner slope stability (Danka & Zhang, 2015; Vorogushyn, Merz, & Apel, 2009). Within the Netherlands, predominantly overtopping and slope instability have been the cause of dike breaches in the past (van Baars & van Kempen, 2009). For this study the probability of a flood is calculated by considering the failure mechanisms overtopping, piping,

and macro-stability. Whether the flood defence fails by a failure mechanism is expressed in an equation called a limit state function:

$$Z = R - S \quad (2.1)$$

where  $Z < 0$  denotes failure,  $R$  is the resistance to failure, and  $S$  is the soliciting load. For overtopping and overflow, the load ( $S$ ) is the amount of water flowing over the dike, while the resistance ( $R$ ) is the capacity of the crest and inner slope to resist the flow of water without eroding (Appendix A.2). For piping, the method of Sellmeijer *et al.* (2011) is used to calculate the stability of the sand particles in the subsoil under a pore water pressure gradient. It is expressed as a critical head difference ( $R$ ) that cannot be exceeded by the head difference across the dike ( $S$ ) (Appendix A.3). Macro stability is calculated within the program D-Geo Stability (Brinkman & Nuttall, 2018) with the stability method by (Van, 2001) and ground water model by (TAW, 2004). The method by Van (2001), like the Bishop (1955) method, calculates the sum of the driving moments ( $S$ ) and the total resisting moment ( $R$ ) along the slip plane (Appendix A.4). However, it also accounts for uplift forces on the interface of aquifers present beneath most dikes. The resulting limit states are:

$$Z_{\text{overflow \& overtopping}} = q_c - q \quad (2.2)$$

$$Z_{\text{piping}} = H_c - H \quad (2.3)$$

$$Z_{\text{macro stability}} = \Sigma M_R - \Sigma M_S \quad (2.4)$$

Here  $q_c$  is the empirically determined critical overtopping discharge,  $q$  is the overtopping discharge calculated according the methods of van der Meer *et al.* (2016) and TAW (2002),  $H_c$  is the critical hydraulic head according to Sellmeijer *et al.* (2011),  $H$  is the difference in water level in front and behind the dike,  $\Sigma M_S$  is the sum of the active moments in the critical slip plane, and  $\Sigma M_R$  is the sum of resisting moment in the critical slip plane.

### 2.3.3. Probabilistic procedure

Multiple procedures are available for calculating the reliability of a flood defence. A fully probabilistic procedure like Monte Carlo relies on evaluating the limit state function for many variations of the random variables and determines the

failure probability as the number of failures over the total number of samples. Meanwhile, a semi-probabilistic approach evaluates the limit state function once and captures uncertainties with (partial) safety factors to determine (non)failure. A probabilistic procedure like the first-order reliability method (FORM) iteratively converges to an approximation of the probability of failure (Hasofer & Lind, 1974) (see Appendix A.5). This option was chosen as it does not require millions of evaluations of the limit state function to assess the small failure probabilities required for dikes while still retaining the probabilistic distribution of the variables otherwise lost in a semi-probabilistic approach.

While the FORM procedure can approximate the failure probability of a single limit state function of a single failure mechanism, a combination of failure mechanisms is more complex to evaluate. When the only dependence between failure mechanisms is assumed to be the water level, each failure mechanism becomes an independent event for each discrete water level such that the probability of failure of the system is:

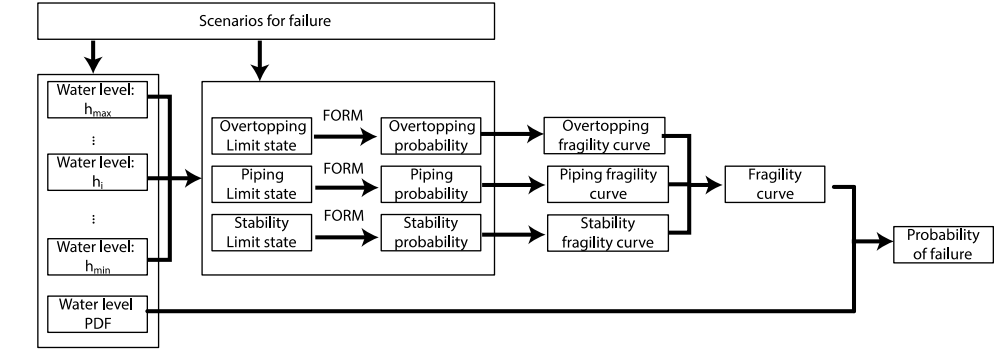
$$P_{f,sys|h} = P_{sys}(f|h) = 1 - \prod_{i=1}^n (1 - P_{f,i|h}) \quad (2.5)$$

Where  $P_{f,i|h}$  is the probability of failure given water level  $h$  for the  $i^{th}$  failure mechanism and  $P_{f,sys|h}$  is the probability of failure given water level  $h$ . Repeating this calculation across all water levels results in the fragility curve of the system to the water level (Bachmann, Huber, Johann, & Schüttrumpf, 2013). The failure probability of the system is computed by integrating the fragility curve of the system ( $F_R(h)$ ) over the probability density function (PDF) of the water level ( $f_h(h)$ ):

$$P_{f,sys} = \int_{h=-\infty}^{h=\infty} f_h(h) * F_R(h) dh \quad (2.6)$$

Eq. 2.6 is discretized to:

$$P_{f,sys} = \sum_{j=1}^m P(h_j) * P_{sys}(f|h_j) \quad (2.7)$$



**Figure 2.3** The probabilistic procedure for calculating the probability of failure of a dike cross section in this study.

2

Low failure probabilities can more easily be expressed in terms of the reliability index which is defined as:

$$\beta = -\Phi^{-1}(P_f) \quad (2.8)$$

Where  $\Phi^{-1}$  is the inverse standard normal cumulative distribution function.

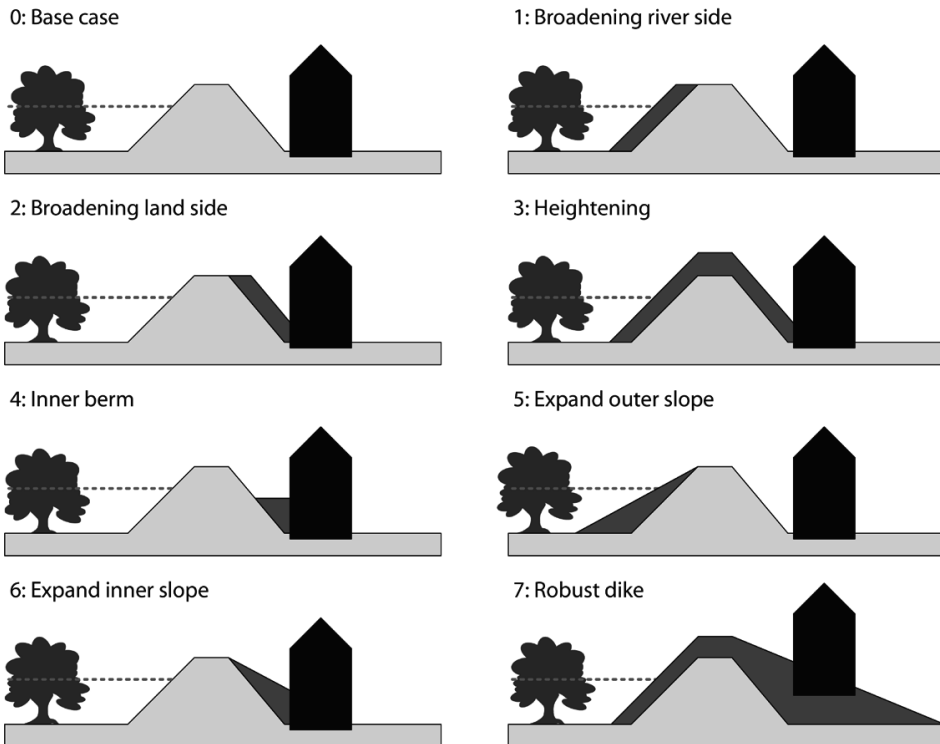
The probabilistic procedure described above has been utilised before successfully by Lendering, Schweckendiek, and Kok (2018) and Bischiniotis *et al.* (2018) to compute the reliability of canal levees and a cost-optimal river dike respectively. An overview of the entire process as applied in this study is schematised in **Figure 2.3**.

## 2.3.4. Case study

### 2.3.4.1. Setting and cross sections

The multifunctional dike for the case study is situated in a riverine area, with nature on the floodplain side and a building on the landward side. To test how a risk approach can affect the calculated level of safety, eight cross sections of multifunctional dike profiles (**Figure 2.4**) are evaluated with three methods: a conservative, a probabilistic, and a monofunctional approach (see 2.3.1).

If a dike does not meet the set safety standards, a reinforcement by adapting the profile, among other options, is explored. Each profile in this study represents a common reinforcement strategy. Broadening the dike by widening the crest or expanding the slope reduces the risk of a piping failure by increasing the piping



**Figure 2.4** Case studies for comparing the conservative and the new probabilistic approach in this study.

length by a few metres. Furthermore, broadening inwards and making the inner slope shallower makes the inner slope more stable. A berm also improves the stability of the inner slope. Finally heightening the dike decreases the risk of overtopping waves and overflow during high water. The final reinforcement strategy is a combination of heightening and decreasing the steepness of the inner slope.

Each multifunctional element can compromise a section of the dike resulting in failure. For the purpose of this study the multifunctional elements have been simplified so these can be incorporated directly in variables of the limit state functions or dike geometry (see Sect. 2.3.4.1). When broadening the dike on the floodplain or making a shallow outer slope (see profiles 1 and 5 in **Figure 2.4**), the hinterland remains unaffected by the dike itself, while in the other alternatives, the building becomes part of the flood defence. By reviewing the options the effect of the multifunctional elements on the safety after the reinforcements is evaluated in each framework.

#### 2.3.4.2. Schematization of multifunctional elements

Effects of multifunctional elements on dike failure are incorporated through scenarios based on the fact sheet by Knoeff (2017). For each mechanism, scenarios are defined in which the element (e.g. tree, structure, and pipeline) affects the failure mechanisms. The probability of failure can then be calculated for each scenario. The total probability of failure for the specific mechanism is computed by weighing the probability of failure of each scenario with the probability of the scenario.

A natural floodplain can add ecological, landscape, and recreational values to the flood protection system. However, elements like trees can penetrate the clay top soil, resulting in cavities within the clay when the tree dies (Zanetti *et al.*, 2011). Following a conservative estimation for the uprooting of trees by TAW (1994), a 2 % annual probability of a cavity within the floodplain is assumed. If a cavity is present, the effective length for piping is reduced to the distance between the dike's inner toe and the location of the disturbance. The trees on the floodplain do not affect the inner slope stability, nor is the tree density in the case study high enough to expect an influence on overtopping by wave dampening properties of trees.

A building on or close to the dike affects multiple failure mechanisms. The weight of the structure is transferred to the underlying soil, where the load increases friction with the subsoil, increasing slope stability, and lateral stress on the soil, decreasing slope stability. On the slope itself, the structure affects the overtopping mechanism through the inner slope cover that prevents erosion. When a structure is present, it acts as a discontinuity in the outer grass cover such that water can more easily erode soil during overtopping and is reflected in a lower critical overtopping rate. When a structure is absent, the space occupied by it in the profile is assumed to be empty. Furthermore there is no grass cover but instead loose bare soil with practically no overtopping resistance (see **Table 2.1**). In the case study the effect of the structure on piping is insignificant as it does not penetrate the aquifer, and pipes can still develop along the outside of the structure rather than directly beneath it.

**Table 2.1** Variation in parameters between reinforcement strategies across profiles (Figure 2.4).

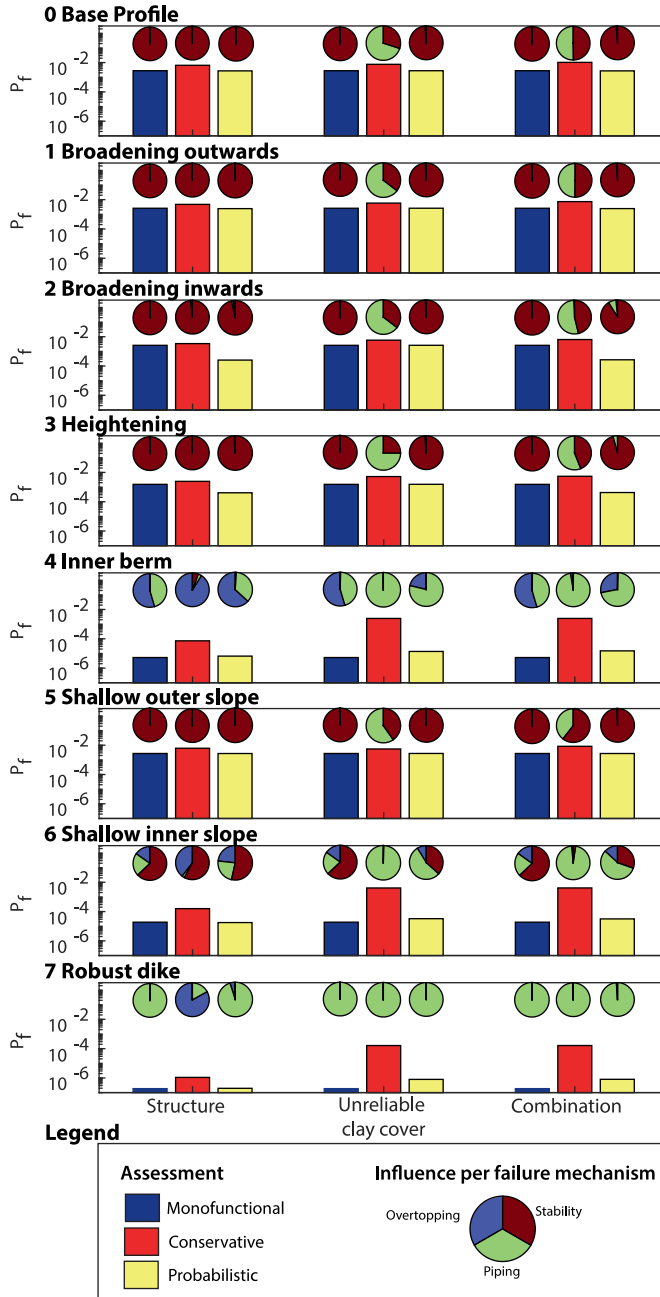
Profile nr.	Inner slope [-]	Outer slope [-]	Crest height [m+REF]	Berm width [m]	Crest width [m]	Flood plain length [m]	Max. overtopping rate ( $\mu$ , $\sigma$ )* [l m <sup>-1</sup> s <sup>-1</sup> ]					
							House intact		House collapsed		No house	
0	1:2.5	1:3	5.5	0	5	100	-	-	-	-	100	120
1	1:2.5	1:3	5.5	0	10	95	-	-	-	-	100	120
2	1:2.5	1:3	5.5	0	10	100	70	80	0.1	0	100	120
3	1:2.5	1:3	6.5	0	5	97	70	80	0.1	0	100	120
4	1:2.5	1:3	5.5	15	5	100	70	80	0.1	0	100	120
5	1:2.5	1:4.5	5.5	0	5	91.75	-	-	-	-	100	120
6	1:4	1:3	5.5	0	5	100	70	80	0.1	0	100	120
7	1:10	1:3	6.5	0	5	97	70	80	0.1	0	100	120

\*parameters of the lognormal distribution based on (van Hoven, 2015)

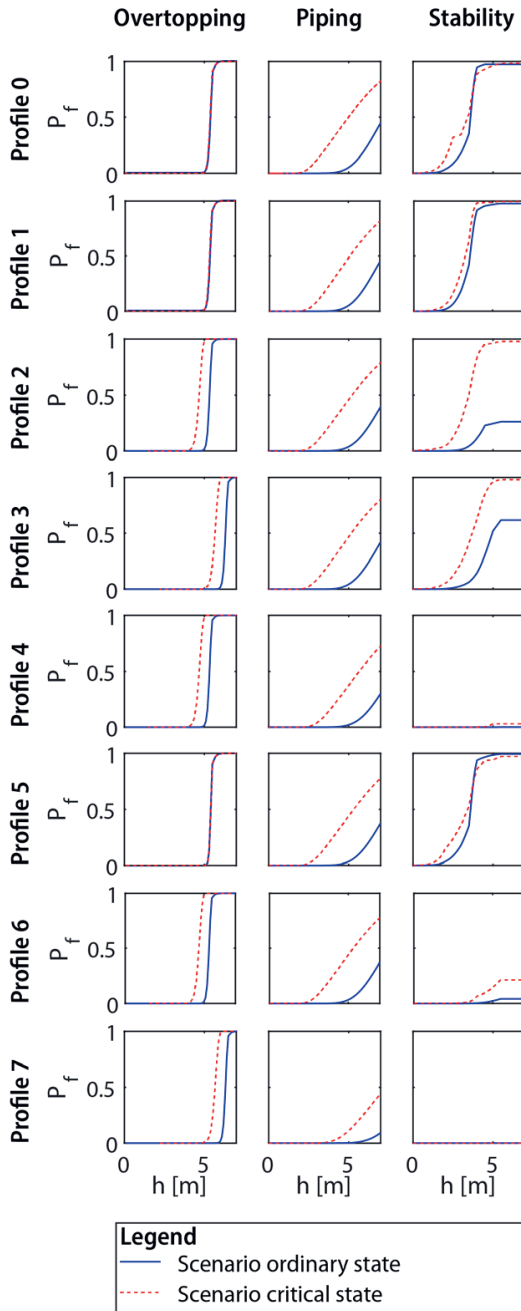
The structure in the case study is located 3 m behind the inner dike toe. The structure is taken to be 15 m wide, exerts a weight of 17 kN m<sup>-1</sup>, and is embedded 1 m into the soil on a shallow foundation without additional geotechnical measures like piles or sheet pile walls. The horizontal position of the structure remains fixed for each reinforcement strategy, while vertically the landward end of the structure is always embedded only 1 m in the soil when the dike is expanded inwards. The probability the structure is absent during a high water event is estimated to be 1 %. This probability is based on the percentage of houses demolished in the Netherlands annually which has varied between 0.13 % and 0.23 % per year (van der Flier and Thomsen, 2006) rather than the probability of structural failure of the house. The structure in its demolished state leaves a discontinuity in the dike profile, exerts no weight on the dike, and exposes bare clay on the dike slope while leaving the remaining dike intact.

## 2.4. Results

The results are presented in **Figure 2.5**. As expected, the conservative approach consistently yields the highest probabilities of failure for the assessed dikes. Both the probabilistic assessment of the additional multifunctional uses and the monofunctional assessment yield a lower probability of failure for each dike profile (**Figure 2.5**).



**Figure 2.5** The probability of failure ( $P_f$ ) for every dike profile (0 to 7) assessed as a monofunctional dike (blue bar), a multifunctional dike with a conservative approach (red bar), and a multifunctional dike using a probabilistic approach (yellow bar) in the situation in which a structure is present (left), an impaired clay cover on the floodplain could be present (middle), and both a structure and unreliable clay cover are present (right). The influence of the three failure mechanisms overtopping (blue), piping (green), and stability (red) is given per bar with a pie chart.



**Figure 2.6** The difference between the fragility curves of the three failure mechanisms and each profile, with both multifunctional elements intact in blue and both multifunctional elements in a critical state in red

### 2.4.1. Slope stability

The weight of the structure can improve the slope stability of the dike in the probabilistic assessment as shown in the assessment of profile 1 with the structure only. The changes in annual failure probabilities are solely due to the presence or absence of weight increasing friction in the passive zone of the slip circle. In the conservative approach the weight of structure is always ignored, leading to a noticeably higher failure probability. This effect is most noticeable in profile 2 with only a structure. The reliability increases by a factor of 10 in the probabilistic assessment compared to a monofunctional dike due to a favourable position of the structure in the critical slip circle (see **Figure 2.6**). In contrast to profile 2, in profile 4 the position of the structure is detrimental to stability, whereby a monofunctional dike has a reliability that is 3 times larger ( $1.6 \times 10^{-8}$  versus  $5.0 \times 10^{-8}$ ) for the probabilistically assessed dike with a structure. Both the structure and berm add weight, but the structure

has the risk of being absent while the risk of a monofunctional berm being absent is negligible. This makes the berm a safer option. Nevertheless this effect on the reliability of profile 4 was insignificant compared to the overall failure probability, which was dominated by piping and overtopping.

### 2.4.2. Overtopping

The presence or absence of the structure had a minor impact on overtopping as can be seen in **Figure 2.6**. This is mainly the result of the relatively high predictability of the mechanism itself (reflected by the steepness of the fragility curve) rather than the direct influence of the structure on the mechanism (reflected by the shift of the fragility curve) or additional uncertainty introduced by the structure (reflected by a decreasing steepness of the fragility curve). Because overtopping has a steep fragility curve, the influence of the structure only affects a limited range of water levels, and thus the net effect of the structure on the safety of the dike is limited.

### 2.4.3. Piping

Including uncertainty because of unmanaged vegetation on the floodplain has a large effect on piping failure, which was ignored in the assessments with the structure. Because the floodplain in the case study is wide, a scenario with a cavity close to the dike results in a major reduction of the piping length in the probabilistic assessment. **Figure 2.6** shows a large difference between the fragility curves of the critical state and the ordinary state. The presence of trees on the floodplain on piping is even more pronounced in the conservative approach because the entire width of the floodplain is automatically excluded in the assessment. This leads to a different assessment of the need for piping specific reinforcement measures, in particular for the conservative assessment. Due to the dominance of the piping failure mechanism in a conservative schematization, there is an increasing discrepancy between the conservative assessment and the other assessments.

### 2.4.4. Assessments

Finally the difference in probability of failure between a monofunctional dike and a multifunctional dike depends on the reliability of the monofunctional dike itself. Unless there are large differences in the schematization of a failure mechanism (as was discussed for piping), differences in failure probabilities between assessments scale roughly by the same order of magnitude as the decrease in failure probability after a reinforcement (**Figure 2.5**; note the log scale for the probability of failure). However, the relative differences become more pronounced leading to proportionally higher failure probabilities in a conservative assessment compared to a probabilistic assessment.

## 2.5. Discussion

The results show a large difference between the reliability assessed between the conservative approach and the probabilistic approach. A prevailing view against the multifunctional use of flood defences is that these require larger dimensions to meet the same safety standard as a traditional dike (Ellen *et al.*, 2011a; van Loon-Steensma *et al.*, 2014c). However, as the case study above illustrated, this perception only holds true for a conservative approach that omits multifunctional elements from the assessment. With a more probabilistic approach towards multifunctional elements, their perceived negative influence was significantly smaller or could even result in a net positive influence. Positive contributions of multifunctional elements under likely conditions can be included as well as the likelihood of the multifunctional elements affecting the flood defence negatively.

A drawback of the probabilistic approach is that it needs specific information about the failures and states of multifunctional elements before an assessment can be conducted. For example, erosion around or over discontinuities during overtopping (possibly due to the presence of multifunctional elements like a road) is highly variable and hard to capture in a generic limit state function, even with well-calibrated models (Bomers *et al.*, 2018; Hoffmans, Akkerman, Verheij, van Hoven, & van der Meer, 2009). Depending on the sensitivity of the failure probability to these processes, assumptions on effects and statistical distributions would need to be increasingly conservative to guarantee the safety level is met.

However, new information on the interaction between multifunctional uses and failure mechanisms is becoming increasingly available through ongoing research (Aguilar-López *et al.*, 2018a; Vuik *et al.*, 2018b). Furthermore, new techniques are being employed to continuously monitor the dikes in detail (Hanssen & van Leijen, 2008; Herle, Becker, & Blankenbach, 2016), while advances in remote sensing allow for closer monitoring of the state of foreshores (Friess *et al.*, 2012; Niedermeier, Hoja, & Lehner, 2005). As a result, a probabilistic approach towards multifunctional elements can capitalize on these advances by updating the previously assumed risks in assessments with observations of the actual performance of MFFDs over time.

Aside from the effects of multifunctional elements themselves, other uncertainties influence how much the multifunctional use of the flood defence can affect the level of safety. For piping, Aguilar-López, Warmink, Schielen, and Hulscher (2015) demonstrated that by reducing the uncertainty in the seepage properties of the soil of a multifunctional dike, the probability of a piping failure is already significantly reduced. Lanzafame (2017) concluded variability introduced by vegetation only has a small effect on the probability of a slope failure due to larger uncertainties in strength and seepage of the soil. In contrast, a relatively small disturbance by burrowing animals in a fragile dike has resulted in a breach under conditions it had previously survived (Orlandini, Moretti, & Albertson, 2015). The observation that the dike's own reliability influences the degree to which multifunctional use can affect the probability of failure of the dike was also found in this study. As the reliability of the dike itself increases, the influence of a multifunctional element on the level of safety decreases as the added variability of the multifunctional element becomes smaller compared to the uncertainties in other parameters the dike was already designed for. This effect of dike reliability on the influence of multifunctional elements has implications. An increase in failure probability due to multifunctional elements is likely to be overestimated in a traditional assessment for dikes with a high protection level, while similarly for these dikes also only a limited decrease in failure probability can be expected from beneficial multifunctional elements. Conversely, dikes with a low protection level

are influenced more by both beneficial and detrimental effects of multifunctional use of the flood defence.

This chapter only looked at the effects of multifunctional use on flood protection. However, multifunctional use comes with its own set of requirements that must be taken into account. For example, structures need to comply with building codes, and flood protection measures in nature reserves can be subject to environmental protection regulations, while to preserve landscape values substantial dike heightening may be unacceptable. How much such additional non-flood protection requirements influence the design of dikes needs to be researched for a successful implementation of MFFDs.

This chapter investigated the assessments of multifunctional flood defences for the current situation. In the design of these defences, however, future conditions, like for example climate change or societal trends, need to be taken into account. Scenarios for future sea-level rise in the coming century vary between 0.23 and 0.98 m (IPCC, 2013). Incorporating beneficial multifunctional uses of flood defences, either natural like marshes or man-made like structures, can become an asset to achieve the levels of flood protection needed in the future.

## 2.6. Conclusions

This chapter analysed how a full probabilistic approach towards multifunctional flood defences can change the assessed safety compared to the commonly applied conservative approach in which multifunctional use of the flood defence can only be shown to have no significant negative influence. Although probabilistic assessments have been used before, the new regulations of the Water Act in the Netherlands necessitate a full probabilistic assessment of flood defences. Therefore, a probabilistic framework incorporating multifunctional elements probabilistically was developed. The overall conclusion is that application of a probabilistic approach towards multifunctional use of the flood defence will lead to a lower assessed risk of flooding compared to conservative assessments because (1) positive contributions of multifunctional elements to safety can be included, even when in a critical state there is a negative contribution to safety, and (2) the risk of multifunctional elements being in such a critical state

is made explicit. Another important aspect is that effects of multifunctional use on safety become smaller as the reliability of the dike increases. Therefore, monofunctional dikes which already have a high reliability are more suitable to be combined with multifunctional uses detrimental to safety, whereas dikes with a low reliability can benefit more from multifunctional uses that contribute to safety.

Based on the results, we recommend that a probabilistic framework is further developed and implemented for including multifunctional elements into dike assessments. While many knowledge gaps are still present in quantifying the effects of multifunctional use of flood defences, incorporating scenarios in which a multifunctional element can harm or help flood protection can already provide insights in synergies that can be exploited or dangers that can be mitigated. These scenarios and associated probabilities will need to rely on expert judgment. However, it is expected that with the growing number of methods to monitor dike performance and ongoing studies on dike failures, these gaps can be filled in the future. To this end, further research is required on the proper scenarios and their associated probabilities that can be used to improve future assessments of multifunctional dikes. Additionally, more research is needed to assess how multifunctional elements influence the safety of dikes over longer periods, especially in relation to the large uncertainties involved in climate change. A real-world case study for design should be used to explore how these aspects can be incorporated in practice.

## Acknowledgements

This work is part of the Perspectief research programme “All risk”, project number P15-21, which is financed by NWO Domain Applied and Engineering Sciences. We thank Wim Kanning for his advice on the probabilistic stability calculations. Furthermore, we would like to thank Harry Schelfhout and Reindert Stellingwerf for the discussions on the current practices for multifunctional dikes. Finally we thank the two anonymous reviewers for their helpful comments.

## Appendices

Appendices to this chapter can be found starting from page 200.



# 3

## Flood risk reduction by parallel flood defences – case-study of a coastal multifunctional flood protection zone

R.J.C. Marijnissen, M. Kok, C. Kroeze, J.M. van Loon-Steensma

This chapter was published as:

Marijnissen, R.J.C., Kok, M., Kroeze, C., & van Loon-Steensma, J.M. (2021). Flood risk reduction by parallel flood defences – Case-study of a coastal multifunctional flood protection zone. *Coastal Engineering*, 167, 103903. <https://doi.org/10.1016/j.coastaleng.2021.103903>



## Abstract

In this chapter the safety of a double-dike system (or twin dikes) is assessed. Such a system consists of two parallel lines of flood defences. During storms the combined strength of the parallel flood defences must prevent flooding of the hinterland. A culvert can be implemented for the tidal exchange of sea water to enable new land-uses in the area between the dikes such as aquaculture, saline agriculture, salt marsh restoration and clay extraction. We develop a general framework for assessing the safety of such double dike systems and apply a simplified version to the Double Dike between Eemshaven and Delfzijl (The Netherlands) to test this method. In doing so, we aim to quantify the flood protection benefits of parallel flood defenses and enable their use in multifunctional flood protection strategies.

Within the framework the transmission of hydraulic loads by the seaward dike to the landward dike in the case-study was described by overtopping, overflow and erosion of the outer slope, alongside discharge through the culvert in the event of a non-closure. For the subset of coastal double dike systems with a tall seaward dike (as in the case-study), the results show only a negligible improvement in flood protection compared to a single dike system. With the addition of a culvert in the first dike, flood risk will only be reduced by the second landward dike if its height is sufficient to retain water in the event of a non-closure during common storm events. These double dike systems are implemented for potential uses of the inter-dike zone, e.g. for nature restoration, rather than as a measure to primarily improve flood protection.


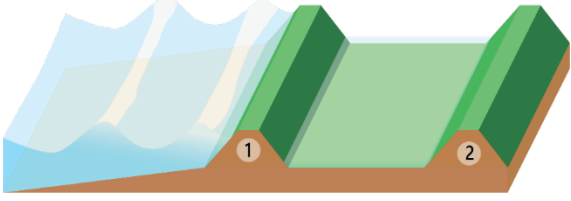
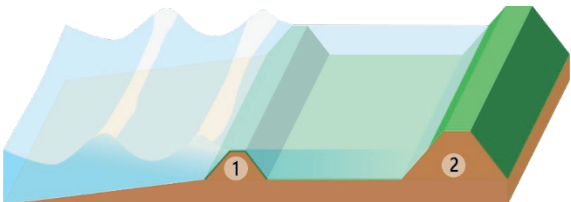
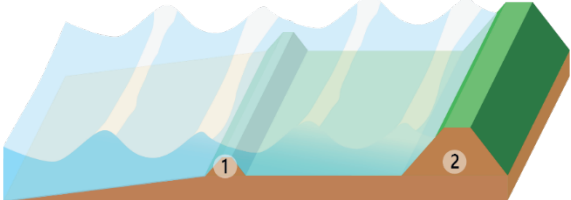

### 3.1. Introduction

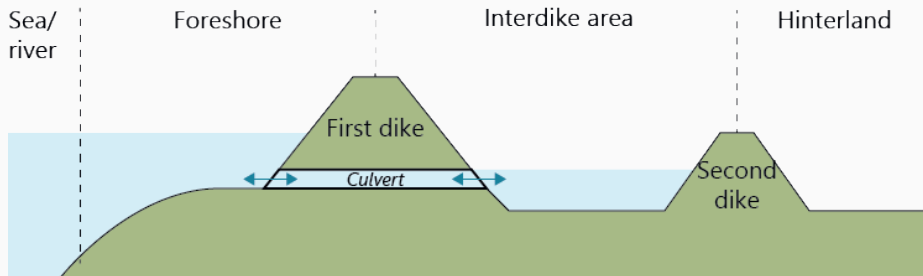
#### 3.1.1. Implementation of double dike systems

The majority of the world's population lives near rivers and coastlines where millions of people are exposed to the threat of flooding. With a growing global population and the influence of climate change, flood risk is expected to increase further unless new flood risk management strategies are implemented, including the introduction of innovative flood protection infrastructure (Hinkel *et al.*, 2014; Vousdoukas *et al.*, 2018; Winsemius *et al.*, 2016). One method to reduce the exposure to floods is the continued heightening and strengthening of existing levees, seawalls and other structures. However, such interventions may not address, or could even aggravate, other pressing problems (Elliott, Day, Ramachandran, & Wolanski, 2019; Jeuken, Haasnoot, Reeder, & Ward, 2014), like loss of marsh and fish habitat (Munsch, Cordell, & Toft, 2017; Schuerch *et al.*, 2018), coastal erosion (Williams, Rangel-Buitrago, Pranzini, & Anfuso, 2018), limited space for urban expansion (Barbier, 2015), and a deteriorating water quality (Kiedrzyńska, Kiedrzyński, & Zalewski, 2015). Therefore, integrated solutions are being investigated to reduce flood risk, while at the same time integrating, improving or restoring other uses within the flood protection system (Stalenberg, 2013; Temmerman *et al.*, 2013; van Loon-Steensma *et al.*, 2014c). A system of multiple parallel dikes (also called double dikes or twin dikes) is one alternative being explored in this context.

Double dike systems are already implemented in many different forms to improve flood protection. A system of multiple dikes has been described in literature in a variety of contexts, using different names to refer to the double dike system and its components. For example, a second dike behind the primary dike can be referred to as a sleeper dike, a ring dike if it encircles an area of interest, a compartment dike designed to limit the flood extent after a breach, or as a regional dike. To aid in the discussion of these systems, we first classify different double dike types based on the probability of a flood ( $P_f$ ) for each dike in the absence of the other (**Table 3.1**). The first dike is always located closest to the sea/river while the second dike is closest to the hinterland regardless of function, size or age (see Box 3.1). In a type I system the strongest dike is located near the source of water. In

**Table 3.1** A classification for different double dike configurations based on the probability of a flood ( $P_f$ ) for each dike in the absence of the other.

Type	Image	Criterium
I		$P_{f,1} < P_{f,2}$
II		$P_{f,1} \approx P_{f,2}$
III		$P_{f,1} > P_{f,2}$
IV		$P_{f,1} \gg P_{f,2}$
V		$P_{f,1} = 1$

**Box 3.1: Definitions used for the components of a double dike system**

The following definitions are used throughout this chapter:

**Double dike system:** A flood defence system where two parallel dikes, including the area between the dikes, protect the hinterland from flooding.

**Foreshore:** The land in front of the first dike which is not permanently inundated with water.

**Culvert (optional):** If present, this structure allows the interdike area to be controllably flooded and drained.

**Interdike area:** The land in between two dikes. Flooding of this area may be managed.

**Hinterland:** The land protected by the flood protection system.

**First/second dike:** Dikes are numbered from the foreshore towards the hinterland, regardless of size, age or function.

a type II system both dikes are about equally strong. In a type III system the strongest dike is located closest to the hinterland. For completeness two additional types are included where the first dike does not offer protection from floods, but may still interact with flows and waves on the foreshore. This is the case for small embankments on the foreshore (type IV) or after a breach is created (type V), e.g. as a part of managed realignment.

Secondary dikes can simply be remnants of defences along former polders, rivers or coastlines and no longer serve a purpose in flood protection. When a second defence is built to support an existing defence its function differs between riverine and coastal environments. Generally, along coastlines an additional dike aims to reduce or mitigate flooding by high (storm) waves. This may be accomplished by making the first dike act as a breakwater in a type III system (Mai, von Lieberman, & Zimmermann, 1999). Alternatively, overtopping water can be contained in the interdike area and prevent damage in the hinterland in a type I or

II system (Pasche *et al.*, 2008). Along rivers, a sufficiently high second dike aims to reduce the (peak) river discharge and the associated flood water levels by providing additional space (Room for the River) in a type I, II or III system (Bornschein & Pohl, 2018). The interdike area is flooded (directly or through a structure) during the peak of the discharge, thereby reducing the peak discharge and water level downstream (Lammersen, Engel, van de Langemheen, & Buiteveld, 2002; Smolders *et al.*, 2020). Smaller “summer” dikes found along rivers only aim to retain water within the river’s main channel for navigation and agriculture in summer, rather than contributing to mitigating flood risk during extreme events, and are classified as a type IV system.

Systems with multiple dikes have often emerged from repeated land reclamation for agriculture or urban expansion. More recently, small polders have also been restored to wetlands across many countries to preserve and create ecosystem services (Esteves, 2014). In many of these coastal examples, the tide was reintroduced via one or several in-/outlet structures in the first dike and a second ring dike was built around the restoration site, thus creating a type I, II or III double dike system (e.g. Kruibeke (BE), Breebaart (NL), Luneplate (GE), Bremerhaven (GE), Beltringharder Koog (GE), Sébastopol (FR)) (Goeldner-Gianella, 2007; Hofstede, 2019; Maris *et al.*, 2007; Peletier, Wanningen, Speelman, & Esselink, 2004; Reise, 2017). In other cases double dikes have been implemented for retaining water and managing floods for agriculture (Ghazavi, Vali, & Eslamian, 2010; Toan, 2014) or to anticipate the loss of primary flood defences by ongoing coastal erosion (Vinh, Kant, Huan, & Pruszek, 1997). While two dikes remain present to retain floods, usually only one dike is assigned the function of flood defence during critical conditions. Finally, systems where the first dike is already breached before a storm are classified as a type V system. While the first dike can no longer prevent flooding by itself, it can still aid in reducing water levels at the second dike, as was studied for the Freiston Shore Managed Realignment site (UK) (Kiesel *et al.*, 2020).

### 3.1.2. Research gap

Double dikes have garnered interest for their potential to integrate coastal functions (e.g. urban development, nature conservation and development,

recreation, aquaculture, saline agriculture, etc.) with flood protection. However, without an extensive local or regional assessment it is not yet clear how an additional dike affects flood protection assessments of such a system.

So far, safety assessments of systems with multiple flood defences have computed the probability of failure of each flood defence individually for the failure mechanisms (Jongejan *et al.*, 2020) and later combine the probabilities into a system reliability. This is achieved by schematising the failures of flood defence components into a system of serial and parallel correlated failures, from which the combined failure probability is assessed with a fault tree analysis (Roscoe, Diermanse, & Vrouwenvelder, 2015; Steenbergen *et al.*, 2004). The applied failure mechanisms to compute these individual failure probabilities are usually defined by critical thresholds rather than by a physical description of dike erosion or deformation. While such thresholds for failure are useful indicators, they give no information regarding the subsequent flows over/through the dike into the interdike area during failure. Therefore this approach is ill-suited for incorporating the dynamic loads on a second flood defence during and after “failure” of the first dike. Generally, a component like the first dike is simply assumed to have one “failed” state in which a breach has developed. This assumption overestimates the failure probability of a double dike system when the residual strength of the first dike remains sufficient to reduce or even prevent loads on the second dike.

The development of a breach and the subsequent flows after failure of the first dike is usually modelled separately as part of the safety assessment of regional compartment dikes, dikes designed to limit the extent of a flood after a breach. These simulations are carried out for pre-defined breach locations, during pre-defined design storm scenarios, under the assumption that breach formation is initiated upon reaching the design water level of the primary defence during the simulated event (Geerse, Stijnen, & Kolen, 2007; Oost & Hoekstra, 2009). As a result, this method substantially simplifies the events initiating failure and relies on the judgement of the engineer to select the proper scenarios.

In this study we aim to quantify the flood protection benefits of parallel flood defences in order to enable their use in multifunctional flood protection strategies. In the current practise the system reliability is assessed by simple failure scenarios for each individual flood defence. In this study a more sophisticated approach is

explored where the first dike of the system is treated similar to a foreshore. Recent studies have demonstrated how complex additional elements on the foreshore like vegetation or sand from dunes can be implemented in probabilistic flood risk assessments (Oosterlo *et al.*, 2018a; Vuik *et al.*, 2018b) and affect flooding once a breach has developed (Zhu *et al.*, 2020). Adopting a similar approach for double dikes allows for greater optimisation in the design of these systems. This chapter proposes a general method for assessing the safety of double dike systems and applies a simplified version to the Double Dike between Eemshaven and Delfzijl (The Netherlands) to demonstrate its applicability.

### 3.1.3. Outline of the chapter

First the methodology to assess the safety of a double dike system is presented in section 3.2, starting with the existing framework for single dikes (3.2.1) and expanding this to a new framework for two dikes (3.2.2). The method (section 3.3) is applied to the case of the double dike between Eemshaven and Delfzijl (3.1). Here the framework is simplified to fit the study area (3.3.2) and the concepts of hydraulic loads (3.3.3), and transmission functions with the probability estimation methods (3.3.4) are described for the case-study. Results of the safety assessment calculations are presented in section 3.4: first for the safety assessment of the first dike (3.4.1), then integrated with a culvert (3.4.2), and finally with a second dike (3.4.3). In section 3.5 the results are discussed: first the reliability of the models (3.5.1), secondly the applicability of the double dike framework (3.5.2), thirdly the applicability of the results of the case-study for other types of double dike systems (3.5.3) and finally other drives for implementing a double dike system beside flood protection (3.5.4). Finally the conclusions are presented in section 3.6.

## 3.2. Assessment of double dike systems

### 3.2.1. Existing approach for flood risk assessments

In general, assessing the safety of dike systems consists of identifying the failure mechanisms of the system, assessing with various models when these failures are expected to occur, and finally determining if the probability of such an event is acceptably low. The failure mechanisms of dikes, levees and other common

flood protection structures are well known and can be found in most engineering manuals, guides, and standards. e.g. (Allsop, 2007; Kok *et al.*, 2017; USACE, 2002). For failure mechanisms “failure” is usually defined as an amount of critical damage of the flood defence or a critical condition in which damage is expected. Examples of such criteria include overflow, a critical overtopping discharge limit (van der Meer *et al.*, 2016), a critical pore pressure gradient for piping (Sellmeijer *et al.*, 2011), or a critical force balance for slope instability (Van, 2001). The probability of failure in these cases is defined as:

$$P_f = P(\mathbf{S} > \mathbf{R}), \quad (3.1)$$

where  $\mathbf{S}$  is the applied load condition on the dike and  $\mathbf{R}$  is the critical load condition for the flood defence.

Solving when the limit state ( $\mathbf{R} = \mathbf{S}$ ) has been reached does not indicate how much water will flood the hinterland. Therefore, in Dutch law a different criterion is used. According to the definition of Kok *et al.* (2017) a flood defence has only failed if it results in at least 0.2 m of water depth in a postcode area in the hinterland. In practice the limit state approach is still used for assessing flood defences. However, exceeding the limit state for a failure mechanism is allowed within safety assessments as long as the flood depth criterion is not exceeded.

### 3.2.2. A framework for double dikes

In case of a single dike, the probability of failure is defined as the moment where the applied hydraulic loads on the system ( $\mathbf{S}$ ) are greater than the resistance of the system ( $\mathbf{R}$ ). In a double dike system, failure of the first dike may not result in a flood as long as the second defence prevents flooding of the hinterland by its height, or when the “failed” first dike sufficiently reduces the hydraulic loads at the second dike. The first dike can be conceived as transmitting ( $T$ ) a portion of the hydraulic loads from the sea/river ( $\mathbf{S}$ ) to the second dike. Under critical conditions dikes can transmit water and waves, similar to a breakwater. A breakwater transmits loads to the other side depending on the properties of the breakwater and its location within the system (d'Angremond, van der Meer, & de Jong, 1997). Dikes will only transmit water and waves by overtopping, overflow, seepage, or after a breach rather than through water pressures in the structure. The second dike needs to resist ( $\mathbf{R}$ ) the loads transmitted by the first dike ( $T(\mathbf{S})$ ). This resistance ( $\mathbf{R}$ ) of the second dike is not affected by the fact that the dike is part of a double dike system.

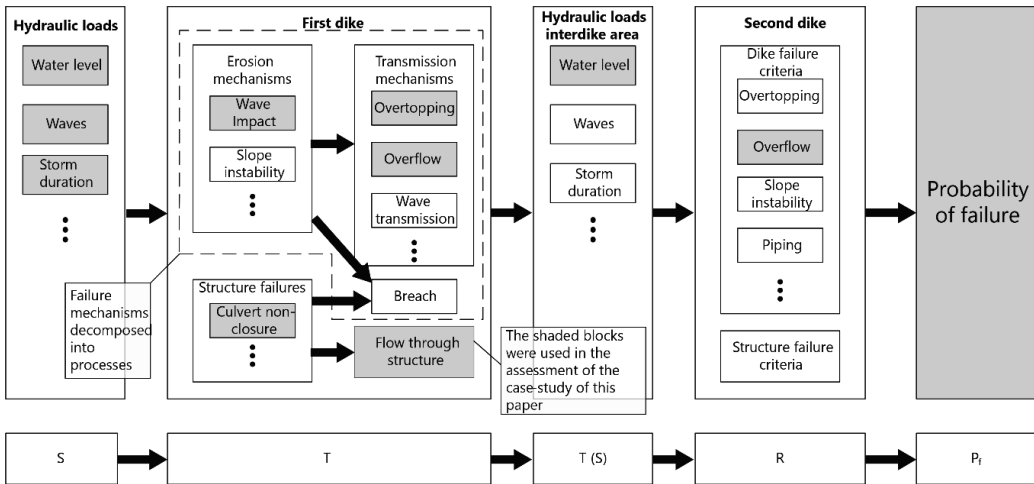
The probability of failure of the system is thus the probability of the transmitted hydraulic loads being greater than the resistance of the second dike. In mathematical terms:

$$P_f = P(T(\mathbf{S}) > \mathbf{R}) \quad (3.2)$$

Comparing Eq. 3.2 to Eq. 3.1 used for single dike systems, the only difference is the addition of a transmission function ( $T$ ). Here  $T$  is a sequence of models describing for any storm event in  $\mathbf{S}$  the corresponding hydraulic loads behind the dike. The idea of properties ( $\mathbf{S}$ ), like water levels and waves, being transmitted through a system ( $T$ ) and comparing it with some critical criteria ( $\mathbf{R}$ ) to decide on the probability of an event ( $P_f$ ) is not uncommon in other fields. In fact, this procedure lies at the core of many machine learning applications where information is transmitted through a network of (simple) models to inform about probabilities of an event.

To follow this procedure, we present in **Figure 3.1** A general framework for assessing the probability of failure for a double dike system. The shaded boxes represent the mechanisms that were considered in the assessment of the case-study between Eemshaven-Delfzijl. a new framework which consists of 5 steps:

1. Retrieve or compute the necessary statistics of hydraulic boundary conditions of the defence ( $\mathbf{S}$ ). These include the water level, the tide, the frequency of (storm) waves, the duration of storms, etc.
2. Identify the relevant failure mechanisms ( $T$ ) of the first dike. In the framework there are three categories of failure mechanisms: the transmission mechanisms which transfer water from one side of a dike to the other (e.g. overtopping and overflow), the erosion mechanisms which damage the flood defence such that transmission mechanisms are enhanced or a breach develops (e.g. soil instability or damage by waves), and the failures of embedded structures which can either allow water to flow through the dike (e.g. a culvert) or can damage the flood defence (e.g. an uprooted tree). Each erosion mechanism is expressed by a model calculating changes in the profile



**Figure 3.1** A general framework for assessing the probability of failure for a double dike system. The grey boxes represent the mechanisms that were considered in the assessment of the case-study between Eemshaven-Delfzijl.

3

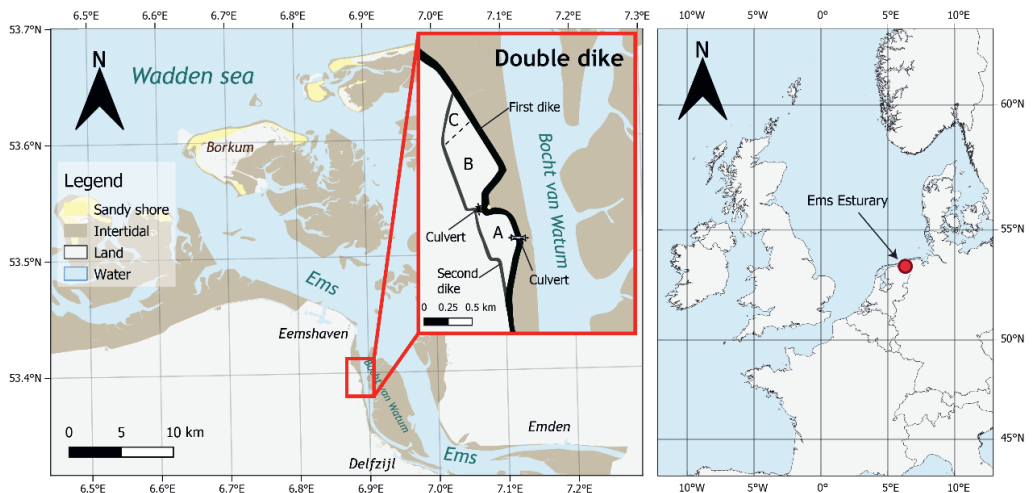
3. over time, and each transmission mechanism is expressed by a model calculating the flow over, through, or beneath the (eroding) dike. Possible failures posed by embedded structures can vary depending on the structure but should be expressed as flows or erosion over time. Finally, if according to one of the failure definitions erosion is too large a breach is assumed. Once the dike is assumed breached, failure mechanisms are no longer calculated and instead hydraulic loads are transmitted unimpeded to the interdike area.
4. Link the models identified in step 2 such that for all combinations of boundary conditions transmitted hydraulic loads into the interdike area are calculated  $T(S)$ .
5. Determine the resistance of the second dike ( $R$ ) to the relevant failure mechanisms. This procedure is identical to descriptions of failure in a situation with a single dike.
6. Select and execute a suitable algorithm to compute the probability of failure. Examples of such algorithms are the first order reliability method (FORM) (Ditlevsen & Madsen, 2007), numerical integration, or different sampling methods (e.g. Monte Carlo, directional sampling, importance sampling, etc.).

To understand how the framework can be employed in practice, a simplified subset of mechanisms (the grey blocks in **Figure 3.1**) are evaluated for the case of the double-dike between Eemshaven and Delfzijl (section 3.3).

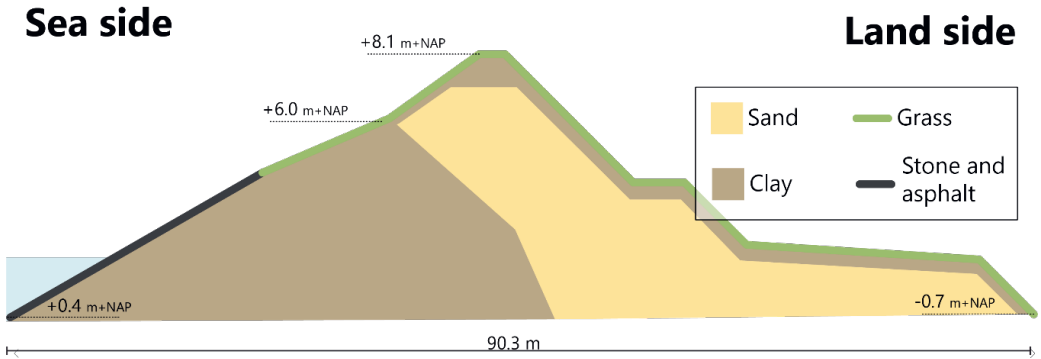
### 3.3. Application to Ems-Dollard double dike

#### 3.3.1. Case study

Like many coasts in the world, the Wadden-sea region will need to prepare for accelerating sea-level rise. The Delta Program, National Flood Protection Program, and local water boards are investigating options to prepare the Dutch Wadden-sea coast for 2100 (Delta Programme, 2014). At the dike section between Eemshaven and Delfzijl the application of a double dike system is investigated to maintain the strict flood protection level under future sea-level rise and subsidence, and explore how additional functions (saline agriculture, aquaculture, nature development, clay mining) can be integrated in this system (Kwakernaak *et al.*, 2015).



**Figure 3.2** The location of the Double Dike between Eemshaven and Delfzijl within the Ems estuary. Sections A, B, C are the different zones planned for different functions, each connected by culverts to the sea. Base map adapted from OpenStreetMaps



**Figure 3.3** A cross-section of the front dike between Eemshaven and Delfzijl

The Double Dike project Eemshaven-Delfzijl is located in the north-east of the Netherlands inside the Ems estuary, in the southern part of the Wadden Sea (see **Figure 3.2**). The parallel dikes (see Box 1 for the definitions of a first and second dike) enclose about 39 ha of land where new uses are explored. The first dike has been reinforced many times and the original clay dike can still be found inside the current dike (**Figure 3.3**). Recently the first dike was reinforced by the construction of the inner berm. A second dike was built behind the dike to a height of approximately 4 m+NAP to create the double dike system (see definitions in Box 1).

The area between the two dikes is split into three sections (**Figure 3.2**). The southernmost section (A) will be connected directly to the Ems through a culvert. In this area clay mining and nature development are planned as additional land-uses within the flood protection system. While an intertidal habitat develops, at yet to be determined locations accumulated clay will be extracted at regular intervals for use in dike construction. Section B will be connected to section A through a smaller culvert and is reserved for aquaculture. Section C is elevated and will feature saline agriculture. At the time of writing the second dike has been constructed, but the culverts in the first dike and between the dike sections, and the functions within the interdike area are not yet implemented.

### 3.3.2. Framework applied to the case-study

The first dike of the double dike system has already been reinforced to prevent breaching from failure mechanisms like piping and geotechnical instabilities up to the required Dutch safety standard for a single dike. For the mechanisms of wave impact and overtopping sufficient safety ought to be provided by the addition of the second dike. The usual overtopping and wave impact criteria assume the flood protection system has failed once the outer grass and roots, asphalt, or stone layer is damaged. Provided no breach develops, damage to the first dike is acceptable since the second dike would prevent water from reaching the hinterland. While this approach suits the specific circumstances of the case-study where an existing primary dike has already been reinforced up to standard, it does not generalise well for designing double dike systems from scratch. Therefore, the integrated framework in section 3.2 is applied to this context.

For the case-study the framework in **Figure 3.1** is substantially simplified to estimate failure of the Double Dike Eemshaven-Delfzijl. In practice all failure mechanisms need to be included for a thorough assessment, but for this study only the shaded parts of the framework in **Figure 3.1** are evaluated. First, we consider only erosion of the outer slope by waves as the erosion mechanism of the first dike. The considered transmission mechanisms as defined in section 3.2.2 are overtopping and overflow. Other failure mechanisms were already addressed during the last round of reinforcement with the construction of the wide inner berm.

Secondly, we consider failure of the structure (i.e. the culvert in the first dike) to only result from non-closure, and assume it will be constructed with a negligibly low probability of structural failure. The second culvert between sections A and B (see **Figure 3.2**) is not considered as it will remain open to fill the interdike area evenly. Therefore, we only consider the flow of water between the sea and interdike area through the culvert in the first dike from here on.

Thirdly, the first dike used to be the primary defence and consequently was designed to prevent overtopping during most storm events. As a result, little wave action can be expected within the interdike area from overtopping of the first dike. A water level increase inside the interdike area is therefore the only transmitted

hydraulic load considered at the second dike. To transform the combined hydraulic load probabilities at the first dike into the water level distribution of the interdike area, a multitude of different storm events were simulated in a probabilistic procedure (see subsection 3.3.4.3 and Appendix B.2).

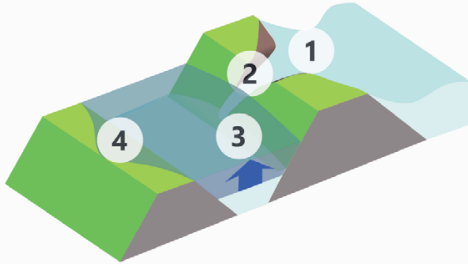
To arrive at the failure probability of the double dike system, the remaining hydraulic load distributions need to be evaluated at the second dike. For simplicity, this study only looks at overflow as a failure mechanism for the second dike, as this mechanism dictates the required height of the second dike. Hence the probability of failure for this particular simplified case reduces to:

$$P_f = P(T(S) > R) = P(h_{interdike} > z_{crest,2}). \quad (3)$$

**Figure 3.4** visualizes the mechanisms that were used to assess the case-study.

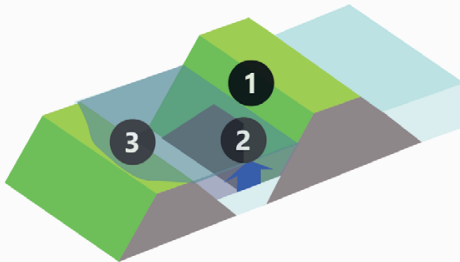
3

#### a. Transmission of loads by the first dike



- 1 Erosion mechanism: *Wave impact*
- 2 Flow mechanism: *Overtopping/overflow*
- 3 Transmitted hydraulic load: *Water level*
- 4 Critical load: *Overflow*

#### b. Transmission of loads by a structure



- 1 Structure failure: *Non-closure*
- 2 Transmitted hydraulic load: *Water level*
- 3 Critical load: *Overflow*

**Figure 3.4** The transmission of loads from the sea into the interdike area as schematised for the case-study in this paper.

### 3.3.3. Hydraulic loads

For many locations along the Dutch coast annual water level and wind statistics derived from over 60 years of measurements are available from gauges and stations. Additionally, the expected wave conditions during different combinations of water levels, wind speeds, and wind directions have been simulated with standardised models of the Dutch coast and are stored in databases for designing and assessing flood protection measures (den Heijer, Vos, Diermanse, Groeneweg, & Tönis, 2008). The most recent version of this hydraulic databases of the studied section of the Wadden Sea coast was used (Rijkswaterstaat WVL, 2017). Hydra-NL is a software-package made available by the Dutch water authorities that combines station statistics and the hydraulic database of simulations to estimate the annual probability of hydraulic load conditions at flood defences (Duits & Kuijper, 2018; Gautier & Groeneweg, 2012). The probabilistic methods employed in Hydra-NL are described by Diermanse and Geerse (2012) and in Hydra-NL's background report (Gautier & Groeneweg, 2012). To simplify computations, probability density functions (PDFs) and correlations were fitted to the water level, wave height and wave period statistics at the case-study site computed by Hydra-NL. Due to the orientation of the case-study site inside the estuary the conditions were simplified further by only considering one wave direction: from the Wadden Sea towards the study-site (see section 3.3.1). The fitted

**Table 3.2** Simplified distributions of maximum annual hydraulic conditions at the case-study site.

\*Note: NAP is the local vertical datum. \*\* Note: the probabilities of extreme values presented belong to the marginal distribution of the variable

Symbol	Variable	Unit	Distribution	Parameters	Extreme values**		Correlations		
					Exceedance Probability	Val.	$\rho_h$	$\rho_{H_s}$	$\rho_{T_p}$
$h$	Water level	$m + NAP^*$	Generalized extreme value	$\mu = 3.28$ , $\sigma = 0.36$ , $\xi = -0.02$ .	1 / 10 1 / 1,000 1 / 1,000,000	4.1 5.6 7.5	1.00	0.68	0.43
$H_s$	Significant wave height	$m$	Weibull	$A = 0.54$ , $B = 1.63$ .	1 / 10 1 / 1,000 1 / 1,000,000	0.9 1.8 2.7	0.68	1.00	0.92
$T_p$	Peak wave period	$s$	Weibull	$A = 2.44$ , $B = 3.56$ .	1 / 10 1 / 1,000 1 / 1,000,000	3.1 4.2 5.1	0.43	0.92	1.00
$\beta_{wave}$	Wave direction	$^\circ$	Constant	69.	-	69	-	-	-

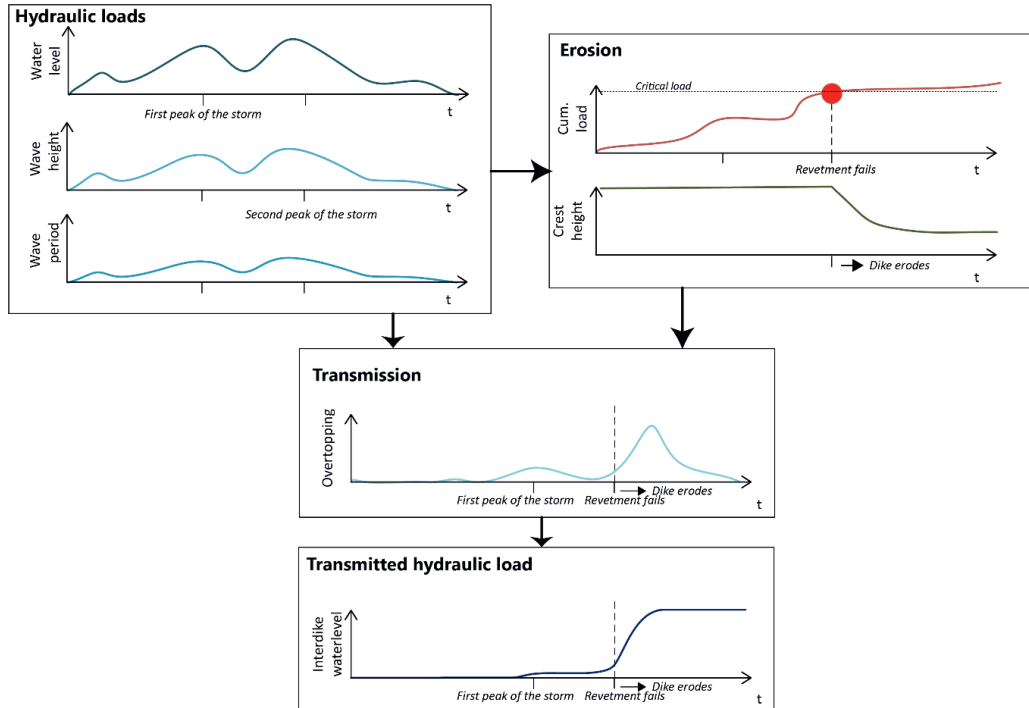
distributions for storm conditions are summarised in **Table 3.2**. The conditions in **Table 3.2** represent the simplified correlated joint probability distribution of annual maximum hydraulic loads at the first dike. This was defined as the collection of hydraulic loads (**S**) in section 3.2.2.

### 3.3.4. Transmission models

#### 3.3.4.1. Overtopping and erosion

For assessing overtopping flows and erosion of the outer revetment simultaneously, a prototype dike erosion model was utilised (Rongen, Stenfert, Dupuits, & Barbosa, 2018). It is based on the extensive research performed on grass dikes during the development of new dike assessment tools in the Netherlands (WTI-2017) (de Waal & van Hoven, 2015a, 2015b; Kaste & Klein Breteler, 2014, 2015; Kaste, Klein Breteler, & Provoost, 2015; Klein Breteler, Capel, Kruse, Mourik, & Kaste, 2012b; Mourik, 2015). The formulas were empirically derived from large-scale wave flume experiments (Klein Breteler, Bottema, Kruse, Mourik, & Capel, 2012a; Wolters, Klein Breteler, & Bottema, 2013). The integration of the different components into a single model was first presented by Kaste *et al.* (2015) and programmed by Rongen *et al.* (2018). While all individual model components are already in use for advanced dike assessments in the Netherlands as part of the WTI-2017 tools, the integrated model is still under development at the time of writing. Minor adjustments were made to the prototype to allow the dike erosion model to run within a probabilistic routine (see 3.3.4.3).

The general steps performed by the model are described here. For the details and formulas see Appendix B.4. First the dike profile needs to be specified in terms of geometry and the different materials (grass cover, clay, sand) like in **Figure 3.3**. Each of these materials has a resistance to being eroded when exposed to wave impacts and wave run-up loads. Secondly, the annual maximum storm loads were converted into a storm event with a time-series of a water-level, wave height and wave period using the 45 hour storm schematization for the region from Chab (2015) (see Appendix B.2 for details). At each time step, the model calculates which part of the dike is exposed to the wave loads, determines whether the critical load



**Figure 3.5** Overtopping of the dike as a result of loads (water level + waves) over time. Once a critical load is realized on a dike section, the dike starts eroding. As the dike is lowered by erosion, more waves overtop the dike as a result and the water level behind the dike rises. (Based on figure 5 of Rongen *et al.* (2018) )

has been exceeded for the exposed material and, if true, calculates the volume of dike material being eroded at that time step (see Appendix B.4). After the erosion processes are evaluated, the overtopping discharge by waves over the possibly eroded dike profile is calculated. The result is a time series of the wave-overtopping discharge (see **Figure 3.5**). The total volume of overtopping during the simulated storm event is divided by the area of the interdike area to determine the rise in water level during the event.

#### 3.3.4.2. Flow through the culvert

The formulas of Borgerhout implemented in Delft-3D (Deltares, 2020) (p. 301-303), based on the flow regimes in French (1985) (p. 368), were used to calculate the flow of water through the culvert in the event of a non-closure (see Appendix B.3 for details). A wide range of 45-hour events, ranging from a regular tide without

storm surge to a 1 in 1,000,000 year storm surge, were simulated in the event of a non-closure (see section 3.4.3 and Appendix B.2). The highest water level reached during the event is the maximum hydraulic load of the event.

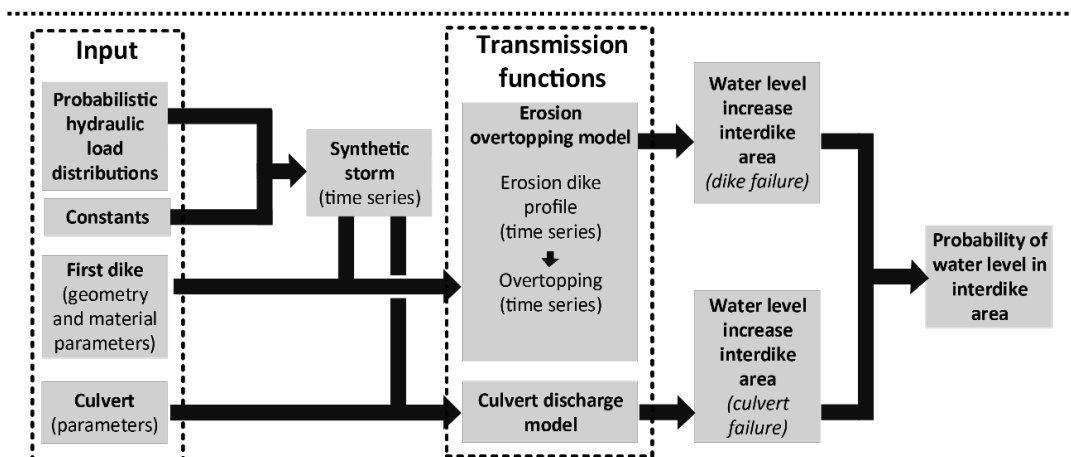
At the time of writing, no final design is made yet for the culverts in the case study, but some dimensions have been proposed. The bottom of the culvert is being set at the bottom level of the inter-dike area (around -0.5 m+NAP), and the height is set at 2 m. Different widths for the culvert in the outer dike are being considered: 3.5 m, 6 m and 12 m. Since the culvert has not been designed yet, the parameters needed to calculate the flow contraction ( $c_D$ ,  $\alpha$  and  $n$ ) are set at default values. These parameters can be determined once a culvert is designed. A non-closure probability for the culvert in the case-study area of  $1.67 \cdot 10^{-4}$  per event was estimated using a score-table of aspects such as preparation, mobilisation, and closure-mechanisms within the guidelines set out by the Dutch national water authority Rijkswaterstaat (Casteleijn & Van Bree, 2017). Since the culvert will be part of a primary flood defence, it is assumed it will be designed and maintained to the strictest safety policies. For comparison, the famous, Maeslandt barrier in Rotterdam, the Netherlands, is only assumed to have a probability of non-closure of 1/100 per event (Bijl, 2006), primarily because it is more difficult to close a large barrier in case of a malfunction. A summary of the dimensions and parameters of the culvert are given in **Table 3.3**.

**Table 3.3** Parameters for calculating flow through the culvert

<b>Culvert</b>	
Probability of non-closure [-]	$1.67 \cdot 10^{-4}$
Bottom elevation [m+NAP]	-0.5
Height [m]	2
Width [m]	3.5, 6, or 12
Length [m]	42
Manning roughness coefficient [ $s \cdot m^{-1/3}$ ]	$6.00 \cdot 10^{-3}$
Energy-loss coefficient ( $c_D$ ) [-]	0.6
Additional energy loss coefficient ( $\alpha$ ) [-]	0.03
Flow directions	2
<b>Interdike area</b>	
Area [ $km^2$ ]	0.39
Elevation [m+NAP]	-0.5
Initial water level [m+NAP]	0.5

### 3.3.4.3. Coupling the models in a probabilistic routine

The probability distribution of the transformed hydraulic loads, in this case only the water level distribution of the interdike area, was evaluated in discrete water depths between 0.2 m to 7 m inside the interdike area. Both the combined erosion-overtopping dike model (section 3.3.4.1) and the culvert model (section 3.3.4.2) only accept discrete storm parameters as inputs, and produce the highest water level in the interdike zone for that event as output (see **Figure 3.6**). The probabilistic routines below iterate hydraulic conditions over these models and converge to the conditions with the highest probability of exceeding a discrete water depth. Because the probability of conditions with both significant overtopping and an open culvert were insignificantly small (in the order of  $10^{-9}$ ) and the erosion-overtopping model is computationally expensive, the interdike water level probability for each mechanism was calculated separately, opting to calculate more steps with the culvert model. The total probability of reaching a water level by each mechanism is calculated by adding the probabilities of exceedance of both mechanisms.



**Figure 3.6** The flow of information between the model inputs, the hydraulic loads (section 3.3.3), the creation of a synthetic storm event (Appendix B.2), the transmission functions for the culvert and first dike (section 3.3.4.1 and 3.3.4.2) and evaluation of the probability by a computational algorithm like FORM or importance sampling. The interdike water level probability for each mechanism was calculated separately as the joint probability of both significant overtopping and a non-closure was low, in the order of  $10^{-9}$ .

For each discrete water depth in the interdike area, first the probability of exceedance and the associated hydraulic conditions at the first dike were estimated with the first order reliability method (FORM) (Ditlevsen & Madsen, 2007). The FORM method starts from an initial design point and reduces the complex set of correlated probability distributions into approximately equivalent standard normal distributions ( $\mathbf{n}$ ) around this design point, e.g. with a Rosenblatt transformation. In the transformed n-space, the distance from the origin represents the likelihood of the conditions. To solve for the likeliest storm (i.e. conditions nearest to the origin in n-space) almost exceeding the limit state definition ( $h_{interdike} = h_i$ ), the Constrained Optimization BY Linear Approximations solver (Cobyla) was used (Powell, 1994), which uses successive linear approximations of the limit state to iterate towards the design point. Mathematically, FORM iteratively solves the optimisation problem:

$$P(h_{interdike} > h_i) = \Phi(-\min(|\mathbf{n}|)), \quad (3.3)$$

$$\text{Constrained by the limit state:} \quad T(\mathbf{S}) - h_{interdike,i} = 0$$

state:

Where:	$h_i$	=	Water level in the area between dikes for which the exceedance probability is being evaluated (m+NAP)
	$h_{interdike}$	=	Water level in the area between dikes (m+NAP)
	$T$	=	The water transfer model across the first dike, i.e. the overtopping and culvert flow
	$\mathbf{S}$	=	The set of correlated hydraulic load parameters
	$\mathbf{n}$	=	Set of independent standard normal distributions of equivalent probability around the design point in $\mathbf{S}$
	$\Phi$	=	Cumulative standard normal distribution

While FORM generally converges quickly to a solution, it cannot converge well around the sudden increase in overtopping when waves erode the crest of the first dike. A more accurate exceedance probability was obtained through

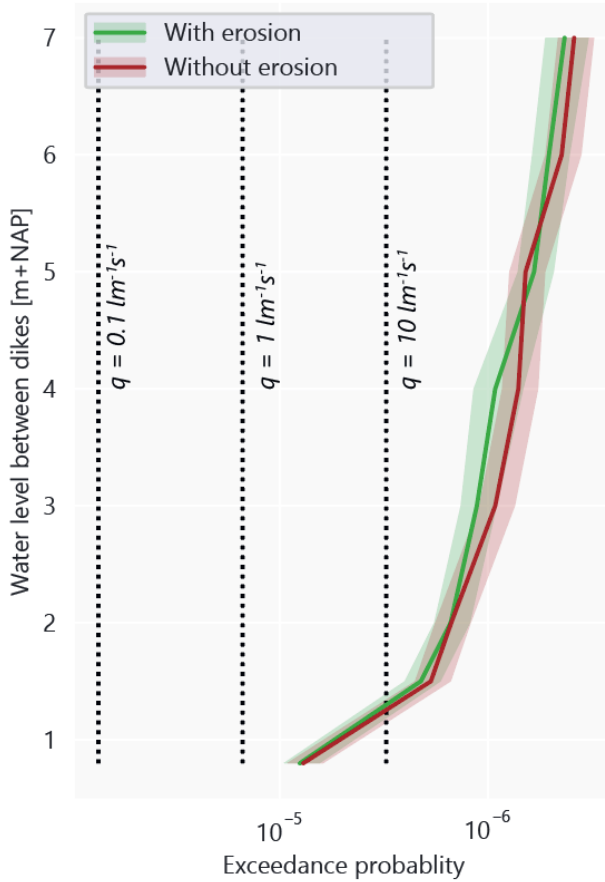
importance sampling (IS) (Robert & Casella, 1999) around the conditions returned by the FORM routine. The IS-routine sampled up to 3000 random storm events within one standard deviation of the design point in standard normal space to compute the probability of a storm causing a failure of the system. Both methods were performed with the open-source toolkit OpenTURNS (Baudin, Dutfoy, Iooss, & Popelin, 2015) in the Python programming language. Interpolating between the computed exceedance probabilities of the water depth behind the first dike gives the full cumulative probability distribution of water depths inside the inter dike area. This water level distribution ( $h_{interdike}$ ) is the distribution of hydraulic loads transformed by the dike ( $T(\mathbf{S})$ ) as defined in section 3.2.2.

## 3.4. Results

### 3.4.1. Overtopping of the first dike

The water level exceedance frequency in the interdike area due to overtopping and erosion of the first dike was obtained by the FORM-IS procedure (see section 3.3.4.3). The results are compared to calculations of the conventionally accepted overtopping limits for a single dike during the peak of a storm (0.1, 1, and 10  $\text{lm}^{-1}\text{s}^{-1}$ ) as well as the water level increase for a model where no erosion of the outer profile is included (see **Figure 3.7**). The conventional overtopping limits are conservative as they assume failure of the first dike immediately when the inner grass experiences this discharge, ignoring the time required for the dike to erode and form a breach.

For conditions with overtopping discharges up to 10  $\text{lm}^{-1}\text{s}^{-1}$  coupling erosion of the seaward slope with overtopping does not affect the expected water level in the interdike area as little erosion is expected from wave impact (see **Figure 3.7**). Following the Dutch design code the dikes in the region have a 1/3000 acceptable annual probability of flooding. Considering the length effect, which requires this dike segment to be split into 3 individual sections for overtopping, and a suggested 24% failure budget for overtopping and overflow, the dike cross-section of the case-study should be designed against an annual failure probability greater than 1/37,500 for overtopping and overflow (Rijkswaterstaat, 2016b). The probability of



3

**Figure 3.7** The probability of water levels in the interdike area due to overtopping alone (red) and the integrated erosion-overtopping model (green) with 95% confidence bands. The horizontal lines are drawn at the calculated exceedance probabilities for conventional overtopping limits of a single dike system of 0.1, 1, and 10  $\text{lm}^{-1}\text{s}^{-1}$ .

exceeding a moderate overtopping limit of 1  $\text{lm}^{-1}\text{s}^{-1}$  under present conditions was calculated at 1/66,200 per year, around the safety criterion as expected.

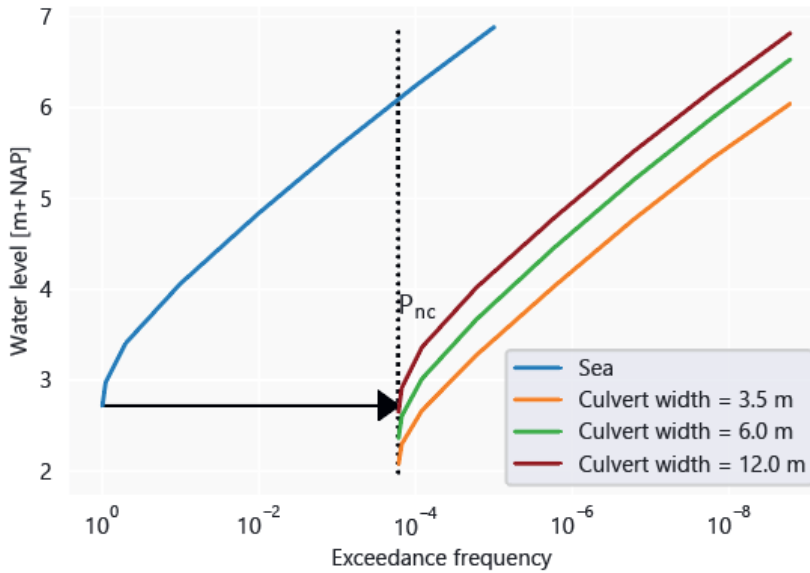
The storm resulting in a water level rising in the interdike area over 0.2 m by overtopping has a return period of 120,000 years, a storm surge of 6.8 m+NAP and a significant wave height up to 2.1 m. As storms grow further in intensity, the outer layer of clay and sand above the old clay core are eroded, resulting in a sudden increase in overtopping and overflow in the interdike area. Conditions where overtopping is enhanced by wave impact erosion can be expected roughly once in a 1,000,000 years. As a result, coupling wave impact erosion with overtopping increased the probability of interdike water levels of 3 and 4 m+NAP

(Figure 3.7). Under conditions with an expected interdiike water level above 5 m+NAP, overtopping appears very sensitive to tiny changes in storm conditions, such that even without erosion an increase in storm intensity is capable of filling up the interdiike area to sea-level. The calculated probabilities for interdiike water levels of 6 m+NAP and 7 m+NAP suggest the flooding probabilities for the coupled model remain generally higher than the model without wave impact erosion, although as the result at 5 m+NAP, shows, variance in the results of the FORM-IS procedure is too large to draw this conclusion. For a storm with an expected return period of approximately 2,300,000 years with a storm surge of 7.3 m+NAP and significant wave height of 2.5 m the dike can be assumed breached as the water level in the interdiike area rises to sea level during the storm event.

As conditions with significant overtopping are likely to erode the dike crest in this case-study, flood protection is only marginally improved by the ability of the second dike to retain water up to its crest level. It can be argued that no safety is gained as the amount of stored overtopping water in these cases would not be sufficient to cause a water level rise of 20 cm in the hinterland of Groningen anyway.

### 3.4.2. Effect of the culvert

The water level behind the first dike with an open culvert under a variety of conditions is presented in **Table 3.4**. There is a trade-off between introducing a tide in the interdiike area and exposing the second dike to high water levels during a storm due to the risk of failure of the culvert. With the smallest culvert (3.5 m wide) there is only 30 cm of tide during regular tides with a polder level at -0.5 m+NAP. During an extreme storm, the small size of the culvert prevents a fast increase in water level of the interdiike area in case of a non-closure. The water level in the interdiike area will be a substantially reduced (approximately 0.8 m less) compared to the outside water level (the extreme sea level). With the widest culvert (12 m) there is substantially more exchange of the tide, but only about 5 cm of reduction in the water level in the event of a non-closure. When accounting for the probability



**Figure 3.8** The frequency of water levels in the interdiike area due to a non-closure of the culvert with probability  $P_{NC}$

**Table 3.4** The variation in water level when the culvert remains open during different events. LW = low water, HW = high water, HHW = highest high water during a storm event.

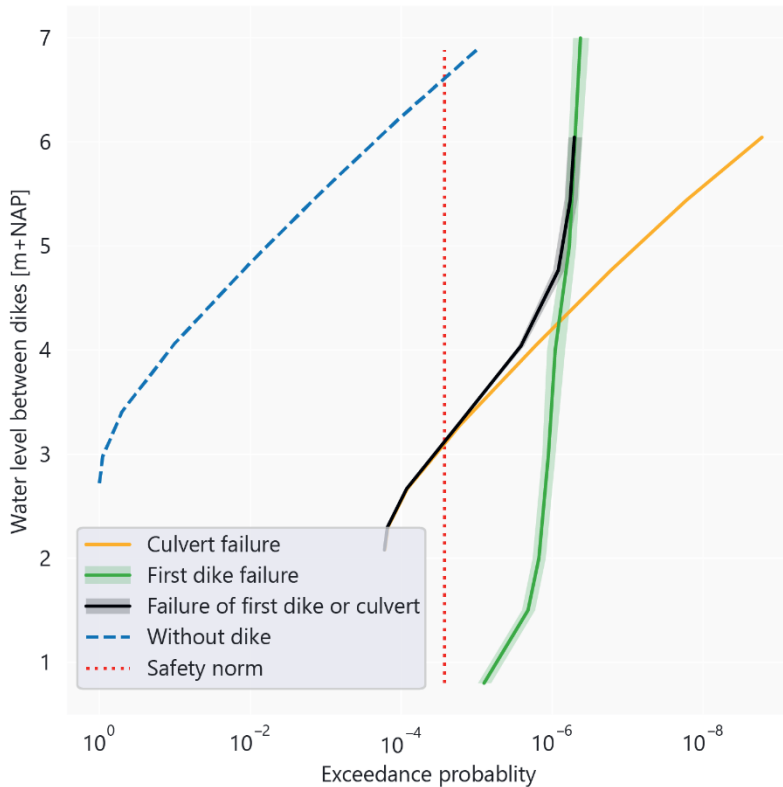
	Regular tide [m+NAP]	1/10 year storm [m+NAP]	1/1000 year storm [m+NAP]	1/100,000 year storm [m+NAP]
<b>At sea</b>	HW = 1.35 LW = -1.64	HHW = 4.06	HHW = 5.56	HHW = 6.88
<b>Culvert width = 3.5 m</b>	HW = 0.88 LW = 0.58	HHW = 3.28	HHW = 4.77	HHW = 6.04
<b>Culvert width = 6 m</b>	HW = 0.98 LW = 0.50	HHW = 3.67	HHW = 5.20	HHW = 6.53
<b>Culvert width = 12 m</b>	HW = 1.18 LW = 0.32	HHW = 4.02	HHW = 5.51	HHW = 6.81

of non-closure, the water level exceedance probabilities are obtained as shown in **Figure 3.8**.

### 3.4.3. Required height second dike

Without the second dike the failure probability would follow from the overtopping criteria used (**Figure 3.7**). With a second dike and no culvert, the probability of overflow of the second dike is the new failure criterion and it follows

from the amount of water overtopped by the first dike. An additional 1 m high second dike decreases the overtopping failure of the system to  $5.5 \cdot 10^{-6}$ . However, further heightening yields diminishing returns as can be seen by the steep green curve from the overtopping failure in **Figure 3.7** and **Figure 3.9**. Heightening the second dike to 2 m+NAP, 4 m+NAP and 6 m+NAP yields only  $1.51 \cdot 10^{-6}$ ,  $9.22 \cdot 10^{-7}$ , and  $5.1 \cdot 10^{-7}$  as the system failure probability respectively. Storm events causing overtopping are rare (**Figure 3.7**) and are drawn from the very tails of the probability distributions (**Table 3.2**) making more severe storms become exponentially less likely. Thus, heightening of the first dike several decimetres in a double dike system with a tall first dike (type I) is far more effective in reducing



**Figure 3.9** The exceedance probability of the water level in the interdike area due to a failure of the culvert or the first dike. The bands represent the 95% confidence interval of the FORM-IS procedure. The culvert width was 3.5 m for this plot. The safety norm for a dike section is  $1/37500$ .

the probability of a flood than heightening of the second dike. Still as mentioned in section 3.4.1, it can be argued that the stored volumes of overtopping would not yet constitute a flood for the hinterland according to the 20 cm water depth criterion and thus no actual flood was prevented.

The frequency of water levels inside the interdike area from a dike or culvert failure are presented in **Figure 3.9**. Because the probability of large overtopping volumes is already low, it is more likely the interdike area will be flooded due to a non-closure of the culvert.. To meet the regional safety norm the dike section of the case-study cannot have an annual failure probability greater than 1/37,500 for overtopping and overflow. As a consequence the second dike should be higher than 3.12 m+NAP with a 3.5m culvert, 3.5 m+NAP with a 6 m wide culvert, and 3.84 m+NAP with a 12 m wide culvert.

3

## 3.5. Discussion

### 3.5.1. Reliability of the results

The application of the framework for the case-study required coupling different models of interactions between hydraulic loads and dike failures. The hydraulic loads were simplified from the distributions returned by Hydra-NL, the official tool used to determine hydraulic boundaries for Dutch flood defences. According to Oosterlo, van der Meer, Hofland, and van Vledder (2018b) the SWAN wave model that is used to compute the wave heights in the hydraulic databases for Hydra-NL, predicts unusually high on-shore directed waves for the Ems-Dollard estuary and therefore requires validation of the complicated nature of wave refraction, wind-wave and wave-wave interactions in the estuary by measurements. Safety assessments are highly sensitive to the hydraulic boundary conditions (Vuik *et al.*, 2018b) and thus updating wave predictions can greatly affect the assessed safety. In the case-study of this paper, the risk from overtopping of the first dike could be smaller if the wave heights stored in the hydraulic database are overpredicted.

Next in the modelling chain are the interactions between the hydraulic loads and the dike itself. The applied models describing the process of wave erosion are empirical, and tuned with results from a limited number of flume experiments

performed over a few decades (Klein Breteler *et al.*, 2012a). Calibration of the formulas is limited by the tested experimental conditions, e.g. wave conditions, slope, and condition of the clay (Klein Breteler *et al.*, 2012a; Wolters *et al.*, 2013). While the formulas represent the most up-to date knowledge to describe the erosion process, they will be updated as more experiments are conducted. The EurOtop wave overtopping formulae have been derived similarly and have become standard models in the field as the number of experiments for verification has increased over the years (van der Meer *et al.*, 2016). Within the context of this study, however, the uncertainty in erosion parameters did not influence the expected failure of the double dike system due to the dominant effect of the culvert.

The probability of non-closure of the culvert proved to be the most influential parameter in our case-study. This probability followed from guideline based estimations of the probabilities of subfailures by Dutch experts (e.g. failing to predict a storm in time, failure to initiate a closure, failure to mobilize a mechanic, etc.) (Casteleijn & Van Bree, 2017). Assuming strict policies on preparation, detection, and mobilization for a culvert with multiple closure-mechanisms in a rural area, the probability of non-closure per event was estimated to be  $1.67 \cdot 10^{-4}$ . The actual probability will of course be determined by the design of the culvert and its operation scheme. Still, considering strict policies on the prediction of closure-events, mobilization, and operation were already presumed, designing a system with a non-closure probability within the same order of magnitude as dike overtopping ( $10^{-5}$  -  $10^{-6}$ ) will pose an engineering challenge.

### 3.5.2. Applicability of the framework

The proposed framework in section 3.2.1 to assess double dike systems was applied to the system between Eemshaven and Delfzijl. The framework itself is based on the probabilistic dike assessment methods already described in literature and applied in practice (Bischiniotis *et al.*, 2018; CUR/TAW, 1990; Schweckendiek, Vrouwenvelder, Calle, Kanning, & Jongejan, 2012; Slomp *et al.*, 2016; Vorogushyn *et al.*, 2010). As a result, the same data, probabilistic techniques, and failure criteria could be employed as in a regular dike assessment. However, the perspective of a dike transmitting hydraulic loads to another flood defence proved novel.

In the framework introduced in this study, a combination of dike erosion and water transmission models are needed to compute loads on the second dike. The coupling of wave erosion and overtopping by Kaste *et al.* (2015) is one of few methods in which erosion processes on the seaward side of the dike and flows over the dike are combined. More methods are being developed that combine other erosion processes with overtopping flows on the inner slope (Aguilar-López *et al.*, 2018a; van Bergeijk, Warmink, Frankena, & Hulscher, 2019), but these are still limited to the upper grass and soil layer. Advances in geotechnical models will allow models to quantify the probability of a breach forming, rather than an initial sliding failure (Remmerswaal, Hicks, & Vardon, 2018). Ideally, erosion of the dike by all failure mechanisms is calculated such that subsequent flows and waves can be evaluated. While such models are not yet available for most failure mechanisms, an integrated model of wave impact erosion combined with overtopping flows is already possible and this setup may serve as an example to integrate other failure mechanisms.

### 3.5.3. Comparison with other double dike systems

A direct comparison of the results from this case-study with other double dike systems is difficult, as flood risk and exposure varies greatly in different contexts. The case-study Eemshaven-Delfzijl represents only a small subset of possible double dike systems which 1) are adjacent to the coast, 2) have a higher first dike and lower second dike (type I in the classification of section 3.1.1), and 3) feature a culvert to accommodate a wetland, agriculture, and clay-mining simultaneously. The interpretation of the results from this study for general double dike systems is discussed below.

Studies so far have found only limited local flood protection benefits from inundating coastal interdike areas compared to benefits of such retention areas along rivers and within estuaries. Huguet, Bertin, and Arnaud (2018) found for a case study in La Faute-sur-mer, France, that water-level reductions are achieved for areas further inside the estuary rather than along the coast. As noted by Hofstede (2019) based on managed realignment in Schleswig-Holstein, Germany, the opened coastal polders have no significance as flood retention areas and thus do not contribute to improving flood protection. If the total length of defences increases,

flood protection is even diminished. In contrast, double dike systems along rivers and inside estuaries (in this context called Flood Retention Areas (FRAs), or buffer zones in other studies) remove water from a confined system and thus reduce the water level at the site as well as downstream, thereby reducing flood risk. Combined with the benefits of wetland restoration, such estuarine retention areas can be implemented as an eco-system based flood protection (Temmerman *et al.*, 2013). Interventions from the Sigmaplan in Belgium, and Room for the River in the Netherlands for example, achieve flood risk reduction mainly from this principle. Additionally, coastal flood protection is subject to higher wave loads than in river settings. Consequently, wave-related failures were considered in this study while for river dikes other failure mechanisms related to a prolonged high water level and water pressure are more likely to be dominant (e.g. piping or macrostability). Flooding of the interdike area can reduce the water level in rivers and estuaries and thus reduce the probability of such failures for both defences in the double dike system. Wave action at the outer defence remains unaffected by flooding of the interdike area in a coastal setting, hence the risks of wave related failures is only reduced for the landward defence of the system. Thus, protection benefits of a double dike system are expected to be higher along rivers and within estuaries compared to the results of the case from study.

The first dike in the double dike of Eemshaven-Delfzijl is taller than the second dike and is an example of a type I system within the classification of double dike systems in section 3.1.1. The safety assessment changes with a low first dike and tall second dike (types II and III). For these types, flooding of the interdike area due to overflow of the low first dike will not risk overflowing the tall second dike. However, wave loads propagating over the low first dike towards the second dike when the interdike area is flooded can no longer be ignored. Within a type III system (a low first dike and high second dike) the first dike acts as a low-crested breakwater, reducing the wave load on the second dike when the interdike area is flooded. The behaviour of these types of structures has already been extensively studied and can realize substantial wave height reductions (d'Angremond *et al.*, 1997; Mai *et al.*, 1999). Because wave action inside the interdike area was insignificant for a type I system, the results do not generalise to type III systems. In river areas where wave loads are insignificant similar results for interdike loads as

presented in **Figure 3.9** can still be expected from a type III system. In type IV and V systems (low embankment and breached first dike) the first dike cannot prevent a flood. Water is not retained by the first dike and only wave and water level attenuation effects can be expected in these systems. Rather than an erosion-overtopping model used in this study, a hydrodynamic wave and flow model is needed to assess the loads propagating towards the second dike in these systems (Kiesel *et al.*, 2020). These examples show that the selection of models needed in the transmission step of the framework greatly depends on the type of system and its context.

The different uses of the interdike area may require a regulated exchange of water through the first dike and pose limits to the acceptable frequency of flooding in the interdike area. As the results show, the probability of flooding of the interdike area by storms in the case in Eemshaven-Delfzijl is small and therefore multifunctional use criteria are hardly relevant. However, there is a trade-off between functions through the configuration of the culvert as designing the culvert for a greater tidal exchange to support multifunctional use of the interdike zone will result in larger water levels (and thus flood risk) in case of a non-closure. Across different documented double dike projects, balancing uses proved to be a design challenge. At the nature restoration site polder Breebaart nearby our case-study, a tide of 27 cm was introduced in the polder through a small culvert in the first dike (Peletier *et al.*, 2004). While a new marsh successfully developed, due to the high turbidity of the Ems-estuary, an average of 30 cm of sediment was deposited annually prompting an unexpectedly rapid succession of vegetation types and habitats (Peletier *et al.*, 2004). As a result, 70,000 m<sup>3</sup> of sediment was eventually dredged in 2019 to restore the diversity of habitats within the marsh (H2O, 2019). Another double dike system where flood protection is combined with functions requiring a tidal exchange is in the dunes of Waterdunen, the Netherlands. The in- and outflow of the tide has to be regulated to allow enough tidal variation for nature development, recreation, and experimental saline agriculture, while preventing overflow of the inner ring dike (Stark, Ravenstijn, Korf, & Walraven, 2006). At the time of writing the project is exploring options for a sufficiently safe operation scheme of the culverts each tidal cycle, while meeting the new strict Dutch flood protection standards. The Controlled Reduced Tide

(CRT) areas of the Belgian Sigmaplan in Kruibeke, Lippenbroek, and Bergenmeersen Belgium, are another example. The combination of several culverts preserves the dynamic tidal variation needed to support a marsh habitat similar to natural marshes outside the dike, while minimising sedimentation that reduces the water storage capacity of the area over time (Cox *et al.*, 2006; Oosterlee, Cox, Temmerman, & Meire, 2019). Nevertheless, the ability to reduce water levels in the Scheldt River by flooding the interdike area during a high-water event was a crucial factor in the design of the in/outlet structures (Cox *et al.*, 2006; Smolders *et al.*, 2020). Given the importance of culverts for both flood protection and multifunctional use, the limitations and synergies between functions imposed on a culvert design should be explored further in detail.

#### 3.5.4. Values beside flood protection

As can be seen in the results of our case-study, double dikes are not necessarily safer than a single dike. Still, the long-term benefits and value generated by its multifunctionality are a strong driver to choose a double dike system over a simple reinforcement. As long as the additional costs of a second dike over a simple reinforcement are outweighed by the costs saved on reinforcing the first dike and the value generated over time in the interdike area, a double dike system is even economically preferable. Economic benefits include specialised saline agriculture, or clay extraction (Kwakernaak *et al.*, 2015). Benefits in a double dike system do not have to be strictly monetary to be viable however. Nature restoration can be another driver for the implementation of such a system, as is the case for many managed realignment projects (Esteves, 2014). Ecosystem service benefits like carbon sequestration, water purification, sediment accretion, as well as natural values, may outweigh the costs of realignment, or in this case a double dike system, after several decades (Luisetti *et al.*, 2011; Turner, Burgess, Hadley, Coombes, & Jackson, 2007). To summarise, double dike systems in the coastal zone are primarily implemented for the potential use of the inter-dike zone, e.g. for nature restoration, rather than as a pure flood protection measure.

### 3.6. Conclusions

Double dike systems have been constructed to manage and control water for different uses as well as providing flood protection for the hinterland. Despite the benefits of combining flood protection with other uses in a double dike system, it was still uncertain how much flood protection is provided by a second dike in the system. The double dike between Eemshaven and Delfzijl was analysed as a case-study to demonstrate a general method for assessing the safety of double dike systems. The probability of failure was assessed using an advanced dike erosion model of the seaward slope (Rongen *et al.*, 2018) coupled with overtopping for 3000 simulated storm events for the area.

The novel general framework for assessing double dike systems developed in this study is based on the same safety principles for flood protection assessment as current practises. However, the distinction and integration needed within the framework between dike failures describing erosion of the dike, and those describing the transfer of water over the dike proved novel and is not present in most failure criteria for dike assessments. This part could only be achieved by a specialised erosion-overtopping model that is still being developed at the time of writing. For the framework to be implemented for other types of failures, integrated models describing both erosion of the dike and the transfer of water during the process of dike failure are needed.

According to the model results, the taller front dike in the case-study area is already unlikely to be overtopped by large volumes of water. Wave conditions during high overtopping events are also likely to erode the dike and rapidly fill the interdike area. Because of its low crest height, the second dike overflows in this scenario and does not reduce the probability of flooding, although it may delay the onset of flooding of the hinterland. Instead of overtopping or breaching of the front dike, water depths up to about 4 m between the dikes are far more likely to be reached from a non-closure of the culvert that connects the inner area with the sea. Thus, the second dike is required to reduce the risks related to the culvert rather than any dike failure. No (significant) reduction in flood risk can be expected from coastal double dike systems in general when the first seaward dike is taller than the second landward dike. The flood risk reduction in other types of double dike

systems depends on potential water-level reductions in estuarine or riverine settings as well as the different dominant failure mechanisms. Further research into the safety of double dikes in these environments is needed to further validate the framework developed in this study.

An interesting trade-off between flood protection and tide within the interdiike area was found. As the culvert width increases, a greater tidal variation can be realised between the dikes to support a functioning tidal ecosystem and clay-mining. However, in the event of a non-closure more water will flood the area between the dikes, thus requiring a higher second dike to prevent flooding. Similar trade-offs between functions through the design of the culverts were found in other double dike projects.

Results of this study show there is not necessarily a substantial flood risk reduction by implementing a double dike system over a single dike system. The value of these systems lies mostly in the integration of other functions, e.g. saline agriculture or nature restoration, rather than as the simplest improvement for flood protection. The framework of this study gives engineers and designers a tool to expand the number of uses around flood protection in a double dike system, while ensuring flood protection safety norms are met.

### **Acknowledgements**

We would like to thank Kees de Jong, Jan Willem Nieuwenhuis and Marco Veendorp from waterboard Noorderzijlvest, whose collaboration and insights made this research possible. A special thanks goes out to Guus Rongen and Joost Stenfert from HKV, who shared the dike erosion-overtopping model for use in this study and provided us with the tools to run the simulations. We would further like to thank Mark Klein Breteler from Deltares for sharing his expertise on the assessment of clay dikes. Finally we thank the two anonymous reviewers who considerably helped to improve the manuscript with their comments.

### **Appendices**

Appendices to this chapter can be found starting from page 209.

# 4

## How natural processes contribute to flood protection - a sustainable adaptation scheme for a wide green dike

R.J.C. Marijnissen, P. Esselink, M. Kok, C. Kroeze, J.M. van Loon-Steensma

This chapter was published as:

Marijnissen, R.J.C., Esselink, P., Kok, M., Kroeze, C., & van Loon-Steensma, J.M. (2020). How natural processes contribute to flood protection-A sustainable adaptation scheme for a wide green dike. *Science of the Total Environment*, 739, 139698. <https://doi.org/10.1016/j.scitotenv.2020.139698>



## Abstract

Effective adaptation to sea-level rise is critical for future flood protection. Nature-based solutions including salt marshes have been proposed to naturally enhance coastal infrastructure. A gently sloping grass-covered dike (i.e. Wide Green Dike) can be strengthened with clay accumulating locally in the salt marsh. This study explores the feasibility of extracting salt-marsh sediment for dike reinforcement as a climate adaptation strategy in several sea-level rise scenarios, using the Wide Green Dike in the Dutch part of the Ems-Dollard estuary as a case study. A 0-D sedimentation model was combined with a wave propagation model, and probabilistic models for wave impact and wave overtopping. This model system was used to determine the area of borrow pits required to supply clay for adequate dikes under different sea-level rise scenarios.

For medium to high sea-level rise scenarios (>102 cm by 2100) thickening of the clay layer on the dike is required to compensate for the larger waves resulting from insufficient marsh accretion. The model results indicate that for our case study roughly 9.4 ha of borrow pit is sufficient to supply clay for 1 km of dike reinforcement until 2100. The simulated borrow pits are refilled within 22 simulation years on average, and infilling is projected to accelerate with sea-level rise and pit depth. This study highlights the potential of salt marshes as an asset for adapting flood defences in the future.

## 4.1. Introduction

Coastlines are expected to become increasingly vulnerable to flooding from a combination of rising sea-levels due to climate change and economic growth (Neumann, Vafeidis, Zimmermann, & Nicholls, 2015; Nicholls, 2004). Accelerated sea-level rise from future ice-loss in the Antarctic, among other factors, considerably raises the sea-level projection for the end of the 21st century (DeConto & Pollard, 2016). The large range in future sea-level rise predictions has prompted the search for robust yet flexible adaptation options for the world's vulnerable delta regions (Hallegatte, 2009). Many studies (Borsje *et al.*, 2011; Möller *et al.*, 2014; Temmerman *et al.*, 2013; van Loon-Steensma, 2015; van Loon-Steensma *et al.*, 2016; Vuik *et al.*, 2018b) stress the capacity and importance of specific coastal ecosystems such as salt marshes and mangroves to dampen wave action and preserving foreshores. Incorporating these systems into coastal management could reduce the need for more costly flood protection measures in the future. As a result, nature-based flood-protection measures have emerged as a potential adaptation option.

The tendency of coastal wetlands to accumulate sediment provides an avenue for incorporating them in flood protection strategies. In natural salt marshes, the vegetation decelerates tidal currents by exerting friction which allows suspended sediment to accumulate on the marsh platform (Bouma *et al.*, 2005) (Christiansen, Wiberg, & Milligan, 2000; Leonard & Croft, 2006). Furthermore, roots bind the marsh bed and reduce erosion during storm conditions. Provided there is a sufficient supply of sediment, a marsh accumulates fine sediment based on the sea-level, the tide, compaction and subsidence processes, organic deposition, and wave action (Allen, 2000b; Davidson-Arnott, van Proosdij, Ollerhead, & Schostak, 2002).

The rising of the marsh platform by sediment accumulating within the marsh has the benefit of reducing the load on flood protection infrastructure (Vuik *et al.*, 2019). Another benefit of sedimentation of salt marshes for flood protection is to supply clay as building material for dike reinforcement, as was done historically. Within the German sector of the Wadden Sea, pits have already been excavated for dike reconstruction and to rejuvenate marsh from a late stage of succession. At Petersgroden in 1998 approximately 150,000 m<sup>3</sup> of clay was extracted from a 300 ×

330 m (10 ha) pit with a depth of 1.2 to 1.5 m. Initially the infilling rate was 15 cm/yr in the first years and decelerated to 4 cm/yr by 2007 (Bartholomä *et al.*, 2013). More recently in 2012 at Elisabethaußengroden 325,000 m<sup>3</sup> of clay was excavated across four pits to cover roughly 1/3 of the clay demand for reinforcing a 27-km long dike section (Menke, 2015). Infilling of the pit, and accretion of marshes in general, relies on inundation by sediment-laden water from the sea. As the bottom elevation of the pit increases, it becomes increasingly reliant on spring- and storm tides to supply additional sediment and the thus the infilling rate decelerates (Bartholomä *et al.*, 2013). From experience pits are refilled within 30 years after excavation (Arens, 2002; Bartholomä *et al.*, 2013).

While sedimentation within marshes can be an asset in flood protection it is yet unclear how future sea-level rise can affect such a strategy in the long term. Both the historic and foreseen response of marshes to sea-level rise has been extensively studied. Many marshes are expected to drown within this century as these will not be able to accrete fast enough to keep pace with sea-level rise (Best *et al.*, 2018; Crosby *et al.*, 2016; Kirwan *et al.*, 2010; Schuerch *et al.*, 2018). The response of borrowing pits within them has, however, not been studied so far. Therefore, the effectiveness of incorporating borrowing pits for dike-building material as a measure for sea-level rise adaptation is still unknown.

This study explores the feasibility of extracting sediment for dike reinforcements from the fringing salt marshes as a climate adaptation strategy in several sea-level rise scenarios, using the Wide Green Dike in the Dutch sector of the Dollard bay in the Ems estuary as a case study. To sustain adaptation of the flood defence by natural sedimentation of the marsh under sea-level rise, two conditions need to be satisfied: the borrow pit will refill to the marsh's level and the dike meets the national flood protection standard. This study explores 1) the feasibility and 2) sustainability of extracting salt marsh sediment for dike reinforcements as a climate adaptation strategy in several sea-level rise scenarios. A 0-D sedimentation model was combined with a wave propagation model, and probabilistic models for wave impact and wave overtopping. This model system was used to determine the dimensions of adequate dikes and borrow pit dimensions under different sea-level rise scenarios.

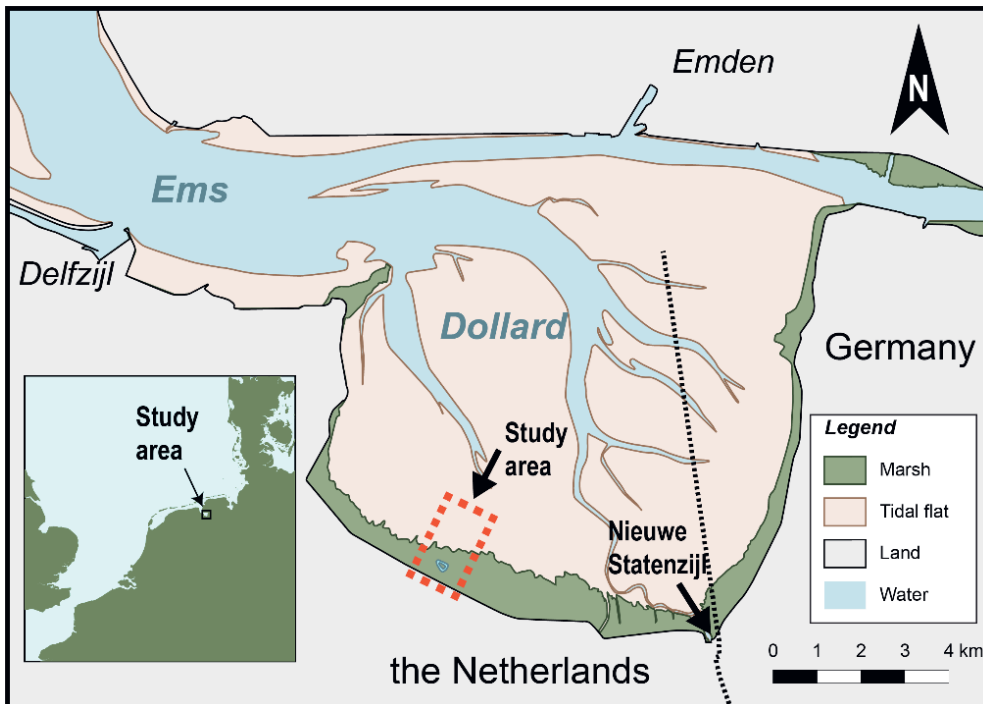
## 4.2. The study area

### 4.2.1. History of the Dollard

The Dollard forms a bay of about 100 km<sup>2</sup> within the Ems estuary located on the Dutch-German border in the Wadden Sea (**Figure 4.1**). Around 80% of the Dollard consists of tidal flats on which approximately 1.1 km<sup>2</sup> of salt marsh is present. The Dollard has a mesotidal regime with a tidal range of 3.3 m and a mean high tide of 1.55 m + NAP (Dutch Ordnance Level).

The bay developed during the Middle Ages and reached its greatest extent in the 16th century after a series of storm surges (Esselink, 2000). Further transgressions were halted by improved management of the dikes. Land was reclaimed from the sea by repeatedly embanking the emerging marshes on the fringes of the diked estuary. The last reclamation was completed in 1924 (Esselink, 2000). In the Dollard, engineering measures to promote salt-marsh development were initiated as early as the 17th century. This was achieved by the construction

4



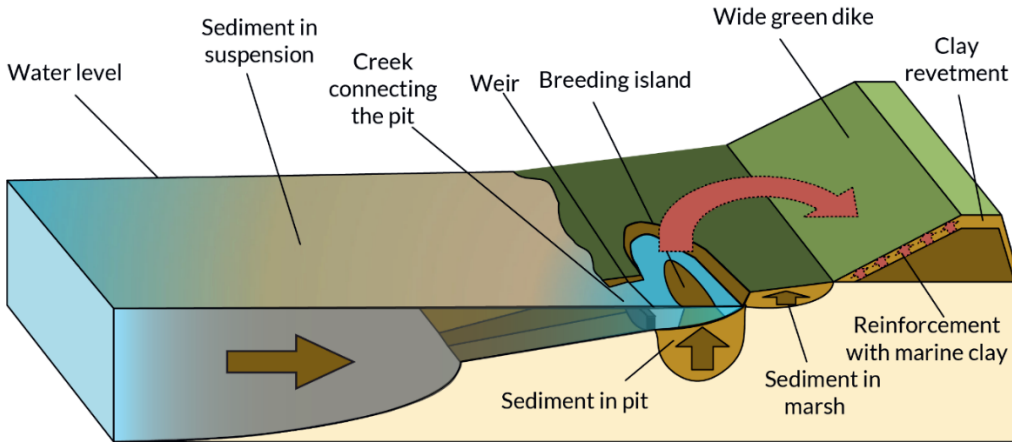
**Figure 4.1** Location of the study area where the pilot study for clay mining is being conducted within the Ems-Dollard estuary

and upkeep of a pattern of low clay-built groynes and a dense drainage network. These works were acquired and expanded by the Provincial Government in 1938 but were discontinued 15 years later. The majority of the present-day salt marshes date back to this period (1938–1953) (Esselink, 1998). The historic loss of intertidal area for the deposition of sediment, among others through deepening of the estuary for navigation and ongoing morphological processes, has been linked to an increasingly high turbidity in the estuary today (van Maren, Oost, Wang, & Vos, 2016) which inhibits the primary production of the local marine ecosystem (DeGroot & de Jonge, 1990).

#### 4.2.2. The Wide Green Dike pilot

Dikes along the Dutch Dollard coast were designed for an acceptable annual failure probability of 1/3000. In the last dike assessment only 20% of the Dollard dikes met the safety standard (van Loon-Steensma & Schelfhout, 2017). The current dikes feature a crest height between 7.7 and 9.3 m + NAP a lower section of the seaward slope at an angle of 1:4 and an upper section at an angle of 1:7. The lower section of the slope is reinforced with asphalt and stones against wave impacts while the remaining upper section consists of grass (van Loon-Steensma & Schelfhout, 2017).

The Province of Groningen aims to remove 1 million ton of sediment from the estuary annually to reduce the high turbidity in the estuary to acceptable levels (Provincie Groningen & Ministerie van Infrastructuur en Milieu, 2018). A so-called “Wide Green Dike” has emerged as an option to reinforce the dikes while reducing turbidity within the estuary. As a pilot 1 km of dike will be reinforced with marine clay extracted locally from the salt marsh (Hunze en Aa's, 2020). The resulting borrow pit will function as a sink for new sediment while the excavated clay is processed for dike reinforcement. The dike will feature a shallow (1:7) grass outer slope along the entire seaward side to withstand the impact of large waves rather than a conventional stone or asphalt revetment. Furthermore, it simplifies future reinforcements with the excavated clay (van Loon-Steensma & Schelfhout, 2013, 2017).



**Figure 4.2** A schematic cross-section of the wide green dike system and its components

The borrow pit will extract sediment from the water by a similar process as the marsh. Water carrying sediment in suspension is transported landward during flood tide. Within the marsh and pit the flow of water is decelerated allowing the suspended sediment to settle. Because of its depth the pit will experience more regular inundations of sediment-laden water than the marsh through a creek leading into it, thereby capturing more suspended sediment from the estuary over time until the pit is filled.

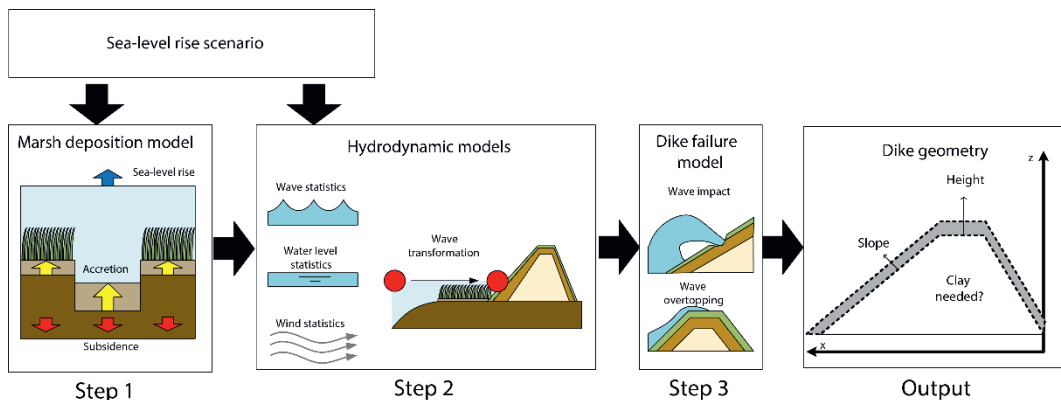
At the time of writing a pilot project of the Wide Green Dike is being conducted in the Dollard (see **Figure 4.2**) (Hunze en Aa's, 2020). In the spring of 2018 45,000 m<sup>3</sup> of clay was excavated from a 4 ha borrow pit with an average depth of 1.6 m (Esselink, Elschot, Tolman, & Veenstra, 2019). The pit is connected to the tidal creek through a weir (of 0.9 m + NAP) which impedes the in- and outflow. At the centre of the pit an elevated section of marsh remains to serve as a breeding island for birds. The excavated clay is being processed to be used as dike clay. Meanwhile the infilling of the borrow pit and ecological impacts are being monitored.

## 4.3. Methods

### 4.3.1. Modelling approach

To assess the feasibility of a wide green dike system under sea-level rise, both the clay required for dike reinforcement and the future clay yield from the pit need to be predicted. We do this in three modelling steps in which we quantify: 1) on the foreshore the accretion of both the marsh and the pit over time, 2) the change in storm conditions over time, 3) the failure probability of a dike design subjected to those storm conditions (see **Figure 4.3**) as assessed with the official Dutch dike assessment tools. The final step is repeated for different dike designs to find the design that requires the lowest amount of clay.

In the first step the vertical marsh growth and infilling of the borrow pit in response to different sea-level rise scenarios is modelled by a 0D numerical deposition model which has been used in many other studies (Allen, 1990; French, 1993; Krone, 1987; Temmerman, Govers, Meire, & Wartel, 2003). The simplicity and speed of the 0D model allows for uncertainties to be quantified by varying the initial elevation and sediment properties in a Monte Carlo fashion (5000 simulations per sea-level rise scenario) (see Section 4.3.3, **Table 4.2** and Appendix C.1 for details). In the second step wave, wind and water level conditions of the



**Figure 4.3** the modelling approach followed in this study starting from a sea-level rise scenario towards computing the optimal dike by 2100. Step 1: determine the accumulation of sediment in the marsh, step 2: determine the storm conditions across the marsh at the dike toe, step 3: determine the probability of failure of different dike designs and return the design with the lowest clay demand as output.

Ems-Dollard estuary from a database developed for Dutch dike assessments (Rijkswaterstaat, 2018) were run across the accreted foreshore predicted by the deposition model in step 1 until the dike toe with the SWAN wave model (Booij, Ris, & Holthuijsen, 1999). The Hydra-NL model (Duits & Kuijper, 2018) is used to compute the associated probability of the storm events to which correlated probability distributions were fitted. In the third step the wave and water level distributions are used to evaluate the probability of failure of different dike configurations by overtopping (van der Meer *et al.*, 2016) and failure of the outer slope by wave action (Kaste *et al.*, 2015; Klerk & Jongejan, 2016; Mourik, 2015). The optimal dike configuration requires the least amount of clay to achieve the required safety level without a hard revetment. With the results of the borrow pit simulations in the first modelling step the area of pit required for 1 km of dike reinforcement is computed.

4

#### 4.3.2. Sea-level rise scenarios

For this study the RCP and KNMI sea-level rise scenarios for the Dutch coast as presented by Haasnoot *et al.* (2018) were selected as a starting point (**Table 4.1**). The RCP scenarios from the IPCC were adapted by Haasnoot *et al.* (2018) from Le Bars, Drijfhout, and de Vries (2017). Dutch flood protection measures, however, were designed based on the delta scenarios that were developed in 2014 by the

Royal Dutch Meteorological Institute (KNMI) (Bruggeman *et al.*, 2013; Bruggeman *et al.*, 2016; KNMI, 2014). The KNMI concluded that: *“observations show decadal-scale variations, but no long-term trend over the past 130+ years. Results from recent state-of-the-art climate models as well as RCM studies suggest no changes in the wind climate [for the Netherlands]. This is true for mean wind conditions, low wind conditions and extreme wind speeds. Modelled changes are statistically insignificant.”* (KNMI, 2014, p. 69). The KNMI based this conclusion on analyses by de Winter, Sterl, and Ruessink (2013) and Sterl, van den Brink, de Vries, Haarsma, and van Meijgaard (2009). Therefore, we decided to follow the KNMI's assessment that there will be no (significant) effects of climate change on storm statistics in our study area.

**Table 4.1** Sea-level rise scenarios for 2050 and 2100 (in cm difference from 2018) adjusted for the Dutch coast by Haasnoot *et al.* (2018), using the KNMI'14 Delta scenarios and RCP scenarios. Values are adjusted by 6 cm for sea-level rise at the Dutch coast between 1995 and 2018 following Baart *et al.* (2019). The low (L), 50% medium (M), and 50% high (H) scenarios used in this study are highlighted in green, yellow, and red respectively.

Scenario	KNMI'14 D/R	KNMI'14 W/S	RCP 4.5			RCP 8.5		
Margin	-	-	5%	50%	95%	5%	50%	95%
This study	L			M			H	
2050	+ 9 cm	+ 34 cm	+ 1 cm	+ 18 cm	+ 35 cm	+ 3 cm	+ 23 cm	+ 41 cm
2100	+ 29 cm	+ 94 cm	+ 23 cm	+ 102 cm	+ 186 cm	+ 69 cm	+ 189 cm	+ 311 cm

The KNMI'14 scenarios do not yet account for recent findings on accelerated ice-loss (DeConto & Pollard, 2016; Haasnoot *et al.*, 2018). No statistically significant acceleration of sea-level rise has been detected yet at stations along the Dutch coast, as the acceleration of sea-level rise accounts for just 0.1% of the variance in observed mean annual water levels (Baart *et al.*, 2019). For this study the KNMI'14 D/R, the median of RCP 4.5, and median of RCP 8.5 scenarios were selected as a low (L), medium (M), and high (H) sea-level rise scenario for 2100. This allows for a range of possible climate change scenarios to be explored (Table 4.1).

### 4.3.3. Marsh deposition model

As the first step, sediment deposition within the marsh is modelled (see Figure 4.3). In this study a basic marsh elevation model similar to various other studies (Allen, 1990; French, 1993; Krone, 1987; Temmerman *et al.*, 2003) was used. It simulates a single idealised point within the marsh. Each tide when the water rises suspended sediment is transported to this point. The suspended sediment sinks towards the bottom and thus raises the elevation of this point over time. It is assumed that vegetation reduces the flow velocity such that all suspended sediment is able to sink without resuspension by turbulence. Furthermore it is assumed that the vegetation reduces wave energy and flows sufficiently to prevent settled sediment from eroding. The approach was first described by Krone (1987) and uses a mass balance as follows:

$$\frac{dz}{dt} = \frac{dS_{min}}{dt} + \frac{dS_{org}}{dt} - \frac{dP}{dt}, \quad (4.1)$$

Where  $z$  is the surface elevation,  $S_{min}$  is the mineral sediment deposition,  $S_{org}$  is the organic deposition and  $P$  is a subsidence term. Organic deposition was omitted in this study as samples from the marsh area contained only a low percentage of organic content (8%) indicating low organic deposition (see Appendix C.1).

Sediment is deposited when suspended sediment carried by the incoming tide settles within the marsh. The process is described by the equations:

$$(h - z) \frac{dC}{dt} = \begin{cases} -w_s C(t) + C_{flood} * \frac{dh}{dt} & \frac{dh}{dt} > 0 \\ -w_s C(t) + C(t) * \frac{dh}{dt} & \frac{dh}{dt} \leq 0 \end{cases} \quad (4.2)$$

$$\frac{dS_{min}}{dt} = \frac{w_s C(t)}{\rho_{sed}} \quad (4.3)$$

Where  $h$  is the water level,  $w_s$  is the sediment fall velocity,  $C_{flood}$  is the suspended sediment concentration (SSC) during flood tide,  $C(t)$  is the SSC at time  $t$ , and  $\rho_{sed}$  is the bulk dry density (BDD) of the deposited sediment layer.

Expanding on the approach by Temmerman *et al.* (2003), the expected deposition during a tidal period was modelled from the distribution of high waters and extrapolated to an annual deposition. However, to include the effect of storm surges lasting multiple cycles, the expected deposition of two tidal cycles rather than one cycle was determined in this study using a basic storm surge schematisation model for the Dutch coast (see Appendix C.2). We assumed no variation in SSC between storm events.

Modelling the behaviour of the borrow pit required a few additions. In order to keep water around the breeding island at low tide, a small weir was constructed in the creek draining the pit (**Figure 4.2**). A formula was calibrated from measurements within the pit to incorporate the effect of the weir on the water level (see Appendix C.2). Compaction of sediment deposited within the pit was included using a variation of the formula proposed by Allen (2000a) which was calibrated with soil samples of the Dollard marsh (see Appendix C.1, Appendix C.4).

The model produces a time series of the elevation of both the marsh and the pit bed. For modelling purposes the pit is considered full when the bed elevation is within 5 cm of the marsh elevation as at this stage the difference in accretion rate between marsh and pit is no longer significant. At that point the pit is re-excavated

to a depth of 1.6 m below the marsh surface identical to the pit in the pilot study. Using this setup, the amount of sediment extracted per sea-level rise scenario from that single pit is stored as a time series.

Because of uncertainty associated with multiple variables ( $\rho_{sed}$ ,  $w_s$ , and the initial marsh elevation  $z_0$ , see Section 4.2.2), a Monte Carlo approach was needed to quantify the uncertainty in accretion. The marsh deposition model was run 5000 times for each scenario, sampling randomly from the probability distributions of these variables. The median result as well as the 5 and 95 percentiles of the accretion time series were stored and passed to the next modelling steps.

#### 4.3.4. Modelling storm conditions

In step 2 the design conditions for the flood defence are determined (see **Figure 4.3**). Water-level, wave and wind statistics on the foreshore of the Dollard were retrieved from a hydraulic database of the Eastern Dutch Wadden sea (Rijkswaterstaat, 2018) and analysed in Hydra-NL (Duits & Kuijper, 2018). Hydra-NL is a programme made available by the Dutch authorities to derive hydraulic loads on flood defences across the country in compliance with the official assessments procedures (Rijkswaterstaat, 2016b). Across the Netherlands, official stations at representative locations measure water levels, wind speeds, and wind directions. Hydra-NL connects the statistical probability of the water level, wind direction, and wind speed derived from the stations, to a database of precomputed wave model simulations for the Wadden Sea area. For locations between stations values are found by interpolation. By doing so, the statistics of storm waves at the coastal defences are estimated. The correlation models employed by Hydra-NL are described in (Diermanse & Geerse, 2012). The effect of sea-level rise is simulated by raising the mean of the water level probability distribution accordingly (Duits & Kuijper, 2018).

A database from Rijkswaterstaat (2018) was selected which contains computed wave characteristics at the marsh foreshore in the eastern Dutch Wadden Sea under various combinations of water levels and wind conditions. This database was adapted to represent storm conditions at the dike toe per sea-level rise scenario. The widely used SWAN wave model (Booij *et al.*, 1999) was applied across

the salt-marsh profile until the dike toe for all entries in the database. SWAN uses an implicit numerical scheme to calculate the evolution of the wave spectrum across the foreshore as described by the spectral action balance equation:

$$\frac{\partial N}{\partial t} + \frac{\partial(c_{g,x}N)}{\partial x} + \frac{\partial(c_{g,y}N)}{\partial y} + \frac{\partial(c_{\sigma}N)}{\partial \sigma} + \frac{\partial(c_{\theta}N)}{\partial \theta} = S_{tot} \quad (4.4)$$

where  $N$  is the wave-action density, defined as spectrum energy density divided by the radian frequency,  $\sigma$  is the relative wave frequency. The first term describes the change in wave action over time, the second and third terms the propagation of wave action in space with velocity components  $c_{g,x}$  and  $c_{g,y}$ , the fourth term represents the shifting of the relative frequency due to depth change, and the fifth term represents depth-induced diffraction. The sum of sink and source terms ( $S_{tot}$ ) accounts for wave breaking, bottom friction, triad wave interactions, and the input of energy from the wind. The model requires an input of water level, wave spectrum properties (i.e. significant wave height, peak period, and wave direction) at the offshore boundary, an elevation profile towards the coast, and additional inputs to compute the processes included as source/sink terms (i.e. wind speed, wind direction, and bottom roughness)(Booij *et al.*, 1999).

To simplify the computations, only a 1D profile of the marsh was used in the SWAN calculation. In this step the elevation change of the salt marsh by sedimentation (see Section 4.3.3) is incorporated in the foreshore profile derived from the AHN2 elevation map (Rijkswaterstaat, 2014) to examine the effect of natural sedimentation of the foreshore on the wave exposure of the dike. The effect of the pit and wave damping by vegetation was not included. A worst-case inundated tidal flat (Manning roughness  $n = 0.02 \text{ m}^{-1/3} \text{ s}$ ) was assumed representative of winter-storm conditions. The off-shore wave boundary conditions and wind speed were retrieved from the original data of Rijkswaterstaat (2018). A new dataset of wave properties at the dike toe was created by running all entries of the original data in SWAN. The new dataset was passed to Hydra-NL to derive the statistics of wave properties at the dike. New simpler probability distributions and correlations of water level, wave height, wave period and wave direction were fitted on the outputs of Hydra-NL. For wave height and wave period a Weibull distribution was fitted, and for water level a generalized extreme

value distribution was fitted. Wave direction was simplified to an empirical distribution from the wind direction, where each bin of 30° in wind direction corresponds to a generated wave direction at the dike. The result is a set of correlated probability distributions describing the frequency of storm wave- and surge conditions at the dike toe for each sea-level rise scenario which is used to design the dike.

#### 4.3.5. Dike failure model

In step 3 the probability of failure for a range of dike designs is calculated (see **Figure 4.3**). The wide green dike must be dimensioned such that the probability of failure of the dike conforms to the Dutch national safety standard (WBI2017). For this study the focus is on the main failure mechanisms that determine the outer dike geometry: overtopping and failure of the revetment by wave erosion. It was previously determined that these failures dictate the outer slope, necessitating a “wide” dike if a “green” grass revetment were to be implemented (van Loon-Steensma & Schelfhout, 2013, 2017). The dike section of the Dollard has a maximum annual failure probability of 1/3000. The norm for a specific cross-section failing by overtopping or erosion of the grass revetment is calculated following the Dutch design guidelines (Rijkswaterstaat, 2016c) as:

$$P_{f,cross-section} = \frac{\omega}{N} P_{f,norm} \quad (4.5)$$

where the fraction of the norm failure probability ( $P_{f,norm}$ ) allocated to overtopping and erosion of the revetment is 29% ( $\omega = 0.29$ ) while the length factor ( $N$ ) of these mechanisms is recommended to be 3 (Rijkswaterstaat, 2017). The result is an allowed failure probability of a cross-section ( $P_{f,cross-section}$ ) of  $3.22 * 10^{-5} \text{ year}^{-1}$  or a minimum reliability index ( $\beta$ ) of 4.0. Whether a dike fails by a mechanism is expressed by a limit state function (LSF). In this study the formulas accepted within the Dutch safety regulations are applied for the mechanism of overtopping and wave impact. Overtopping is a type of failure of the dike where water from waves flows over the crest onto the inner slope eroding the dike in the process. The amount of overtopping was calculated by the method described in van der Meer *et al.* (2016) and TAW (2002). The limit state has been reached when the overtopping discharge ( $q$ ) exceeds the critical discharge the dike is able to resist ( $q_c$ ).

$$Z_{\text{overtopping}} = q_c - q \quad (4.6)$$

Erosion from wave impact on the outer slope was calculated according to the descriptions in Kaste *et al.* (2015), Klerk and Jongejan (2016), and Mourik (2015). The limit state function is reached when the duration of the storm ( $t_{\text{storm}}$ ) exceeds the amount of the time required to damage the grass ( $t_{\text{grass}}$ ), the root zone ( $t_{\text{root}}$ ) and erode the clay below ( $t_{\text{clay}}$ ). See Appendix C.5 for details on the calculation of each of these durations.

$$Z_{\text{wave impact}} = t_{\text{grass}} + t_{\text{root}} + t_{\text{clay}} - t_{\text{storm}} \quad (4.7)$$

The probability of failure for a dike design is determined by probabilistically evaluating the LSF's under the hydraulic boundary conditions and uncertainties with the first order reliability method (FORM) Low and Tang (2007):

$$\beta_{Z(\mathbf{x})=0} = \min \left( \sqrt{\mathbf{n}^T \mathbf{R}^{-1} \mathbf{n}} \right) \quad (4.8)$$

Here  $\beta$  is the reliability index,  $\mathbf{n}$  is the vector of the normalised stochastic input variables in  $\mathbf{x}$  and  $\mathbf{R}$  is the correlation matrix of the stochastic input variables. Vector  $\mathbf{x}$  contains the values of the hydraulic load such as water level and wave parameters, as well as stochastic variables related to modelling wave impact and overtopping (see Appendix C.5). A value of variable ( $x_i$ ) is normalised as:

$$n_i = \Phi^{-1}(F(x_i)) \quad (4.9)$$

Where  $F$  is the cumulative distribution function (CDF) for that variable and  $\Phi^{-1}$  is the inverse standard normal CDF. The routine was programmed in MATLAB and solved for the two LSF's ( $Z(\mathbf{x})=0$ ) with the built-in nonlinear solver called `fmincon`.

Since both overtopping and large wave impacts are dependent on storm conditions it is reasonable to assume both mechanisms are fully dependent. As a result, the reliability of the system is the minimum reliability of these mechanisms:

$$\beta_{\text{system}} = \min(\beta_{\text{overtopping}}, \beta_{\text{wave impact}}) \quad (4.10)$$

While the 1:7 outer slope was maintained, a range of crest height and clay thickness combinations were evaluated. The optimal outcome for each sea-level

rise scenario was determined as the combination where  $\beta_{system}$  matched the safety standard of 4 and the required amount of clay was lowest.

## **4.4. Trust in the model system**

### **4.4.1. Model selection**

The series of models described in Section 4.3.3, with the exception of the marsh deposition model, were all selected for their use in and compliance with the official Dutch dike assessment instruments (WBI2017). Both the SWAN and Hydra-NL model (including their precursors) have been used extensively in determining hydraulic loads along the Dutch coast (Rijkswaterstaat, 2016b; Slomp *et al.*, 2016). The applied overtopping and wave impact models are directly incorporated in the official Dutch dike assessment instruments or were developed specifically as an addition to these instruments (Rijkswaterstaat, 2016c). Given that these models were developed for Dutch systems already, no further validation or calibration of these models was conducted. By applying these specific models, this study will align as close as possible to the dike that would be built in practise, even if better and more advanced models are available.

Despite the fact that it is required to consider the foreshore for determining hydraulic loads on the dike (Rijkswaterstaat, 2016b), modelling the changes of the foreshore over time is not common in the Netherlands. As a result, a model had to be selected for this purpose. Highly advanced methods exist for predicting the accretion of marshes over time e.g. (Best *et al.*, 2018; Elmilady, van der Wegen, Roelvink, & Jaffe, 2019; Temmerman, de Vries, & Bouma, 2012), but would be computationally intensive for an exploratory study which is not focused specifically on marsh morphology. Instead a comparatively simple method employed extensively in sea-level rise studies (Allen, 1990; French, 1993; Krone, 1987; Temmerman *et al.*, 2003) was used that could be calibrated for the Dollard estuary with the first observations from the pilot. Owing to its relative simplicity, multiple combinations of parameter inputs could be quickly assessed making this approach better suited for the study.

#### 4.4.2. Implementation and evaluation of the marsh deposition model

For the implementation of the marsh deposition model suitable data of water level ( $h$ ), elevation ( $z$ ), sediment settling velocity ( $w_s$ ), sediment density ( $\rho$ ), and suspended sediment concentration in flood water ( $C_{flood}$ ) is needed (see section 4.3.3). For the water level ( $h$ ), a record of water levels from a local gauge at Nieuwe Statenzijl was retrieved from the water authority Rijkswaterstaat and the water level within the borrow pit has been monitored as part of the ongoing pilot. The elevation of the marsh ( $z$ ) was based on information from the national elevation database (Rijkswaterstaat, 2014) and checked with point measurements of the marsh taken just before implementation of the pilot (Esselink, Veenstra, Daniels, & Veenstra, 2018). Sediment characteristics on bulk dry density ( $\rho$ ) were derived from local soil investigations (Raadgevend Ingenieursbureau Wiertsema & Partners, 2016; Sweco Nederland B.V., 2018) and initial measurements (Esselink *et al.*, 2019) (see Appendix C.1). Sediment fall velocities ( $w_s$ ) and suspended sediment concentrations (SSC) ( $C_{flood}$ ) were retrieved from literature. Sediment settling velocities are reported to vary between 1 and 3 mm/s (Ridderinkhof, van der Ham, & van der Lee, 2000; van der Lee, 2000). There is a great variation in measured SSC in the estuary, differing between years, seasons, within spring-neap cycles and daily by weather conditions (Dankers, Binsbergen, Zegers, Laane, & van der Loeff, 1984; de Haas & Eisma, 1993; Dyer *et al.*, 2000; Kornman & de Deckere, 1998; Ridderinkhof *et al.*, 2000; Taal, Schmidt, Brinkman, Stolte, & Van Maren, 2015; van der Lee, 2000; van Maren *et al.*, 2016). To generalise the model across these different seasons and conditions, a representative value for SSC during the incoming tide had to be found by calibration.

An overview of all modelling parameters is presented in **Table 4.2**. Over the period 1984–2003 the average accretion rate within the marsh has been 8 mm/yr, though large variations exist across the marsh between 0 and 20 mm/yr (Esselink, 1998, 2007). The model was run for 1 year at elevations  $0.32 \pm 0.12$  m above mean high tide (MHT) with different values for the representative SSC ( $C_{flood}$ ). A representative SSC of  $0.19 \text{ kg/m}^3$  best reproduced these observations (**Figure 4.4**). To evaluate the performance of the same deposition model for the borrow pit the

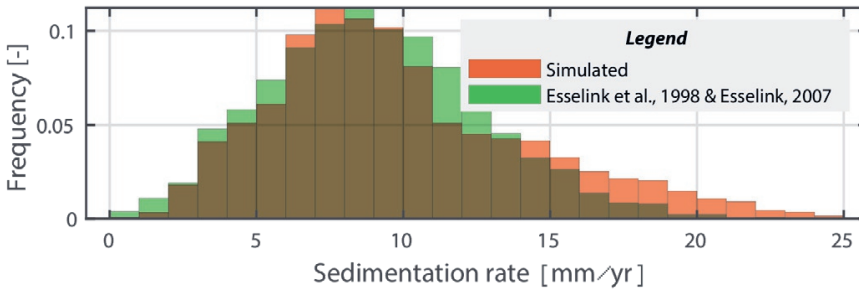
**Table 4.2** Inputs of the model. Probability distributions: deterministic (D), empirical (E), and normal (N).

	Value	Unit	Distribution	Source
<b>Water level</b>				
High water peak level	<i>From distribution</i>	m+NAP	E	Tide gauge at Nw. Statenzijl (Rijkswaterstaat)
Sea-level rise	<i>From scenario</i>	m	D	<i>See section 3.2</i>
<b>Weir in borrow pit:</b>				
Weir crest elevation	0.9	m+NAP	D	(Esselink <i>et al.</i> , 2019)
Weir flow resistance term	$R_{in} = 3.5$ $R_{out} = 2.7$ $R_{over} = 13.5$	m	D	Calibrated (See Appendix B)
<b>Elevation:</b>				
Initial marsh elevation	$\mu = 1.86$ $\sigma = 0.12$	m+NAP	N	Based on AHN2 (Rijkswaterstaat, 2014)
Initial bed elevation of the pit	0.41	m+NAP	D	Based on excavation depth of pit
Subsidence	2.6	mm/yr	D	(NCG, 2018)
<b>Sediment:</b>				
Representative sediment concentration during flood	0.19	kg/m <sup>3</sup>	D	Calibrated (This section)
Sediment settling velocity	$\mu=2.7$ $\sigma=1$	mm/s	N	(van der Lee, 2000)
Bulk dry density of deposited sediment	$\mu = 398$ $\sigma = 87$	kg/m <sup>3</sup>	N	See Appendix A
Bulk dry density within marsh	$\mu = 873$ $\sigma = 72$	kg/m <sup>3</sup>	N	See Appendix A

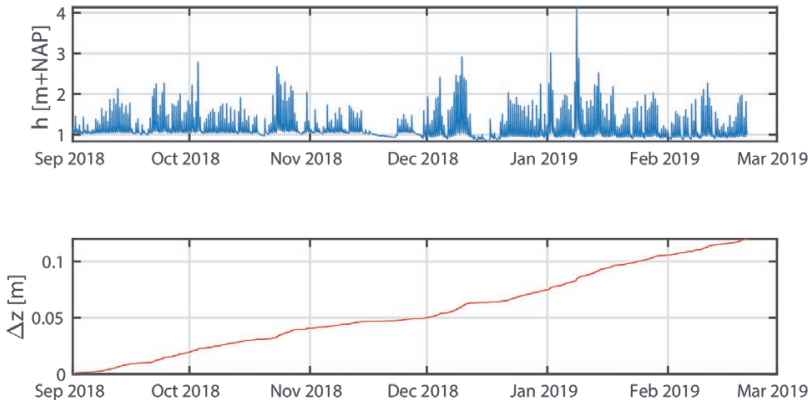
model was run with the exact water level time series measured at the pit between September of 2018 and March 2019, and compared the results with the deposition measured. For the initial half year of the pilot 0.13 m of elevation change was measured (Esselink *et al.*, 2019). Subsequent measurements show a further 0.13 m of elevation change between September of 2018 and March 2019. A representative SSC of 0.25 kg/m<sup>3</sup> reproduced the reported elevation change (**Figure 4.5**).

Both SSCs found are within the range of values that was expected from literature. A higher representative SSC of 0.25 kg/m<sup>3</sup> during the winter of 2018 than the 0.19 kg/m<sup>3</sup> for 1984 to 2003 also seems consistent with seasonal differences

observed in previous studies resulting from wave action and decreased biological activity in winter (de Haas & Eisma, 1993; Dyer *et al.*, 2000; Kornman & de Deckere, 1998). For this study, however, we consider the first value of  $0.19 \text{ kg/m}^3$  more appropriate as it was calibrated over a longer timespan with an elevation more representative for the long-term rather than the initial bed elevation of the pit. However, an extensive study of seasonal SSC variations is required to properly validate this specific value. Despite the limitations in validation we consider the model to be satisfactory for an exploratory study until validation can be performed on a longer time series.



**Figure 4.4** Distribution of calibrated model results of the average sedimentation rate for the period 1984–2003 in orange and the distribution of measured sedimentation rates between 1984 and 2003 by Esselink in green.



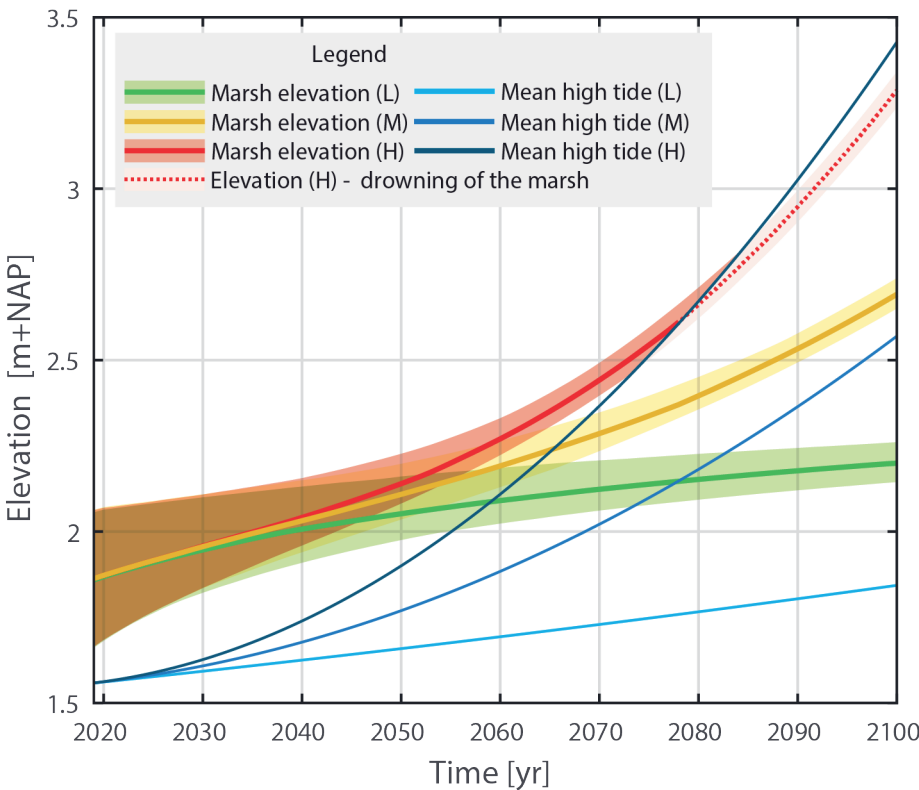
**Figure 4.5** Modelled sedimentation over time (bottom panel) from the water level time series measured at the borrow pit (top panel). Input parameters:  $C_{flood} = 0.25 \text{ kg/m}^3$ ;  $\rho_{sed} = 372 \text{ kg/m}^3$ ;  $w_s = 2.7 \cdot 10^{-3} \text{ m/s}$ .

## 4.5. Results

### 4.5.1. Marsh elevation

The predicted effect of sea-level rise on vertical accretion of the marsh surface is substantial (see **Figure 4.6**). In the lowest sea-level rise scenario, the marsh accretes in pace with sea-level rise. For the medium scenario the deposition rate decreases until around 2050 when sea-level rise outpaces the deposition rate. From this point onward inundation depths increase with each year enhancing deposition but never catching up to the increasing rate of sea-level rise. The high sea-level rise scenario is similar to the medium scenario but is outpaced by 2035. In this scenario

---



**Figure 4.6** Development of the marsh elevation over time as predicted by the model simulations for the low sea-level rise scenario (L) in green, medium sea-level rise scenario (M) in yellow, and high sea-level rise scenario (H) in red. The band represents 90% of simulation results and the line is the median of all simulations.

the marsh is projected to be below mean high water around the year 2078. Since marsh vegetation requires a minimum period of dry conditions to survive, the marsh may not persist at this stage of drowning and the assumptions underlying the model will no longer hold. That is, as vegetation cover is lost, more turbulence and wave action will inhibit sediment for settling and enable erosion. Hence, the model tends to overestimate the sediment accumulation of a drowning marsh. In a worst-case scenario, run-away erosion of the marsh could be initiated resulting in a net loss of sediment, rather than accretion.

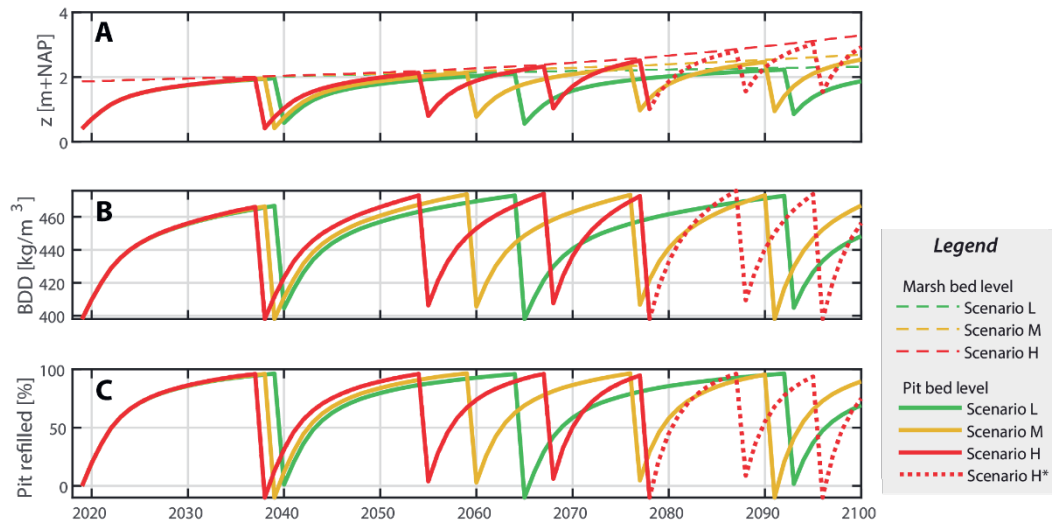
As **Figure 4.6** shows, the relative water depth above the marsh during high tide does only vary in the order of centimetres between scenarios by 2050. Towards 2100 the relative water depth has remained constant for low sea-level rise, increased under medium sea-level rise and increased substantially with a high sea-level rise scenario. The 90% band of simulations decreases under strongly accelerated sea-level rise suggesting a decreasing influence of settling velocity, bulk dry density and variance in initial elevation for the deposition rate compared to the increasing inundation depth by sea-level rise. The uncertainty in initial conditions is the result of heterogenous processes in the marsh (e.g. creeks, patches of denser vegetation, etc.). The model does not capture these features, so variance across the marsh will be larger in 2100 than the model suggests. However, it does indicate that the initial uncertainty of a “representative marsh elevation” has a diminishing influence on long-term accretion trends.

4

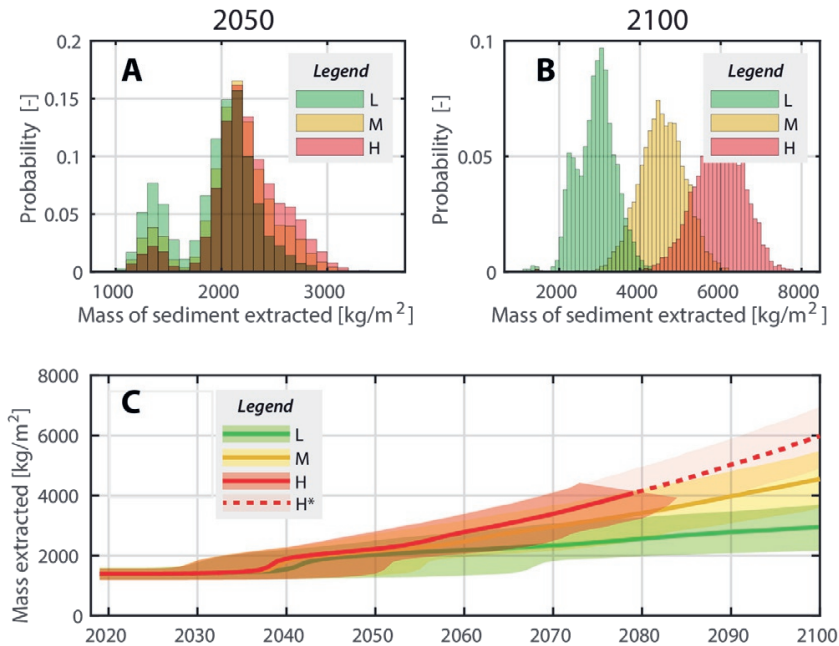
#### 4.5.2. Infilling of the borrow pit

For the same reasons as discussed in section 4.5.1, until 2050 the expected deposition within the borrow pit is similar between scenarios until 2050 (see **Figure 4.7**, **Figure 4.8**). The pit excavated in 2018 is expected to be refilled by 2040 for all scenarios. At the earliest the pit is already filled by 2029 for all scenarios in 5% of the simulations. At the latest the pit is refilled in 2068 for the low sea-level rise scenario, 2056 for the medium scenario and 2052 for the high scenario according to 95% of simulations.

The majority of infilling takes place during the initial years after excavation of the borrow pit. Within the first 10 years approximately 75% of the pit is already



**Figure 4.7** The influence of sea-level rise scenario L, M and H on A) elevation, B) the bulk dry density within the pit, and C) the infilling rate of the borrow pit until 2100 with all parameters fixed at average values. Note (\*) that for scenario H after 2078 results are not reliable (see **Figure 4.6**).



**Figure 4.8** The mass of clay extracted from the borrow pit by A) 2050, B) 2100 and C) cumulative over time for the low (L) sea-level rise scenario in green, the medium (M) sea-level rise scenario in yellow, and the high (H) sea-level rise scenario in red. For each scenario, the band represents 90% of all simulation results and the solid line the median. Note (\*) that for scenario H after 2078 results are not reliable (see **Figure 4.6**)

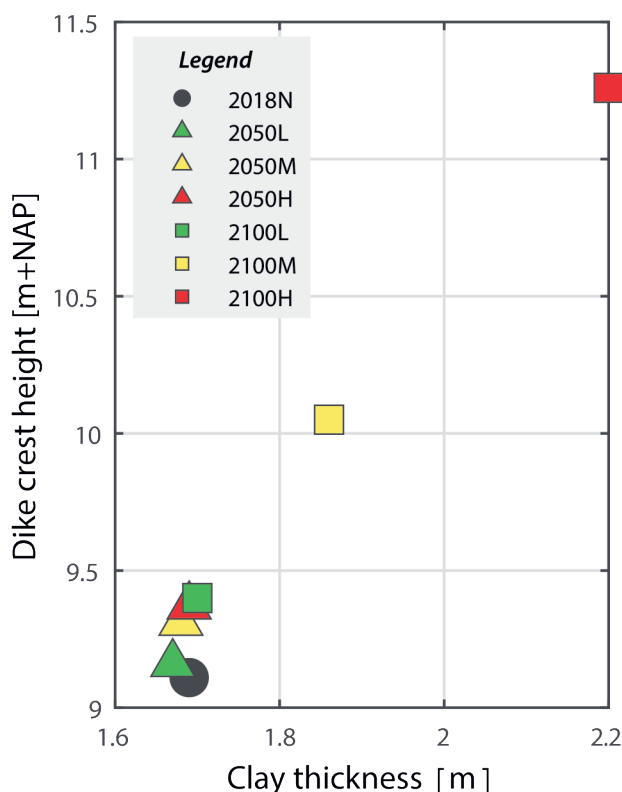
refilled. Initially, the relative depth to mean high tide is largest, resulting in frequent inundation and thus ample opportunities for sedimentation. Inundation frequency decreases exponentially with increasing elevation explaining the decreasing deposition within the pit over time. It further suggests that a greater initial depth of borrow pit is more efficient in capturing sediment than a pit with a shallow depth. As the rate of sea-level rise accelerates, so does the inundation frequency and thus deposition rate within the borrow pit relative to the marsh surface. The modelling results suggest an acceleration of the infilling process as a result of the acceleration in sea-level rise which results in a higher clay yield from a continuous exploitation of the borrow pit.

The model also suggests the sediment density of an infilled pit remains significantly lower than the density of the surrounding marsh, which has on average a density of  $873 \text{ kg/m}^3$  (see **Figure 4.7B**). On average, the infilled pit will contain only 54% of the mass of clay compared to the surrounding undisturbed marsh. The 5th and 95th percentiles of simulations show a large range in BDD within the pit upon refilling: from 37% to 74% of the BDD in the marsh. Uncertainty in the density of sediment within the pit upon re-excavation is a major influence on the total clay yield by 2100 as it directly affects the mass of clay in the pit at the end of each extraction cycle (**Figure 4.8**).

4

#### 4.5.3. Optimal dike dimensions in 2050 and 2100

The deposition rate on the foreshore has a large influence on the design of the dike. If the marsh keeps pace with sea-level rise, the dike stays subjected to similar waves as initially. However, if the inundation depth increases as a result of sea-level rise the dike will be exposed to higher waves. The effects on the required dike dimensions are presented in **Figure 4.9**. The required dike height is primarily governed by the absolute sea-level rise. Lower crest heights become increasingly likely to overtop as the water level rises. The required clay layer on the dike's outer slope is primarily affected by the impact of waves on the outer slope. For all dikes in 2050 and scenario L in 2100 the optimal thickness was found to be around 1.7 m when a 1:7 slope is maintained (**Figure 4.9**). With increasing wave heights under



**Figure 4.9** The dike dimension for the three sea-level rise scenarios in 2050 and 2100 when the minimal amount of clay is applied on the dike slope. The black dot represents the optimal wide green dike design for 2018, the triangles represent 2050 dike dimensions and the squares 2100 dike dimensions. The colour of the squares and triangles indicate the sea-level rise scenario: green for scenario L, yellow for scenario M and red for scenario H.

extreme storm conditions, the clay layer is eroded more rapidly from wave impacts. By 2100 the required thickness has increased to 1.9 m and 2.2 in scenarios M and H respectively. In scenario H however, because of potential drowning of the marsh a lower foreshore may be present than predicted. Thus, stronger waves may reach the dike and larger dike dimensions will be required.

#### 4.5.4. Matching clay demand for dikes with supply from the pits

A representative dike profile of the current Dollard dike was adapted to the dimensions calculated in section 4.5.3. The amount of clay applied on the outside of the dike was computed to achieve the optimal minimal clay thickness where any

space left was filled by sand. Assuming a clay density of  $1200 \text{ kg/m}^3$  the volume of clay was converted in a demand for the mass of clay per reinforcement. This amount was converted to an area of pit using the results of section 4.5.2 of the mass retrieved from each  $\text{m}^2$  of pit.

The first reinforcement is conducted as part of the pilot in which in 2025 the dike is reinforced to the dimensions meeting the safety criteria in 2050 as calculated in 4.5.3 with clay extracted from the pit since 2018. Ordinarily dikes are reinforced for a time horizon of 50 years, but given the fact this reinforcement is part of pilot for other dike sections in the Dollard and the uncertainty in sea-level rise by 2075, a 25 years' time horizon is more applicable. The necessary area of a pit 1.6 m deep

**Table 4.3** The area of pit required in hectares to reinforce 1 km of dike to the 2050 safety level in the low (L), medium (M) and high (H) sea-level rise scenario with the 5%, 50% and 95% uncertainty margins.

Area of pit required (in ha) per km of dike reinforcement by 2050	L	M	H
5%	4.6	5.1	5.8
50%	7.3	7.3	7.9
95%	8.6	9.2	9.4

**Table 4.4** The area of pit required in hectares to reinforce 1 km of dike to the 2100 safety level in the low (L), medium (M) and high (H) sea-level rise scenario with the 5%, 50% and 95% uncertainty margins.

Area of pit required (in ha) per km of dike reinforcement by 2100	L	M	H
Strategy 1: New pits			
5%	3.5	3.8	4.7
50%	4.3	4.4	5.5
95%	5.2	6.5	8.2
Strategy 2a: Re-excavating pit up to 2050			
5%	4.5	4.4	5.3
50%	5.9	5.7	6.9
95%	9.9	11.7	13.8
Strategy 2b: Re-excavating pit up to 2075			
5%	3.5	3.1	3.3
50%	4.9	3.8	4.1
95%	6.6	6.7	6.7

to meet the clay needed for the dike in each 2050 scenario with uncertainty margins is presented in **Table 4.3**. The area of pit required in hectares to reinforce 1 km of dike to the 2050 safety level in the low (L), medium (M) and high (H) sea-level rise scenario with the 5%, 50% and 95% uncertainty margins.. As the rise in sea level remains modest until 2050, there is little difference between dike dimensions and thus clay demand for each scenario. The area of pit needed lies between 4.6 and 9.4 ha with an expected area of 7.3 ha across all scenarios.

A decision will have to be made about the reinforcement strategy for 2100 based on the results of the pilot and the projected sea-level rise. We look at 2 strategies: 1) excavate a new pit elsewhere in the marsh after the first one is refilled or 2) a continuous exploitation of the same pit as shown in **Figure 4.8**. In strategy 1 we assume 2 pits of equal of equal area are dug and refilled by 2100. In strategy 2 clay is collected until either (a) 2050 or (b) 2075. The required borrow pit area for each scenario and strategy is presented in **Table 4.4**. For a reinforcement until 2100 similarly-sized pits are needed as for a 2050 reinforcement despite the higher and thicker dikes in 2100, mostly because first the slope had to be flattened from 1:4 to 1:7. It can be seen that for the low sea-level rise scenario excavating a new pit yields more clay per hectare than excavating an existing pit once (up to 2050) or twice (2075). This is the result of the low density of clay within an infilled pit compared to the surrounding marsh. Infilling of the borrow pit is projected to accelerate with sea-level rise. As a result in scenarios M and H a large amount of additional clay can be extracted up to 2075 and cyclically excavating the pit requires less area of pit per kilometre of dike than excavating a new pit once when a reinforcement is needed.

## **4.6. Discussion**

Different types of nature-based solutions in flood protection have been proposed to enhance coastal protection. Ecosystems like reefs, marshes, mangroves, and oyster reefs are typically effective in wave damping and/or stabilising sediment (Narayan *et al.*, 2016; Scheres & Schüttrumpf, 2019), but their survival and performance as flood protection measures may suffer from accelerated sea-level rise (Crosby *et al.*, 2016; Kirwan *et al.*, 2010; Perry *et al.*, 2018;

Ridge *et al.*, 2015). In this regard, the ability of the ecosystems to (partially) mitigate relative sea-level rise by accumulating sediment is a more promising avenue for long-term nature-based solutions. This study explores whether utilising sedimentary processes of a salt marsh-dike system can sustainably adapt a dike system against sea-level rise. Successes of clay mining in Lower Saxony, Germany, have encouraged the concept to be reintroduced in the Netherlands (Bartholomä *et al.*, 2013; Karle & Bartholomä, 2008; van Loon-Steensma & Schelfhout, 2017; van Loon-Steensma & Vellinga, 2019). Exploratory studies suggested a Wide Greed Diike constructed with clay from the marsh could be successfully implemented in the Dutch Dollard estuary to adapt the flood defences for future sea-level rise (van Loon-Steensma & Schelfhout, 2013, 2017; van Loon-Steensma *et al.*, 2014a). As a result the Wide Green Diike pilot was initiated to further explore the concept (Hunze en Aa's, 2020).

Future sea-level rise has a profound effect on the implementation of an adaptation strategy involving sedimentary processes for flood protection. The first aspect relates to the vertical accretion of the foreshore. Vuik *et al.* (2019) demonstrated vertical accretion of the marsh contributes to flood risk reduction against sea-level rise by the dissipation of wave energy across the foreshore. A similar result was produced by the combination of a 0-D marsh deposition model and SWAN wave model in this study. When the relative water depth on the foreshore is maintained by accretion, the design storm waves will remain unchanged and only increasing the dike crest height is necessary. Otherwise reinforcement of the outer slope will be necessary.

Our simulations with the sea-level rise scenarios representing the RCP 4.5 and 8.5 scenarios of the IPCC (scenarios M and H in this study) indicate accretion rates for our case study for 2100 could be insufficient to mitigate the accelerated sea-level rise, whereas in the low KNMI'14 scenario (scenario L in this study) the marsh does keep pace with sea-level rise. Whether the marsh fronting the dike maintains its elevation relative to mean sea level until 2100 is therefore uncertain. Kirwan *et al.* (2010) suggested an environment like the Dollard should be capable persisting under sea-level rise upwards of 80 mm/yr but in our simulation only 9 mm/yr (90% interval: 4–12 mm/yr) could be accommodated. In

the Scheldt estuary at a representative suspended sediment concentration of one fifth of the Dollard ( $0.04 \text{ kg/m}^3$ ) accretion was measured around  $1.6 \text{ cm/yr}$  (Temmerman *et al.*, 2003), almost twice the accumulation rate of  $8.5 \text{ mm/yr}$  observed in the Dollard (Esselink, 1998, 2007). Comparing our model parameters with the parameters from the Scheldt marsh from Temmerman *et al.* (2003), a high bulk dry density on the foreshore is the most important factor explaining the low deposition rate in the Dollard. Given the large influence, close consideration of bulk dry density on the foreshore is required when comparing the resilience of different estuaries to sea-level rise.

Model simulations suggest the borrow pits are expected to be refilled after 22 years (range: 11–50 years across scenarios) under present day sea-level rise rates with initial infilling in the order of  $10 \text{ cm/yr}$  and decelerating as the pit fills. This rate is comparable to the pits of Jade Bay in the German Wadden Sea, which take about 30 years to refill (Arens, 2002). Furthermore, the model predicts sediment in the refilled clay pit will not exceed a bulk dry density of  $500 \text{ kg/m}^3$  mirroring the observations in Jade bay of former clay puts (Bartholomä *et al.*, 2013; Karle & Bartholomä, 2008). As the infilling rate is directly related to the depth of the pit (see section 4.5.2), a small yet deeper pit is more effective in trapping sediment than a wide but shallow pit. However a deeper pit will remain inundated for longer meaning it will take longer for the marsh to rejuvenate. Marsh rejuvenation was another reason for the construction of borrow pits in the Jade Bay (Bartholomä *et al.*, 2013). In this sense the objectives of nature restoration and sediment extraction may not necessarily align.

A prediction of the model is an increasing infill rate of the pit as sea-level rise accelerates. This would be a unique property for a borrowing-pit adaptation scheme compared to other nature-based solutions in which its effectiveness increases as the sea-level rise accelerates. However, in this study it was assumed the marsh locally surrounding the pit always shelters the pit from erosion by wave action and currents. In practise the effectiveness of the borrow pit will be constrained by the adaptive capacity of the marsh to sea-level rise. Furthermore, a key assumption in this study was that the sediment concentration within the estuary would remain constant. If large scale efforts to reduce the turbidity within the estuary are successful, borrow pits being one of them, a reduced amount of

sediment will be available for accumulation on the marshes and pits on the long term.

The effects of local topography and horizontal processes governing the marsh and pit were not included in the methodology for this study. However, such processes can contribute to the developments on a long time-scale (Best *et al.*, 2018; Elmilady *et al.*, 2019). Within Jade Bay clay mining was carried out in combination with ecological restoration by redesigning an artificially developed salt marsh into a more natural marsh with natural creeks and levees (Bartholomä *et al.*, 2013; Esselink, 2007). Across the pit the elevation changes varied greatly depending on emerging drainage patterns, relative elevation differences and the emergence of vegetation (Bartholomä *et al.*, 2013; Karle & Bartholomä, 2008). Also within the Dollard marsh such differences in accretion rates exist, and which are not accounted for in our approach (Esselink, 1998). Such processes may hinder the capacity of the marsh to accrete locally in response to sea-level rise, resulting in e.g. the formation of ponds (Mariotti, 2016; Watson *et al.*, 2017). Lateral erosion of the salt marsh edge also plays a role in the development of the marsh. Multiple studies have revealed collapse of the marsh can be triggered by wave action at the marsh edge, rather than by direct drowning of the marsh through sea-level rise (Fagherazzi, Mariotti, Wiberg, & McGlathery, 2013; Mariotti & Fagherazzi, 2013; van de Koppel, van der Wal, Bakker, & Herman, 2005). This is relevant for the high sea-level rise scenarios in this study, in which an increase in wave action across the marsh was predicted. Marsh erosion from wave action leads to a smaller marsh platform, larger waves reaching the dike and thus more reinforcement of the dike. Local processes within the marsh should therefore be included in future assessments of high sea-level rise scenarios.

The use of borrow pits can be considered for other regions outside of the Dollard and the Wadden Sea as long as similar conditions can be satisfied that allow for the refilling of a pit: an abundance of suspended sediment, a sufficiently wide marsh to avoid erosive wave action at the pit, and a sufficient tidal range for sediment transport towards the marsh. Other deltas with marshes and a historic record of sediment accumulation (e.g. the Yangtze and Mississippi) should possess these qualities unless human interventions have altered these conditions.

In the Dutch case, marshes have historically been managed to further promote sediment accumulation in the marsh. Understanding the present hydrodynamics and morphology, both daily and during extreme storms, is vital to assess the balance between natural sediment accumulation, and the required sediment for flood defences. The Dutch case presented in this study allowed for the use of tools, hydrodynamic databases, and marsh monitoring efforts over decades. In the absence of such knowledge, data gathering of marsh sediment accumulation, as well as storm conditions, is necessary before the methods presented in this study can be applied.

## **4.7. Conclusions**

Effective adaptation to sea-level rise is one of the major challenges of this century. The sedimentary processes within marshes fronting flood defences are an adaptation option to reinforce or improve flood defences for future sea-level rise. Using the “Wide green dike project” in the Dutch Dollard as a case, we combined models quantifying the vertical sedimentation processes within the marsh with hydraulic models and design formulas for dike assessments to explore the feasibility of such a nature-based adaptation strategy under different sea-level rise scenarios.

For a low sea-level rise scenario (+29 cm by 2100) we simulate accretion of the foreshore in pace or faster than the rate of sea-level rise. For medium to high sea-level rise scenarios (over +102 cm by 2100) vertical accretion is outpaced by sea-level rise leading to a relatively lower foreshore and higher waves impacting the dike. As long as the marsh keeps pace with sea-level rise the grass dike can maintain an outer slope of approximately 1:7 and a clay layer of approximately 1.7 m thick. To meet safety standards by 2100 under the high sea-level rise scenario (+189 cm by 2100) the clay layer on the outer slope needs to be thickened to 2.2 m.

Clay mined from the marsh fronting the dike can supply clay for dike reinforcement. According to the model simulations the borrow pit will refill in 22 years (range: 11–50 years across scenarios) but will contain sediment of only 54% (range: 37–74%) the density of the original marsh. The model predicts that the infilling rate of the pit decreases asymptotically when the bottom elevation

increases relative to the mean high tide. This results in an increasing clay yield with sea-level rise if the pits are repeatedly re-excavated upon reaching the elevation of the surrounding marsh. Depending on the scenario 7.3 ha (range: 4.6–9.4 ha) of borrow pit is necessary to reinforce the outer slope of a 1 km dike section by 2050. To construct a dike meeting the safety standards by 2100 re-excavating a new pit of 4.3 ha twice (range: 3.5–5.2 ha) is most efficient for the clay yield per hectare in the low sea-level rise scenario. In a high sea-level rise scenario with strongly accelerated sea-level rise infilling of the pit is projected to accelerate substantially. Here re-excavating a pit up to 2075 requires the smallest borrow pit of 4.1 ha (range: 3.3–6.7 ha).

This study highlights the important role sedimentary processes can play in future flood protection. Even though the study focusses on the marsh in the Dollard estuary, in principle other sediment rich estuaries suitable for marsh, e.g. within the Yangtze Delta, can utilise borrow pits in their flood protection strategies provided these pits remain sheltered from erosion within the marsh. Maintaining natural foreshores can thus be an important asset for adapting flood defences in the future.

4

## Acknowledgments

We would like to thank Erik Jolink from the water board Hunze en Aa's and project leader of the Wide Green Dike project for his help and collaboration that made this research possible. We would further like to thank Mark Klein Breteler from Deltares for his explanation on the assessment of clay dikes. Finally we thank Matthijs Duits at HKV for his great help in understanding and applying the Hydra-NL model.

## Appendices

Appendices to this chapter can be found starting from 216.



# 5

## The Sensitivity of a Dike-Marsh System to Sea-Level Rise—A Model-Based Exploration

R.J.C. Marijnissen, M. Kok, C. Kroeze,  
J.M. van Loon-Steensma

This chapter was published as:

Marijnissen, R.J.C., Kok, M., Kroeze, C., & van Loon-Steensma, J.M. (2020). The Sensitivity of a Dike-Marsh System to Sea-Level Rise—A Model-Based Exploration. *Journal of Marine Science and Engineering*, 8(1), 42. <https://doi.org/10.3390/jmse8010042>



## Abstract

Integrating natural components in flood defence infrastructure can add resilience to sea-level rise. Natural foreshores can keep pace with sea-level rise by accumulating sediment and attenuate waves before reaching the adjacent flood defences. In this study we address how natural foreshores affect the future need for dike heightening. A simplified model of vertical marsh accretion was combined with a wave model and a probabilistic evaluation of dike failure by overtopping. The sensitivity of a marsh-dike system was evaluated in relation to a combination of processes: (1) sea-level rise, (2) changes in sediment concentration, (3) a retreat of the marsh edge, and (4) compaction of the marsh. Results indicate that foreshore processes considerably affect the need for dike heightening in the future. At a low sea-level rise rate, the marshes can accrete such that dike heightening is partially mitigated. But with sea-level rise accelerating, a threshold is reached where dike heightening needs to compensate for the loss of marshes, and for increasing water levels. The level of the threshold depends mostly on the delivery of sediment and degree of compaction on the marsh; with sufficient width of the marsh, lateral erosion only has a minor effect. The study shows how processes and practices that hamper or enhance marsh development today exacerbate or alleviate the challenge of flood protection posed by accelerated sea-level rise..

## 5.1. Introduction

To protect the growing number of people living in deltas against flooding, flood protection measures are required. In many deltas “grey” solutions like dikes, levees and storm surge barriers have been implemented (Powell, Tyrrell, Milliken, Tirpak, & Staudinger, 2019; Scheres & Schüttrumpf, 2019; Schoonees *et al.*, 2019). In general these measures are designed to function over long periods, yet are relatively inflexible to unforeseen accelerated sea-level rise (Borsje *et al.*, 2011; Powell *et al.*, 2019; Temmerman *et al.*, 2013; Vuik *et al.*, 2019). Moreover, many grey solutions can be detrimental to ecosystems by confining the intertidal area (coastal squeeze) or affecting the natural hydro- morphological processes (Firth *et al.*, 2014; Leo, Gillies, Fitzsimons, Hale, & Beck, 2019; Powell *et al.*, 2019).

Nature-based solutions, where “green” ecosystems aid in flood protection, have recently garnered a great deal of attention (Borsje *et al.*, 2011; Temmerman *et al.*, 2013). Ecosystems like salt marshes promote accretion on the foreshore of a flood defence through interacting with the tide, dampen waves, and attenuate storm surges (Allen, 2000a; Costanza *et al.*, 2008; Möller *et al.*, 2014; van Loon-Steensma *et al.*, 2016). A major benefit of marsh ecosystems in flood protection is their ability to naturally adapt to sea-level rise under the right conditions (Kirwan & Temmerman, 2009; Kirwan, Temmerman, Skeehean, Guntenspergen, & Fagherazzi, 2016). However, mitigating flood risk with nature-based solutions alone may not always be feasible. As a result, hybrid flood defences, incorporating both traditional flood defences structures and natural elements, are an attractive strategy to protect deltas (Borsje *et al.*, 2011; Temmerman *et al.*, 2013; Vuik *et al.*, 2019).

A combination of dikes with salt-marshes are considered to be an effective hybrid flood defence (Temmerman *et al.*, 2013; van Loon-Steensma, 2015; Vuik, Jonkman, Borsje, & Suzuki, 2016). Yet, the inherent variability and uncertainty about the development of the marsh is an obstacle for implementation in an integrated dike-marsh flood protection scheme where only small risks are acceptable (Scheres & Schüttrumpf, 2019; van Loon-Steensma & Kok, 2016). Marshes are dynamic systems which expand and retreat periodically in response to the complex interactions between waves, elevation and seedling establishment

(Bouma *et al.*, 2016; van de Koppel *et al.*, 2005). Furthermore, the marshes will respond directly to future human activities that affect the availability of sediments like dredging or upstream dam construction (Aaron & Turner, 1997; Yang, Ding, & Chen, 2001). Large uncertainties about the effectiveness of a marsh for flood protection could negate its potential contributions and preference may be given to a more traditional flood defence rather than to a hybrid flood defence (Möller, 2019).

So far, few studies tried to translate processes affecting marshes into the required adaptations of dikes. The connection between marshes and flood risk reduction concepts was qualitatively described by van Loon-Steensma and Kok (2016). Vuik *et al.* (2018b) were the first to apply these concepts for a safety assessment of a flood defence. In Vuik *et al.* (2019) this type of assessment was used to compare the cost-effectiveness of a natural foreshore against regular reinforcement measures with sea-level rise, assuming all other factors governing the marsh would remain constant. In this study we explore how dike reinforcement is affected in case those factors do not remain constant.

The aim of this study is, therefore, to address how the processes on a natural foreshores affect the future need for dike heightening. More specifically, we consider the effects of sea-level rise, sediment availability, marsh erosion, and compaction on the dike crest elevation in a marsh-dike flood protection system. To do so, a simplified model of vertical marsh accretion was combined with the SWAN wave model and a probabilistic evaluation of dike failure by overtopping. The modelled foreshore, hydraulic conditions and dike design were taken from the Ems estuary in the Dutch Wadden sea as a case-study. Through this modelling system the required dike reinforcement over time as a result of human interventions and dynamic processes in the marsh are explored.

## **5.2. Marsh processes and flood protection**

### **5.2.1. Marsh development and human influence**

Salt marshes are coastal ecosystems on the fringes between land and sea. Vegetation within the marsh has adapted to frequent submergence by the tide. Typically the edge of marshes can be found above mean high neap tide (MHNT)

where submergence times are tolerable only for the most well-adapted plants (Allen, 2000b). When tides inundate the marsh, the vegetation exerts a drag force on the water decelerating the flow. In the decelerated flow sediment suspended in the water can settle while the turbulent motions of waves are dampened (Leonard & Reed, 2002; Möller *et al.*, 2014; van Loon-Steensma *et al.*, 2016). Furthermore, the root structure reinforces the soil which becomes more resistant to erosion (Silliman *et al.*, 2012). As a result, the marsh platform accumulates sediment over time and grows in elevation, allowing for a succession of plants less tolerant to submergence on the higher elevations (Allen, 2000b). In this way the pioneering plants in the ecosystem “engineer” their environment to facilitate the establishment of more vegetation (Bouma, de Vries, & Herman, 2010).

Sea-level rise directly affects the water level and through the interactions described above will affect the development of the marsh. The resilience of marshes to sea-level rise is highly debated in literature. Crosby *et al.* (2016) predict as many as 60-90% of marshes globally are under threat of drowning this century. Spencer *et al.* (2016) estimate a loss of 46-78% and Craft *et al.* (2009) 20 to 45%. Schuerch *et al.* (2018) predict only 0-30% of global wetlands will be lost if no new accommodation space for marsh is created. Kirwan explains key determinants of marsh resilience are the rate of sea-level rise, tidal range, the amount of sediment suspended in the coastal water, and the capacity of marshes to retreat to higher elevations (Kirwan *et al.*, 2010; Kirwan & Megonigal, 2013; Kirwan & Temmerman, 2009; Kirwan *et al.*, 2016). Without considering the feedbacks between these processes the resilience of marshes can be greatly underestimated (Kirwan *et al.*, 2010). Other studies (Fagherazzi *et al.*, 2013; Mariotti & Fagherazzi, 2013; van de Koppel *et al.*, 2005) point out marshes can still be lost by lateral erosion from increased wave action, even if vertical accretion of the marsh surface supersedes the rate of sea-level rise.

Human actions in the larger delta system will play a crucial role in the development of marshes. Land reclamation has already resulted in a direct loss of roughly one third of coastal wetlands, including marshes, worldwide (McLeod *et al.*, 2011). However, human interventions can affect the marsh further by disrupting the flow sediment. For instance, the expansion of marshes in the Yangtze delta has been halted or turned to retreat as a result of dams constructed upstream blocking

the flow of sediments to the coast (Yang *et al.*, 2001; Yang *et al.*, 2006). Meanwhile, the retreat of marshes on Sturgeon Bank, Vancouver, B.C., Canada, has been caused in part by the reduction in sediment supply as a result of dredging in the Fraser River and the redirection of its outflow by a jetty (Atkins, Tidd, & Ruffo, 2016). In Jamaica bay, New York city US, mineral sediment supply was reduced by 60% in the past two centuries due to urbanisation, but sediment supply was compensated by enhanced organic deposition after intense fertilization of the marsh by wastewater pollution (Peteet *et al.*, 2018). Ironically, improving water quality in Jamaica bay would probably lead to a reduced resilience of its marshes to sea-level rise. Other such examples of human interventions are numerous and reveal the extent of the influences these can have (Kirwan & Megonigal, 2013).

In the light of historic marsh losses, preserving or restoring marsh habitat for coastal protection has become increasingly important. Measures like e.g. depoldering of agricultural land (Rupp-Armstrong & Nicholls, 2007), applying sediment onto or near tidal flats (Baptist *et al.*, 2019; Ford, Cahoon, & Lynch, 1999), and promoting sedimentation with groynes or dams (van Loon-Steensma & Slim, 2013), have been employed to restore marsh land. While these interventions aim to restore and/or preserve marsh habitat, these projects can also aid in flood protection.

### 5.2.2. Flood protection services by marshes

Flood protection measures aim to reduce the risk of areas being inundated. Structures like dikes fail when the hydraulic load is too great to prevent water (pressure) from: flowing over the dike (i.e. overflow and overtopping), eroding or destabilising the structure resulting in collapse (e.g. macro-stability and erosion), or excessive seepage in the ground below (i.e. piping). The hydraulic load is composed of characteristics of the extreme event, e.g. the water level, wave characteristics, storm duration, etc. . Flood protection services are provided when the marsh interacts with one or more components of the hydraulic load.

The attenuation of waves by the marsh is one of the benefits for flood protection. Many studies find significant wave height reductions within the first 10's of metres of marsh (Möller *et al.*, 2014; Möller, Spencer, French, Leggett, &

Dixon, 1999; Schoutens *et al.*, 2019; Vuik *et al.*, 2016; Ysebaert *et al.*, 2011). Waves are dampened further with distance travelled across the marsh. Möller *et al.* (2014) measured 60% of the wave height reduction during storm surges could be attributed to the plants themselves. Studies tend to highlight the large reductions achieved with wave heights below 1 m and biomass under peak summer conditions. Field studies find a strong seasonality in wave attenuation corresponding to seasonal changes in vegetation density (Möller & Spencer, 2002; Schoutens *et al.*, 2019; Vuik *et al.*, 2016). Vuik showed that the capacity of marshes to attenuate waves is hampered by the breaking of stems under high wave loads (Vuik, Suh Heo, Zhu, Borsje, & Jonkman, 2018a; Vuik *et al.*, 2018b). Moreover, field studies have consistently shown the wave dampening capacity diminishes when the marsh is considerably inundated (Foster-Martinez, Lacy, Ferner, & Variano, 2018; Möller *et al.*, 2001; Vuik *et al.*, 2016). Well-known models of wave dampening by vegetation predict a continuously stronger decrease in drag-force from vegetation as the inundation depth exceeds the height of the vegetation (Baptist *et al.*, 2007; Dalrymple, Kirby, & Hwang, 1984; Mendez & Losada, 2004). Taken together, the direct effect of wave dampening by the presence of vegetation during extreme events becomes limited once storm surges are expected to be substantially higher than MHT and typical wave heights are sufficient to break all stems remaining in winter.

Another benefit of coastal wetlands is storm surge attenuation. A recent review of attenuation rates by Glass, Garzon, Lawler, Paquier, and Ferreira (2018) suggests marshes can attenuate water levels about 4 to 5 cm/km with extremes reported at -2.2 and 70 cm/km. Stark, Van Oyen, Meire, and Temmerman (2015) explain the ability of marshes to attenuate water levels is determined by the combination of friction effects along the tidal channels and their convergence. Models suggest a small-shallow tidal channel system will result in more attenuation than one with wide deep channels (Stark, Plancke, Ides, Meire, & Temmerman, 2016). Attenuation is strongest for surges up to about 1 m above the marsh platform and diminish with higher inundation levels and longer lasting events (Stark *et al.*, 2015; Wamsley, Cialone, Smith, Atkinson, & Rosati, 2010). Furthermore, the presence of dikes or levees reduces the attenuation as these block

the water from moving further inland. Consequently, the marsh platform inundates faster and the rate of storm surge attenuation reduces (Stark *et al.*, 2016).

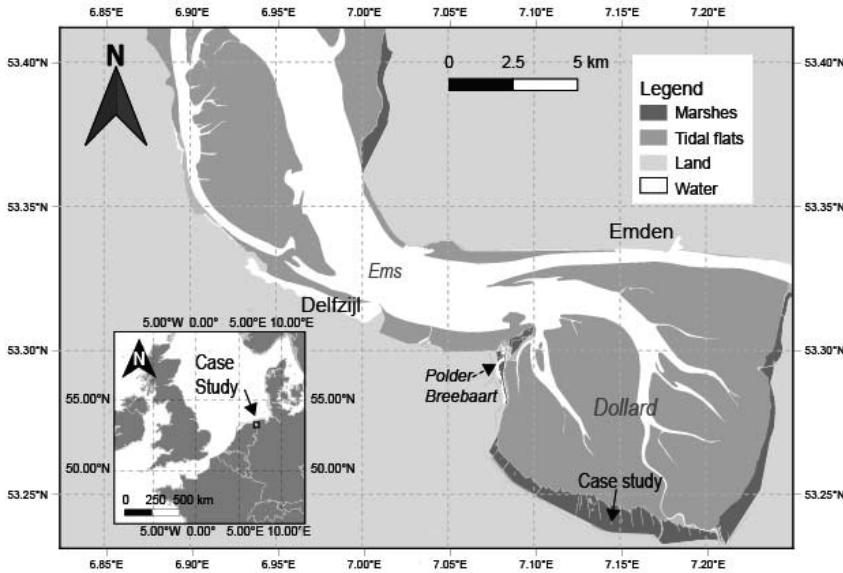
The highest value of marshes for coastal protection during extreme events lies instead in the ability of marshes to grow in elevation over time, thereby limiting the water depth waves can travel through before reaching the flood defence. Waves break and dissipate energy when the water depth decreases sufficiently (Battjes & Stive, 1985). Thus, as long as the marsh accretes faster than the rate of sea-level rise, wave heights at the flood defence can be expected to diminish over time. Furthermore, during storm events strong winds actively generate waves across the inundated tidal flats and marshes. The wave height generated by the wind is limited by the water depth (Young & Verhagen, 1996). The effect of marsh accretion thus diminishes both the generation and progression of waves on the marsh platform.

### **5.3. Methods**

#### **5.3.1. Case-study description**

The interplay between flood protection, nature conservation and human interventions within a delta system is one of the challenges in the Ems-Dollard estuary, the Netherlands (**Figure 5.1**). Over centuries a large portion of the marshes was converted into farmland until the final reclamation in 1924 (Esselink, 2000). Accretion of the marsh was still promoted with a system of ditches and clay dams until the 1950s when maintenance of the ditches and dams ceased. Since then the parts of the marsh have remained stable or show retreat (Esselink, 2000; Esselink, Dijkema, Sabine, & Geert, 1998). Today the marshes are part of a protected nature reserve, with sections that are privately owned and used for grazing livestock.

The loss of sediment major sinks like marshes, the frequent dredging of the shipping lanes and harbours, and morphological processes within the estuary itself, have resulted in a high turbidity in the estuary. Over the past 20 years the mean annual sediment concentration has increased between 0.7 to 4 mg/l annually (van Maren *et al.*, 2016) and without intervention a further increase is likely.



**Figure 5.1** The case-study site in the Dollard within the Dutch Ems estuary. The map is adapted from OpenStreetMap © layers.

The high turbidity is of concern for the local ecological quality of the estuary as the turbid water negatively affects the primary production of the ecosystem. It was, therefore, decided by the provincial government to remove 1 Mt of sediment per year from the estuary by 2050 (Provincie Groningen & Ministerie van Infrastructuur en Milieu, 2018). Measures proposed to do so include creating and maintaining sediment sinks like de-poldered Polder Breebaart, creating a sediment sink between the twin dikes at Delfzijl, and by digging borrowing pits in the current marsh itself that refill from sediment in the estuary within the Wide Green Dike project. The new sediment sinks are used as nature reserves while borrowing pits are dug such that these create islands for birds to breed undisturbed. Furthermore a pilot is being conducted to process clay dredged from the local harbour at Delfzijl and the clay periodically extracted from the marshes as material for dike construction.

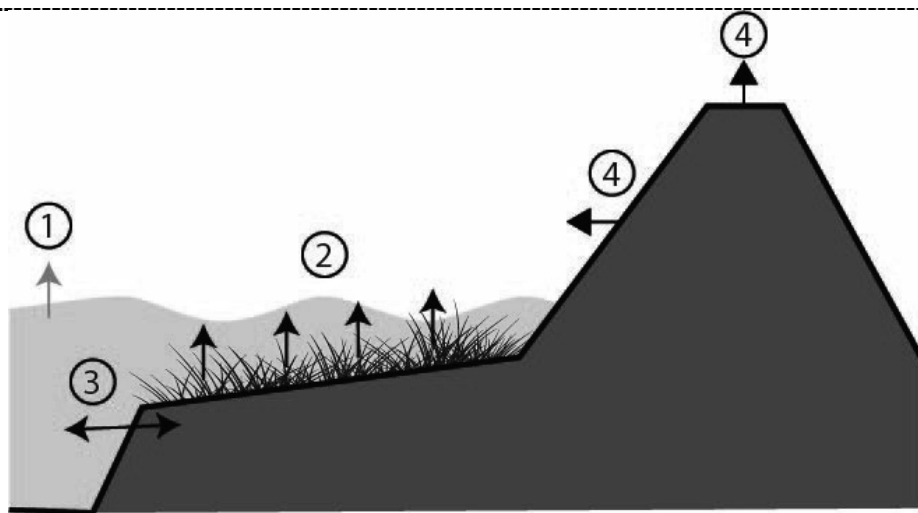
The goal of these projects is threefold: 1) to improve the water quality in the estuary to acceptable levels by reducing turbidity, 2) to create new or enhance existing natural values of marshes and 3) to retrieve building material for future dike reinforcements. The dynamics of the marsh-foreshore are affected by the

interventions in the sediment dynamics of the system. In turn, changes in the foreshore will affect the hydraulic load on the dike. Furthermore, both the marshes and the dikes are affected by sea-level rise in the future. This complicates assessing the extent to which the dikes should be reinforced to combat sea-level rise, while these other processes are at play. Therefore, in this chapter we examine the

sensitivity of dike reinforcement against sea-level rise to the processes affecting the foreshore.

### 5.3.2. Model framework

To explore the sensitivity of the required dimension of the dikes along the Dollard to sea-level rise and other interventions in the estuary, we look at a simple representation of one dike and marsh cross-section. The hydraulic forcing at the marsh edge was adapted from Rijkswaterstaat's hydraulic boundary conditions database for the detailed dike assessments of the Wadden Sea (Rijkswaterstaat, 2011) and analysed with the statistical model for the Dutch coast Hydra-NL (Duits & Kuijper, 2018). A constant slope of 1/4000 across the Dollard marsh was determined from the AHN2 elevation map (Rijkswaterstaat, 2014) as well as a representative width of the marsh of 750 m. We did not consider the attenuation of storm surges or the attenuation of waves by stems of vegetation and instead



**Figure 5.2** The processes modelled within the framework. 1) sea-level rise, 2) vertical sediment accretion and compaction, 3) marsh retreat and 4) dike reinforcement.

focused solely on the effect of marsh accretion as wave heights and marsh inundation are expected to be too severe under design storm conditions (see **Table 5.2** and section 5.3.5) for a significant influence.

We employ a similar approach as used in Chapter 4 to determine dike dimensions in a wide green dike system. The accretion of the marsh by suspended sediment is simulated under a constant sea-level rise rate (processes 1 and 2 in **Figure 5.2**, see section 5.3.3) for a 20 year period. Within this relatively short morphological period both sediment concentration and sea-level rise are assumed to remain constant. The SWAN wave model (Booij *et al.*, 1999) was run under a variety of wind-, wave- and water-level conditions to calculate the expected wave attenuation by the foreshore (see section 5.3.4). From here an optimal dike crest height is determined (see section 5.3.5). The foreshore is then adapted with the modelled amount of accretion and the amount of marsh retreat in the scenario. The wave attenuation under the sea-level rise conditions and altered foreshore is recalculated and used to calculate new dike dimensions (see section 5.3.4). From this we estimate the required rate of dike reinforcement under a particular scenario.

We varied four parameters: the rate of sea-level rise, the suspended sediment concentration, the rate of marsh retreat, and the bulk dry density in the marsh. Each represents expected or already observed processes affecting the Dollard marshes. The rates of sea-level rise were chosen between 3 and 20 mm/yr to cover the range of sea-level rise rates for the Wadden Sea in RCP scenarios for this century (Vermeersen *et al.*, 2018). The suspended sediment concentration was taken from

**Table 5.1** The parameters affecting the marsh and dike varied in this chapter

Variable	Description	Values	Unit
SLR	Sea-level rise rate	3, 5, 10, 20	$\frac{mm}{yr}$
SSC	Suspended sediment concentration	0.1, 0.2, 0.4	$\frac{kg}{m^3}$
MR	Marsh edge retreat	0, 1, 2	$\frac{m}{yr}$
BDD	Bulk dry density of sediment	398, 873, 1208	$\frac{kg}{m^3}$

Chapter 4 and halved or doubled to cover a wide range of potential futures and measures affecting the sediment supply. The marsh edge retreat rate was based on a scenario of marsh conservation and/or no retreat, and rates of 1 and 2 m/yr of retreat. Observed rates of retreat average between +0.4 and -1.7 m/yr (Esselink *et al.*, 2011). Finally we consider different marsh management scenarios based on the three classes of sediment density found in the marsh (Chapter 4, Appendix C.1). A value of 398 kg/m<sup>3</sup> represents no compaction or little compaction, 873 kg/m<sup>3</sup> represents compaction under the current management with grazing of the marsh, and 1208 kg/m<sup>3</sup> represents heavy compaction from extensive use of the marsh with heavy equipment. In total 108 combinations of these parameters were run for analysis (**Table 5.1**).

### 5.3.3. Vertical marsh accretion

A basic sedimentation model was applied to simulate accretion of the marsh. It was simplified from existing numerical models of marsh accretion under sea-level rise conditions (Allen, 1990; French, 1993; Krone, 1987). The model is a balance between the total load of sediment above the marsh platform, the amount of sediment deposited and elevation change. Every time the water exceeds the elevation of the marsh platform ( $z_{marsh}$ ), a water column with a concentration of suspended sediment ( $C_{flood}$ ) is present. A fraction of suspended sediment deposits ( $f_d$ ) and settles with a certain density ( $\rho_{deposit}$ ) on the marsh. Here  $f_d$  is a simple constant combining the effects of sediment fall velocity, tidal asymmetry, and erosion. It was calibrated using observed deposition rates between 1984 and 2003 (Esselink, 2007; Esselink *et al.*, 1998). The high waters from the nearby tide gauge station at Nieuw Statenzijl ( $h_{HW}$ ) were analysed and the expected number of inundations with each water level per year was computed ( $n_{events}$ ). Sea-level rise is incorporated by raising the water-level at each inundation frequency by the total amount of sea-level rise. Summing the deposition during each water level and subtracting subsidence results in the net elevation change for a given year (Eq. 5.1). Details on the parameters and probability distributions can be found in Appendix D.1.

$$\frac{dz}{dt} = \sum_{i=1}^n \frac{n_{events,i} * C_{flood} * (h_{HW,i} - z_{marsh}) * f_d}{\rho_{deposit}} - S_{subsidence} \quad (5.1)$$

### 5.3.4. Wave forcing and attenuation by the foreshore

The SWAN wave model was used to compute wave attenuation across the foreshore (Booij *et al.*, 1999). It incorporates the effects of wave breaking, the influence of the wind, and bottom friction. The friction across the marsh platform was incorporated as a bottom roughness with a Manning coefficient of 0.02 m<sup>-1/3</sup>s representing flats under worst-case open-water conditions (Wamsley *et al.*, 2010).

The water level, wave and wind conditions at the marsh edge were retrieved from Rijkswaterstaat's hydraulic database for foreshores in the Wadden Sea (Rijkswaterstaat, 2011) and processed with Hydra-NL (Table 5.2).

For each of the 108 scenarios over 600 different combinations of wave height, period, water level, and wind speed with exceedance probabilities between 10<sup>-0.1</sup> to 10<sup>-6</sup> yr<sup>-1</sup> were run across the foreshore. The results were stored in a database. Only waves and winds from the north-west along the strait connecting the Dollard to the Wadden Sea were considered as, because of the orientation of the Dollard (see Figure 5.1), only these can result in the critical storm surges and wave heights. The generated database of SWAN computations was used to interpolate arbitrary combinations of wave, wind and water levels in front of the marsh into hydraulic parameters at the dike toe without the need to rerun the SWAN model itself. This sped up the iterative dike failure computation (see section 5.3.5) which requires in the order of 100's of evaluations of the attenuation provided by foreshore under changing hydraulic parameters to compute the failure probability of the dike under a specific scenario.

5

**Table 5.2** Return periods of inundation depth ( $d$ ), significant wave height ( $H_s$ ) and wave peak period ( $T_p$ ) at the edge of the Dollard marshes as calculated with Hydra-NL

Return period [yr]	$d$ [m]	$H_s$ [m]	$T_p$ [s]
10	2.78	1.34	4.14
100	3.69	1.85	4.90
1,000	4.47	2.35	5.52
10,000	5.18	2.85	6.05
100,000	5.84	3.37	6.52

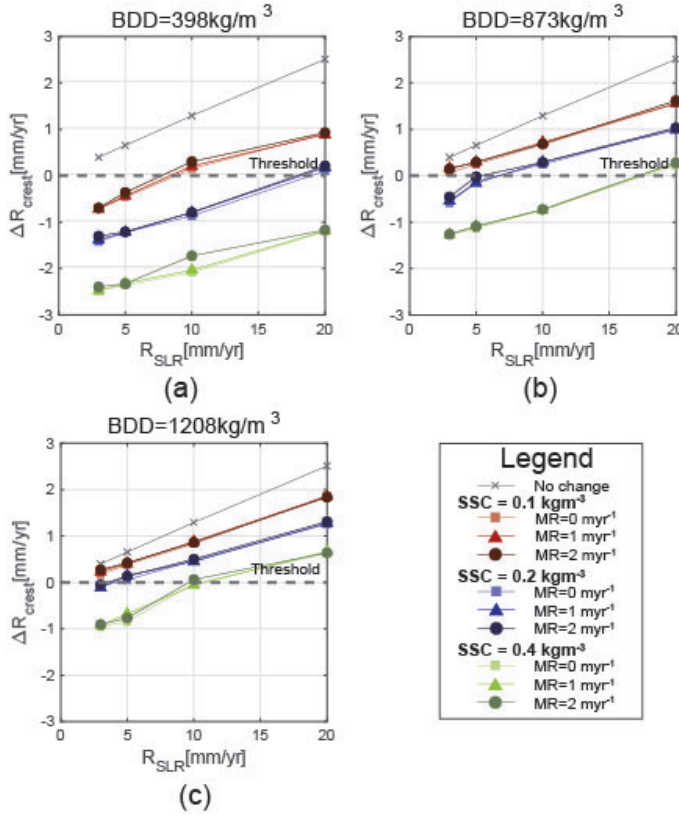
### 5.3.5. Dike reinforcement calculation

Dikes need to be high enough to limit the risk of waves eroding the dike by overtopping to an acceptable level. For dikes along the Dollard the safety level for dike failure is  $1/4000 \text{ yr}^{-1}$ . As dikes can fail by multiple mechanisms across the length of the transect, a correction factor needs to be applied when evaluating a cross-section of a specific failure mechanism. In accordance with the Dutch guideline “*Designing with flooding probabilities*” (Rijkswaterstaat, 2017) the acceptable level of overtopping for a given cross-section should be approximately  $1/200,000 \text{ yr}^{-1}$ .

The amount of wave overtopping is computed with the formulas in the Eurotop manual (van der Meer *et al.*, 2016). The dike is considered to have failed when the amount of overtopping exceeds the critical amount of overtopping to initiate erosion (see Appendix D.1 for parameter values and Appendix D.2 for the formulas). The risk of such a failure was calculated with the First Order Reliability Method (FORM) algorithm by Low and Tang (2007) implemented in the non-linear optimizer `fmincon` in MATLAB. The procedure iteratively searches the likeliest set of input parameters where failure is initiated. The dike crest height was varied and evaluated with the FORM algorithm until a crest height was found meeting the safety standard (see Appendix B for details). In this manner a crest height was computed for each of the 108 scenarios with varying sea-level rise, suspended sediment concentration, marsh retreat rate and foreshore compaction. The reinforcement is simply the difference between the required crest height at the end of the 20-year scenario and the start of the scenario.

## 5.4. Results

The required rate of dike reinforcement for all different combinations of bulk dry density (BDD), suspended sediment concentration (SSC), sea-level rise (SLR) and marsh retreat scenarios (MR) (Table 5.1) are shown in Figure 5.3. Intuitively one would expect that for every millimetre of sea-level rise requires an equivalent amount of dike reinforcement would be necessary. The difference between the rate of sea-level and the year-averaged amount of dike heightening required ( $\Delta R_{\text{crest}}$ ) depends on the relative amount of marsh accretion and retreat compared to sea-



**Figure 5.3** The year-averaged dike heightening rate ( $\Delta R_{\text{crest}}$ ) on top of sea-level rise ( $R_{\text{SLR}}$ ) for the Dollard in the Dutch Wadden sea. The grey line represents a static foreshore without any morphological changes. The colours suspended sediment concentrations. The marsh retreat rate scenarios are denoted by the symbols and variations in shade of colour. The dashed black line at  $\Delta R_{\text{crest}}=0$  is the threshold, above which the year-averaged rate of dike reinforcement exceeds the anticipated rate of sea-level rise

**Table 5.3** Fitted parameters of the generalised linear model of Eq. 5.2. See text for the symbols

	Estimate	95% confidence range	Unit
$a_{\text{SLR}}$	8.76E-02	8.2E-2 — 9.4 E-2	-
$a_{\text{Cflood}}$	-4.90E-03	-5.2E-3 — -4.6E-3	$\frac{\text{m}^4}{\text{kg} * \text{yr}}$
$a_{\text{marsh}}$	3.13E-05	-1.8E-5 — 8.0E-5	-
$a_{\text{BDD}}$	1.60E-06	1.5E-6 — 1.7E-6	$\frac{\text{m}^4}{\text{kg} * \text{yr}}$
$b$	-1.23E-03	-1.4E-3 — -1.1E-3	$\frac{\text{m}}{\text{yr}}$
<b>Goodness of fit:</b>			
$R^2$	0.96		-
RMSE	2.1E-4		$\frac{\text{m}}{\text{yr}}$

level rise resulting in more or less attenuation of waves.

To infer the sensitivity of the dike reinforcement rate to the changes, a linear model (LM) was fit to the results in the form of:

$$(R_{crest} - R_{SLR}) = a_{SLR} * R_{SLR} + a_{cflood} * C_{flood} + a_{marsh} * R_{marsh} + a_{BDD} * \rho_{deposit} + b \quad (5.2)$$

Where  $R_{crest}$  is the required rate of dike heightening,  $R_{SLR}$  is the rate of sea-level rise,  $R_{marsh}$  is rate of marsh retreat,  $\rho_{deposit}$  is the density of deposited sediment,  $a_{SLR}$ ,  $a_{cflood}$ ,  $a_{marsh}$ ,  $a_{BDD}$ , represent the local sensitivity to each of these variables and  $b$  is a model constant. The threshold, above which dike reinforcement outpaces sea-level rise is found by rearranging Eq. 5.2 as follows:

$$R_{SLR,crit} = \frac{-a_{cflood}C_{flood} - a_{marsh}R_{marsh} - a_{BDD}\rho_{deposit} - b}{a_{SLR}} \quad (5.3)$$

First of all the least-squares fit of the sensitivity parameters  $a$  and constant  $b$  approximates the solutions of the modelling procedure well (**Table 5.3**). This suggests that, at least for this specific case-study, a LM is sufficient to describe the influences between the dike reinforcement rate, the rate of sea-level rise, sediment concentration in the estuary and the average density of deposited soil on the foreshore for the immediate future (up to 20 years). From the LM it is substantially easier to infer the relative influences of the future processes on dike reinforcement.

There is only a small effect expected of erosion of the marsh edge on failure of the dike by overtopping at its current width of 750 m. This is clearly visible in **Figure 5.3** and in the p-value computed for the marsh width in the linear regression (p=0.21). A p-value higher than 5% from the t-test is not sufficient to accept the hypothesis that marsh retreat has an influence on future dike reinforcement. Interpreted physically, the marsh width remains sufficient to dampen waves close to its full potential under extreme conditions for the foreseeable future in spite of the marsh receding.

In the current situation of the Dollard with an average 0.2 kg/m<sup>3</sup> suspended sediment concentration (SSC), 1 m/year erosion of the marsh edge, and a bulk dry density on the foreshore of 873 kg/m<sup>3</sup>, the critical rate of sea-level rise for dike reinforcement is estimated to be 8.9 mm/yr. The sediment concentration is thus contributing substantially to mitigating future dike reinforcements. Halving the SSC 0.1 kg/m<sup>3</sup> reduces the critical rate of sea-level rise to only 3.3 mm/yr while a doubling of SSC to 0.4 kg/m<sup>3</sup> increases it to 20 mm/yr. In other words, halving or

doubling of the present-day suspended sediment concentration determines whether dike reinforcement needs to accelerate beyond sea-level rise in the near future, or only at sea-level rise rates found in the highest projections.

The range of bulk dry densities tested had a large influence on the results. While in the current situation the critical rate of sea-level rise was found to be 8.9 mm/yr, if in the future compaction of the foreshore would be limited to 400 kg/m<sup>3</sup> the critical rate of sea-level rise moves to 17.6 mm/yr. On the other hand if in an extreme case human activity would fully compact the foreshore to 1200 kg/m<sup>3</sup> present-day sea-level rise would already result in a dike reinforcement rate higher than sea-level rise. Changing management to limit compaction (400 kg/m<sup>3</sup>) or allow almost full compaction of the clay (1200 kg/m<sup>3</sup>) of the foreshore is roughly equivalent to doubling or halving SSC on the marshes for the rate of dike reinforcement.

## 5.5. Discussion

The question this paper set out to explore was how influential the dynamics of a natural foreshore are for future reinforcements of a dike-wetland system. The results of the Dollard case-study show that interventions altering the supply of sediment and management of the foreshore strongly affect the rate of dike reinforcement. There are examples of cases where the sediment supply has been halved (Yang *et al.*, 2006) and marsh soil was strongly compacted after extensive agricultural use (Tempest, Harvey, & Spencer, 2015). Effective adaptation thus should strongly consider the impact of other uses on the foreshore as and developments within the delta that could affect the sedimentary processes of the marsh.

The focus on sedimentary processes exclusively for dike reinforcement in this case-study, rather than biological factors, is an indirect result of the extreme hydraulic loads that need to be withstood to meet the desired safety level. Under design conditions waves of at least 2.5 m high and water depths over 4.5 m deep were expected. The breaking of stems (Vuik *et al.*, 2018a), and large inundation reducing drag forces by vegetation (Mendez & Losada, 2004) as well as the storm surge attenuation capacity (Stark *et al.*, 2015), leave only the elevation created

through accretion of the marsh as a viable contribution of the marsh. It can be expected that for other areas where the desired safety level is lower and the dike is more sheltered from extreme loads these processes can significantly contribute to flood protection and should be incorporated for an accurate assessment.

For the case-study in the Dollard marsh recession was not significantly affecting dike reinforcement in the foreseeable future. The 750 m width of the marsh is still sufficient to cope with recession. While direct dampening by stems was not included in this study, this agrees with many observations that most waves break at the edge of the marsh and further dampening decays landward (Möller *et al.*, 2014; Möller & Spencer, 2002; Schoutens *et al.*, 2019). According to Möller *et al.* (2014) a width of 40 m is sufficient to already reduce 15% of the incoming waves height. As our study shows, the modelled lateral dynamics of marshes do not conflict with flood protection objectives as long as a sufficient width is maintained.

The future sediment concentration, and subsequently the turbidity of the Ems-estuary, is still highly uncertain. If the water quality is improved by reducing the amount of suspended sediment the accretion of the marshes is negatively affected and more dike reinforcement is necessary. This is not the full picture if the reduction in turbidity was achieved by new wetlands or borrowing pits designed to capture sediment for re-use in dike reinforcement. In that case the measures would locally increase the required dike reinforcement from decreased sedimentation, but still aid in flood protection by capturing more sediment as a building material for use in flood protection on a larger scale.

This modelling study demonstrates the importance of sediment transport towards marshes has for future dike reinforcements. Human actions like damming rivers, dredging, or building coastal infrastructure can similarly result in a lower supply (Peteet *et al.*, 2018; Yang *et al.*, 2001) and thereby necessitate more dike reinforcement. On the flipside adding sediment through suppletions can also be a viable addition to flood adaptation strategies (Baptist *et al.*, 2019; Ford *et al.*, 1999). The suppleted sediment has to accumulate on the marsh for longer time-scales and not degrade other areas of the system (Baptist *et al.*, 2019; Ganju, 2019). Doing so effectively requires extensive knowledge of the local hydrodynamics and morphology. Baptist *et al.* (2019) mention the Dollard as a location where suppletion would be possible, but is undesirable because it conflicts with water

quality objectives. Furthermore as Vuik *et al.* (2019) noted, while promoting the process of sediment accretion in the marsh decreases the probability of failure of the flood defence, artificial break waters in the marsh can still be more cost-effective in the short-term. Suppletion would therefore not be a preferred option for the Dollard.

Finally this study also suggests compaction of the marsh by human use affects dike reinforcements in the future. While we did not investigate what types of uses or processes in the marsh contribute to compaction of the marsh, it is reasonable to posit that limiting compaction within the marsh will improve the resilience of both the marsh and dike system to sea-level rise. Grazing on the marsh is one such process that contributes to compaction. Studies did find higher compaction and overall shorter vegetation at grazed sites, but are yet to find a statistically significant difference in accretion rates between grazed and ungrazed sites (Elschot, Bouma, Temmerman, & Bakker, 2013; Nolte *et al.*, 2013). Spatial processes affecting the distribution of sediments across the marsh were found to be more important for accretion rates than grazing (Nolte *et al.*, 2013). A better site-specific understanding of grazing, compaction and accretion processes is needed for assessing the impacts of grazing specifically for a flood protection strategy.

The modelled results of this study show that sea-level rise will necessitate dike reinforcements under the modelled conditions. Extrapolating the LM of the Dollard beyond its range suggests that only an increase of SSC to  $0.7 \text{ kg/m}^3$  is sufficient to fully mitigate the effects of the present-day sea-level rise for flood protection through marsh accretion. Regardless of whether a tripling of SSC is physically feasible, it would conflict with the ambitions to improve the water quality by reducing SSC. Many marshes are inundated with lower SSC concentrations than found in the Dollard. Therefore it is infeasible marshes alone will be sufficient to mitigate the increasing flood risk from sea-level rise. Instead of a replacement for traditional reinforcement measures, marshes act as buffers for the effects of sea-level rise while simultaneously providing valuable services to the ecosystem.

Apart from the marsh component, the modelling approach we used to assess hydraulic loads and overtopping is widely accepted for analyses of dikes in the Netherlands (Slomp *et al.*, 2015). The modelled marsh behaviour was, however,

simplified to a large degree. Important spatial morphological processes and features were omitted like: resuspension and erosion events, creek formation, vegetation growth and distribution, and the feedbacks between these spatial processes. Superior models exist that resolve these interactions and the approach of this study should only be considered an exploration. Feedbacks like described in Mariotti and Fagherazzi (2013) could accelerate recession. Furthermore, rare events could result in a sudden large scale die-off of marsh affecting its evolution over time (e.g. a year of extensive herbivory or a significant storm event). Nevertheless, simple models still tend to be the most suitable for a simple exploration of the general behaviour of wetlands (Fagherazzi *et al.*, 2012).

## **5.6. Conclusions**

In recent years, it has been recognized that marsh ecosystems play a role in flood protection, because of their wave- and storm surge attenuation properties. Few studies, however, quantified the processes affecting marshes in relation to the challenge of reinforcing defences against sea-level rise.

Studies from the past two decades focussed on three main contributions of marshes to flood protection: (1) wave attenuation by vegetation, (2) storm surge attenuation, and (3) stabilisation and accretion of foreshores. Accretion of foreshores directly counter-acts the effects of sea-level rise on the propagation of waves. The effectiveness of wave attenuation by vegetation and storm surge attenuation is limited for high storm surges with high wave heights. Therefore, accretion is the most important process to consider in flood protection schemes. Furthermore anecdotal evidence from literature reveals that the sediment supply needed for accretion can be greatly influenced by human actions in the delta.

A simple marsh accretion model of the Dollard marsh-dike system was combined with the design procedures for dikes to explore the effects of sediment supply, marsh retreat and marsh compaction on sea-level rise adaptation schemes. At present day conditions, a sea-level rise exceeding 8.9 mm/yr would require dikes to be heightened at a faster pace than the rate of sea-level rise. Halving the supply of sediment to the marsh reduces the threshold to a sea-level rise rate of 3.3 mm/yr while doubling the sediment supply increases it to 20 mm/yr. Similarly if the bulk

dry density of the deposited soil would remain low this threshold is at 17.6 mm/yr while if the soil would be highly compacted by human activity marsh accretion would already be insufficient at present day sea-level rise. In short, suspended sediment concentration, as well as management of the foreshore to limit compaction of the marsh determines whether dike reinforcement needs to accelerate beyond sea-level rise in the near future, or only at sea-level rise rates found in the highest projections

Our results and modelling approach are also interesting for other regions. While the focus of flood risk adaptation schemes is usually on sea-level rise itself, the results of this study show there is a great deal of influence people have on the extent of future dike reinforcements through the management of marshes.

## **Acknowledgments**

We would like to thank Erik Jolink from the water board Hunze en Aa's and project leader of the Wide Green Dike project for his help and collaboration that made this research possible. We would further like to thank Peter Esselink for sharing his knowledge and experience with the Dollard marshes to the authors. Finally, we want to thank the two anonymous reviewers for their comments that improved the manuscript.

## **Appendices**

Appendices to this chapter can be found starting from page 225.



# 6

# General Framework

R.J.C. Marijnissen

This chapter uses sections from the conference paper:

Marijnissen, R.J.C., Kok, M. Kroeze, C., van Loon-Steensma, J.M. (2021) . The four components to combine flood protection with other functions. Paper presented as part of the proceedings of the online FLOODRisk2020 conference (June 2021). [https://floodrisk2020.net/uploads/papers/12\\_3/12\\_3-FLOOD-risk2020\\_full%20paper\\_RM\\_5Jan-1610016805.pdf](https://floodrisk2020.net/uploads/papers/12_3/12_3-FLOOD-risk2020_full%20paper_RM_5Jan-1610016805.pdf)



## 6.1. Introduction

Throughout the previous chapters methods for assessing the safety of multifunctional flood protection have been discussed. As explained in Chapter 1, an existing probabilistic framework for assessing flood defences (WBI2017) (Slomp *et al.*, 2016) was used as a starting point for defining a multifunctional framework. In this framework, the presence of any function must not lead to an unacceptably high probability of failure of the flood defence. The probability of failure is calculated from analysing the failure mechanisms of the flood defence. The most common modes of failure of a flood defence are overflow, overtopping, piping, and macro (in)stability (Allsop, 2007; Danka & Zhang, 2015). Assessing the probability of failure of these mechanisms can vary from empirical relations based on tests, to numerical simulations (**Table 6.1**).

Regardless of the methods used, at the core of any safety assessment is a limit state function ( $Z = R - S$ ). When  $Z < 0$  failure of the flood defence is assumed as the soliciting loads ( $S$ ) are greater than the resistance ( $R$ ) of the flood defence. The loads are most often hydraulic loads like water level, wave characteristics, and the duration of the storm or high water. The resistance is determined by the design of the flood defence (e.g. the crest height). Both  $S$  and  $R$  are composed of uncertain factors and hence  $Z$  will be uncertain. These uncertainties are modelled as probability density functions (PDFs). The goal of a designer of a flood defence is to ensure that the probability of  $Z < 0$  remains below the safety norm.

A designer of a flood defence has several methods to ensure the flood defence meets the safety norm. Some loads are subject to the design itself (e.g. the external weight of an additional structure). The main tool for a designer to meet the safety standard is through the design of the flood defence itself. The resistance to the loads must be delivered by the different elements of the flood defence. The flood defence can be decomposed in: the geometry (its height, width, slope angles, etc.), and the material composition (sand, clay, asphalt, etc.). The dike composition is further broken down based on its location:

- the revetment, i.e. the outer shell,
- the core,
- and the soil beneath the dike including features like sheet pile walls.

**Table 6.1** The failure mechanisms and methods to assess them. Common procedures for Dutch dike assessments are presented in Rijkswaterstaat (2016c).

Failure mechanism	Description	Assessment Methods in the Dutch assessment procedures
<i>Overflow and overtopping</i>	Flow of water across the dike crest and inner slope	Wave overtopping: (van der Meer <i>et al.</i> , 2016), (TAW, 2002), (de Waal, 1999) Overtopping resistance: Critical overtopping discharge, (van der Meer <i>et al.</i> , 2016), (Rijkswaterstaat, 2016c)
<i>Piping</i>	Excessive flow of groundwater beneath the dike resulting in erosion of the subsoil	Uplift: Basic force balance (Rijkswaterstaat, 2016c) Heave: Empirical critical heave gradient (Rijkswaterstaat, 2016c) Erosion: (Sellmeijer <i>et al.</i> , 2011)
<i>Macro stability inner slope</i>	Sliding of the soil at the inner slope	Basic methods: (Bishop, 1955), (Morgenstern & Price, 1965), (Spencer, 1967), (Janbu, 1973), Lift-(Van, 2001) Advanced methods: Finite elements modelling, e.g. (Griffiths & Fenton, 2007), (Bakker <i>et al.</i> , 2019)
<i>Erosion of grass revetment on outer slope</i>		Empirical cumulative overload method (de Waal & van Hoven, 2015a, 2015b; Rijkswaterstaat, 2016c)
<i>Erosion of other type of revetment on outer slope</i>	Damage and erosion of the protective outer layer of the dike by waves	Asphalt: GOLFKLAP model: (de Looft, 't Hart, Montauban, & van de Ven, 2012) Empirical uplift criterion (Rijkswaterstaat, 2016c) Stone: Stability under uplift: force balance, e.g. (Klein Breteler, Mourik, & Provoost, 2014) Stability against sliding: force balance (Rijkswaterstaat, 2016c) Other: sub-failures have been omitted from this table.
<i>Other</i>	-	-

6

**Table 6.2** Connections between dike elements, storm conditions, and failure mechanisms. A "X" denotes a connection.

	Resistance factors						Load factors			
	Dike geometry			Dike composition			Hydraulic loads			Other
	Crest height	Berm /dike width	Dike slope	Revetment material	Core material(s)	Subsoil	Water level	Wave action	Event duration	External loads
<i>Overflow &amp; Overtopping</i>	X	X	X	X	(X)*		X	X	(X)*	
<i>Piping</i>		X				X	X		(X)*	
<i>Macro stability</i>		X	X	X	X	X	X		(X)*	X
<i>Revetment failure</i>			X	X	X		X	X	X	

\*Usually omitted or substantially simplified for basic assessments and/or design calculations

Connections between the components of the dike resisting failure mechanisms are presented in **Table 6.2**. For an additional function in a multifunctional flood defence to affect its safety it needs to interact with the dike geometry, dike composition or the loads (the columns in **Table 6.2**).

As introduced in Chapter 1, the aim of this PhD research is to investigate how combining different activities on or near flood defences affects the safety provided by flood defences assessed using a risk-based approach. In the previous chapters case-studies have been explored to quantify the flood protection provided by different multifunctional flood protection designs. Based on these case-studies, changes to the probabilistic assessment framework have been proposed. In this chapter the explored changes to the probabilistic assessment framework are summarised into one framework for assessing multifunctional flood defences. Furthermore, this chapter describes how these multifunctional elements and flood protection are linked through the design of a flood protection measure. This will help designers and managers of flood defences to better assess the safety implications of multifunctional use on flood defences.

Section 6.2 presents a reflection on the case-studies. The different multifunctional elements encountered are summarised along with the influenced design features of the flood defence. Furthermore, it presents the changes to the assessment framework made to quantify flood risk in the case-study. Section 6.3 generalises these insights by linking multifunctional elements through the flood defence design to flood risk (6.3.1), then links these design elements to changes in the assessment procedure (6.3.2) to finally arrive at the framework for assessing the safety of multifunctional protection (6.3.3). The framework is discussed (6.4) and finally the conclusions are presented (6.5).

## **6.2 Reflection on the case-studies**

### **6.2.1 Multifunctional use along river dikes**

The first case was presented in Chapter 2 and represents a “prototypical” multifunctional river dike (**Figure 6.1**). In the original framework (WBI2017, see (Rijkswaterstaat, 2016c)) other uses are not mentioned explicitly, but are represented by non-water retaining objects (NWOs). The functions covered are:

nature in the form of woody vegetation, infrastructure in the form of pipelines, and structures for e.g. housing. An exception is transportation. The loads on the flood defence by cars and trucks need to be considered in stability calculations if they can plausibly be expected on the dike in flood scenarios. Other functions, e.g. recreation, are often not considered to have an effect on safety.

According to the Dutch WBI guidelines (Rijkswaterstaat, 2016c), but also international standards like the levee handbook (Sharp *et al.*, 2013), the dike should be dimensioned such that the objects do not interfere with the minimal profile needed to retain water under extreme conditions unless the safety of a MFFD can be demonstrated with tailored studies. In **Figure 6.1** for example, the subsoil is penetrated by the roots of vegetation. This poses a risk of water seeping into a sandy layer below the dike and result in piping beneath the flood defences. The basic method suggested in the WBI is to pad the dike geometry, such that these functions no longer interfere with the minimal required profile, e.g. adding a stability or piping berm. In effect, the regions of the dike affected by multifunctional use are excluded from the assessed dike profile.

As Chapter 2 demonstrates, this conservative approach in the guidelines can result in overestimating the probability of failure by several orders of magnitude. Instead, Chapter 2 proposes the use of scenarios to account for changes in the dike geometry (e.g. a hole from an exploded pipeline), or the properties of materials (e.g. the resistance of grass to overtopping) due to the multifunctional use. This approach allows for benefits of multifunctional use (e.g. a building stabilising soil at the dike toe) to be incorporated in the design.

### 6.2.2 Multifunctional use by multiple defences

The Double Dike at Delfzijl (**Figure 6.2**) was analysed in Chapter 3 as an example of a multifunctional flood protection with multiple flood protection structures. Rather than a single structure, the combination of structures must comply with the safety standards. In the case-study, the multiple defences allow the area in between to be used for trapping silt in the Ems estuary (similar to the Wide Green Dike), nature development, aquaculture, and saline agriculture. Thus, the addition of other uses resulted in the addition of a culvert and a second dike.



**Figure 6.1** Example of a river dike with common multifunctional elements like trees, a house and a pipeline in the inner dike toe.



**Figure 6.2.** The Double Dike as implemented between Eemshaven and Delfzijl, the Netherlands. At the top a section is dedicated to nature and clay extraction and the bottom is designated for agri- and aquaculture. Each section is connected by structures through the dike.



**Figure 6.3.** The Wide Green Dike, as implemented in the Dutch Dollard estuary. Left of the dike is the marsh with the extraction pit around the bird island. Right of the dike there is an area to process and store extracted clay.

For the analysed case the seaward dike was wider and higher than the landward dike, hence flood protection was primarily provided by the seaward dike (see Chapter 3). Furthermore, in the assessed case-study a culvert will be made in the seaward dike, introducing an additional failure mechanism, i.e. failure to close the culvert. Only in cases of non-closure of the culvert, excessive overtopping of the first dike, or a breach of the first dike, additional flood protection is provided by the second dike. Thus, loads on the landward dike depend on processes at the seaward dike. Chapter 3 proposes to consider parallel flood defences as objects transmitting hydraulic loads from the river or sea towards the final flood defence. After transforming the hydraulic load distributions sequentially across the foreshore and parallel defences, the safety of the entire system is evaluated from the transmitted hydraulic loads and the resistance of the last flood protection structure.

### 6.2.3 Long-term use of multifunctional dikes

The Wide Green Dike concept was analysed in Chapters 4 and 5 as an example of a flood defence designed for long-term benefits of multifunctional use. It is located in the Dutch Dollard region of the Ems estuary in the Wadden Sea near the border between Germany and the Netherlands. It features a shallow slope of approximately 1:7 at the seaward side (hence “wide”) with only a grass revetment (hence “green”) (see **Figure 6.3**) (van Loon-Steensma *et al.*, 2014c). The grass revetment extends into the extensive Dollard salt marshes. The concept is to reinforce the dike with clay extracted locally from borrowing pits in the salt marsh. Furthermore, the pit acts a sediment sink to improve water quality while the middle of the pit features a breeding island for birds. The multifunctional aspect of the Wide Green Dike concept is primarily through the connections between the dike reinforcement and the uses of the foreshore. The use of clay from local clay pits to reinforce the outer slope resulted in a design with a shallow outer slope and a thick clay layer.

In Chapter 4 the concept of retrieving sediment from the foreshore for future reinforcements against sea-level rise was explored. Modelling the sedimentation on the foreshore, the pit is expected to be refilled within 20 years, after which it can be re-excavated. While clay pits do re-create pioneer marsh vegetation (Vöge, Reiss, & Kröncke, 2008), large scale clay extraction should be managed to avoid trade-offs for nature values, further permanent marsh loss or impede the marsh’s capacity to accrete in response to sea-level rise. Chapter 5 analysed the interaction between sea-level rise, sedimentation on the foreshore, and the hydraulic loads on the flood defence. Chapter 5 concludes the accretion on foreshores dampens the need for dike reinforcements with sea-level rise. However, the extent of this dampening is strongly affected by the sediment supply and the management of the foreshore. While both chapters do not propose changes to the assessment framework for dikes, they do consider the management of the foreshore through the interactions with hydraulic loads as a feature of the flood protection measure.

## 6.3 General framework for multifunctional dike design

### 6.3.1 Linking multifunctional design to flood risk

To incorporate multifunctional use in a flood defence several components may be added or changed (**Figure 6.4**). These correspond with the components already identified in **Table 6.2**, but with the addition of the foreshore. This was motivated by both the Wide Green Dike and Double Dike cases. Most of the multifunctionality of the Wide Green Dike was derived from the foreshore of the system, rather than any multifunctional use of the dike itself. Foreshore elevation (e.g. by marsh accretion) and composition (e.g. the higher roughness of a marsh substrate) can work in conjunction to decrease loads (e.g. through wave breaking and friction) (Chapter 5). The case of the Double Dike can be evaluated from another perspective, as the primary seaward dike can also be perceived as an object transmitting hydraulic loads to the final landward dike (Chapter 3). However, when the seaward defence provides most safety against flooding, like in the case-study of Chapter 3, it may seem counter-intuitive to classify a seaward flood defence providing the bulk of the safety against flooding as an “*object*” within the safety framework rather than as a flood defence. Indeed, if little safety is provided by the landward defence a practical approach could be to assess the seaward defence with minor adjustments to the failure criteria based on the presence of the second defence (e.g. allowing larger amounts of overtopping). Nevertheless, the approach suggested in this thesis is intended to be generalisable to other configurations of systems with multiple defences (Chapter 5).

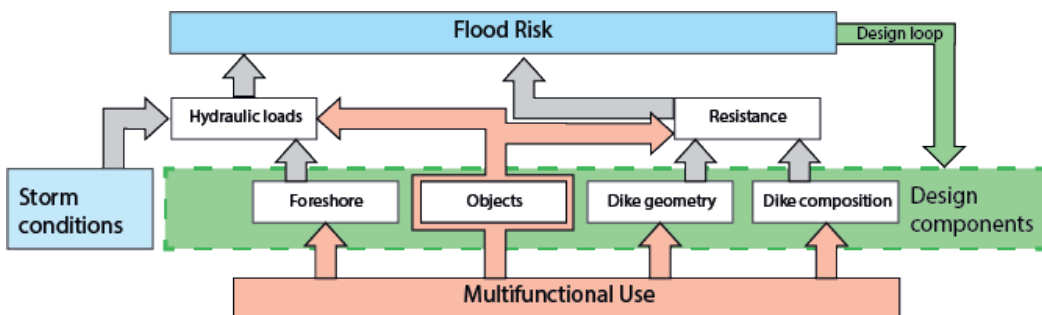
Allowing multifunctional use by changes in dike geometry has been the default approach as for example suggested by van Loon-Steensma and Vellinga (2014). This approach has been used for the concepts of delta dike, unbreachable dike, and the super dike (de Moel *et al.*, 2010; Knoeff & Ellen, 2011; Nakamura, 2016; Silva & van Velzen, 2008). While these dike concepts differ in geometry from traditional designs due to multifunctional elements, these geometry changes are a consequence of excluding multifunctional elements in conservative safety assessments rather than optimisation in multifunctional design (Chapter 2). Also in the case-study of the Wide Green Dike, multifunctional use did affect the dike

geometry. Because of the choice to preserve the landscape value of a green grass dike and re-use clay extracted from the estuary, the dike's slope was made less steep to increase the resistance of the dike to wave impacts (Chapter 4). Thus, multifunctional use directed the design of the dike's geometry.

Dike composition is another way to introduce multifunctional use. The grass cover on the Wide Green Dike for landscape values is one such example where the material was not (primarily) chosen for its effectiveness in flood protection. A similar concept in which the dike's ecological value is enhanced by flowers or weeds on its outer cover, is another example. The erosion-resistance of the dike cover is primarily governed by the root density and the overall root depth (Scheres & Schüttrumpf, 2019; Vannoppen, Poesen, Peeters, de Baets, & van de Voorde, 2016).

Introducing additional vegetation species to improve the ecological value of the dike therefore has a direct influence on the dike design when it affects the allowable amount of water flowing on the inner slope without erosion (e.g. in deciding the necessary crest height against overtopping). Another example of multifunctional design is integrating the wall of a house as a retaining wall (van Veelen *et al.*, 2015).

Objects can be anything on a dike that interacts with the movement of water on, within, or beneath the dike, can apply loads on the dike, or alter properties of the dike (e.g. damage). This makes objects a broad category. Objects traditionally found on flood defences are fences, trees, houses, cables, pipes, pavements, roads, etc.. Some objects, e.g. in the case of a pipeline, may result in such severe damages



**Figure 6.4** The connection between multifunctional use, flood risk, and the design choices within a flood defence. Red arrows denote the influence of multifunctional use, the green block contains design elements, and the blue blocks represent flood conditions.

that it can be considered a separate failure mechanism (Schelfhout *et al.*, 2020). While the types of risks, opportunities, and uncertainties vary greatly between objects, in general objects can be considered to affect flood risk through interactions on the (local) hydraulic loads, applying loads directly, or by influences on the resistance of a dike to a failure mechanisms (e.g. by introducing damages). Objects also introduce uncertainty when the object can be in different states during a potential flood event, each state resulting in different interactions with hydraulic loads and/or the resistance of the dike. As demonstrated in Chapter 2, not only the worst-case negative interactions of an object affect flood risk, but the variability in both negative and positive interactions determines the influence an object has on flood risk.

### 6.3.2. Implementation of multifunctionality in dike safety assessments

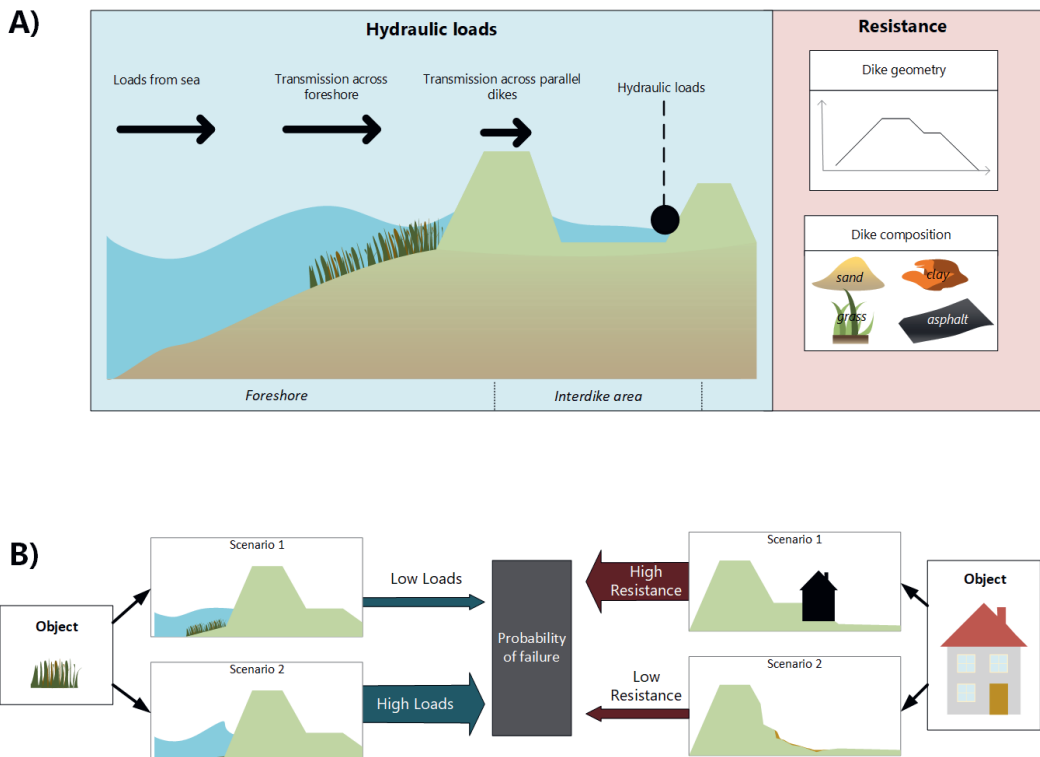
The four types of multifunctional design components require each a different implementation in the risk framework. **Figure 6.5** presents how the multifunctional components from **Figure 6.4** fit into assessment of failure mechanisms through hydraulic loads and resistance factors (**Table 6.2**).

Foreshore components reduce the hydraulic loads before the flood defence is reached (**Figure 6.5**). Tools and models (e.g. SWAN, X-Beach, Delft-3D) are already present to simulate the behaviour of waves and storm surges across foreshores of different compositions. Foreshores can be dynamic morphological systems and change in composition and geometry over time. Incorporating future changes of the foreshore (whether natural changes or by human intervention) is crucial to assess the hydraulic loads and thus the safety of the flood defence in the future.

Dike geometry and dike composition are integrated in the resistance of a flood defence and are already included in any safety assessment (**Figure 6.5**). Geometry parameters in particular, like steepness of a slope, can already be varied in most design formulas and approaches. Incorporating changes in dike composition can be more challenging if the relevant material properties (e.g. the erosion of marsh clay in the Wide Green Dike case) are uncertain. However, such uncertainties can be reduced by experimentally testing the properties or by employing measures to ensure quality standards are met. In a probabilistic analysis the uncertainties in

material properties are represented by probability distributions. Objects embedded into a material can also be considered as a change in the material property. For example, Aguilar-López *et al.* (2018b) demonstrate a pipeline below a dike can be conceived as a change in hydraulic conductivity of the subsoil rather than as an object within the assessment of the piping failure mechanism.

Objects can possess their own interactions with the hydraulic loads to decrease the resistance of the system (see Chapter 2). These interactions were observed in the treatment of roads (with traffic) and structures in the first example of a proto-typical river dike. Additional loads were applied to the dike directly in conjunction with the hydraulic loads (Rijkswaterstaat, 2019). The interactions between objects, hydraulic loads, and resistance greatly depend on the specifics of the object, how it is used during a high water event, and the particular failure



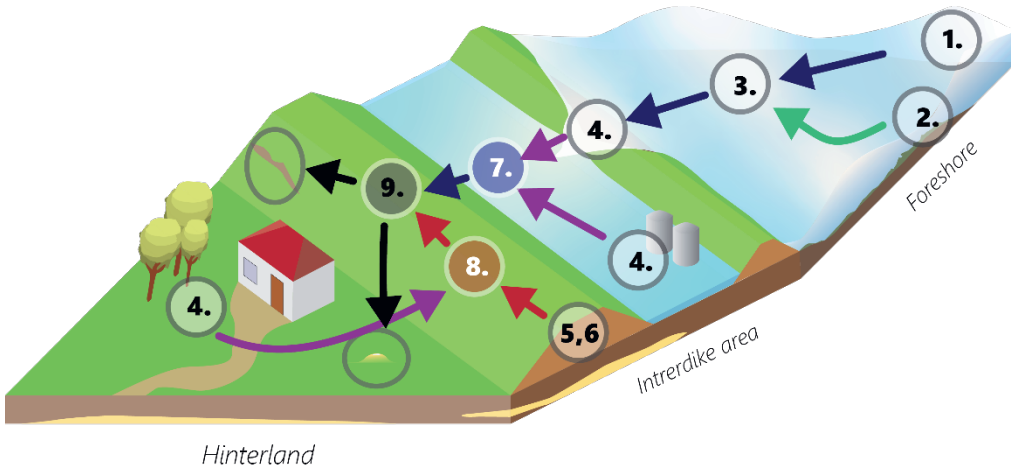
**Figure 6.5** A) Representing the dike geometry, composition and foreshore as part of the hydraulic loads and resistance factors used to assess the stability of flood defences. B) Representing the scenario-approach for objects in terms of hydraulic load and resistance factors for assessing the safety of a flood defence

mechanisms the object interacts with. A scenario-based approach is needed with scenarios for the state of the object during a high water event (including a worst-case one), and attribute probabilities to each scenario (**Figure 6.5**). These scenarios are then evaluated for the relevant failure mechanisms and combined into a single probability with fragility curves (See Chapter 2).

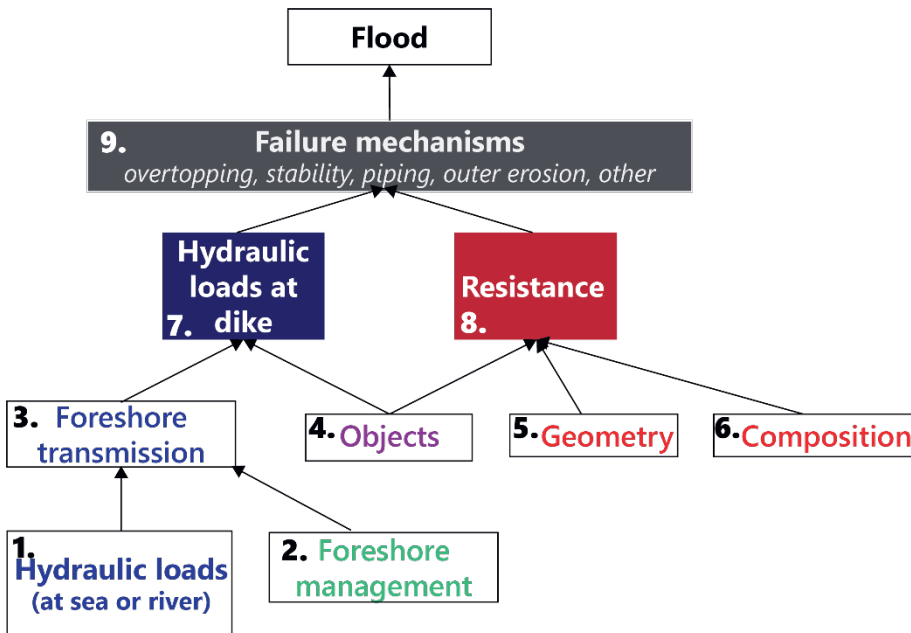
Often the presence of natural features on foreshores like marshes are not included, as relying on these features for flood protection lacks certainty about their presence under changing conditions. Such features can also be considered as objects and assessed with a scenario-based approach. For example, by assessing scenarios of likely extends of vegetated foreshores during critical conditions. Parallel flood defences also fall within this category of objects (**Figure 6.5**). The front dike in the system reduces hydraulic loads on the landward dike by reducing the probability of waves and surges at the final landward defence (see Chapter 3). To determine the erosion and subsequent flows over/through the first defence, complex models are required and makes the assessment of parallel defences challenging. However, once reductions in hydraulic loads are accounted for, the assessment process can proceed as for monofunctional dikes (see Chapter 3). Ideally, a transmission model like in Chapter 3 is determined to directly translate hydraulic loads at the outer defence into hydraulic loads at the landward defence. Otherwise a scenario-based approach can be used.

### 6.3.3. Summary of the adapted framework

After linking the design concepts from the case-studies (section 6.2) to elements for multifunctional dike design (section 6.3.1) and incorporating these in methods for safety assessments (section 6.3.2), this section summarises the framework developed in this thesis. This framework for assessing the safety of multifunctional flood defences is extended from the current Dutch flood protection framework (Kok *et al.*, 2017; Rijkswaterstaat, 2016a, 2016b, 2016c). The steps to design or assess the safety of a multifunctional flood defence are presented visually in **Figure 6.6** and **Figure 6.7**. Chapters exploring steps of the framework in more detail, propose additions, or suggest changes to this framework are presented in between brackets.



**Figure 6.6** A representation of a multifunctional flood protection zone with the numbered components of the risk framework (see Figure 6.7)



**Figure 6.7** The fault tree used to assess the risk of flooding for a flood protection zone (see Figure 6.6)

1. Determine the hydraulic loads within the environment of the food defence using local measurements, hydraulic models, and statistical models.
2. Investigate the changes on the foreshore over time and consider implementing management practises to enhance load reducing capabilities of foreshore land-uses (e.g. accretion and wave damping by marsh vegetation), or reduce the impact of detrimental uses (e.g. reduction in sediment supply by dams). [Chapters 4 and 5]
3. Calculate the impact of foreshore features on the transmission of hydraulic loads from the sea/river [Chapters 4 and 5]
4. Determine a transmission model or set of scenarios with corresponding probabilities for objects interacting with the hydraulic loads and/or the strength of the dike. [Chapters 2 and 3]
5. Evaluate/design changing the dike geometry to enable additional uses of the flood defence [Chapters 2, 3, 4 and 5]
6. When designing, evaluate whether materials synergise with additional uses of or near the flood defence (e.g. a grass revetment with flowers to enhance biodiversity, incorporating local clay, etc.). [Chapters 4, 6]
7. Evaluate the hydraulic loads and associated return periods at the flood defence.
8. Evaluate the parameters and uncertainties thereof to evaluate the resistance of the dike.
9. Compute the probability of failure of the flood defence to all failure mechanisms with the hydraulic load and resistance probabilities.

### 6.4. Discussion

Many dikes are already multifunctional. They may serve a transportation function by a road on top or its slope may be part of a nature reserve. This was covered by the “prototypical” river dike example in this paper. Both traditional assessment standards (Ministerie van Verkeer en Waterstaat, 2007; Rijkswaterstaat, 2016c) and other literature (van Loon-Steensma & Vellinga, 2014) assert a negative effect of functions for a design of a flood defence to ensure a safe design. This is understandable, as functions do not necessarily provide direct benefits for flood protection or those benefits are uncertain (van Loon-Steensma & Kok, 2016). As a

consequence, however, defences will not gain any safety benefits from other functions in this approach.

Voorendt, Vrijling, and Voortman (2017) distinguish different levels of functional integration based on the overlap of functions with water structural elements of the flood defence. Voorendt identified 8 types of structural elements multifunctional for MFFDs (Voorendt, 2017; Voorendt *et al.*, 2017). The underlying idea is that multifunctional design can only improve safety if an element required for multifunctional use can fulfil the function of a structural element of a flood defence (e.g. the walls of a parking garage that also serve at the same time as retaining walls). However, these types of functions were not included in the rural case-studies explored in this thesis, as these are more common in urban settings (Stalenberg, 2013; Voorendt, 2017). This view of multifunctionality ties in neatly with the dike composition elements identified in this chapter, where material or composition design choices are motivated by multifunctional use.

The frameworks for MFFDs so far had only a limited scope of multifunctionality of dike design. However, there is a push to look beyond the dike itself in developing integrated multifunctional flood protection solutions. For example, a growing body of scientific literature is starting to connect natural processes in foreshore ecosystems like coral reefs, salt marshes, and mangroves, to flood risk mitigation (Borsje *et al.*, 2011; Ferrario *et al.*, 2014; Guannel, Arkema, Ruggiero, & Verutes, 2016; Vuik *et al.*, 2016) (Borsje *et al.*, 2011; Ferrario *et al.*, 2014; Guannel, Arkema, Ruggiero, & Verutes, 2016; Vuik *et al.*, 2016). Such opportunities to enhance flood protection are overlooked when reinforcement is only focussed on the dike itself, rather than entire flood protection zone. The cases in this thesis furthermore highlight that multifunctionality can be integrated across the entire flood protection zone, from the foreshore until multiple lines of flood defences. The framework presented in this thesis thus allows for a wider application of MFFDs than other studies had so far.

While the links between multifunctional use and flood protection cover a wide range of practical applications, it does not consider the benefits of a flexible design over a static one. This may further alter the design choices, provided safety remains guaranteed during the design period. Studies have suggested natural elements can add flexibility and resilience to regular defences under a changing

climate (van Slobbe *et al.*, 2013; van Wesenbeeck *et al.*, 2014). Building with nature measures like the suppletion of sand or silt on marsh foreshores are such examples (Baptist *et al.*, 2019; Stive *et al.*, 2013). Under favourable conditions, natural systems can adapt to a changing environment and reduce the need for future reinforcements. Flexibility and adaptability aspects are usually not captured in designs made on to basis of assessments at the end of the flood defence's design life. In the long term, not accounting for these leads to more expensive designs for both monofunctional and multifunctional dikes (Anvarifar *et al.*, 2017).

Finally, it is important to stress that flood protection and costs are never the only factors governing the choice for a multifunctional flood defence. A proper integration of other functions will add other values to the area by for example various ecosystem services by nature, recreation, etc. . These benefits need to be accounted for in the costs of alternative safe dike designs.

## **6.5. Conclusions**

Multifunctional flood defences are of growing interest to protect deltas from floods. In this chapter an extended framework for assessing the safety of multifunctional flood defences is presented based on lessons learned in the previous chapters.

The three examples of multifunctional dike design concepts from the previous chapters were discussed, from which four categories of multifunctional design components were identified: 1) foreshore, 2) dike geometry, 3) dike composition, and 4) dike objects. Multifunctional foreshore elements affect hydraulic loads directly and can be incorporated in dike assessments via accounting for these changes. Similarly, existing dike assessment procedures can be followed when additional functions affect the geometry of the flood defence and/or the choice of materials used in dike elements. When additional functions are facilitated by objects, dike assessments need to be adapted. Objects may introduce additional loads, or interact with the hydraulic loads or directly affect elements of the dike itself. A scenario-based approach is needed to quantify risks in different possible states of the object. Furthermore, objects in front of the dike affecting hydraulic loads may also be modelled by transmission models. These four

types of elements were used to expand the existing risk framework for flood defences to include steps for multifunctional elements.

In the existing approach, multifunctional use is conservatively assessed by a worst-case scenario. The extended framework for multifunctional flood protection with a scenario-based approach allows for benefits and synergies between multifunctional use and flood protection to be quantified. Furthermore, connections to the foreshore and areas between multiple defences are made in the framework in order to capture flood benefits and risks across the entire flood protection zone.

Designs of multifunctional flood defences will vary across different environments and function combinations. Nevertheless, the framework in this chapter will aid in guiding safe multifunctional flood protection solutions.



# 7

# Synthesis

R.J.C. Marijnissen



## 7.1 Introduction

In this synthesis chapter the results and insights across the previous chapters are discussed as well as the wider implications of this research for multifunctional flood protection. Section 7.2 first summarises the key findings of the thesis. Section 7.3 presents a discussion on the strengths and weaknesses of the framework for multifunctional flood defences presented in the thesis. Section 7.4 presents an outlook for multifunctional use of flood defences in the future and provides recommendations for further research. Finally, section 7.5 discusses how the lessons could be applied within the Dutch Flood Protection Program (HWBP).

## 7.2 Key findings and novelties for multifunctional flood defences

In this sections the key findings from the previous chapters are summarised. In these chapters, three research questions were explored:

1. How can a dike assessment framework be adapted to probabilistically evaluate multifunctional use of a flood defence?
2. How can additional defences constructed for multifunctional use of the flood protection zone be incorporated and evaluated within a probabilistic evaluation framework?
3. How can a probabilistic framework account for long-term climate adaption benefits of multifunctional use within a flood protection zone?

Together, these questions serve the main aim of the research: *to investigate how combining different activities on or near flood defences affects the safety provided by flood defences within a risk-based approach*. An overview of all highlights is presented in **Figure 7.1**. The highlights are elaborated further throughout this section.

## Safety framework for flood defences

### Narrow scope

2

- Assessments of multifunctional flood defences should include multiple scenarios rather than only the worst-case scenario
- Effects of multifunctional use on safety become smaller as the reliability of the dike increases

Case:

Proto-typical river dike

3

- A new method for assessing parallel flood defences was applied.
- Double dikes should be assessed using the transmitted loads of parallel defences, rather than failure of individual defences.
- Flood protection is negligibly improved by a low dike landward of a tall dike at the coast.
- A trade-off is made between flood risk and other functions by the culvert in the dike.

Case:

Double dike

4

- Pits accumulate sufficient clay for reinforcements until 2100 under sea-level rise.
- The infill rate of the borrow pit increases with its depth.
- Infilling of the pit is projected to accelerate with sea-level rise.

Case:

Wide green dike

5

- Foreshore processes considerably affect future dike heightening
- Dike heightening needs to compensate for loss of marshes
- Management of sediment on foreshores considerably affects the need for dike reinforcements under accelerated sea-level rise

Case:

Wide green dike

### Wide scope

## Safety framework for sustainable multifunctional flood defence zones

6

- Multifunctional use can be included in assessments through dike geometry, dike composition, foreshore, and objects
- The extended framework with a scenario-based approach allows for benefits and synergies with flood protection to be quantified

7

**Figure 7.1** The highlights of each chapter in the thesis in expanding from a safety framework for single flood defences with little multifunctional elements, towards a safety framework for multifunctional flood defences encompassing the wider flood protection zone.

### 7.2.1 Probabilistic assessment of multifunctional elements on flood defences

The probabilistic assessment of multifunctional use was investigated within Chapter 2. The research followed the suggestion published in a memo by Knoeff (2017) to consider failures by objects as scenarios when evaluating failure mechanisms within the reliability framework. To see whether this approach is feasible and how it affects the results from safety assessments, the approach was applied to a schematisation of a typical river dike where different objects (a house and a tree) are present after different reinforcement measures.

The main finding of the study was the large degree to which a conservative approach can reduce the assessed safety level compared to the probabilistic implementation with scenarios. A conservative approach inherently penalises the safety of a flood defence for other land-uses present as only the worst state of the different objects on a flood defence are considered while benefits are omitted. Thus, if an object can strongly influence a failure mechanism, regardless of the probability of the object reaching this critical state (a tree affecting piping in the example of Chapter 2), this failure mechanism becomes more dominant for the probability of failure of the defence. When the feasibility of a critical scenario and potential benefits (e.g. stabilisation of the slope by the weight of a building) are accounted for results can vary significantly. Chapter 2 highlights the probability of failure in the conservative approach can be multiple orders of magnitude higher than probabilistic approach for the same defence (**Figure 2.6**). Thus, in cases where multifunctional use has the potential to strongly increase the odds of a failure mechanism, a conservative approach can inform a drastically different implementation of a function than a probabilistic assessment would.

Another finding from Chapter 2 was that the magnitude of the influence of multifunctional use on flood protection is shown to be inversely proportional to the protection level of the dike itself. Thus, dikes with a lower probability of failing will not be affected as much by multifunction use, either positively or negatively, as dikes with a higher probability of failure. In practice, the risks as well as flood protection benefits of multifunctional use of a flood defence decrease as the dike increases in size. Previously, “robust” dikes have already been proposed to be

combined with other uses for this exact reason (de Moel *et al.*, 2010; Knoeff & Ellen, 2011; Silva & van Velzen, 2008; van Loon-Steensma & Vellinga, 2014). However, the proportional loss of flood protection benefits from other uses with robust dikes has so far received little attention.

### 7.2.2 Probabilistic assessment of additional flood defences

In Chapter 3 the case of the Double Dike near Delfzijl is studied to investigate how the additional flood defence constructed for both flood protection and land-uses like saline agriculture affects flood protection. Prior to this study, several other studies had investigated this specific system. Gautier, Schelfhout, and van Meurs (2015) concluded the Double Dike would meet the flood protection norm by virtue of the tall first dike alone as the clay core would not significantly erode during critical storm conditions for a breach, nor would overtopping be significant. The additional dike would instead need to be designed according to the water management of the area in between the dikes. Wauben (2019) applied the updated Dutch reliability framework (WBI2017) but found the methods in this framework remained inadequate for multiple defences. Instead he applied a new model (Rongen *et al.*, 2018) to assess dike failure by wave impact at the first dike by the amount of overtopping into the interdike area resulting from erosion of the dike by waves. Despite these efforts, a probabilistic evaluation of the system where both defences are assessed is missing.

In Chapter 3 a framework to assess multiple flood defences was developed. Recognising that effects of foreshores and structures like breakwaters can be modelled by adjusting hydraulic loads at the flood defence within the Dutch reliability framework (Rijkswaterstaat, 2016b), the same approach can be applied for additional defences. This novel approach for treating flood defences in Chapter 3 considers the first flood defence by the mechanisms that can erode it (erosion mechanisms), and the mechanisms that can transfer hydraulic loads (transmission mechanisms). The transmitted hydraulic loads are then evaluated at the most landward defence to assess the protection level of the system. The approach of Chapter 3 can be applied to many combinations of defences by selecting the relevant erosion- and transmission mechanisms for the assessment.

The framework was applied to the case-study of the Double Dike in Delfzijl. The advanced erosion-overtopping model conceptualised by Kaste and Klein Breteler (2015); (Kaste *et al.*, 2015) , programmed by Rongen *et al.* (2018) and subsequently demonstrated for application to the Double Dike (Wauben, 2019) was adapted in Chapter 3 for a probabilistic scheme. The failure models of the seaward dike are recontextualised as a hydraulic transmission function where erosion by wave impact contributes to the volume of water transmitted into the interdike area. An additional transmission mechanism was introduced by the culvert inside the seaward dike which was added to the model. Like previous studies (Gautier *et al.*, 2015; Wauben, 2019), this study found the Double Dike system at Delfzijl gained little additional flood protection from the additional dike. However, it did reveal the transmission of loads by the culvert had a significantly more effect on safety than previously assumed, necessitating a compromise between the tidal exchange through the culvert for activities in the interdike zone and flood protection. The novel approach was capable of confirming earlier results, as well as provide a more general understanding of the safety provided by additional defences. It has also informed further research on the safety of the Double Dike concept (van Steeg & Diermanse, 2021).

### 7.2.3 Incorporating long-term benefits of multifunctional flood protection

Chapters 4 and 5 studied the Wide Green Dike case to investigate the long-term potential of multifunctional use of flood defence systems for flood protection. Prior to this thesis, van Loon-Steensma and Schelfhout (2017) had analysed the feasibility of a “Wide Green Dike” (a grass-covered dike with a shallow outer slope smoothly merging with the salt-marsh). While their calculations showed the concept was feasible and cheaper than traditional reinforcement when local clay is extracted, the importance of the marsh for the adapting the foreshore with sea-level rise and accumulating the necessary clay for reinforcement was not yet incorporated in their assessment.

In Chapter 4 the clay accumulating in man-made pits for dike reinforcements with sea-level rise is discussed, while Chapter 5 investigates how the conditions

governing natural sediment accretion of the marsh affect the required dike reinforcement to mitigate sea-level rise for flood protection. Introducing these components to the safety assessment of the flood defence has led to two main conclusions.

Firstly, excavating pits on a salt marsh foreshore for capturing sediment as reinforcement material from a turbid estuary is feasible as a long-term adaptation strategy. Sediment capture is positively linked to sea-level rise, allowing more sediment to be used in reinforcement. Thus the additional demand for clay as sea-level rise accelerates is dampened by the additional sediment capture. Within the reliability framework, the pits on the foreshore are expressed by the additional clay used in reinforcements of the dike and the resulting change in dike geometry after each reinforcement cycle.

Secondly, the sediment accretion on the marsh acts as a buffer against sea-level rise, reducing the need for future dike heightening. Managing the suspended sediment concentration in the Dollard and the compaction of the marsh determines whether dike reinforcements will need to outpace sea-level rise (i.e. over 1 mm of dike heightening needed for each millimetre of sea-level rise) in the near future or only at the end of this century within the highest sea-level rise scenarios. Thus, managing foreshores and the factors governing their evolution is crucial to design future-proof flood protection. Within the reliability framework, managing the foreshore should be considered as a design element to limit future hydraulic loads at the flood defence.

### **7.3 Strengths and weaknesses**

Based on the results presented in Chapters 2 to 5, Chapter 6 assembles these lessons into a new integrated framework for assessing multifunctional flood defence systems. In this section, the advances for the assessment of multifunctional flood protection systems by the framework in Chapter 6 are discussed.

### 7.3.1. Comparison to different flood risk management approaches

Probabilistic assessments have been available and performed in flood risk management internationally, e.g. in Germany and the UK (Apel *et al.*, 2006; Hall *et al.*, 2003). Still, methods for the probabilistic assessment of multifunctional components on a dike have remained limited. This thesis has contributed by expanding an existing probabilistic framework with methods to consider multifunctional uses on the dike (Chapter 2) and near the dike (Chapters 3, 4, 5). These new insights may aid in the optimisation of multifunctional flood protection designs internationally. This thesis has mainly focussed on adapting and improving the reliability assessment framework as applied within the Dutch flood risk policy. Here the findings of this thesis are discussed through the lens of different flood risk approaches.

First of all, the framework in this thesis is characterised by advanced assessments of the reliability of the defences, using both probabilistic algorithms and detailed descriptions of failure mechanisms. Many other approaches can be employed to simplify the assessment of flood defences, e.g. with deterministic design storms, or performance indicators (Sharp *et al.*, 2013). While simpler approaches like indicators may be less accurate, these are often sufficient to already identify key weaknesses in flood protection infrastructure (Vuillet, Peyras, Serre, & Diab, 2012). The type of advanced assessment proposed in this thesis may simply be infeasible when many flood defences need to be considered in a limited time or data required for advanced assessments is unavailable.

Still, there are more fundamental concerns with adapting a framework for multifunctional use from the Dutch flood risk management approach. One of its main criticisms is the strong emphasis on reducing the probability of flooding through engineering measures rather than addressing the vulnerability to flooding (Klijn, de Bruijn, Knoop, & Kwadijk, 2012). The consequences of a flood, i.e. economic damage, the number of people affected, and the likelihood of casualties during a flood event, are only reflected within the official safety norms for flood protection measures expressed as a maximum allowable flooding probability. These norms are set independently of the designs of flood defences themselves. Multifunctional flood defences not only affect the probability of flooding, their

designs can greatly affect the vulnerability of the hinterland should a flood occur. For example, the value of marshes in reducing the flow through a breach, thereby reducing the speed and extent of flooding in the hinterland (Zhu *et al.*, 2020). The “robust” broad dikes (Silva & van Velzen, 2008; van Loon-Steensma & Vellinga, 2014; Vellinga, 2008) not only aim to increase the robustness of dikes for multifunctional use of the defences, these broad dike are primarily concerned with reducing the probability of sudden breaches that threaten to quickly inundate the hinterland. As a result of a slower flooding, there would be more time for emergency measures, evacuation and potentially less damage to the hinterland. Other multifunctional concepts relocate critical land-uses to higher or less exposed locations, e.g. placing buildings on the super levee (Kundzewicz & Takeuchi, 1999), while incorporating land-uses that may benefit from occasional flooding (e.g. nature creation in a double dike system). Since these benefits are outside of the scope of reducing the probability of flooding as defined in the Dutch Water Act, these benefits remain unaccounted for within the Dutch reliability framework, and thereby in the dike design process.

Aside from the approach described above which considers risk as the product of probabilities and consequences ( $R = P * C$ ), other approaches consider risk as the intersection of hazards and vulnerabilities ( $R = H \cap V$ ). For example, the Japanese flood risk management approach regulates the vulnerability of exposed areas by a combination of zoning policies, flood-proofing of structures, as well as structural measures like parallel or ring dikes (Fan & Huang, 2020; Ichidate, Tsuji, Taki, & Nakamura, 2016; Takeuchi, 2002). These different approaches are reconciled by considering how measures can affect the exposure ( $E$ ) of the hinterland to floods (Klijn, Kreibich, de Moel, & Penning-Rowsell, 2015). Exposure encompasses the characteristics of the flood hazard ( $H = P * E$ ) like flood extent, flood depth, and flow velocities which determine the consequences for vulnerable assets in the hinterland ( $C = E \cap V$ ). A treatment of the exposure within the framework of this thesis enables its use within hazard-oriented flood risk management approaches.

Because the reliability framework developed in thesis is rooted within Dutch reliability framework it inherits both its strengths and weaknesses as discussed above. However, the methodology for handling parallel defences from Chapter 3

may provide a way forward for addressing the exposure of the hinterland in the assessment framework. In Chapter 3 the first dike of the system is considered as transmitting hydraulic loads to the interdike zone behind it. The result is a new set of hydraulic loads within the interdike zone. Instead of evaluating the failure mechanisms to determine a probability of failure for the flood defence, one could similarly calculate the loads transmitted by the final dike towards the hinterland. As these transmitted hydraulic loads (i.e. water level and waves) are evaluated probabilistically, the result is actually the flood hazard as defined earlier. Thus, the framework from this thesis is a first a step to bridge the gap between different flood risk management approaches. Nevertheless, adapting the framework from this thesis to include exposure of the hinterland will require further study as well as a redefinition of the Dutch flood protection norm.

### 7.3.2. Discussion on supporting models

Implementing the framework presented in this thesis requires a suite of models to evaluate all processes leading up to failure as well as assess the probability of such an event. There are three types of models needed for implementing the framework: hydraulic models to compute the flow of water, models of failure mechanisms to compute if a dike fails, and finally statistical methods to assess the probability of events. This subsection discusses the models used throughout the thesis and discusses their strengths and weakness, as well as points out alternative methods to assess the same processes within the risk framework.

#### 7.3.2.1. *Hydro-morphological models:*

Hydraulic models are used to determine the hydraulic boundary conditions of the environment like water levels and wave conditions, as well their changes when travelling towards flood defences. Throughout this thesis Hydra-NL (Duits & Kuijper, 2018) was used to determine the hydraulic boundary conditions of the case-studies. Hydra-NL combines observations of water levels and wind speeds at stations throughout the Netherlands with a database of precomputed wave simulations from a SWAN wave-model (Booij *et al.*, 1999) of the Dutch coast to extrapolate conditions along the Dutch coast during extreme events. To account

for changing conditions on the foreshore a separate SWAN model was used to model the final stretch of foreshore toward the defence (Chapters 4 and 5). This approach follows directly the procedure in the WBI (Rijkswaterstaat, 2016b) and thus produces consistent results with dike design practises in the Netherlands. This advanced approach is suitable for the Netherlands where many decades of measurements have verified the accuracy of these hydraulic models. However, there are concerns about limitations of the SWAN model, e.g. infra-gravity waves on shallow foreshores (Lashley, Bricker, van der Meer, Altomare, & Suzuki, 2020) or interactions between waves in complex estuaries like the Dollard (Oosterlo *et al.*, 2018b). Alternative models like XBeach (Roelvink *et al.*, 2015) or calibration of the models for specific areas may resolve such shortcomings. Addressing limitations is paramount for designing flood defences, as inaccuracies will be magnified in the extrapolation of extreme (storm) events. To implement advanced wave models sufficient data needs to be available for extrapolating hydraulic loads, calibrating the wave models, and verifying the results. This data may not be available for other areas in the world.

Aside from the propagation of waves across the foreshores, models are needed to determine the changes on the foreshore itself before hydrodynamic models can predict the future loads on a flood defence. A basic sedimentation model for marsh accretion based solely on tidal inundation and suspended sediment was applied in this thesis (Chapters 4 and 5). While such models are useful for predicting the general behaviour of salt marshes (Kirwan *et al.*, 2010), it omits the many complex interactions between vegetation, morphology and hydrodynamics. Complex models are available to model these interactions, e.g. (Best *et al.*, 2018; Breda *et al.*, 2021; D'Alpaos *et al.*, 2007). Such models are both computationally intensive and require more extensive data collection for proper calibration and validation. For implementation in a risk approach the main objective of a foreshore model is not to accurately predict all foreshore features, but rather to assess the effect of the on hydraulic loads at the flood defence foreshore across a range of potential future scenarios. As such, implementing a simple model (like in Chapter 4) capable of running many simulations quickly across multiple scenarios is best suited for a risk framework. This does require attention to the limitations of the model as a result of the assumptions and simplifications. Finding

sufficiently accurate yet fast models is one of the main challenges in probabilistically assessing future hydraulic loads on flood defences.

### 7.3.2.2. Failure mechanisms

Throughout the thesis the failure mechanisms of piping (Chapter 2), macrostability (Chapter 2), overtopping and overflow (Chapters 2, 3, 4, and 5), and wave impact (Chapters 3 and 4), were considered. **Table 7.1** presents an overview of the applied methods in this thesis. For implementation into a risk framework, descriptions of failure mechanisms must fit the definition of a limit state ( $Z = R - S$ ) where failure is denoted when the loads ( $S$ ) exceed the capacity of a flood defence ( $R$ ). As long as failure models can be rewritten in this form other methods can be implemented as well. It should be noted that exceeding the presented limit states does not necessarily result in a flood, but rather reflects some critical state prior to the actual flooding. As a result, the limit state definition of the same mechanism may vary across models. For example, overtopping is usually evaluated by a critical overtopping discharge (van der Meer *et al.*, 2016), but in the model by van Bergeijk *et al.* (2019) it is defined as 20 cm of erosion depth on the dike's inner slope. Aside from practical considerations (e.g. computational time, accuracy, etc.), the choice of models for failure mechanisms is of little consequence for their implementation in the risk framework. This is useful as different (combinations of) models may be better equipped to incorporate effects of specific types of multifunctional use, e.g. (Aguilar-López *et al.*, 2018a; Aguilar-López *et al.*,

**Table 7.1** Summary of failure mechanisms, models, and limit states utilised throughout the thesis. The relevant chapters are presented between brackets.

Failure mechanism	Model utilised	Limit state implemented**
Overtopping and overflow	(van der Meer <i>et al.</i> , 2016), (Ch 2, 3, 4, 5) (Rongen <i>et al.</i> , 2018), (Ch 3)*	Overflow: $Z = z_{crest} - h$ Overtopping: $Z = q_c - q$
Wave impact	(Klein Breteler, 2015), (Ch 4)	$Z = t_{erosion} - t_{storn}$
Piping	(Sellmeijer <i>et al.</i> , 2011) (Ch 2)	$Z = H_c - H$
Slope stability	(Van, 2001), (Ch 2)	$Z = \Sigma M_R - \Sigma M_S$

\* This model was only implemented for the first parallel defence and was not evaluated as a limit state (see Chapter 3)

\*\* Symbols:  $Z$  = limit state,  $z_{crest}$ =dike crest height,  $h$ =water level,  $q_{(c)}$ = (critical) overtopping discharge,  $t_{erosion}$ =time required to erode the revetment,  $t_{storn}$ = storm duration,  $H_{(c)}$ =(critical) hydraulic pressure gradient,  $\Sigma M$ = the sum of (resisting or driving) moments on a slab of soil

2018b). **Table 7.1** presents the limit state definitions applied across this thesis. As explained in Chapter 3, limit states should only be evaluated for the last line of flood defences in order to account for all processes transmitting hydraulic loads through the other defences.

Within the risk framework, all failure mechanisms are assumed to be independent. However, it is known there are connections between these failure mechanisms. One such connection was implemented for wave impact and overtopping (Chapter 3) where wave impact lowers the crest height and enhances overtopping. Other examples of connections are: the connection between infiltration during overflow/overtopping, and saturation of the dike resulting in a loss of soil stability (Gasmo, Rahardjo, & Leong, 2000), and the correlations among soil parameters affecting both the formation of pipes and the stability of the soil above (Aguilar-López *et al.*, 2015; Van, 2001). Coupling mechanisms is not standard practice, but may be required to properly assess multifunctional use when present on the interface between mechanisms. For example, pores in the outer revetment of a dike as a result dead roots from woody vegetation enhances the infiltration of water into the dike body (Zanetti *et al.*, 2011), which during overflow increases the risk of slope instabilities. Coupling of failure mechanisms is required to study such effects. While assuming independence simplifies calculations (see Chapter 2), the framework can still be utilised for complex interactions between multifunctional use and failure mechanisms by combining mechanisms (see Chapter 3).

#### 7.3.2.3. *Reliability models*

Evaluating the probability of events in which a flood defence fails requires the use of statistical models and computational algorithms. Reliability analyses are classified in three levels: level I for semi-probabilistic methods like the use of safety factors, level II for methods which simplify distributions like the First Order Reliability Method (FORM), and level III for fully probabilistic methods like Monte-Carlo or importance sampling (CUR/TAW, 1990). Throughout the thesis FORM has been utilised (Chapters 2, 3, 4, and 5), as well as Importance Sampling (Chapter 3) to quantify the probability of failure of a flood defence (Ditlevsen & Madsen, 2007; Low & Tang, 2007; Robert & Casella, 1999). Since a level I procedure requires safety

factors derived by a higher level assessment, this type of analysis cannot be performed for multifunctional elements of which the effects (and thus the required safety factors) are not known beforehand.

The choice for a level II algorithm over a level III algorithm was motivated by the balance between accuracy in estimating the probability failure, while keeping computational times relatively short. The limitations of a level II procedure became apparent in Chapters 2 and 3. The FORM procedure is best suited for continuous, monotonically increasing limit state functions, otherwise convergence is not guaranteed. For the failure mechanism of macrostability (Chapter 2) the evaluation of different slip planes can present sudden jumps in the evaluation of the limit state function between iterations, resulting in several times in poor convergence and inaccurate failure probabilities as a result. A similar issue was present in the case of wave impact erosion on the first dike of a double dike system (Chapter 3). Once waves have eroded the clay on the outer revetment, the acceleration in erosion at the sand core and the increased overtopping as a result presents a sudden discontinuity of the limit state definition. This could only be resolved by resorting to a level III routine. Thus, while level II routines can be implemented in the risk framework for multifunctional use, care should be taken to avoid errors resulting from discontinuous limit state definitions.

Finally, in many applications of flood risk management indicators are used rather than reliability analyses (Sharp *et al.*, 2013; Vuillet *et al.*, 2012). Indicators may be used to quickly identify weaknesses in flood protection infrastructure and prioritise reinforcements or further investigations. While indicators are a useful tool, they are only qualitative in nature. As such, these are not compatible with the risk framework presented in this thesis which aims to quantify the reliability of flood defences.

### 7.3.3. Summary of strengths and weaknesses

In this subsection the main strengths and weaknesses of the framework are summarised from the discussions in subsections 7.3.1 and 7.3.2:

#### **Strengths:**

- Uncertainties of multifunctional use are made explicit (through scenarios)

- Layers of (parallel) flood defences can be assessed
- Management practises of foreshore are quantifiable as flood risk reduction measures over time
- Multifunctional use across the flood protection zone can be quantified in terms of flood risk through evaluation of the affected design elements (dike geometry, dike composition, objects, and foreshore)

### **Weaknesses:**

- The framework considers reducing flood risk only by reducing the probability of flooding, not by reducing the vulnerability or exposure of the hinterland.
- A collection of (complex) statistical models, hydro-morphological models, models of failure processes, and reliability algorithms need to be calibrated, validated and integrated. Expertise to implement and recognise the limitations of the models, as well as data for calibrating and validating the models is required. Data and expertise may not always be available.

## **7.4 Outlook**

### **7.4.1 Integration of Nature-Based Solutions in flood protection**

Nature-based flood protection, where flood protection services are provided by eco-systems like marshes, is often proposed as a promising form of future flood protection (Temmerman *et al.*, 2013; van Wesenbeeck *et al.*, 2014). In salt marsh ecology there is well-known principle called “windows of opportunity”; an ecosystem needs sufficient time without major disturbances from the sea to establish before the next storm arrives (Balke *et al.*, 2011; Hu *et al.*, 2015). Similarly, there is a limited window of opportunity for the establishment of ecosystems in a nature-based flood protection scheme due to sea-level rise. Coastal ecosystems like salt marshes can adapt to, and even expand with, a gradual increase in sea-level rise due to their ability to enhance sediment deposition and/or retreating landward (Cahoon, McKee, & Morris, 2020; Kirwan *et al.*, 2010; Kirwan *et al.*, 2016). Still, global trends are narrowing the window of opportunity for nature-based flood protection. Sea-level rise in the Dutch Wadden Sea is projected to accelerate from

about 2 mm/yr in 2014 to between 2.2 mm/yr (lower bound RCP 2.6) and 18 mm/yr (upper bound RCP 8.5) by 2100 (Vermeersen *et al.*, 2018). According to the analysis performed in Chapter 4 marshes in the Dollard part of the Wadden Sea can only be expected to persist up to a sea-level rise rate of 8.9 mm/yr before drowning under current environmental conditions. The Dollard area has a relatively high availability of sediment compared to most deltas. Worldwide the construction of dams, as well as other human influences, has reduced the amount of sediment reaching coastal ecosystems from the river (Walling & Fang, 2003).

From the perspective of flood risk, relying on ecosystem services for additional protection long-term is contentious if their own adaptive capacity is in question. As discussed in Chapter 4, severe compaction of the foreshore from agricultural use or a drastic decrease of the sediment supply results can equally increase in flood risk over time similar to the highest sea-level rise scenarios when relying on marsh accretion for protection. Furthermore, a wide-scale implementation of eco-engineering measures based on accretion will be limited by the amount of sediment naturally available within the delta system (Oost *et al.*, 2021). Therefore, long-term nature-based flood protection can only be successful if integral policies are present and enforced to ensure conditions remain favourable for the ecosystem. Still, as long as conditions remain within the “window of opportunity”, Chapter 4 demonstrates substantial benefits are gained from coupling dike reinforcement with a salt marsh through wave damping and the extraction of clay for dike construction from pits. As flood management plans start to shift towards more nature-based solutions (Wesseling *et al.*, 2016), managing sediment budgets and other anthropomorphic influences within the delta becomes crucial for the success of these softer measures (Hoitink *et al.*, 2020).

A final consideration for nature-based solutions is the required protection level. As the protection level increases, flood protection measures need to be designed for increasingly extreme wave and water level conditions. While studies found a substantial attenuation of waves by vegetation under regular storm conditions (Möller *et al.*, 2014; Yang *et al.*, 2012), attenuation reduces for extremer situations due the breaking of stems (Vuik *et al.*, 2018a), seasonal die-off (Schoutens *et al.*, 2019), and deeper submergence. For the Dutch case studies in this thesis extreme conditions with annual probabilities lower than 1/1000 were considered.

For simplicity, this thesis opted not to include direct wave dampening effects from vegetation in the case-studies in these conditions, even though these can still be incorporated in the dike assessment framework from Chapter 6 using the scenario approach for different vegetation conditions introduced in Chapter 2. Still, Willemssen, Borsje, Vuik, Bouma, and Hulscher (2020) found a positive, albeit diminished, contribution to wave attenuation can be expected from vegetated foreshores under extreme conditions. As a result, nature-based solutions may improve flood protection more so than this thesis suggests, in particular when a high failure probability is acceptable.

To summarise, building with nature concepts of multifunctional use of flood defences are promising to improve the protection against floods. However, one must realise the contribution of nature-based elements to flood protection will diminish over time with extremer sea-level rise scenarios, increasingly strict protection standards for flood defences, and poor management of foreshores and sediment budgets in the estuary.

## 7.4.2 The future of multifunctional use in flood protection strategies

For the next 30 years the flood protection strategies as applied today can still guarantee sufficient safety against flooding once all reinforcement projects in the HWBP are completed. For the long-term, 2100 and beyond, the uncertainty in climate change and sea-level rise specifically will become an important factor.

Continued heightening and strengthening of flood defences in combination with pumping remains a technical option for the future (Kwadijk *et al.*, 2010). Dikes will inevitably need to expand in and around urban centres and will increasingly need to resemble the “super levee” concept already implemented in regions of Japan, integrating massive flood defences into the urban fabric (Nakamura, 2016). As explained in Chapter 2, the influence of multifunctional use on flood protection from the added uncertainty in loads or dike strength will decrease as the magnitude of the hydraulic loads or dike’s resistance increase, either to meet stricter safety norms or due to increasing loads expected loads from e.g. sea-level rise. Put simply, the influence of multifunctional use on safety decreases with the size of the dike. In a way, this reinforces the call for more robust-multifunctional flood defences

previously (van Loon-Steensma & Vellinga, 2014), although this time motivated from a probabilistic perspective. Additionally, even the inclusion of a highly uncertain system like a salt-marsh within a safety-assessment has shown uncertainty in the dike's strength parameters remains the largest source of uncertainty for a dike's performance (Vuik *et al.*, 2018b). Thus, opportunities for integrating multifunctional use with flood defences will increase in the scenario of continued dike strengthening.

An alternative adaptation method is the inclusion of multifunctional flood defence zones with nature-based solutions in addition to dike strengthening of the flood defences. Multiple studies have suggested shifting towards softer nature-based solutions in response to sea-level (Baptist *et al.*, 2019; Haasnoot *et al.*, 2019; Temmerman *et al.*, 2013; van Wesenbeeck *et al.*, 2014). It is actually one of the preferred coastal adaption options for the Wadden Sea within the Dutch Delta program (Delta Programme, 2014) and is one of the reasons for the pilots of the Wide Green Dike and the Double Dike. These concepts for a multifunctional flood protection zone were analysed in this thesis.

Chapters 4 and 5 discuss how the wave damping and sediment accumulation processes of natural foreshores can be utilised to reduce the need and materials for improving flood defences against sea-level rise. Still, as posed in section 7.4.1, effective flood protection by ecosystems has a limited window of opportunity where flood risk is reduced when sea-level rise quickly accelerates and sediment sources in the Delta decrease. Therefore, this adaptation is most effective for the lowest climate scenarios and decreases in effectiveness with higher sea-level rise scenarios. The presence of an ecosystem will still aid in flood protection, even if additional measures are needed to counteract sea-level rise.

Double dike systems allow for the creation of new land-uses such as nature creation, aquaculture and saline agriculture while improving flood protection (Chapter 3) and may add economic value to the adaptation strategy. Furthermore, the interdike area can be used to establish ecosystems with same benefits as natural foreshores in places where none are possible on the existing foreshore. As Chapter 3 discussed however, only a marginal improvement in flood protection is achieved along the Dutch Wadden sea coast by the construction of an additional low dike behind the existing tall defences. Instead, double dike systems can be implemented

along the coast to slowly raise a second line of defences and anticipate a future retreat scenario while preserving flood risk protection and land-use benefits. This use of double systems can already be found along the Vietnamese coast in response to coastal erosion (Vinh *et al.*, 1997). Double dike systems with a small first dike reducing waves loads on the second dike, or where water storage from flooding of the interdike zone can reduce loads downstream show most promise (see Chapter 3).

In conclusion, the safety of multifunctional dikes will be highly relevant for dike reinforcements now and in the future, regardless of the climate adaptation pathway.

### 7.4.3 Recommendations for science

Based on the limitations raised in 7.3.3, and the foreseen knowledge gaps in 7.4.1 and 7.4.2 this subsection presents a list of recommendations for developing the framework for multifunctional use further.

- *Incorporate the effects of multifunctional use on the exposure and vulnerability of the hinterland.* The current framework does not consider the effects of land-uses on/near the dike on the vulnerability of and exposure of the hinterland. For example, buildings on the super levee are elevated above the surrounding area (Nakamura, 2016) making them less likely to be flooded when another section of levee fails, but their presence on the levee makes them vulnerable to the collapse of the specific levee they are built on. The net safety gain or loss for by multifunctional use of the levee cannot be evaluated within the framework of this thesis.
- *Incorporate serviceability limit states of other uses.* The framework only considers whether the dike will meet flood protection criteria. However, it does not consider whether the dike or the surrounding area is fit for the intended uses. Incorporating serviceability limit states alongside the safety limit states would enable designs to be evaluated both based on flood protection criteria, as well as the needs for the other uses.

- Development of probabilistic foreshore models. The complex interactions between tides, waves, sediment, and possibly vegetation are difficult to model. Yet, identifying the range and probability of future foreshore scenarios is crucial to determine future loads on flood defences, especially with regards to sea-level rise. Running accurate multi-year models repeatedly to find critical future foreshore states is computationally expensive. However, models that can run quickly within probabilistic procedures are simplistic and require the omission or simplification of many processes. Therefore, more work is needed to develop a model procedure which can identify the risk of future foreshore states detrimental to flood protection efficiently, while retaining as many crucial complex interactions as possible.

## **7.5 Implications for the Dutch Flood Protection Program**

One of the countries with the greatest need for flood protection is the Netherlands. Dutch flood defences are maintained and reinforced by the Flood Protection Program (abbreviated as *HWBP* in Dutch). This section discusses how the framework from Chapter 6 of the thesis can be used to improve the existing practices in the *HWBP* and compares them with the recent technical recommendations by studies across projects in the *HWBP* (known as *POVs* in Dutch).

When the probabilistic assessment framework for Dutch flood defences (*WBI2017*) was introduced in 2017 based on the methodology by *VNK2* (2012), a probabilistic approach towards multifunctional elements was yet to be determined. In Chapter 2 the approach detailed by *Knoeff* (2017) of failure scenarios for objects introduced for other uses was investigated. The recent *POV* studies (*Roode et al.*, 2019; *Schelfhout et al.*, 2020) identify two options to include scenarios in assessments: 1) either incorporate scenarios directly within the assessment of failure mechanisms, or 2) include dike failure after the failure of an object as a separate mechanism in the assessment. *POV* cables and pipelines (*Schelfhout et al.*, 2020) prefers the second option for pipelines as the safety assessments of the

conventional failure mechanisms can be maintained while POV foreshores (Roode *et al.*, 2019) suggests the first option for objects on foreshores.

In the current approach all direct failure mechanisms are conservatively assessed assuming the worst-case scenario for the state of objects to guarantee the safety standards are met. However, as the calculation of the effect of a house in Chapter 2 exemplifies, uses can, depending on the implementation, both contribute to flood protection in one state and reduce flood protection in another. The net effect of an object (both benefits and risks) on the safety of the dike is strongly affected by the uncertainties in the failure mechanisms it affects. For example, if the uncertainties in slope stability are already large due to uncertainties in the soil strength, the effect of the house on flood protection will be smaller than if the soil strength parameters are well-known. Such connections are less clear if the failure state of an object is evaluated separately as a new failure mechanism, making it more difficult to evaluate a design across the direct failure mechanisms like overtopping or stability. Therefore, in this thesis, Chapters 2 and 6 specifically, scenarios for objects have been incorporated directly within the assessment of direct failure mechanisms similar to the suggestion by POV foreshores (Roode *et al.*, 2019). Nevertheless, incorporating objects, e.g. pipelines, wind turbines, etc., as additional failure mechanisms in the HWBP's assessments is more practical when little flood protection benefits can be expected while damage from the object to the flood defence can be extensive enough to trigger a dike failure.

An integrated approach between uses on the foreshore and the safety of a flood defence is gaining traction within the HWBP. The recent POVs foreshores and Wadden Sea dikes strongly advocate for incorporating foreshores in dike assessments by default (Roode *et al.*, 2019; Steetzel, Groeneweg, & Vuik, 2020). Like the framework presented in Chapter 6, the POVs suggest (elements on) foreshores are considered by a scenario approach when directly affecting failure mechanisms of the flood defence (Roode *et al.*, 2019), or as a change in the hydraulic load conditions (Steetzel *et al.*, 2020). A safety framework evaluating the flood protection by multiple flood defences is still missing however. This has made flood protection concepts like the Double Dike in Chapter 3 more difficult to evaluate.

Based on the Double Dike case in Chapter 3 this thesis proposes to consider parallel defences as objects transmitting hydraulic loads to the most landward

defence similar in concept to transforming hydraulic loads by a foreshore. When multiple elements can retain a flood (e.g. with multiple dikes or a sand dune with dike) a scenario approach is usually applied based on the probability of failure of each defence. However, as discussed in Chapter 3, defining failure criteria for the flood protection system at the first defence is ambiguous due to the interactions between hydraulic loads, erosion mechanisms, and the resulting transmission of hydraulic loads over time. In this case a scenario-based approach with a breached scenario ignores the time required for the formation of a breach during a storm event, resulting in an overestimation of the probability of a system failure if emergency repairs are not possible.

The framework presented in Chapter 3 proposes to model parallel dikes by a hydraulic transmission model similar to a transformation of loads by a foreshore, rather than by scenarios. The required safety level is assessed at the last defence protecting the hinterland given the transmitted hydraulic loads. Theoretically, transmitted hydraulic loads are zero if the seaward defences already provide sufficient safety during an event. Consequently, in this thesis the transmission of hydraulic loads is regarded as an integral part of the design of a flood protection system itself, rather than a boundary condition to which flood protection infrastructure is designed. A downside of this approach is that modelling flows across an eroding dike is complex, requiring models and schematisations of both the relevant erosion mechanisms of a dike and the resulting flows. Therefore, this approach may not yet be feasible for most dike assessments. While small adjustments can be made to failure criteria of the strongest dike to accommodate the effect of another defence, this approach does not generalise easily to other projects. Especially now integrated multifunctional flood protection measures with double dikes are explored for multiple areas in the Netherlands (de Mesel, Ysebaert, & Kamermans, 2013; van Loon-Steensma, de Vries, Bouma, & Schelfhout, 2020), the HWBP may consider to research the more general concept of transmission models for dikes in order to assess the safety of such concepts in the future.

Finally, one of the major tasks of the HWBP is reinforcing flood defences to meet the safety standards before 2050. Understandably, many flood protection designs and assessments within the HWBP are therefore geared towards analyses

of the near future. However, cases like the Double Dike and Wide Green Dike are presented as long-term solutions (2100 and beyond) with elements intended to reduce the effects of future sea-level rise (e.g. by accretion of the foreshore). Yet, probabilistic safety assessments of these systems have so far been limited to the near future (Gautier *et al.*, 2015; van Loon-Steensma & Schelfhout, 2013; van Loon-Steensma *et al.*, 2014a). Chapters 4 and 5 present a long-term perspective for flood defences through the Wide Green Dike study, and conclude sediment accretion on foreshores and mining from clay pits can indeed contribute to mitigating sea-level rise. In doing so, management of the foreshore, e.g. sediment suppletion, grazing, marsh restoration, etc., as well management of sediment within the delta system, is revealed to be a key factor for the design of future flood protection measures along the Wadden Sea in the HWBP. The monitoring and management of sediment is already practised along the sandy coast of the Netherlands for decades. It is recommended foreshore management is considered within reinforcement projects along the muddy coasts as well.

Based on the framework in this thesis some types of multifunctional flood protection concepts are more promising than others. As a general rule of thumb, the effects of multifunctional (both positive and negative) are inversely proportional to the size of the dike (i.e. large dike equals small effect). Primary flood defences meeting high safety standards are designed for coping with large uncertainties. Therefore, these defences will not be as significantly affected by minor cases of shared-use a conservative estimate from a worst-case scenario would suggest. Furthermore, promising avenues for multifunctional use of the flood defence zone lie in the use foreshores, as these have the capacity to dampen the need for additional reinforcements in the future. Special attention is required for multifunctional use across multiple defences, as the construction of additional low inland defences will generally not significantly contribute to flood protection in the short term. Instead, these defences offer an avenue for long-term adaptation plans, or for accommodating specific types of land-uses requiring access to seawater.



# Bibliography

- Aaron, S. B., & Turner, R. E. (1997). Relationships between Salt Marsh Loss and Dredged Canals in Three Louisiana Estuaries. *J. Coast. Res.*, 13(3), 895-903. Retrieved from [www.jstor.org/stable/4298682](http://www.jstor.org/stable/4298682)
- Adams, H., Adger, W. N., & Nicholls, R. J. (2018). Ecosystem Services Linked to Livelihoods and Well-Being in the Ganges-Brahmaputra-Meghna Delta. In R. J. Nicholls, C. W. Hutton, W. N. Adger, S. E. Hanson, M. M. Rahman, & M. Salehin (Eds.), *Ecosystem Services for Well-Being in Deltas: Integrated Assessment for Policy Analysis* (pp. 29-47). Cham: Springer International Publishing.
- Aguilar-López, J. P. (2016). *Probabilistic safety assessment of multi-functional flood defences*. (PhD). Universiteit Twente, Enschede, Netherlands.
- Aguilar-López, J. P., Warmink, J. J., Bomers, A., Schielen, R. M. J., & Hulscher, S. J. M. H. (2018a). Failure of Grass Covered Flood Defences with Roads on Top Due to Wave Overtopping: A Probabilistic Assessment Method. *J. Mar. Sci. Eng.*, 6(3), 74. Retrieved from <https://www.mdpi.com/2077-1312/6/3/74>
- Aguilar-López, J. P., Warmink, J. J., Schielen, R. M. J., & Hulscher, S. J. M. H. (2015). Correlation Effect in Probabilistic Design against Piping in Multi-Functional Flood Defences. In T. Schweckendiek, A. F. Van Tol, D. Pereboom, A. Van Staveren, & P. M. C. B. M. Cools (Eds.), *Geotechnical Safety and Risk V* (pp. 239-244): IOS Press.
- Aguilar-López, J. P., Warmink, J. J., Schielen, R. M. J., & Hulscher, S. J. M. H. (2018b). Piping erosion safety assessment of flood defences founded over sewer pipes. *Eur. J. Environ. Civ. En.*, 22(6), 707-735. doi:<https://doi.org/10.1080/19648189.2016.1217793>
- Allen, J. R. L. (1990). Salt-marsh growth and stratification: A numerical model with special reference to the Severn Estuary, southwest Britain. *Mar. Geol.*, 95(2), 77-96. doi:[https://doi.org/10.1016/0025-3227\(90\)90042-I](https://doi.org/10.1016/0025-3227(90)90042-I)
- Allen, J. R. L. (2000a). Holocene coastal lowlands in NW Europe: autocompaction and the uncertain ground. *Geological Society, London, Special Publications*, 175(1), 239-252. doi:<https://doi.org/10.1144/gsl.Sp.2000.175.01.18>
- Allen, J. R. L. (2000b). Morphodynamics of Holocene salt marshes: a review sketch from the Atlantic and Southern North Sea coasts of Europe. *Quaternary Sci. Rev.*, 19(12), 1155-1231. doi:[https://doi.org/10.1016/S0277-3791\(99\)00034-7](https://doi.org/10.1016/S0277-3791(99)00034-7)
- Allsop, W. (2007). *FLOODsite: failure mechanisms for flood defence structures*. (T04-06-01). Retrieved from HR Wallingford: [https://d1rkab7tlqy5f1.cloudfront.net/TBM/Over%20faculteit/Afdelingen/Values%2C%20Technology%20and%20Innovation/People/Full%20Professors/Pieter%20van%20Gelder/Books/T04\\_06\\_01\\_failure\\_mechanisms\\_D4\\_1\\_v1\\_1\\_p01.pdf](https://d1rkab7tlqy5f1.cloudfront.net/TBM/Over%20faculteit/Afdelingen/Values%2C%20Technology%20and%20Innovation/People/Full%20Professors/Pieter%20van%20Gelder/Books/T04_06_01_failure_mechanisms_D4_1_v1_1_p01.pdf).
- Anvarifar, F., Oderkerk, M., van der Horst, B. R., & Zevenbergen, C. (2013). Cost-effectiveness study on preventive interventions: A survey of multifunctional flood defences. In F. Klijn & T. Schweckendiek (Eds.), *Comprehensive Flood Risk Management: research for policy and practice* (pp. 891-899). London: Taylor Francis Group.
- Anvarifar, F., Voorendt, M. Z., Zevenbergen, C., & Thissen, W. (2017). An application of the Functional Resonance Analysis Method (FRAM) to risk analysis of multifunctional flood defences in the Netherlands. *Reliab. Eng. Syst. Safe.*, 158, 130-141. doi:<https://doi.org/10.1016/j.res.2016.10.004>

- Anvarifar, F., Zevenbergen, C., Thissen, W., & Islam, T. (2016). Understanding flexibility for multifunctional flood defences: a conceptual framework. *J. Water Clim. Change*, 7(3), 467. doi:<https://doi.org/10.2166/wcc.2016.064>
- Apel, H., Thieken, A. H., Merz, B., & Blöschl, G. (2004). Flood risk assessment and associated uncertainty. *Nat. Hazard Earth Sys.*, 4(2), 295-308. doi:<https://doi.org/10.5194/nhess-4-295-2004>
- Apel, H., Thieken, A. H., Merz, B., & Blöschl, G. (2006). A Probabilistic Modelling System for Assessing Flood Risks. *Nat. Hazards*, 38(1), 79-100. doi:<https://doi.org/10.1007/s11069-005-8603-7>
- Arens, S. (2002). *Entwicklung und ökologische Wertigkeit von Kleinnahmestellen in Salzwiesen - Dienstbericht Forschungsstelle Küste 14/2002*. Retrieved from NLO, Norderney & Wilhelmshaven, Germany.
- Atkins, R. J., Tidd, M., & Ruffo, G. (2016). Sturgeon Bank, Fraser River Delta, BC, Canada: 150 Years of Human Influences on Salt Marsh Sedimentation. *J. Coast. Res.*, 75(sp1), 790-794, 795. Retrieved from <https://doi.org/10.2112/SI75-159.1>
- Baart, F., Rongen, G., Hijma, M., Kooi, H., de Winter, R. C., & Nicolai, R. (2019). *Zeespiegelmonitor 2018; De stand van zaken rond de zeespiegelstijging langs de Nederlandse kust* (11202193-000-ZKS-0004). Retrieved from Deltares, Delft, Netherlands: <https://www.deltares.nl/app/uploads/2019/03/Zeespiegelmonitor-2018-final.pdf>.
- Bachmann, D., Huber, N. P., Johann, G., & Schüttrumpf, H. (2013). Fragility curves in operational dike reliability assessment. *Georisk: Assessment and Management of Risk for Engineered Systems and Geohazards*, 7(1), 49-60. doi:<https://doi.org/10.1080/17499518.2013.767664>
- Bakker, H. L., Haasnoot, J. K., Goeman, D. G., Simanjuntak, T. D. Y. F., de Koning, M., & Kaspers, E. J. (2019). *PMMS—Probabilistic Model Macro Stability—with layer boundary uncertainties. General description and example*. Paper presented at the Proceedings of the 17th European Conference on Soil Mechanics and Geotechnical Engineering, Reykjavik, Iceland.
- Bakker, W. T., & Vrijling, J. K. (1980). Probabilistic Design of Sea Defences. In *Coastal Engineering 1980* (pp. 2040-2059).
- Balke, T., Bouma, T. J., Horstman, E. M., Webb, E. L., Erftemeijer, P. L. A., & Herman, P. M. J. (2011). Windows of opportunity: thresholds to mangrove seedling establishment on tidal flats. *Mar. Ecol. Prog. Ser.*, 440, 1-9. doi:<https://doi.org/10.3354/meps09364>
- Baptist, M. J., Babovic, V., Rodríguez Uthurburu, J., Keijzer, M., Uittenbogaard, R. E., Mynett, A., & Verwey, A. (2007). On inducing equations for vegetation resistance. *J. Hydraul. Res.*, 45(4), 435-450. doi:<https://doi.org/10.1080/00221686.2007.9521778>
- Baptist, M. J., Gerkema, T., van Prooijen, B. C., van Maren, D. S., van Regteren, M., Schulz, K., . . . van Puijenbroek, M. E. B. (2019). Beneficial use of dredged sediment to enhance salt marsh development by applying a 'Mud Motor'. *Ecol. Eng.*, 127, 312-323. doi:<https://doi.org/10.1016/j.ecoleng.2018.11.019>
- Barbier, E. B. (2015). Climate change impacts on rural poverty in low-elevation coastal zones. *Estuar. Coast. Shelf S.*, 165, A1-A13. doi:<https://doi.org/10.1016/j.ecss.2015.05.035>
- Barbier, E. B. (2017). Marine ecosystem services. *Curr. Biol.*, 27(11), R507-R510. doi:<https://doi.org/10.1016/j.cub.2017.03.020>
- Bartholomä, A., Dittmann, T., Exo, K. M., Karle, M., Metzinger, D., & Vöge, S. (2013). *Wiederverlandung einer Pütte; Forschungsergebnisse zu Chancen und Risiken von Kleinentnahmen in Salzwiesen für den Deichbau* (D. Metzinger Ed.). Oldenburg, Germany: III. Oldenburgischer Deichband.
- Bastola, S., Murphy, C., & Sweeney, J. (2011). The sensitivity of fluvial flood risk in Irish catchments to the range of IPCC AR4 climate change scenarios. *Sci. Total Environ.*, 409(24), 5403-5415. doi:<https://doi.org/10.1016/j.scitotenv.2011.08.042>

- Battjes, J. A., & Stive, M. J. F. (1985). Calibration and verification of a dissipation model for random breaking waves. *J. Geophys. Res.-Oceans*, 90(C5), 9159-9167.  
doi:<https://doi.org/10.1029/JC090iC05p09159>
- Baudin, M., Dufloy, A., Iooss, B., & Popelin, A. L. (2015). Open TURNS: An industrial software for uncertainty quantification in simulation. *arXiv preprint*. doi:<https://arxiv.org/abs/1501.05242>
- Bernardara, P., Schertzer, D., Sauquet, E., Tchiguirinskaia, I., & Lang, M. (2008). The flood probability distribution tail: how heavy is it? *Stoch. Env. Res. Risk A*, 22(1), 107-122.  
doi:10.1007/s00477-006-0101-2
- Best, Ü. S. N., van der Wegen, M., Dijkstra, J., Willemsen, P. W. J. M., Borsje, B. W., & Roelvink, D. J. A. (2018). Do salt marshes survive sea level rise? Modelling wave action, morphodynamics and vegetation dynamics. *Environ. Modell. Softw.*, 109, 152-166.  
doi:<https://doi.org/10.1016/j.envsoft.2018.08.004>
- Bijl, W. (2006). *Achterlandstudie Maeslantkering* (ISBN 90-369-4823-1). Retrieved from Rijkswaterstaat, Delft, Netherlands: [https://puc.overheid.nl/doc/PUC\\_125106\\_31/1/#b8fb7ee8-c6ec-4aff-9272-af91513fc218](https://puc.overheid.nl/doc/PUC_125106_31/1/#b8fb7ee8-c6ec-4aff-9272-af91513fc218).
- Bischiniotis, K., Kanning, W., Jonkman, S. N., & Kok, M. (2018). Cost-optimal design of river dikes using probabilistic methods. *J. Flood Risk Manag.*, 11(S2), S1002-S1014.  
doi:<https://doi.org/10.1111/jfr3.12277>
- Bishop, A. W. (1955). The use of the slip circle in the stability analysis of slopes. *Géotechnique*, 5(1), 7-17. doi:<https://doi.org/10.1680/geot.1955.5.1.7>
- Bomers, A., Aguilar-López, J. P., Warmink, J. J., & Hulscher, S. J. M. H. (2018). Modelling effects of an asphalt road at a dike crest on dike cover erosion onset during wave overtopping. *Nat. Hazards*. doi:<https://doi.org/10.1007/s11069-018-3287-y>
- Booij, N., Ris, R. C., & Holthuijsen, L. H. (1999). A third-generation wave model for coastal regions: 1. Model description and validation. *J. Geophys. Res.-Oceans*, 104(C4), 7649-7666.  
doi:<https://doi.org/10.1029/98JC02622>
- Bornschein, A., & Pohl, R. (2018). Land use influence on flood routing and retention from the viewpoint of hydromechanics. *J. Flood Risk Manag.*, 11(1), 6-14.  
doi:<https://doi.org/10.1111/jfr3.12289>
- Borsje, B. W., van Wesenbeeck, B. K., Dekker, F., Paalvast, P., Bouma, T. J., van Katwijk, M. M., & de Vries, M. B. (2011). How ecological engineering can serve in coastal protection. *Ecol. Eng.*, 37(2), 113-122. doi:<https://doi.org/10.1016/j.ecoleng.2010.11.027>
- Bouma, T. J., de Vries, M. B., & Herman, P. M. J. (2010). Comparing ecosystem engineering efficiency of two plant species with contrasting growth strategies. *Ecology*, 91(9), 2696-2704.  
doi:<https://doi.org/10.1890/09-0690.1>
- Bouma, T. J., de Vries, M. B., Low, E., Kusters, L., Herman, P. M. J., Tanczos, I. C., . . . van Regenmortel, S. (2005). Flow hydrodynamics on a mudflat and in salt marsh vegetation: identifying general relationships for habitat characterisations. *Hydrobiologia*, 540(1), 259-274. doi:<https://doi.org/10.1007/s10750-004-7149-0>
- Bouma, T. J., van Belzen, J., Balke, T., van Dalen, J., Klaassen, P., Hartog, A. M., . . . Herman, P. M. J. (2016). Short-term mudflat dynamics drive long-term cyclic salt marsh dynamics. *Limnol. Oceanogr.*, 61(6), 2261-2275. doi:<https://doi.org/10.1002/lno.10374>
- Bouwer, L. M., Bubeck, P., & Aerts, J. C. J. H. (2010). Changes in future flood risk due to climate and development in a Dutch polder area. *Global Environ. Chang.*, 20(3), 463-471.  
doi:<https://doi.org/10.1016/j.gloenvcha.2010.04.002>
- Breda, A., Saco, P. M., Sandi, S. G., Saintilan, N., Riccardi, G., & Rodríguez, J. F. (2021). Accretion, retreat and transgression of coastal wetlands experiencing sea-level rise. *Hydrol. Earth Syst. Sci.*, 25(2), 769-786. doi:<https://doi.org/10.5194/hess-25-769-2021>

- Brinkman, R., & Nuttall, J. D. (2018). *Failure mechanisms – MacroStability kernel; Scientific Background* (11201523-001). Retrieved from Deltares, Delft, Netherlands.
- Bruggeman, W., Dammers, E., van den Born, G. J., Rijken, B., van Bommel, B., Bouwman, A., . . . te Linde, A. (2013). *Deltascenario's voor 2050 en 2100; Nadere uitwerking 2012-2013*. Retrieved from Deltares, KNMI, PBL, CPB & LEI, Delft, Netherlands: [https://www.deltacommissaris.nl/binaries/deltacommissaris/documenten/publicaties/2014/05/27/deltascenarios-voor-2050-en-2100-nadere-uitwerking-2012-2013/Deltascenario%27s+voor+2050+en+2100\\_tcm309-351190.pdf](https://www.deltacommissaris.nl/binaries/deltacommissaris/documenten/publicaties/2014/05/27/deltascenarios-voor-2050-en-2100-nadere-uitwerking-2012-2013/Deltascenario%27s+voor+2050+en+2100_tcm309-351190.pdf).
- Bruggeman, W., Kwadijk, J. C. J., van den Hurk, B., Beersma, J. J., van Dorland, R., van den Born, G. J., & Matthijsen, J. (2016). *Verkenning actualiteit Deltascenario's*. Retrieved from Deltares, KNMI, PBL, Delft, Netherlands: <https://www.deltares.nl/app/uploads/2016/09/20160906-verkenning-houdbaarheid-deltascenarios-incl-bijlagen.pdf>.
- Cahoon, D. R., McKee, K. L., & Morris, J. T. (2020). How Plants Influence Resilience of Salt Marsh and Mangrove Wetlands to Sea-Level Rise. *Estuaries Coasts*. doi:10.1007/s12237-020-00834-w
- Casteleijn, A., & Van Bree, B. (2017). *Werkwijze bepalen kans op niet sluiten per sluitoraag met scoretabellen: Actualisatie van de gedetailleerde methode van betrouwbaarheid sluiten van kunstwerken voor beoordelen en ontwerpen*. Retrieved from Rijkswaterstaat, Netherlands: [https://www.helpdeskwater.nl/publish/pages/157133/werkwijze\\_bepalen\\_kans\\_op\\_niet\\_sluiten\\_per\\_sluitvraag\\_met\\_scoretabellen\\_definitief\\_v1\\_2.pdf](https://www.helpdeskwater.nl/publish/pages/157133/werkwijze_bepalen_kans_op_niet_sluiten_per_sluitvraag_met_scoretabellen_definitief_v1_2.pdf).
- Chab, H. (2015). *Waterstandsverlopen kust : Wettelijk Toetsinstrumentarium WTI-2017* (1220082-002-HYE-0003). Retrieved from Deltares, Delft, Netherlands: <https://edepot.wur.nl/458925>.
- Chen, X., Jonkman, S. N., Pasterkamp, S., Suzuki, T., & Altomare, C. (2017). Vulnerability of Buildings on Coastal Dikes due to Wave Overtopping. *Water*, 9(6), 394. doi:doi:10.3390/w9060394
- Christiansen, T., Wiberg, P. L., & Milligan, T. G. (2000). Flow and Sediment Transport on a Tidal Salt Marsh Surface. *Estuar. Coast. Shelf S.*, 50(3), 315-331. doi:<https://doi.org/10.1006/ecss.2000.0548>
- Costanza, R., Pérez-Maqueo, O., Martinez, M. L., Sutton, P., Anderson, S. J., & Mulder, K. (2008). The Value of Coastal Wetlands for Hurricane Protection. *AMBIO*, 37(4), 241-248, 248. doi:[https://doi.org/10.1579/0044-7447\(2008\)37](https://doi.org/10.1579/0044-7447(2008)37)
- Cox, T., Maris, T., de Vleeschauwer, P., de Mulder, T., Soetaert, K., & Meire, P. (2006). Flood control areas as an opportunity to restore estuarine habitat. *Ecol. Eng.*, 28(1), 55-63. doi:<https://doi.org/10.1016/j.ecoleng.2006.04.001>
- Craft, C., Clough, J., Ehman, J., Joye, S., Park, R., Pennings, S., . . . Machmuller, M. (2009). Forecasting the effects of accelerated sea-level rise on tidal marsh ecosystem services. *Front. Ecol. Environ.*, 7(2), 73-78. doi:<https://doi.org/10.1890/070219>
- Crosby, S. C., Sax, D. F., Palmer, M. E., Booth, H. S., Deegan, L. A., Bertness, M. D., & Leslie, H. M. (2016). Salt marsh persistence is threatened by predicted sea-level rise. *Estuar. Coast. Shelf S.*, 181, 93-99. doi:<https://doi.org/10.1016/j.ecss.2016.08.018>
- CUR/TAW. (1990). *Probabilistic design of flood defences* (Report 141). Retrieved from Centre for Civil Engineering Research and Codes (CUR), Technical Advisory Committee on Water Defences (TAW), Gouda, the Netherlands.
- D'Alpaos, A., Lanzoni, S., Marani, M., Bonometto, A., Cecconi, G., & Rinaldo, A. (2007). Spontaneous tidal network formation within a constructed salt marsh: Observations and morphodynamic modelling. *Geomorphology*, 91(3), 186-197. doi:<https://doi.org/10.1016/j.geomorph.2007.04.013>

- d'Angremond, K., van der Meer, J. W., & de Jong, R. J. (1997). Wave Transmission at Low-Crested Structures. In *Coastal Engineering 1996* (pp. 2418-2427).
- Dalrymple, R. A., Kirby, J. T., & Hwang, P. A. (1984). Wave Diffraction Due to Areas of Energy Dissipation. *J. Waterw. Port Coast.*, 110(1), 67-79. doi:[https://doi.org/10.1061/\(ASCE\)0733-950X\(1984\)110:1\(67\)](https://doi.org/10.1061/(ASCE)0733-950X(1984)110:1(67))
- Danka, J., & Zhang, L. M. (2015). Dike Failure Mechanisms and Breaching Parameters. *J. Geotech. Geoenviron.*, 141(9), 04015039. doi:[doi:10.1061/\(ASCE\)GT.1943-5606.0001335](https://doi.org/10.1061/(ASCE)GT.1943-5606.0001335)
- Dankers, N., Binsbergen, M., Zegers, K., Laane, R., & van der Loeff, M. R. (1984). Transportation of water, particulate and dissolved organic and inorganic matter between a salt marsh and the Ems-Dollard estuary, The Netherlands. *Estuar. Coast. Shelf S.*, 19(2), 143-165. doi:[https://doi.org/10.1016/0272-7714\(84\)90061-1](https://doi.org/10.1016/0272-7714(84)90061-1)
- Davidson-Arnott, R. G. D., van Proosdij, D., Ollerhead, J., & Schostak, L. (2002). Hydrodynamics and sedimentation in salt marshes: examples from a macrotidal marsh, Bay of Fundy. *Geomorphology*, 48(1), 209-231. doi:[https://doi.org/10.1016/S0169-555X\(02\)00182-4](https://doi.org/10.1016/S0169-555X(02)00182-4)
- Day, J. W., Gunn, J. D., Folan, W. J., Yáñez-Arancibia, A., & Horton, B. P. (2007). Emergence of complex societies after sea level stabilized. *Eos, Transactions American Geophysical Union*, 88(15), 169-170. doi:<https://doi.org/10.1029/2007EO150001>
- de Haas, H., & Eisma, D. (1993). Suspended-sediment transport in the Dollard estuary. *Neth. J. Sea Res.*, 31(1), 37-42. doi:[https://doi.org/10.1016/0077-7579\(93\)90014-I](https://doi.org/10.1016/0077-7579(93)90014-I)
- de Looft, A. K., 't Hart, R., Montauban, K., & van de Ven, M. F. C. (2012). Golfklap a model to determine the impact of waves on dike structures with an asphaltic concrete layer. In *Coastal Engineering 2006* (pp. 5106-5115): World Scientific Publishing Company.
- de Mesel, I. G., Ysebaert, T., & Kamermans, P. (2013). *Klimaatbestendige dijken: het concept wisselpolders*. Retrieved from IMARES, Yerseke, Netherlands: <https://edepot.wur.nl/274605>.
- de Moel, H., Beijersbergen, J., van den Berg, F., de Goei, J., Koch, R. C., Koelewijn, A. R., . . . Zantinge, A. M. (2010). *De Klimaatdijk in de Praktijk : gebiedsspecifiek onderzoek naar nieuwe klimaatbestendige dijkverbeteringsalternatieven langs de Nederrijn en Lek*. In H. de Moel (Ed.). Retrieved from <http://publicaties.minienm.nl/documenten/de-klimaatdijk-in-de-praktijk-gebiedsspecifiek-onderzoek-naar-nieuwe-klimaatbestendige-dijkverbeteringsalternatieven-langs-de-nederrijn-en-lek>
- de Waal, H., & van Hoven, A. (2015a). *Failure Mechanism Module Grass Wave Impact Zone: Requirements and Functional Design* (1220043-002-HYE-0025). Retrieved from Deltares, Delft, Netherlands.
- de Waal, H., & van Hoven, A. (2015b). *Failure Mechanism Module Grass Wave Runup Zone: Requirements and Functional Design* (1220043-002-HYE-0004). Retrieved from Deltares, Delft, Netherlands.
- de Waal, J. P. (1999). Deelrapport 9: Modelleren dammen, voorlanden en golfoploop. In *Achtergronden hydraulische belastingen dijken IJsselmeergebied* (pp. 50): Lelystad : RIZA
- de Winter, R. C., Sterl, A., & Ruessink, B. G. (2013). Wind extremes in the North Sea Basin under climate change: An ensemble study of 12 CMIP5 GCMs. *J. Geophys. Res.-Atmos.*, 118(4), 1601-1612. doi:<https://doi.org/10.1002/jgrd.50147>
- DeConto, R. M., & Pollard, D. (2016). Contribution of Antarctica to past and future sea-level rise. *Nature*, 531(7596), 591-597. doi:<https://doi.org/10.1038/nature17145>
- DeGroot, E. G., & de Jonge, V. N. (1990). Effects of changes in turbidity and phosphate influx on the ecosystem of the Ems estuary as obtained by a computer simulation model. *Hydrobiologia*, 195(1), 39-47. doi:<https://doi.org/10.1007/BF00026812>

- Delta Programme. (2014). *Delta Programme 2015. Working on the Delta: The Decisions to Keep The Netherlands Safe and Liveable*. Retrieved from Ministry of Infrastructure and the Environment and Ministry of Economic Affairs,, The Hague, Netherlands.
- Deltares. (2020). *Delft3D-FLOW: User Manual*. Retrieved from Deltares, Delft, Netherlands: [https://content.oss.deltares.nl/delft3d/manuals/Delft3D-FLOW\\_User\\_Manual.pdf](https://content.oss.deltares.nl/delft3d/manuals/Delft3D-FLOW_User_Manual.pdf).
- Deltares. (2021). *Riskeer; Gebruikershandleiding*. Retrieved from Deltares, Delft, Netherlands: <https://www.helpdeskwater.nl/onderwerpen/applicaties-modellen/applicaties-per/omgevings/omgevings/riskeer/>.
- den Heijer, F., Vos, R. J., Diermanse, F. L. M., Groeneweg, J., & Tönis, R. (2008). *Achtergrondrapport HR 2006 voor de Zee en Estuaria* (RWS RIKZ rapport 2006.029. ISBN 9036914930). Retrieved from Rijkswaterstaat, Deventer, Netherlands: <https://www.helpdeskwater.nl/publish/pages/157168/b2006-029achtergrondrapporthr2006voordezeenestuaria.pdf>.
- Der Kiureghian, A., & Dakessian, T. (1998). Multiple design points in first and second-order reliability. *Struct. Saf.*, 20(1), 37-49. doi:[https://doi.org/10.1016/S0167-4730\(97\)00026-X](https://doi.org/10.1016/S0167-4730(97)00026-X)
- Diermanse, F. L. M., & Geerse, C. P. M. (2012). Correlation models in flood risk analysis. *Reliab. Eng. Syst. Safe.*, 105, 64-72. doi:<https://doi.org/10.1016/j.res.2011.12.004>
- Ditlevsen, O., & Madsen, H. O. (2007). Generalized reliability index. In *Structural Reliability Methods* (Internet edition 2.3.7 ed., pp. 87 - 109). Kongens Lyngby, Denmark: Department of Mechanical Engineering, Technical University of Denmark.
- Duits, M. T., & Kuijper, B. (2018). *Hydra-NL – Systeemdokumentatie – Versie 2.4*. Retrieved from HKV, Lelystad, Netherlands.
- Dyer, K. R., Christie, M. C., Feates, N., Fennessy, M. J., Pejrup, M., & van der Lee, W. (2000). An Investigation into Processes Influencing the Morphodynamics of an Intertidal Mudflat, the Dollard Estuary, The Netherlands: I. Hydrodynamics and Suspended Sediment. *Estuar. Coast. Shelf S.*, 50(5), 607-625. doi:<https://doi.org/10.1006/ecss.1999.0596>
- Edmonds, D., Caldwell, R., Baumgardner, S., Paola, C., Roy, S., Nelson, A., & Nienhuis, J. (2017). *A global analysis of human habitation on river deltas*. Paper presented at the EGU General Assembly 2017, Vienna, Austria. <https://ui.adsabs.harvard.edu/abs/2017EGUGA..1910832E>
- Ellen, G. J., Boers, M., Knoeff, H., Schelfhout, H. A., Tromp, E., van den Berg, F., . . . Rengers, J. (2011a). *Multifunctioneel medegebruik van de waterkering: beantwoording signaleringsvraag #5 van de Deltacommissaris* (1204871-000). Retrieved from Deltares: <http://docplayer.nl/38173956-Multifunctioneel-medegebruik-van-de-waterkering.html>.
- Ellen, G. J., Hommes, S., Kalweit, A. M., Lamoën, F. v., Melisie, E., Maring, L., . . . Steingrover, E. G. (2011b). *Multifunctioneel landgebruik als adaptatiestrategie - Puzzelen met ondernemers en beleidsmakers*. Retrieved from Kennis voor klimaat: <http://edepot.wur.nl/198714>.
- Elliott, M., Day, J. W., Ramachandran, R., & Wolanski, E. (2019). Chapter 1 - A Synthesis: What Is the Future for Coasts, Estuaries, Deltas and Other Transitional Habitats in 2050 and Beyond? In E. Wolanski, J. W. Day, M. Elliott, & R. Ramachandran (Eds.), *Coasts and Estuaries* (pp. 1-28). Amsterdam, Netherlands; Oxford, United Kingdom; Cambridge, United States: Elsevier.
- Elmilady, H., van der Wegen, M., Roelvink, D., & Jaffe, B. E. (2019). Intertidal Area Disappears Under Sea Level Rise: 250 Years of Morphodynamic Modeling in San Pablo Bay, California. *J. Geophys. Res.-Earth*, 124(1), 38-59. doi:<https://doi.org/10.1029/2018JF004857>
- Elschot, K., Bouma, T. J., Temmerman, S., & Bakker, J. P. (2013). Effects of long-term grazing on sediment deposition and salt-marsh accretion rates. *Estuar. Coast. Shelf S.*, 133, 109-115. doi:<https://doi.org/10.1016/j.ecss.2013.08.021>

- Esselink, P. (1998). *Het Eems-Dollard estuarium : interacties tussen menselijke beïnvloeding en natuurlijke dynamiek*. Haren, Netherlands: RIKZ.
- Esselink, P. (2000). *Nature management of coastal salt marshes : interactions between anthropogenic influences and natural dynamics*. (Doctoral thesis Proefschrift Rijksuniversiteit Groningen). University of Groningen, Haren, Netherlands.
- Esselink, P. (2007). *Hoogteontwikkeling verwaarloosde landaanwinningsskwelder: Opslibbing van de Dollardkwelders in de periode 1991 – 2003 en een vergelijking met de periode 1984 – 1991* (Report 2007-009). Retrieved from Koeman en Bijkerk b.v., Haren, Netherlands.
- Esselink, P., Bos, D., Oost, A. P., Dijkema, K. S., Bakker, H. L., & de Jong, R. J. (2011). *Verkenning afslag Eems-Dollardkwelders* (PUCCIMAR rapport 02, A&W rapport 1574). Retrieved from PUCCIMAR Ecologisch Onderzoek & Advies, Altenburg & Wymenga ecologisch onderzoek, Vries, Feanwâlden, Netherlands.
- Esselink, P., Dijkema, K. S., Sabine, R., & Geert, H. (1998). Vertical Accretion and Profile Changes in Abandoned Man-Made Tidal Marshes in the Dollard Estuary, the Netherlands. *J. Coast. Res.*, 14(2), 570-582. Retrieved from [www.jstor.org/stable/4298810](http://www.jstor.org/stable/4298810)
- Esselink, P., Elschoot, K., Tolman, M., & Veenstra, W. (2019). *Monitoring Demonstratieproject Brede Groene Dijk (fase 1 en 2): vervolgmonitoring ontwateringssstelsel, kwelderafslag, opslibbing en vegetatie* (2018) (rapport 18). Retrieved from PUCCIMAR, Vries, the Netherlands.
- Esselink, P., Veenstra, W., Daniels, P., & Veenstra, W. (2018). *Monitoring Demonstratieproject Brede Groene Dijk (fase 1 en 2): nulmeting ontwateringssstelsel, kwelderafslag en vegetatie* (2017) (PUCCIMAR-report 16). Retrieved from PUCCIMAR, Vries, Netherlands.
- Esteves, L. S. (2014). Examples of Relevant Strategies and Policies. In L. S. Esteves (Ed.), *Managed Realignment : A Viable Long-Term Coastal Management Strategy?* (pp. 45-60). Dordrecht: Springer Netherlands.
- Fagherazzi, S., Kirwan, M. L., Mudd, S. M., Guntenspergen, G. R., Temmerman, S., D'Alpaos, A., . . . Clough, J. (2012). Numerical models of salt marsh evolution: Ecological, geomorphic, and climatic factors. *Rev. Geophys.*, 50(1). doi:<https://doi.org/10.1029/2011rg000359>
- Fagherazzi, S., Mariotti, G., Wiberg, P. L., & McGlathery, K. J. (2013). Marsh Collapse Does Not Require Sea Level Rise. *Oceanography*, 26(3), 70-77. doi:<https://doi.org/10.5670/oceanog.2013.47>
- Fan, J., & Huang, G. (2020). Evaluation of Flood Risk Management in Japan through a Recent Case. *Sustainability*, 12(13), 5357. doi:<https://doi.org/10.3390/su12135357>
- Ferrario, F., Beck, M. W., Storlazzi, C. D., Micheli, F., Shepard, C. C., & Airolidi, L. (2014). The effectiveness of coral reefs for coastal hazard risk reduction and adaptation. *Nat. Commun.*, 5(1), 3794. doi:<https://doi.org/10.1038/ncomms4794>
- Firth, L. B., Thompson, R. C., Bohn, K., Abbiati, M., Airolidi, L., Bouma, T. J., . . . Hawkins, S. J. (2014). Between a rock and a hard place: Environmental and engineering considerations when designing coastal defence structures. *Coast. Eng.*, 87, 122-135. doi:<https://doi.org/10.1016/j.coastaleng.2013.10.015>
- Ford, M. A., Cahoon, D. R., & Lynch, J. C. (1999). Restoring marsh elevation in a rapidly subsiding salt marsh by thin-layer deposition of dredged material. Mention of trade names or commercial products does not constitute an endorsement or recommendation for use by the US Government.1. *Ecol. Eng.*, 12(3), 189-205. doi:[https://doi.org/10.1016/S0925-8574\(98\)00061-5](https://doi.org/10.1016/S0925-8574(98)00061-5)
- Foster-Martinez, M. R., Lacy, J. R., Ferner, M. C., & Variano, E. A. (2018). Wave attenuation across a tidal marsh in San Francisco Bay. *Coast. Eng.*, 136, 26-40. doi:<https://doi.org/10.1016/j.coastaleng.2018.02.001>

- French, J. R. (1993). Numerical simulation of vertical marsh growth and adjustment to accelerated sea-level rise, North Norfolk, U.K. *Earth Surf. Proc. Land.*, 18(1), 63-81.  
doi:<https://doi.org/10.1002/esp.3290180105>
- French, R. H. (1985). *Open-channel hydraulics* (J. Zselezky & R. Margolies Eds. 2nd Printing ed.). New York, United States of America: McGraw-Hill
- Friess, D. A., Spencer, T., Smith, G. M., Möller, I., Brooks, S. M., & Thomson, A. G. (2012). Remote sensing of geomorphological and ecological change in response to saltmarsh managed realignment, The Wash, UK. *Int. J. Appl. Earth Obs.*, 18, 57-68.  
doi:<https://doi.org/10.1016/j.jag.2012.01.016>
- Ganju, N. K. (2019). Marshes Are the New Beaches: Integrating Sediment Transport into Restoration Planning. *Estuaries Coasts*, 42(4), 917-926. doi:<https://doi.org/10.1007/s12237-019-00531-3>
- Gasmo, J. M., Rahardjo, H., & Leong, E. C. (2000). Infiltration effects on stability of a residual soil slope. *Comput. Geotech.*, 26(2), 145-165. doi:[https://doi.org/10.1016/S0266-352X\(99\)00035-X](https://doi.org/10.1016/S0266-352X(99)00035-X)
- Gautier, C., & Groeneweg, J. (2012). *Achtergrondrapportage hydraulische belasting voor zee en estuaria* (1204143-002-HYE-0037). Retrieved from Deltares, Delft, Netherlands:  
[http://publications.deltares.nl/1204143\\_002.pdf](http://publications.deltares.nl/1204143_002.pdf).
- Gautier, C., Schelfhout, H. A., & van Meurs, G. A. M. (2015). *Dijkversterking Eemshaven-Delfzijl; waterveiligheid van een dubbele dijk* (1220600-000-GEO-0004-gbh). Retrieved from Deltares, Delft, Netherlands.
- Geerse, C. P. M., Stijnen, J., & Kolen, B. (2007). *Richtlijnen normering compartimenteringskeringen* (2007-03 ORK). Retrieved from STOWA:  
<https://www.stowa.nl/sites/default/files/assets/PUBLICATIES/Publicaties%202000-2010/Publicaties%202005-2009/STOWA%202007-03%20ORK.pdf>.
- Ghazavi, R., Vali, A., & Eslamian, S. (2010). Impact of Flood Spreading on Infiltration Rate and Soil Properties in an Arid Environment. *Water Resour. Manag.*, 24(11), 2781-2793.  
doi:<https://doi.org/10.1007/s11269-010-9579-y>
- Glass, E. M., Garzon, J. L., Lawler, S., Paquier, E., & Ferreira, C. M. (2018). Potential of marshes to attenuate storm surge water level in the Chesapeake Bay. *Limnol. Oceanogr.*, 63(2), 951-967.  
doi:<https://doi.org/10.1002/lno.10682>
- Goeldner-Gianella, L. (2007). Perceptions and attitudes towards de-polderisation in Europe : a comparison of five opinion surveys in France and the UK. *J. Coast. Res.*, 23(5), 1218-1230.  
doi:<https://doi.org/10.2112/04-0416R.1>
- Griffiths, D. V., & Fenton, G. A. (2007). The Random Finite Element Method (RFEM) in Slope Stability Analysis. In *Probabilistic Methods in Geotechnical Engineering* (pp. 317-346). Vienna, Austria: Springer Vienna.
- Guannel, G., Arkema, K., Ruggiero, P., & Verutes, G. (2016). The Power of Three: Coral Reefs, Seagrasses and Mangroves Protect Coastal Regions and Increase Their Resilience. *PLOS ONE*, 11(7), e0158094. doi:<https://doi.org/10.1371/journal.pone.0158094>
- Gulvanessian, H. (2009). EN 1990 Eurocode "Basis of structural design" – the innovative head Eurocode. *Steel Construction*, 2(4), 222-227. doi:<https://doi.org/10.1002/stco.200910030>
- H2O. (2019). Natuurherstel Polder Breebaart gestart, slib wordt klei voor Brede Groene Dijk H2O. Retrieved from <https://www.h2owaternetwerk.nl/h2o-actueel/natuurherstel-polder-breebaart-van-start>
- Haasnoot, M., Bouwer, L., Diermanse, F., Kwadijk, J., van der Spek, A., Oude Essink, G., . . . Mosselman, E. (2018). *Mogelijke gevolgen van versnelde zeespiegelstijging voor het Deltaprogramma: Een verkenning* (11202230-005-0002.). Retrieved from Deltares, Delft, Netherlands:

- <https://www.deltacommissaris.nl/binaries/deltacommissaris/documenten/publicaties/2018/09/18/dp2019-b-rapport-deltares/DP2019+B+Rapport+Deltares.pdf>.
- Haasnoot, M., Brown, S., Scussolini, P., Jimenez, J. A., Vafeidis, A. T., & Nicholls, R. J. (2019). Generic adaptation pathways for coastal archetypes under uncertain sea-level rise. *Environ. Res. Comm.*, 1(7), 071006. doi:<http://dx.doi.org/10.1088/2515-7620/ab1871>
- Hall, J. W., Dawson, R. J., Sayers, P. B., Rosu, C., Chatterton, J. B., & Deakin, R. (2003). *A methodology for national-scale flood risk assessment*. Paper presented at the Proceedings of the Institution of Civil Engineers-Water Maritime and Engineering.
- Hallegatte, S. (2009). Strategies to adapt to an uncertain climate change. *Glob. Environ. Change*, 19(2), 240-247. doi:<https://doi.org/10.1016/j.gloenvcha.2008.12.003>
- Halter, W. R. (2015). *Flood Safety on Dikes with Wind Turbines*. Paper presented at the Geotechnical Safety and Risk V, Rotterdam, Netherlands.
- Hanssen, R. F., & van Leijen, F. J. (2008). *Monitoring deformation of water defense structures using satellite radar interferometry*. Paper presented at the Proceedings of the 13th FIG Symposium on Deformation Measurement and Analysis, Lisbon, Portugal.
- Hasofer, A. M., & Lind, N. C. (1974). Exact and invariant second-moment code format. *J. Eng. Mech. Div.-ASCE*, 100(1), 111-121.
- Herle, S., Becker, R., & Blankenbach, J. (2016). Smart sensor-based geospatial architecture for dike monitoring. *IOP Conference Series: Earth and Environmental Science*, 34(1), 012014. Retrieved from <http://stacks.iop.org/1755-1315/34/i=1/a=012014>
- Hinkel, J., Lincke, D., Vafeidis, A. T., Perrette, M., Nicholls, R. J., Tol, R. S. J., . . . Levermann, A. (2014). Coastal flood damage and adaptation costs under 21st century sea-level rise. *P. Natl. Acad. Sci. USA*, 111(9), 3292. doi:<https://doi.org/10.1073/pnas.1222469111>
- Hinkel, J., van Vuuren, D. P., Nicholls, R. J., & Klein, R. J. T. (2013). The effects of adaptation and mitigation on coastal flood impacts during the 21st century. An application of the DIVA and IMAGE models. *Climatic Change*, 117(4), 783-794. doi:<https://doi.org/10.1007/s10584-012-0564-8>
- Hirabayashi, Y., Mahendran, R., Koirala, S., Konoshima, L., Yamazaki, D., Watanabe, S., . . . Kanae, S. (2013). Global flood risk under climate change. *Nat. Clim. Change*, 3, 816. doi:<http://dx.doi.org/10.1038/nclimate1911>
- Hoffmans, G., Akkerman, G. J., Verheij, H., van Hoven, A., & van der Meer, J. W. (2009). The erodibility of grassed inner dike slopes against wave overtopping. In *Coastal Engineering 2008* (pp. 3224-3236): World Scientific Publishing Company.
- Hofstede, J. L. A. (2019). On the feasibility of managed retreat in the Wadden Sea of Schleswig-Holstein. *J. Coast. Conserv.*, 23(6), 1069-1079. doi:<https://doi.org/10.1007/s11852-019-00714-x>
- Hoitink, A. J. F., Nittrouer, J. A., Passalacqua, P., Shaw, J. B., Langendoen, E. J., Huismans, Y., & van Maren, D. S. (2020). Resilience of River Deltas in the Anthropocene. *J. Geophys. Res.-Earth*, 125(3), e2019JF005201. doi:<https://doi.org/10.1029/2019JF005201>
- Holthuijsen, L. H. (1980). *Methoden voor golfvoorspelling* (P80-01). Retrieved from TAW/ENW, Delft, Netherlands: <http://resolver.tudelft.nl/uuid:4e0d4d55-986d-488a-9bb6-04e7088b231d>.
- Hu, Z., van Belzen, J., van der Wal, D., Balke, T., Wang, Z. B., Stive, M. J. F., & Bouma, T. J. (2015). Windows of opportunity for salt marsh vegetation establishment on bare tidal flats: The importance of temporal and spatial variability in hydrodynamic forcing. *J. Geophys. Res.-Biogeo.*, 120(7), 1450-1469. doi:<https://doi.org/10.1002/2014JG002870>
- Huguet, J. R., Bertin, X., & Arnaud, G. (2018). Managed realignment to mitigate storm-induced flooding: A case study in La Faute-sur-mer, France. *Coast. Eng.*, 134, 168-176. doi:<https://doi.org/10.1016/j.coastaleng.2017.08.010>

- Hunze en Aa's. (2020). Dijkversterking zeedijk - Brede Groene Dijk. Retrieved from <https://www.hunzeenaas.nl/projecten/brede-groene-dijk/>
- HWBP. (2020). *Projectenboek HWBP 2021*. Utrecht, Netherlands: Programmabureau van het HWBP.
- Ichidate, S., Tsuji, M., Taki, K., & Nakamura, H. (2016). The Risk-Based Floodplain Regulation of Shiga Prefecture in Japan. *E3S Web Conf.*, 7, 13008. doi:<https://doi.org/10.1051/e3sconf/20160713008>
- IPCC. (2013). *Climate Change 2013: The Physical Science Basis. Contribution of Working Group I to the Fifth Assessment Report of the Intergovernmental Panel on Climate Change* (T. F. Stocker, D. Qin, G.-K. Plattner, M. Tignor, S. K. Allen, J. Boschung, A. Nauels, Y. Xia, V. Bex, & P. M. Midgley Eds.). Cambridge, United Kingdom: Cambridge University Press.
- Janbu, N. (1973). Slope stability computations. In E. Hirschfield & S. Poulos (Eds.), *Embankment Dam Engineering (Casagrande Memorial Volume)* (pp. 47-86). New York: John Wiley.
- Jeuken, A., Haasnoot, M., Reeder, T., & Ward, P. J. (2014). Lessons learnt from adaptation planning in four deltas and coastal cities. *J. Water Clim. Change*, 6(4), 711-728. doi:<https://doi.org/10.2166/wcc.2014.141>
- Jongejan, R. B., Diermanse, F., Kanning, W., & Bottema, M. (2020). Reliability-based partial factors for flood defenses. *Reliab. Eng. Syst. Safe.*, 193, 106589. doi:<https://doi.org/10.1016/j.res.2019.106589>
- Jongejan, R. B., Maaskant, B., Ter, W., Havinga, F., Roode, N., & Stefess, H. (2013). *The VNK2-project: A fully probabilistic risk analysis for all major levee systems in the Netherlands*.
- Jongman, B., Ward, P. J., & Aerts, J. C. J. H. (2012). Global exposure to river and coastal flooding: Long term trends and changes. *Global Environ. Chang.*, 22(4), 823-835. doi:<https://doi.org/10.1016/j.gloenvcha.2012.07.004>
- Jonkman, S. N., Kok, M., Van Ledden, M., & Vrijling, J. K. (2009). Risk-based design of flood defence systems: a preliminary analysis of the optimal protection level for the New Orleans metropolitan area. *J. Flood Risk Manag.*, 2(3), 170-181. doi:<https://doi.org/10.1111/j.1753-318X.2009.01036.x>
- Karle, M., & Bartholomä, A. (2008). Salt marsh sediments as natural resources for dike construction – sediment recycling in clay pits. *Senck. Marit.*, 38(2), 83. doi:<https://doi.org/10.1007/BF03055283>
- Kaste, D., & Klein Breteler, M. (2014). *Sensitivity study into residual strength of dikes after block revetment failure, given as preliminary safety factor* (1207811-010-HYE-0005). Retrieved from Deltares, Delft, Netherlands.
- Kaste, D., & Klein Breteler, M. (2015). *Rekenmodel voor kleierosie bij variërende waterstand* (1209832-010-HYE-0001). Retrieved from Deltares, Delft, the Netherlands: [https://www.zeeweringenwiki.nl/images/a/ab/Rekenmodel\\_voor\\_kleierosie\\_bij\\_variërende\\_waterstand\\_definitief.pdf](https://www.zeeweringenwiki.nl/images/a/ab/Rekenmodel_voor_kleierosie_bij_variërende_waterstand_definitief.pdf).
- Kaste, D., Klein Breteler, M., & Provoost, Y. (2015). *Development of a numerical model to predict the erosion of a dike after the failure of the revetment using time dependent boundary conditions*. Paper presented at the 36th IAHR World Congress, the Hague, Netherlands.
- Kheradmand, S., Seidou, O., Konte, D., Batoure, B., & Bohari, M. (2018). Evaluation of adaptation options to flood risk in a probabilistic framework. *J. Hydrol.: Regional Stud.*, 19, 1-16. doi:<https://doi.org/10.1016/j.ejrh.2018.07.001>
- Kiedrzyńska, E., Kiedrzyński, M., & Zalewski, M. (2015). Sustainable floodplain management for flood prevention and water quality improvement. *Nat. Hazards*, 76(2), 955-977. doi:<https://doi.org/10.1007/s11069-014-1529-1>

- Kiesel, J., Schuerch, M., Christie, E. K., Möller, I., Spencer, T., & Vafeidis, A. T. (2020). Effective design of managed realignment schemes can reduce coastal flood risks. *Estuar. Coast. Shelf S.*, 242, 106844. doi:<https://doi.org/10.1016/j.ecss.2020.106844>
- Kirwan, M. L., Guntenspergen, G. R., D'Alpaos, A., Morris, J. T., Mudd, S. M., & Temmerman, S. (2010). Limits on the adaptability of coastal marshes to rising sea level. *Geophys. Res. Lett.*, 37(23). doi:<https://doi.org/10.1029/2010GL045489>
- Kirwan, M. L., & Megonigal, J. P. (2013). Tidal wetland stability in the face of human impacts and sea-level rise. *Nature*, 504(7478), 53-60. doi:<https://doi.org/10.1038/nature12856>
- Kirwan, M. L., & Temmerman, S. (2009). Coastal marsh response to historical and future sea-level acceleration. *Quaternary Sci. Rev.*, 28(17), 1801-1808. doi:<https://doi.org/10.1016/j.quascirev.2009.02.022>
- Kirwan, M. L., Temmerman, S., Skeehan, E. E., Guntenspergen, G. R., & Fagherazzi, S. (2016). Overestimation of marsh vulnerability to sea level rise. *Nat. Clim. Change.*, 6(3), 253-260. doi:<https://doi.org/10.1038/nclimate2909>
- Klein Breteler, M. (2015). *Residual strength of grass on clay in the wave impact zone: Basis for safety assessment method of WTI-2017, product 5.10* (1209437-011-HYE-0004). Retrieved from Deltares, Delft, Netherlands.
- Klein Breteler, M., Bottema, M., Kruse, G. A. M., Mourik, G. C., & Capel, A. (2012a). Resilience of dikes after initial damage by wave attack. *Coastal Engineering Proceedings*, 1(33). doi:<https://doi.org/10.9753/icce.v33.structures.36>
- Klein Breteler, M., Capel, A., Kruse, G., Mourik, G. C., & Kaste, D. (2012b). *Erosie van een dijk na bezwijken van de steenzetting door golven - SBW reststerkte; analyse Deltagootproeven* (1204200-008). Retrieved from Deltares, Delft, Netherlands.
- Klein Breteler, M., & Mourik, G. C. (2019). *Invloed hoek van golfaanval op graserosie op dijken*. Retrieved from Deltares, Delft, the Netherlands.
- Klein Breteler, M., Mourik, G. C., & Provoost, Y. (2014). Stability of placed block revetments in the wave run-up zone. *Coastal Engineering Proceedings*, 1(34), 24. doi:10.9753/icce.v34.structures.24
- Klerk, W. J., & Jongejan, R. B. (2016). *Semi-probabilistic assessment of wave impact and runoff on grass revetments* (1220080-005-ZWS-0003). Retrieved from Deltares, Delft, Netherlands: <https://www.helpdeskwater.nl/publish/pages/132669/1220080-005-zws-0003-r-semi-probabilistic-assessment-of-wave-impact-and-runup-on-grass-revetment.pdf>
- Klijn, F., de Bruijn, K. M., Knoop, J., & Kwadijk, J. (2012). Assessment of the Netherlands' Flood Risk Management Policy Under Global Change. *AMBIO*, 41(2), 180-192. doi:<https://doi.org/10.1007/s13280-011-0193-x>
- Klijn, F., Kreibich, H., de Moel, H., & Penning-Rowsell, E. (2015). Adaptive flood risk management planning based on a comprehensive flood risk conceptualisation. *Mitig. Adapt. Strat. Gl.*, 20(6), 845-864. doi:<https://doi.org/10.1007/s11027-015-9638-z>
- KNMI. (2014). *KNMI'14: Climate Change scenarios for the 21st Century – A Netherlands perspective* (KNMI scientific report WR 2014-01). Retrieved from KNMI, De Bilt, The Netherlands: [www.climatescenarios.nl](http://www.climatescenarios.nl).
- Knoeff, H. (2017). *Factsheet indirecte mechanismen* (11200574-007-GEO-0001). Retrieved from Deltares, Delft, Netherlands: <https://www.helpdeskwater.nl/publish/pages/157143/11200574-007-geo-0001-factsheet-indirecte-mechanismen.pdf>.
- Knoeff, H., & Ellen, G. J. (2011). *Verkenning deltadijken* (1204259-000-ZWS-0004). Retrieved from Deltares, Delft, Netherlands.

- Kok, M., Jongejan, R. B., Nieuwjaar, M., & Tanczos, I. (2017). *Fundamentals of flood protection*. Retrieved from <https://www.enwinfo.nl/images/pdf/Grondslagen/GrondslagenEN-lowresspread3-v.3.pdf>
- Koks, E. E., Jongman, B., Husby, T. G., & Botzen, W. J. W. (2015). Combining hazard, exposure and social vulnerability to provide lessons for flood risk management. *Environ. Sci. Policy*, 47, 42-52. doi:<https://doi.org/10.1016/j.envsci.2014.10.013>
- Kornman, B. A., & de Deckere, E. M. G. T. (1998). Temporal variation in sediment erodibility and suspended sediment dynamics in the Dollard estuary. *Geol. Soc. Sp.*, 139(1), 231-241. doi:10.1144/gsl.Sp.1998.139.01.19
- Krone, R. B. (1987). A method for simulating historic marsh elevations. In N. C. Krause (Ed.), *Coastal sediments '87* (pp. 316-323). New York, NY: ASCE.
- Kundzewicz, Z. W., & Takeuchi, K. (1999). Flood protection and management: quo vadimus? *Hydrolog. Sci. J.*, 44(3), 417-432. doi:<https://doi.org/10.1080/02626669909492237>
- Kwadijk, J. C. J., Haasnoot, M., Mulder, J. P. M., Hoogvliet, M. M. C., Jeuken, A. B. M., van der Krogt, R. A. A., . . . de Wit, M. J. M. (2010). Using adaptation tipping points to prepare for climate change and sea level rise: a case study in the Netherlands. *WIREs Climate Change*, 1(5), 729-740. doi:<https://doi.org/10.1002/wcc.64>
- Kwakernaak, C., Lenselink, G., van der Hoek, D. J., Paulissen, M. P. C. P., Jansen, H. M., Kamermans, P., . . . van Ek, R. (2015). *Economische en ecologische perspectieven van een dubbele dijk langs de Eems-Dollard : waarderen en verzilveren van ecosysteemdiensten en versterken van biodiversiteit bij een Multifunctionele Dubbele Keringzone voor de dijkversterking Eemshaven & Delfzijl*. Retrieved from Alterra, Wageningen-UR, Wageningen: <https://edepot.wur.nl/347025>.
- Lammersen, R., Engel, H., van de Langemheen, W., & Buiteveld, H. (2002). Impact of river training and retention measures on flood peaks along the Rhine. *J. Hydrol.*, 267(1), 115-124. doi:[https://doi.org/10.1016/S0022-1694\(02\)00144-0](https://doi.org/10.1016/S0022-1694(02)00144-0)
- Lanzafame, R. C. (2017). *Reliability Analysis of the Influence of Vegetation on Levee Performance*. (PhD). UC Berkeley, Retrieved from <https://escholarship.org/uc/item/8r38c7gx>
- Lashley, C. H., Bricker, J. D., van der Meer, J. W., Altomare, C., & Suzuki, T. (2020). Relative Magnitude of Infragravity Waves at Coastal Dikes with Shallow Foreshores: A Prediction Tool. *J. Waterw. Port Coast.*, 146(5), 04020034. doi:[https://doi.org/10.1061/\(ASCE\)WW.1943-5460.0000576](https://doi.org/10.1061/(ASCE)WW.1943-5460.0000576)
- Le Bars, D., Drijfhout, S., & de Vries, H. (2017). A high-end sea level rise probabilistic projection including rapid Antarctic ice sheet mass loss. *Environ. Res. Lett.*, 12(4), 044013. doi:<https://doi.org/10.1088/1748-9326/aa6512>
- Lee, J. E., Heo, J.-H., Lee, J., & Kim, N. W. (2017). Assessment of Flood Frequency Alteration by Dam Construction via SWAT Simulation. *Water*, 9(4). doi:<https://doi.org/10.3390/w9040264>
- Lendering, K., Schweckendiek, T., & Kok, M. (2018). Quantifying the failure probability of a canal levee. *Georisk*, 1-15. doi:<https://doi.org/10.1080/17499518.2018.1426865>
- Lenders, H. J. R., Huijbregts, M. A. J., Aarts, B. G. W., & van Turnhout, C. A. M. (1999). Assessing the degree of preservation of landscape, natural and cultural-historical values in river dike reinforcement planning in the Netherlands. *Regul. River*, 15(4), 325-337. doi:[https://doi.org/10.1002/\(SICI\)1099-1646\(199907/08\)15:4<325::AID-RRR545>3.0.CO;2-G](https://doi.org/10.1002/(SICI)1099-1646(199907/08)15:4<325::AID-RRR545>3.0.CO;2-G)
- Leo, K. L., Gillies, C. L., Fitzsimons, J. A., Hale, L. Z., & Beck, M. W. (2019). Coastal habitat squeeze: A review of adaptation solutions for saltmarsh, mangrove and beach habitats. *Ocean. Coast. Manage.*, 175, 180-190. doi:<https://doi.org/10.1016/j.ocecoaman.2019.03.019>

- Leonard, L. A., & Croft, A. L. (2006). The effect of standing biomass on flow velocity and turbulence in *Spartina alterniflora* canopies. *Estuar. Coast. Shelf S.*, 69(3), 325-336. doi:<https://doi.org/10.1016/j.ecss.2006.05.004>
- Leonard, L. A., & Reed, D. J. (2002). Hydrodynamics and Sediment Transport Through Tidal Marsh Canopies. *J. Coast. Res.*, 36(sp1), 459-469, 411. doi:<https://doi.org/10.2112/1551-5036-36.sp1.459>
- Low, B. K., & Tang, W. H. (2007). Efficient Spreadsheet Algorithm for First-Order Reliability Method. *J. Eng. Mech.*, 133(12), 1378-1387. doi:[https://doi.org/10.1061/\(ASCE\)0733-9399\(2007\)133:12\(1378\)](https://doi.org/10.1061/(ASCE)0733-9399(2007)133:12(1378))
- Luisetti, T., Turner, R. K., Bateman, I. J., Morse-Jones, S., Adams, C., & Fonseca, L. (2011). Coastal and marine ecosystem services valuation for policy and management: Managed realignment case studies in England. *Ocean. Coast. Manage.*, 54(3), 212-224. doi:<https://doi.org/10.1016/j.ocecoaman.2010.11.003>
- Mai, S., von Lieberman, N., & Zimmermann, C. (1999). *Interaction of foreland structures with waves*. Paper presented at the Proc. of the XXVIII IAHR congress, Graz, Austria.
- Mariotti, G. (2016). Revisiting salt marsh resilience to sea level rise: Are ponds responsible for permanent land loss? *J. Geophys. Res.-Earth*, 121(7), 1391-1407. doi:<https://doi.org/10.1002/2016JF003900>
- Mariotti, G., & Fagherazzi, S. (2013). Critical width of tidal flats triggers marsh collapse in the absence of sea-level rise. *P. Natl. Acad. Sci. USA*, 110(14), 5353-5356. doi:<https://doi.org/10.1073/pnas.1219600110>
- Maris, A. G., Blocq, V. E., van Kuffeler, V. J. P., Harmsen, W. J. H., Jansen, P. P., Nijhoff, G. P., . . . van der Wal, L. T. (1961). *Rapport Deltacommissie. Deel 1. Eindverslag en interimadviezen*. Retrieved from: <https://repository.tudelft.nl/islandora/object/uuid:0e28dfd8-4e67-4267-a443-54b74a062bcb?collection=research>.
- Maris, T., Cox, T., Temmerman, S., De Vleeschauwer, P., Van Damme, S., De Mulder, T., . . . Meire, P. (2007). Tuning the tide: creating ecological conditions for tidal marsh development in a flood control area. *Hydrobiologia*, 588(1), 31-43. doi:<https://doi.org/10.1007/s10750-007-0650-5>
- Marsooli, R., Lin, N., Emanuel, K., & Feng, K. (2019). Climate change exacerbates hurricane flood hazards along US Atlantic and Gulf Coasts in spatially varying patterns. *Nat. Commun.*, 10(1), 3785. doi:<https://doi.org/10.1038/s41467-019-11755-z>
- Mcleod, E., Chmura, G. L., Bouillon, S., Salm, R., Björk, M., Duarte, C. M., . . . Silliman, B. R. (2011). A blueprint for blue carbon: toward an improved understanding of the role of vegetated coastal habitats in sequestering CO<sub>2</sub>. *Front. Ecol. Environ.*, 9(10), 552-560. doi:<https://doi.org/10.1890/110004>
- Mendez, F. J., & Losada, I. J. (2004). An empirical model to estimate the propagation of random breaking and nonbreaking waves over vegetation fields. *Coast. Eng.*, 51(2), 103-118. doi:<https://doi.org/10.1016/j.coastaleng.2003.11.003>
- Menke, W. (2015). Die Entwicklung des Brutvogelbestands im Elisabeth-Außengroden. In M. Janssen, H. Jöns, & S. Wolters (Eds.), *Nachrichten des Marschenrates zur Förderung der Forschung im Küstengebiet der Nordsee* (pp. 57-72). Wilhelmshaven, Germany: Marschenrat zur Förderung der Forschung im Küstengebiet der Nordsee e. V.
- Regeling van de Minister van Infrastructuur en Milieu, van 2 december 2016, nr. IENM/BSK-2016/283517, ter uitvoering van de artikelen 2.3, eerste lid, en 2.12, vierde lid, van de Waterwet, houdende regels voor het bepalen van de hydraulische belasting en de sterkte en procedurele regels voor de beoordeling van de veiligheid van primaire waterkeringen, (2016).

- Ministerie van Verkeer en Waterstaat. (2007). *Voorschrift Toetsen op Veiligheid Primaire Waterkeringen*. Den Haag: Ministerie van Verkeer en Waterstaat.
- Möller, I. (2019). Applying Uncertain Science to Nature-Based Coastal Protection: Lessons From Shallow Wetland-Dominated Shores. *Front. Ecol. Environ.*, 7(49). doi:<https://doi.org/10.3389/fenvs.2019.00049>
- Möller, I., Kudella, M., Rupprecht, F., Spencer, T., Paul, M., van Wesenbeeck, B. K., . . . Schimmels, S. (2014). Wave attenuation over coastal salt marshes under storm surge conditions. *Nature Geoscience*, 7(10), 727-731. doi:10.1038/ngeo2251
- Möller, I., & Spencer, T. (2002). Wave dissipation over macro-tidal saltmarshes: Effects of marsh edge typology and vegetation change. *J. Coast. Res.*, 36(sp1), 506-521, 516. Retrieved from <https://doi.org/10.2112/1551-5036-36.sp1.506>
- Möller, I., Spencer, T., French, J. R., Leggett, D. J., & Dixon, M. (1999). Wave Transformation Over Salt Marshes: A Field and Numerical Modelling Study from North Norfolk, England. *Estuar. Coast. Shelf S.*, 49(3), 411-426. doi:<https://doi.org/10.1006/ecss.1999.0509>
- Möller, I., Spencer, T., French, J. R., Leggett, D. J., & Dixon, M. (2001). The Sea-Defence Value of Salt Marshes: Field Evidence From North Norfolk. *Water Environ. J.*, 15(2), 109-116. doi:<https://doi.org/10.1111/j.1747-6593.2001.tb00315.x>
- Morgenstern, N. R., & Price, V. E. (1965). The Analysis of the Stability of General Slip Surfaces. *Géotechnique*, 15(1). doi:<https://doi.org/10.7939/R3IS9HF63>
- Mourik, G. C. (2015). *Prediction of the erosion velocity of a slope of clay due to wave attack: WTI-2017 Product 5.21*. Retrieved from Deltares, Delft, Netherlands.
- Munsch, S. H., Cordell, J. R., & Toft, J. D. (2017). Effects of shoreline armouring and overwater structures on coastal and estuarine fish: opportunities for habitat improvement. *J. Appl. Ecol.*, 54(5), 1373-1384. doi:<https://doi.org/10.1111/1365-2664.12906>
- Nakamura, H. (2016). Possibilities of neighborhood evacuation within a district in the event of a large-scale flood in a low-lying area: A case study of Shinden district in Tokyo. *E3S Web Conf.*, 7, 19005. doi:<https://doi.org/10.1051/e3sconf/20160719005>
- Narayan, S., Beck, M. W., Reguero, B. G., Losada, I. J., van Wesenbeeck, B. K., Pontee, N., . . . Burks-Copes, K. A. (2016). The Effectiveness, Costs and Coastal Protection Benefits of Natural and Nature-Based Defences. *PLOS ONE*, 11(5), e0154735. doi:<https://doi.org/10.1371/journal.pone.0154735>
- Neal, J., Keef, C., Bates, P., Beven, K., & Leedal, D. (2013). Probabilistic flood risk mapping including spatial dependence. *Hydrol. Process.*, 27(9), 1349-1363. doi:<https://doi.org/10.1002/hyp.9572>
- NEN. (2012). NEN 3651:2012 nl: Additional requirements for pipelines in or nearby important public works. In.
- Neumann, B., Vafeidis, A. T., Zimmermann, J., & Nicholls, R. J. (2015). Future Coastal Population Growth and Exposure to Sea-Level Rise and Coastal Flooding - A Global Assessment. *PLOS ONE*, 10(3), e0118571. doi:<https://doi.org/10.1371/journal.pone.0118571>
- Nicholls, R. J. (2004). Coastal flooding and wetland loss in the 21st century: changes under the SRES climate and socio-economic scenarios. *Glob. Environ. Change*, 14(1), 69-86. doi:<https://doi.org/10.1016/j.gloenvcha.2003.10.007>
- Niedermeier, A., Hoja, D., & Lehner, S. (2005). Topography and morphodynamics in the German Bight using SAR and optical remote sensing data. *Ocean Dynam.*, 55(2), 100-109. doi:<https://doi.org/10.1007/s10236-005-0114-2>
- Nolte, S., Müller, F., Schuerch, M., Wanner, A., Esselink, P., Bakker, J. P., & Jensen, K. (2013). Does livestock grazing affect sediment deposition and accretion rates in salt marshes? *Estuar. Coast. Shelf S.*, 135, 296-305. doi:<https://doi.org/10.1016/j.ecss.2013.10.026>

- Oost, A. P., Colina Alonso, A., Esselink, P., Wang, Z. B., van Kessel, T., van Maren, B., . . . Firet, M. (2021). *Where mud matters : towards a mud balance for the trilateral Wadden Sea Area: mud supply, transport and deposition*. Leeuwarden, Netherlands: Wadden Academy.
- Oost, J., & Hoekstra, A. Y. (2009). Flood damage reduction by compartmentalization of a dike ring: comparing the effectiveness of three strategies. *J. Flood Risk Manag.*, 2(4), 315-321. doi:<https://doi.org/10.1111/j.1753-318X.2009.01050.x>
- Oosterlee, L., Cox, T. J. S., Temmerman, S., & Meire, P. (2019). Effects of tidal re-introduction design on sedimentation rates in previously embanked tidal marshes. *Estuar. Coast. Shelf S.*, 244, 106428. doi:<https://doi.org/10.1016/j.ecss.2019.106428>
- Oosterlo, P., McCall, R. T., Vuik, V., Hofland, B., Van der Meer, J. W., & Jonkman, S. N. (2018a). Probabilistic Assessment of Overtopping of Sea Dikes with Foreshores including Infragravity Waves and Morphological Changes: Westkapelle Case Study. *J. Mar. Sci. Eng.*, 6(2), 48. Retrieved from <https://www.mdpi.com/2077-1312/6/2/48>
- Oosterlo, P., van der Meer, J. W., Hofland, B., & van Vledder, G. (2018b). Wave modelling in a complex estuary: study in preparation of field measurement campaign Eems-Dollard estuary. *Coast. Eng. Proc.*, 1(36). doi:<https://doi.org/10.9753/icce.v36.papers.66>
- Orlandini, S., Moretti, G., & Albertson, J. D. (2015). Evidence of an emerging levee failure mechanism causing disastrous floods in Italy. *Water Resour. Res.*, 51(10), 7995-8011. doi:<https://doi.org/10.1002/2015WR017426>
- Özer, I. E., van Damme, M., & Jonkman, S. N. (2020). Towards an International Levee Performance Database (ILPD) and Its Use for Macro-Scale Analysis of Levee Breaches and Failures. *Water*, 12(1), 119. doi:<https://doi.org/10.3390/w12010119>
- Pasche, E., Ujeyl, G., Goltermann, D., Meng, J., Nehlsen, E., & Wilke, M. (2008). Cascading flood compartments with adaptive response. *WIT Trans. Ecol. Envir.*, 118, 303-312. doi:<https://doi.org/10.2495/FRIAR080291>
- Peletier, H., Wanningen, H., Speelman, B., & Esselink, P. (2004). Resultaten van een gedempt getijdenregime in polder Breebaart. *De Levende Natuur*, 105(5), 191-194. Retrieved from <https://library.wur.nl/WebQuery/hydrotheek/1733893>
- Perry, C. T., Alvarez-Filip, L., Graham, N. A. J., Mumby, P. J., Wilson, S. K., Kench, P. S., . . . Macdonald, C. (2018). Loss of coral reef growth capacity to track future increases in sea level. *Nature*, 558(7710), 396-400. doi:<https://doi.org/10.1038/s41586-018-0194-z>
- Peteet, D. M., Nichols, J., Kenna, T., Chang, C., Browne, J., Reza, M., . . . Stern-Protz, S. (2018). Sediment starvation destroys New York City marshes' resistance to sea level rise. *P. Natl. Acad. Sci. USA*, 115(41), 10281. doi:<https://doi.org/10.1073/pnas.1715392115>
- Pontee, N., Narayan, S., Beck, M. W., & Hosking, A. H. (2016). Nature-based solutions: lessons from around the world. *P. I. Civil Eng.-Mar. En.*, 169(1), 29-36. doi:<https://doi.org/10.1680/jmaen.15.00027>
- Powell, E. J., Tyrrell, M. C., Milliken, A., Tirpak, J. M., & Staudinger, M. D. (2019). A review of coastal management approaches to support the integration of ecological and human community planning for climate change. *J. Coast. Conserv.*, 23(1), 1-18. doi:<https://doi.org/10.1007/s11852-018-0632-y>
- Powell, M. J. D. (1994). A Direct Search Optimization Method That Models the Objective and Constraint Functions by Linear Interpolation. In S. Gomez & J.-P. Hennart (Eds.), *Advances in Optimization and Numerical Analysis* (pp. 51-67). Dordrecht: Springer Netherlands.
- Provincie Groningen, & Ministerie van Infrastructuur en Milieu. (2018). *Programma Eems-Dollard 2050*. Retrieved from Provincie Groningen, Groningen, Netherlands: [https://eemsdollard2050.nl/wp-content/uploads/2018/03/ED2050\\_Rapport\\_DEF.pdf](https://eemsdollard2050.nl/wp-content/uploads/2018/03/ED2050_Rapport_DEF.pdf).

- Purvis, M. J., Bates, P. D., & Hayes, C. M. (2008). A probabilistic methodology to estimate future coastal flood risk due to sea level rise. *Coast. Eng.*, 55(12), 1062-1073.  
doi:<https://doi.org/10.1016/j.coastaleng.2008.04.008>
- Raadgevend Ingenieursbureau Wiertsema & Partners. (2016). *Onderzoek kwelderklei; Onderzoek naar de samenstelling van klei in de kwelders te Nieuwe Statenzijl en de mogelijkheden voor toepassing in een dijk* (VN-63304-1). Retrieved from Wiertsema & Partners, Tolbert, Netherlands.
- Rackwitz, R., & Flessler, B. (1978). Structural reliability under combined random load sequences. *Comput. Struct.*, 9(5), 489-494. doi:[https://doi.org/10.1016/0045-7949\(78\)90046-9](https://doi.org/10.1016/0045-7949(78)90046-9)
- Reise, K. (2017). Facing the Third Dimension in Coastal Flatlands: Global Sea Level Rise and the Need for Coastal Transformations. *GAIA*, 26(2), 89-93.  
doi:<https://doi.org/10.14512/gaia.26.2.6>
- Remmerswaal, G., Hicks, M. A., & Vardon, P. J. (2018). *Ultimate limit state assessment of dyke reliability using the random material point method*. Paper presented at the Book of extended abstracts 4th international symposium on computational geomechanics, Assisi, Italy.
- Ridderinkhof, H., van der Ham, R., & van der Lee, W. T. B. (2000). Temporal variations in concentration and transport of suspended sediments in a channel-flat system in the Ems-Dollard estuary. *Cont. Shelf. Res.*, 20(12), 1479-1493. doi:[https://doi.org/10.1016/S0278-4343\(00\)00033-9](https://doi.org/10.1016/S0278-4343(00)00033-9)
- Ridge, J. T., Rodriguez, A. B., Joel Fodrie, F., Lindquist, N. L., Brodeur, M. C., Coleman, S. E., . . . Theuerkauf, E. J. (2015). Maximizing oyster-reef growth supports green infrastructure with accelerating sea-level rise. *Sci. Rep.-UK*, 5(1), 14785. doi:<https://doi.org/10.1038/srep14785>
- Rijkswaterstaat. (2011). WTI2011\_Waddenzee\_voorlanden.mdb. Retrieved from <https://www.helpdeskwater.nl/>
- Rijkswaterstaat. (2014). Actueel Hoogtebestand Nederland 2 (AHN2) WMS In: Publieke Dienstverlening Op de Kaart (PDOK).
- Rijkswaterstaat. (2016a). *Regeling veiligheid primaire waterkeringen 2017: Bijlage I Procedure*. Retrieved from: [https://www.helpdeskwater.nl/onderwerpen/waterveiligheid/primaire/beoordelen-\(wbi\)/producten-wbi/](https://www.helpdeskwater.nl/onderwerpen/waterveiligheid/primaire/beoordelen-(wbi)/producten-wbi/).
- Rijkswaterstaat. (2016b). *Regeling veiligheid primaire waterkeringen 2017: Bijlage II Voorschriften bepaling hydraulische belasting primaire waterkeringen*. Retrieved from: [https://www.helpdeskwater.nl/onderwerpen/waterveiligheid/primaire/beoordelen-\(wbi\)/producten-wbi/](https://www.helpdeskwater.nl/onderwerpen/waterveiligheid/primaire/beoordelen-(wbi)/producten-wbi/).
- Rijkswaterstaat. (2016c). *Regeling veiligheid primaire waterkeringen 2017: Bijlage III Sterkte en veiligheid*. Retrieved from: [https://www.helpdeskwater.nl/onderwerpen/waterveiligheid/primaire/beoordelen-\(wbi\)/producten-wbi/](https://www.helpdeskwater.nl/onderwerpen/waterveiligheid/primaire/beoordelen-(wbi)/producten-wbi/).
- Rijkswaterstaat. (2017). *Handreiking ontwerpen met overstromingskansen; Veiligheidsfactoren en belastingen bij nieuwe overstromingskansen-normen* (OI2014v4). Retrieved from Rijkswaterstaat, Lelystad, the Netherlands: [https://www.helpdeskwater.nl/publish/pages/142605/handreiking\\_ontwerpen\\_met\\_overstromingskansen\\_feb2017.pdf](https://www.helpdeskwater.nl/publish/pages/142605/handreiking_ontwerpen_met_overstromingskansen_feb2017.pdf).
- Rijkswaterstaat. (2018). WTI2011\_Waddenzee\_voorlanden.mdb. Retrieved from: <https://www.helpdeskwater.nl/>
- Rijkswaterstaat. (2019). *Schematiseringshandleiding Macrostabiteit; WBI 2017* Retrieved from Rijkswaterstaat: <https://www.helpdeskwater.nl/onderwerpen/waterveiligheid/primaire/beoordelen/@205756/schematiseringshandleiding-macrostabiteit/>.

- Rijkswaterstaat WVL. (2017). *WBI2017\_Waddenzee\_Oost\_6-7\_v03*. Retrieved from: <https://www.helpdeskwater.nl/>
- Robert, C., & Casella, G. (1999). Monte Carlo Integration. In G. Casella, S. Fienberg, & I. Olkin (Eds.), *Monte Carlo statistical methods* (pp. 71 -138). New York, United States: Springer Science & Business Media.
- Roelvink, D. J. A., Van Dongeren, A., McCall, R., Hoonhout, B., Van Rooijen, A., Van Geer, P., . . . Quataert, E. (2015). *XBeach technical reference: Kingsday release*. Retrieved from Deltares, Delft, Netherlands.
- Rongen, G., Stenfort, J., Dupuits, G., & Barbosa, C. M. (2018). *Time dependent load on revetments: A prototype to provide insight in the sensitivity of grass revetments to varying loads over time* (PR3876.10). Retrieved from HKV, Lelystad.
- Roode, N., Maaskant, B., & Boon, M. (2019). *Handreiking Voorland*(pp. 160). Retrieved from [www.povvoorlanden.nl](http://www.povvoorlanden.nl)
- Roscoe, K., Diermanse, F., & Vrouwenvelder, T. (2015). System reliability with correlated components: Accuracy of the Equivalent Planes method. *Struct. Saf.*, 57, 53-64. doi:<https://doi.org/10.1016/j.strusafe.2015.07.006>
- Rupp-Armstrong, S., & Nicholls, R. J. C. (2007). Coastal and Estuarine Retreat: A Comparison of the Application of Managed Realignment in England and Germany. *J. Coast. Res.*, 236, 1418-1430. doi:<https://doi.org/10.2112/04-0426.1>
- Salathé, E. P., Hamlet, A. F., Mass, C. F., Lee, S. Y., Stumbaugh, M., & Steed, R. (2014). Estimates of Twenty-First-Century Flood Risk in the Pacific Northwest Based on Regional Climate Model Simulations. *Journal of Hydrometeorology*, 15(5), 1881-1899. doi:10.1175/JHM-D-13-0137.1
- Schelfhout, H. A., Nurmohamed, N., Janssen, J., & de Koning, M. (2020). *Veiligheidsraamwerk POV K&L; Toepassing in de praktijk*. Retrieved from Stuurgroep POV K&L;: <https://drive.google.com/file/d/1PHIzNNYxCEXh8ZERLerb1GK3ebziMfe0/view>.
- Scheres, B., & Schüttrumpf, H. (2019). Enhancing the Ecological Value of Sea Dikes. *Water*, 11(8), 1617. doi:<https://doi.org/10.3390/w11081617>
- Schilling, K. E., Gassman, P. W., Kling, C. L., Campbell, T., Jha, M. K., Wolter, C. F., & Arnold, J. G. (2014). The potential for agricultural land use change to reduce flood risk in a large watershed. *Hydrol. Process.*, 28(8), 3314-3325. doi:<https://doi.org/10.1002/hyp.9865>
- Schoonees, T., Gijón Mancheño, A., Scheres, B., Bouma, T. J., Silva, R., Schlurmann, T., & Schüttrumpf, H. (2019). Hard Structures for Coastal Protection, Towards Greener Designs. *Estuaries Coasts*, 42(7), 1709-1729. doi:<https://doi.org/10.1007/s12237-019-00551-z>
- Schoutens, K., Heuner, M., Minden, V., Schulte Ostermann, T., Silinski, A., Belliard, J. P., & Temmerman, S. (2019). How effective are tidal marshes as nature-based shoreline protection throughout seasons? *Limnol. Oceanogr.*, 64(4), 1750-1762. doi:<https://doi.org/10.1002/lno.11149>
- Schuerch, M., Spencer, T., Temmerman, S., Kirwan, M. L., Wolff, C., Lincke, D., . . . Brown, S. (2018). Future response of global coastal wetlands to sea-level rise. *Nature*, 561(7722), 231-234. doi:<https://doi.org/10.1038/s41586-018-0476-5>
- Schweckendiek, T., Vrouwenvelder, A. C. W. M., Calle, E. O. F., Kanning, W., & Jongejan, R. B. (2012). Target reliabilities and partial factors for flood defenses in the Netherlands. In P. Arnold, G. A. Fenton, M. A. Hicks, T. Schweckendiek, & B. Simpson (Eds.), *Modern Geotechnical Codes of Practice* (Vol. 1, pp. 311-328). Amsterdam, Netherlands: IOS Press BV.
- Sellmeijer, H., de la Cruz, J. L., van Beek, V. M., & Knoeff, H. (2011). Fine-tuning of the backward erosion piping model through small-scale, medium-scale and IJkdijk experiments. *Eur. J. Environ. Civ. En.*, 15(8), 1139-1154. doi:<https://doi.org/10.1080/19648189.2011.9714845>

- Sharp, M., Wallis, M., Deniaud, F., Hersch-Burdick, R., Tourment, R., Matheu, E., . . . Wallis, M. (2013). *The International Levee Handbook*. Londres: CIRIA.
- Silliman, B. R., van de Koppel, J., McCoy, M. W., Diller, J., Kasozi, G. N., Earl, K., . . . Zimmerman, A. R. (2012). Degradation and resilience in Louisiana salt marshes after the BP–Deepwater Horizon oil spill. *P. Natl. Acad. Sci. USA*, 109(28), 11234-11239.  
doi:<https://doi.org/10.1073/pnas.1204922109>
- Silva, W., & van Velzen, E. (2008). *De dijk van de toekomst? : quick scan doorbraakvrije dijken* (2008.052; Q4558.32). Retrieved from Rijkswaterstaat; Deltares, Delft:  
<http://publicaties.minienm.nl/documenten/de-dijk-van-de-toekomst-quick-scan-doorbraakvrije-dijken>.
- Slomp, R. (2012). *Flood risk and water management in the Netherlands : a 2012 update* (WD0712RE205). Retrieved from Rijkswaterstaat:  
[https://puc.overheid.nl/rijkswaterstaat/doc/PUC\\_139770\\_31/](https://puc.overheid.nl/rijkswaterstaat/doc/PUC_139770_31/).
- Slomp, R., Knoeff, H., Bizzarri, A., Bottema, M., & de Vries, W. (2016). *Probabilistic flood defence assessment tools*. Paper presented at the E3S Web of Conferences.
- Slomp, R. M., Diemanse, F., de Waal, H., Stijnen, J., Noort, J., & Wentholt, L. (2015). *A consistent suite of models for flood risk management*. Paper presented at the 36th IAHR World Congress, The Hague, the Netherlands.
- Smolders, S., João Teles, M., Leroy, A., Maximova, T., Meire, P., & Temmerman, S. (2020). Modeling Storm Surge Attenuation by an Integrated Nature-Based and Engineered Flood Defense System in the Scheldt Estuary (Belgium). *J. Mar. Sci. Eng.*, 8(1).  
doi:<https://doi.org/10.3390/jmse8010027>
- Spencer, E. (1967). A method of analysis of the stability of embankments assuming parallel inter-slice forces. *Géotechnique*, 17(1), 11-26. doi:<https://doi.org/10.1680/geot.1967.17.1.11>
- Spencer, T., Schuerch, M., Nicholls, R. J., Hinkel, J., Lincke, D., Vafeidis, A. T., . . . Brown, S. (2016). Global coastal wetland change under sea-level rise and related stresses: The DIVA Wetland Change Model. *Global Planet Change*, 139, 15-30.  
doi:<https://doi.org/10.1016/j.gloplacha.2015.12.018>
- Stalenberg, B. (2013). Innovative flood defences in highly urbanised water cities. In J. C. J. H. Aerts, W. J. W. Botzen, M. J. Bowman, P. J. Ward, & P. Dircke (Eds.), *Climate Adaptation and Flood Risk in Coastal Cities* (pp. 145-164). London - New York: Earthscan.
- Stark, J., Plancke, Y., Ides, S., Meire, P., & Temmerman, S. (2016). Coastal flood protection by a combined nature-based and engineering approach: Modeling the effects of marsh geometry and surrounding dikes. *Estuar. Coast. Shelf S.*, 175, 34-45.  
doi:<https://doi.org/10.1016/j.ecss.2016.03.027>
- Stark, J., Van Oyen, T., Meire, P., & Temmerman, S. (2015). Observations of tidal and storm surge attenuation in a large tidal marsh. *Limnol. Oceanogr.*, 60(4), 1371-1381.  
doi:<https://doi.org/10.1002/lno.10104>
- Stark, M., Ravenstijn, P., Korf, J., & Walraven, R. (2006). *Inlaatuiker Waterdunen; Definitief rapport* (162531). Retrieved from Oranjewoud, Middelburg, the Netherlands:  
[http://www.waterdunen.com/sites/zl-waterdunen/files/onderzoek\\_getijdeduiker\\_oranjewoud\\_hoofdrapport.pdf](http://www.waterdunen.com/sites/zl-waterdunen/files/onderzoek_getijdeduiker_oranjewoud_hoofdrapport.pdf).
- Steenbergen, H. M. G. M., Lassing, B. L., Vrouwenfelder, A. C. W. M., & Waarts, P. H. (2004). Reliability analysis of flood defence systems. *Heron*, 49(1).
- Steetzel, H., Groeneweg, J., & Vuik, V. (2020). *Effectiviteit Voorlanden HR Samenvattende rapportage*;

- Samenvatting resultaten, handreiking en aanbevelingen* (WFN.1714325). Retrieved from HWBP: <http://pov-waddenzeedijken.nl/wp-content/uploads/2020/01/EFVHR-Product-4-Samenvattende-rapportage.pdf>.
- Sterl, A., van den Brink, H., de Vries, H., Haarsma, R., & van Meijgaard, E. (2009). An ensemble study of extreme storm surge related water levels in the North Sea in a changing climate. *Ocean Sci.*, 5(3), 369-378. doi:<https://doi.org/10.5194/os-5-369-2009>
- Stive, M. J. F., de Schipper, M. A., Luijendijk, A. P., Aarninkhof, S. G. J., van Gelder-Maas, C., van Thiel de Vries, J. S. M., . . . Ranasinghe, R. (2013). A New Alternative to Saving Our Beaches from Sea-Level Rise: The Sand Engine. *J. Coast. Res.*, 29(5), 1001-1008, 1008. doi:<https://doi.org/10.2112/COASTRES-D-13-00070.1>
- STOWA. (2000). *Bomen op en nabij waterkeringen, achtergrondrapport*: Hageman Fulfiiment.
- STOWA. (2010). *Addendum op de leidraad toetsen op veiligheid regionale waterkeringen betreffende de boezemkaden*. Amersfoort: STOWA,.
- Sweco Nederland B.V. (2018). *Grondstromenplan Demonstratieproject Brede Groene Dijk; Fase 1 en 2* (SWNL0220816). Retrieved from De Bilt, Netherlands.
- Taal, M. D., Schmidt, C. A., Brinkman, A. G., Stolte, W., & Van Maren, D. S. (2015). *Slib en primaire productie in het Eems-estuarium; Een samenvatting van vier jaar meten, modelleren, kennis bundelen en verwerven*. Retrieved from Deltares, Imares & Rijkswaterstaat, Delft: [https://eemsdollard2050.nl/wp-content/uploads/2018/05/Slib\\_en\\_primaire\\_productie\\_in\\_Eems-estuarium.pdf](https://eemsdollard2050.nl/wp-content/uploads/2018/05/Slib_en_primaire_productie_in_Eems-estuarium.pdf).
- Takeuchi, K. (2002). Flood Management in Japan—From Rivers to Basins. *Water Int.*, 27(1), 20-26. doi:<https://doi.org/10.1080/02508060208686974>
- TAW. (1985). *Leidraad voor het ontwerpen van rivierdijken: Deel 1, Bovenrivierengebied* (Staatsuitgeverij Ed.). 's-Gravenhage: Technische Adviescommissie voor de Waterkeringen (TAW).
- TAW. (1994). *Handreiking Constructief ontwerpen: Onderzoek en berekening naar het constructief ontwerp van de dijkversterking (L9)*. Retrieved from Technische Adviescommissie voor de Waterkeringen (TAW): [https://puc.overheid.nl/rijkswaterstaat/doc/PUC\\_81057\\_31/](https://puc.overheid.nl/rijkswaterstaat/doc/PUC_81057_31/).
- TAW. (2002). *Technisch Rapport Golfploop en Golfoverslag bij Dijken (TR33)*. Retrieved from Technische Adviescommissie voor de Waterkeringen (TAW): [https://puc.overheid.nl/rijkswaterstaat/doc/PUC\\_37942\\_31/](https://puc.overheid.nl/rijkswaterstaat/doc/PUC_37942_31/).
- TAW. (2004). *Technisch Rapport Waterspanningen bij dijken* (ISBN-90-369-5565-3). Retrieved from Technische Adviescommissie voor de Waterkeringen (TAW): <https://repository.tudelft.nl/islandora/object/uuid:bf74eeaf-dc41-43fc-9c94-acd70f4a8340?collection=research>.
- Temmerman, S., de Vries, M. B., & Bouma, T. J. (2012). Coastal marsh die-off and reduced attenuation of coastal floods: A model analysis. *Global Planet Change*, 92-93, 267-274. doi:<https://doi.org/10.1016/j.gloplacha.2012.06.001>
- Temmerman, S., Govers, G., Meire, P., & Wartel, S. (2003). Modelling long-term tidal marsh growth under changing tidal conditions and suspended sediment concentrations, Scheldt estuary, Belgium. *Mar. Geol.*, 193(1), 151-169. doi:[https://doi.org/10.1016/S0025-3227\(02\)00642-4](https://doi.org/10.1016/S0025-3227(02)00642-4)
- Temmerman, S., Meire, P., Bouma, T. J., Herman, P. M. J., Ysebaert, T., & de Vriend, H. J. (2013). Ecosystem-based coastal defence in the face of global change. *Nature*, 504(7478), 79-83. doi:<http://dx.doi.org/10.1038/nature12859>
- Tempest, J. A., Harvey, G. L., & Spencer, K. L. (2015). Modified sediments and subsurface hydrology in natural and recreated salt marshes and implications for delivery of ecosystem services. *Hydrol. Process.*, 29(10), 2346-2357. doi:<https://doi.org/10.1002/hyp.10368>
- Toan, T. Q. (2014). 9 - Climate Change and Sea Level Rise in the Mekong Delta: Flood, Tidal Inundation, Salinity Intrusion, and Irrigation Adaptation Methods. In N. D. Thao, H.

- Takagi, & M. Esteban (Eds.), *Coastal Disasters and Climate Change in Vietnam* (pp. 199-218). Oxford: Elsevier.
- Turner, R. K., Burgess, D., Hadley, D., Coombes, E., & Jackson, N. (2007). A cost-benefit appraisal of coastal managed realignment policy. *Global Environ. Chang.*, 17(3), 397-407. doi:<https://doi.org/10.1016/j.gloenvcha.2007.05.006>
- USACE. (2002). *Coastal Engineering Manual*. Retrieved from US Army Corps of Engineers,, Washington, DC. , US: <https://www.publications.usace.army.mil/USACE-Publications/Engineer-Manuals>.
- van Baars, S., & van Kempen, I. M. (2009). The causes and mechanisms of historical dike failures in the Netherlands. *E-Water Official Publication of the European Water Association*, 1-14. Retrieved from <http://resolver.tudelft.nl/uuid:a44dbb70-8116-4dec-bf9d-e5879df3f678>
- van Bergeijk, V., Warmink, J. J., Frankena, M., & Hulscher, S. J. M. H. (2019). Modelling dike cover erosion by overtopping waves: the effects of transitions. In N. Goseberg & T. Schlurmann (Eds.), *Coastal Structures 2019* (pp. 1097-1106). Hannover, Germany: Bundesanstalt für Wasserbau.
- van der Lee, W. T. B. (2000). Temporal variation of floc size and settling velocity in the Dollard estuary. *Cont. Shelf. Res.*, 20(12), 1495-1511. doi:[https://doi.org/10.1016/S0278-4343\(00\)00034-0](https://doi.org/10.1016/S0278-4343(00)00034-0)
- van der Meer, J. W., Allsop, N. W. H., Bruce, T., De Rouck, J., Kortenhaus, A., Pullen, T., & Zanuttigh, B. (2016). EurOtop 2016: Manual on wave overtopping of sea defences and related structures. An overtopping manual largely based on European research, but for worldwide application. In: Retrieved from [www.overtopping-manual.com](http://www.overtopping-manual.com).
- van Gelder, P., Buijs, F., Horst, W., Kanning, W., Mai Van, C., Rajabalinejad, M., . . . van Erp, N. (2008). Reliability analysis of flood defence structures and systems in Europe. In P. Samuels, S. Huntington, W. Allsop, & J. Harrop (Eds.), *Flood Risk Management: Research and Practise* (pp. 603-611). London, UK: Taylor & Francis Ltd.
- van Houwelingen, A. W. (2012). *BomenT fase 3, Gedetailleerde toets* (LW-AF20122371). Retrieved from DHV B.V., Amersfoort, the Netherlands: [https://www.helpdeskwater.nl/publish/pages/132670/rapport\\_fase\\_3\\_d1\\_boment\\_fase\\_3\\_gedetailleerde\\_toets.pdf](https://www.helpdeskwater.nl/publish/pages/132670/rapport_fase_3_d1_boment_fase_3_gedetailleerde_toets.pdf).
- van Hoven, A. (2015). *Verderlingen kritisch overslagdebiet WTI2017* (220086-005-HYE-0003). Retrieved from Deltares, Delft, Netherlands: [https://www.helpdeskwater.nl/publish/pages/132665/1220086-005-hye-0003-m-verdelingen\\_kritisch\\_overslagdebiet\\_wti2017\\_final.pdf](https://www.helpdeskwater.nl/publish/pages/132665/1220086-005-hye-0003-m-verdelingen_kritisch_overslagdebiet_wti2017_final.pdf).
- van Loon-Steensma, J. M. (2015). Salt marshes to adapt the flood defences along the Dutch Wadden Sea coast. *Mitig. Adapt. Strat. Gl.*, 20(6), 929-948. doi:<https://doi.org/10.1007/s11027-015-9640-5>
- van Loon-Steensma, J. M., de Vries, M. B., Bouma, T. J., & Schelfhout, H. A. (2020). *Weerbare Waddenkust; Aanzet tot een conceptueel raamwerk en beslisregels voor een lange termijn handelingsperspectief waterveiligheid en landgebruik bij extreme zeespiegelstijging*. (pp. 52). Retrieved from [https://www.waddenacademie.nl/fileadmin/inhoud/pdf/04-bibliotheek/2020-07\\_Weerbare\\_Wadden.pdf](https://www.waddenacademie.nl/fileadmin/inhoud/pdf/04-bibliotheek/2020-07_Weerbare_Wadden.pdf)
- van Loon-Steensma, J. M., Hu, Z., & Slim, P. A. (2016). Modelled Impact of Vegetation Heterogeneity and Salt-Marsh Zonation on Wave Damping. *J. Coast. Res.*, 32(2), 241-252. doi:<https://doi.org/10.2112/JCOASTRES-D-15-00095.1>
- van Loon-Steensma, J. M., & Kok, M. (2016). Risk reduction by combining nature values with flood protection? *E3S Web Conf.*, 7. doi:<https://doi.org/10.1051/e3sconf/20160713003>

- van Loon-Steensma, J. M., & Schelfhout, H. A. (2013). *Pilotstudie Groene Dollard Dijk; een verkenning naar de haalbaarheid van een brede groene dijk met flauw talud en een breed voorland* (Alterra-rapport 2437, Deltares: 18050-000-ZKS-0004). Retrieved from Alterra, Wageningen, Netherlands.
- van Loon-Steensma, J. M., & Schelfhout, H. A. (2017). Wide Green Dikes: A sustainable adaptation option with benefits for both nature and landscape values? *Land Use Policy*, 63, 528-538. doi:<https://doi.org/10.1016/j.landusepol.2017.02.002>
- van Loon-Steensma, J. M., Schelfhout, H. A., Broekmeyer, M. E. A., Paulissen, M. P. C. P., Oostenbrink, W. T., Smit, C., . . . Jolink, E. (2014a). *Nadere verkenning Groene Dollard Dijk : een civieltechnische, juridische en maatschappelijke verkenning naar de haalbaarheid van een brede groene dijk en mogelijke kleiwinning uit de kwelders*. Retrieved from Alterra, Wageningen, Netherlands: <http://library.wur.nl/WebQuery/wurpubs/fulltext/302530>.
- van Loon-Steensma, J. M., Schelfhout, H. A., van Hattum, T., Smale, A., Gözüberk, I., & van Dijken, M. (2014b). *Innovatieve dijken als strategie voor een veilig en aantrekkelijk Waddengebied : Samenvatting van het Deltaprogramma Waddengebied onderzoek naar innovatieve dijken*. Retrieved from Ministerie van Infrastructuur en Milieu, Den Haag, Netherlands: <https://edepot.wur.nl/320454>.
- van Loon-Steensma, J. M., Schelfhout, H. A., & Vellinga, P. (2014c). Green adaptation by innovative dike concepts along the Dutch Wadden Sea coast. *Environ. Sci. Policy*, 44, 108-125. doi:<http://dx.doi.org/10.1016/j.envsci.2014.06.009>
- van Loon-Steensma, J. M., & Slim, P. A. (2013). The Impact of Erosion Protection by Stone Dams on Salt-Marsh Vegetation on Two Wadden Sea Barrier Islands. *J. Coast. Res.*, 29(4), 783-796. doi:<https://doi.org/10.2112/jcoastres-d-12-00123.1>
- van Loon-Steensma, J. M., & Vellinga, P. (2014). Robust, multifunctional flood protection zones in the Dutch rural riverine area. *Nat. Hazard Earth Sys.*, 3857-3889. doi:<https://doi.org/10.5194/nhess-14-1085-2014>
- van Loon-Steensma, J. M., & Vellinga, P. (2019). How “wide green dikes” were reintroduced in The Netherlands: a case study of the uptake of an innovative measure in long-term strategic delta planning. *J. Environ. Plann. Man.*, 1-20. doi:<https://doi.org/10.1080/09640568.2018.1557039>
- Van, M. A. (2001). New approach for uplift induced slope failure. In *Proceedings of the 15th international conference on soil mechanics and geotechnical engineering* (Vol. 3, pp. 2285-2288): AA Balkema Publishers.
- van Maren, D. S., Oost, A. P., Wang, Z. B., & Vos, P. C. (2016). The effect of land reclamations and sediment extraction on the suspended sediment concentration in the Ems Estuary. *Mar. Geol.*, 376, 147-157. doi:<https://doi.org/10.1016/j.margeo.2016.03.007>
- van Slobbe, E., de Vriend, H. J., Aarninkhof, S., Lulofs, K., de Vries, M., & Dircke, P. (2013). Building with Nature: in search of resilient storm surge protection strategies. *Nat. Hazards*, 66(3), 1461-1480. doi:<https://doi.org/10.1007/s11069-013-0612-3>
- van Steeg, P., & Diermanse, F. (2021). *Dubbele dijk fase 2* (11201593-002-HYE-0001). Retrieved from Deltares, Delft, Netherlands.
- van Veelen, P., Voorendt, M. Z., & van der Zwet, C. (2015). Design challenges of multifunctional flood defences. A comparative approach to assess spatial and structural integration. *Research in Urbanism Series*, 275-292%V 273. doi:10.7480/rius.3.841
- van Wesenbeeck, B. K., Mulder, J. P. M., Marchand, M., Reed, D. J., de Vries, M. B., de Vriend, H. J., & Herman, P. M. J. (2014). Damming deltas: A practice of the past? Towards nature-based flood defenses. *Estuar. Coast. Shelf S.*, 140, 1-6. doi:<https://doi.org/10.1016/j.ecss.2013.12.031>

- van de Koppel, J., van der Wal, D., Bakker, J. P., & Herman, P. M. J. (2005). Self-Organization and Vegetation Collapse in Salt Marsh Ecosystems. *Am. Nat.*, 165(1), E1-E12. doi:<https://doi.org/10.1086/426602>
- Vannoppen, W., Poesen, J., Peeters, P., de Baets, S., & van de Voorde, B. (2016). Root properties of vegetation communities and their impact on the erosion resistance of river dikes. *Earth Surf. Proc. Land.*, 41(14), 2038-2046. doi:<https://doi.org/10.1002/esp.3970>
- Vellinga, P. (2008). Hightide in the Delta: inaugural speech at the acceptance of the position of professor in Climate Change [in Dutch]. In.
- Vermeersen, B. L. A., Slangen, A. B. A., Gerkema, T., Baart, F., Cohen, K. M., Dangendorf, S., . . . van der Wegen, M. (2018). Sea-level change in the Dutch Wadden Sea. *Neth. J. Geosci.*, 97(3), 79-127. doi:<https://doi.org/10.1017/njg.2018.7>
- Vinh, T. T., Kant, G., Huan, N. N., & Pruszek, Z. (1997). Sea Dike Erosion and Coastal Retreat at Nam Ha Province, Vietnam. In *Coastal Engineering 1996* (pp. 2820-2828).
- VNK2. (2012). *Flood Risk in the Netherlands - VNK2: the Method in Brief*. Retrieved from Rijkswaterstaat, Utrecht, Netherlands: [https://www.helpdeskwater.nl/publish/pages/132367/vnk\\_nader\\_verklaard\\_uk-lr\\_1.pdf](https://www.helpdeskwater.nl/publish/pages/132367/vnk_nader_verklaard_uk-lr_1.pdf).
- Vöge, S., Reiss, H., & Kröncke, I. (2008). Macrofauna succession in an infilling salt marsh clay pit. *Senck. Marit.*, 38(2), 93-106. doi:<https://doi.org/10.1007/BF03055284>
- Voorendt, M. Z. (2017). *Design principles of multifunctional flood defences*. Delft University of Technology, Delft. Retrieved from <https://edepot.wur.nl/418295> (Ph.D. thesis Delft University of Technology, 2017)
- Voorendt, M. Z., Vrijling, J. K., & Voortman, H. G. (2017). Structural Evaluation of Multifunctional Flood Defenses Using Generic Element Types. In *Coastal Structures and Solutions to Coastal Disasters 2015* (pp. 365-374).
- Vorogushyn, S., Merz, B., & Apel, H. (2009). Development of dike fragility curves for piping and micro-instability breach mechanisms. *Nat. Hazards Earth Syst. Sci.*, 9(4), 1383-1401. doi:<https://doi.org/10.5194/nhess-9-1383-2009>
- Vorogushyn, S., Merz, B., Lindenschmidt, K. E., & Apel, H. (2010). A new methodology for flood hazard assessment considering dike breaches. *Water Resour. Res.*, 46(8). doi:<https://doi.org/10.1029/2009WR008475>
- Vousdoukas, M. I., Mentaschi, L., Voukouvalas, E., Verlaan, M., Jevrejeva, S., Jackson, L. P., & Feyen, L. (2018). Global probabilistic projections of extreme sea levels show intensification of coastal flood hazard. *Nat. Commun.*, 9(1), 2360. doi:<https://doi.org/10.1038/s41467-018-04692-w>
- Vrijling, J. K. (1987). Probabilistic Design of Water-Retaining Structures. In L. Duckstein & E. J. Plate (Eds.), *Engineering Reliability and Risk in Water Resources* (pp. 115-134). Dordrecht: Springer Netherlands.
- Vrijling, J. K. (2001). Probabilistic design of water defense systems in The Netherlands. *Reliab. Eng. Syst. Safe.*, 74(3), 337-344. doi:[https://doi.org/10.1016/S0951-8320\(01\)00082-5](https://doi.org/10.1016/S0951-8320(01)00082-5)
- Vuik, V., Borsje, B. W., Willemsen, P. W. J. M., & Jonkman, S. N. (2019). Salt marshes for flood risk reduction: Quantifying long-term effectiveness and life-cycle costs. *Ocean. Coast. Manage.*, 171, 96-110. doi:<https://doi.org/10.1016/j.ocecoaman.2019.01.010>
- Vuik, V., Jonkman, S. N., Borsje, B. W., & Suzuki, T. (2016). Nature-based flood protection: The efficiency of vegetated foreshores for reducing wave loads on coastal dikes. *Coast. Eng.*, 116, 42-56. doi:<https://doi.org/10.1016/j.coastaleng.2016.06.001>
- Vuik, V., Suh Heo, H. Y., Zhu, Z., Borsje, B. W., & Jonkman, S. N. (2018a). Stem breakage of salt marsh vegetation under wave forcing: A field and model study. *Estuar. Coast. Shelf S.*, 200, 41-58. doi:<https://doi.org/10.1016/j.ecss.2017.09.028>

- Vuik, V., van Vuren, S., Borsje, B. W., van Wesenbeeck, B. K., & Jonkman, S. N. (2018b). Assessing safety of nature-based flood defenses: Dealing with extremes and uncertainties. *Coast. Eng.*, 139, 47-64. doi:<https://doi.org/10.1016/j.coastaleng.2018.05.002>
- Vuillet, M., Peyras, L., Serre, D., & Diab, Y. (2012). Decision-making method for assessing performance of large levee alignment. *Journal of Decision Systems*, 21(2), 137-160. doi:10.1080/12460125.2012.680354
- Walling, D. E., & Fang, D. (2003). Recent trends in the suspended sediment loads of the world's rivers. *Global Planet Change*, 39(1), 111-126. doi:[https://doi.org/10.1016/S0921-8181\(03\)00020-1](https://doi.org/10.1016/S0921-8181(03)00020-1)
- Wamsley, T. V., Cialone, M. A., Smith, J. M., Atkinson, J. H., & Rosati, J. D. (2010). The potential of wetlands in reducing storm surge. *Ocean Eng.*, 37(1), 59-68. doi:<https://doi.org/10.1016/j.oceaneng.2009.07.018>
- Watson, E. B., Wigand, C., Davey, E. W., Andrews, H. M., Bishop, J., & Raposa, K. B. (2017). Wetland Loss Patterns and Inundation-Productivity Relationships Prognosticate Widespread Salt Marsh Loss for Southern New England. *Estuaries Coasts*, 40(3), 662-681. doi:<https://doi.org/10.1007/s12237-016-0069-1>
- Wauben, C. (2019). *Flood Protection Using Multiple Lines of Dikes: A Case Study of the Twin Dike Eemshaven-Delfzijl Project*. (MSc. MSc.). Delft University of Technology, Delft, Netherlands. Retrieved from <http://resolver.tudelft.nl/uuid:e13ae6bc-f5f9-47d8-814b-bc699abf4ca6>
- Weinberger, G., Amiri, S., & Moshfegh, B. (2017). On the benefit of integration of a district heating system with industrial excess heat: An economic and environmental analysis. *Appl. Energ.*, 191, 454-468. doi:<https://doi.org/10.1016/j.apenergy.2017.01.093>
- Wesselink, A., Warner, J., Syed, M. A., Chand, F., Tran, D. D., Huq, H., . . . Zegwaard, A. (2016). Trends in flood risk management in deltas around the world: Are we going 'soft'? *International Journal of Water Governance*(4). doi:<https://doi.org/10.7564/15-ijwg90>
- Willemsen, P. W. J. M., Borsje, B. W., Vuik, V., Bouma, T. J., & Hulscher, S. J. M. H. (2020). Field-based decadal wave attenuating capacity of combined tidal flats and salt marshes. *Coast. Eng.*, 156, 103628. doi:<https://doi.org/10.1016/j.coastaleng.2019.103628>
- Williams, A. T., Rangel-Buitrago, N., Pranzini, E., & Anfuso, G. (2018). The management of coastal erosion. *Ocean Coast. Manage.*, 156, 4-20. doi:<https://doi.org/10.1016/j.ocecoaman.2017.03.022>
- Winsemius, H. C., Aerts, J. C. J. H., van Beek, L. P. H., Bierkens, M. F. P., Bouwman, A., Jongman, B., . . . Ward, P. J. (2016). Global drivers of future river flood risk. *Nat. Clim. Change*, 6(4), 381-385. doi:<https://doi.org/10.1038/nclimate2893>
- Wolters, G., Klein Breteler, M., & Bottema, M. (2013). *Dike erosion strength after initial damage - Large scale model testing*. Paper presented at the Coastal Structures 2011, Yokohama, Japan.
- Yang, S. L., Ding, P. X., & Chen, S. L. (2001). Changes in progradation rate of the tidal flats at the mouth of the Changjiang (Yangtze) River, China. *Geomorphology*, 38(1), 167-180. doi:[https://doi.org/10.1016/S0169-555X\(00\)00079-9](https://doi.org/10.1016/S0169-555X(00)00079-9)
- Yang, S. L., Li, M., Dai, S. B., Liu, Z., Zhang, J., & Ding, P. X. (2006). Drastic decrease in sediment supply from the Yangtze River and its challenge to coastal wetland management. *Geophys. Res. Lett.*, 33(6). doi:<https://doi.org/10.1029/2005GL025507>
- Yang, S. L., Shi, B. W., Bouma, T. J., Ysebaert, T., & Luo, X. X. (2012). Wave Attenuation at a Salt Marsh Margin: A Case Study of an Exposed Coast on the Yangtze Estuary. *Estuaries Coasts*, 35(1), 169-182. doi:<https://doi.org/10.1007/s12237-011-9424-4>
- Young, I. R., & Verhagen, L. A. (1996). The growth of fetch limited waves in water of finite depth. Part 1. Total energy and peak frequency. *Coast. Eng.*, 29(1), 47-78. doi:[https://doi.org/10.1016/S0378-3839\(96\)00006-3](https://doi.org/10.1016/S0378-3839(96)00006-3)

- Ysebaert, T., Yang, S. L., Zhang, L. M., He, Q., Bouma, T. J., & Herman, P. M. J. (2011). Wave Attenuation by Two Contrasting Ecosystem Engineering Salt Marsh Macrophytes in the Intertidal Pioneer Zone. *Wetlands*, 31(6), 1043-1054. doi:<https://doi.org/10.1007/s13157-011-0240-1>
- Zanetti, C., Vennetier, M., Mériaux, P., Royet, P., & Provansal, M. (2011). Managing woody vegetation on earth dikes: Risks assessment and maintenance solutions. *Procedia Environ. Sci.*, 9(Supplement C), 196-200. doi:<https://doi.org/10.1016/j.proenv.2011.11.030>
- Zhu, Z., Vuik, V., Visser, P. J., Soens, T., van Wesenbeeck, B. K., van de Koppel, J., . . . Bouma, T. J. (2020). Historic storms and the hidden value of coastal wetlands for nature-based flood defence. *Nat. Sustain.* doi:<https://doi.org/10.1038/s41893-020-0556-z>

# Appendices

The appendices included contain additional background information, model descriptions and results. Supplementary material to chapters 3 and 4 is available online as a part of the published research articles

**Table A.0.1** References to the published research articles per chapter

Chapter	Research article
2	Marijnissen, R. J. C., Kok, M., Kroeze, C., & van Loon-Steensma, J. M. (2019). Re-evaluating safety risks of multifunctional dikes with a probabilistic risk framework. <i>Nat. Hazards Earth Syst. Sci.</i> , 19(4), 737-756. doi: <a href="https://doi.org/10.5194/nhess-19-737-2019">https://doi.org/10.5194/nhess-19-737-2019</a>
3	Marijnissen, R. J. C., Kok, M., Kroeze, C., & van Loon-Steensma, J. M. (2021). Flood risk reduction by parallel flood defences – case-study of a coastal multifunctional flood protection zone. <i>Coastal Engineering</i> , 167, 103903. doi: <a href="https://doi.org/10.1016/j.coastaleng.2021.103903">https://doi.org/10.1016/j.coastaleng.2021.103903</a>
4	Marijnissen, R. J. C., Esselink, P., Kok, M., Kroeze, C., & van Loon-Steensma, J. M. (2020). How natural processes contribute to flood protection - A sustainable adaptation scheme for a wide green dike. <i>Science of The Total Environment</i> , 739, 139698. doi: <a href="https://doi.org/10.1016/j.scitotenv.2020.139698">https://doi.org/10.1016/j.scitotenv.2020.139698</a>
5	Marijnissen, R. J. C., Kok, M., Kroeze, C., & van Loon-Steensma, J. M. (2020). The Sensitivity of a Dike-Marsh System to Sea-Level Rise – A Model-Based Exploration. <i>Journal of Marine Science and Engineering</i> , 8(1), 42. doi: <a href="https://doi.org/10.3390/jmse8010042">https://doi.org/10.3390/jmse8010042</a>

## Appendix A: Appendices belonging to Chapter 2

### A.1 Case-study parameters

The dike geometry of the base case is captured by the variables in Table A1.1.

**Table A1.1** The standard geometry parameters for the dikes in the hypothetical case-study

Symbol	Description	Distribution	Parameters	
			$\mu$	$\sigma$
$Z_{\text{hinter}}$	elevation of the hinterland [m] above REF	Deterministic	0	-
$Z_{\text{crest}}$	elevation of the crest [m] above REF	Deterministic	5.5	-
$Z_{\text{fore}}$	elevation of the foreshore (at the dike toe) [m] above REF	Deterministic	0	-
$Z_{\text{deep}}$	the average bed level, [m] above NAP along the fetch of the wind	Deterministic	-0.8	-
$\tan(\alpha_{\text{in}})$	inner slope angle [-]	Deterministic	1/2.5	-
$\tan(\alpha_{\text{out}})$	outer slope angle [-]	Deterministic	1/3	-
$B_{\text{crest}}$	crest width [m]	Deterministic	5	-
$L_f$	length of the foreshore	Lognormal	100	10

The soil was divided into 3 layers: the dike core, the blanket layer and the aquifer. Representative values for the soil layers were taken from known soil types in the Dutch riverine area (Table A1.2, Table A1.3 and Table A1.4).

**Table A1.2** Standard parameters of the blanket layer for the dikes in the hypothetical case-study

Symbol	Description	Distribution	Parameters	
			$\mu$	$\sigma$
$d_{\text{blanket}}$	blanket layer thickness [m]	Lognormal	2	0.6
$\gamma_{\text{sat,blanket}}$	saturated volumetric weight of the blanket layer [kN/m <sup>3</sup> ]	Normal	18.8	0.1
$k_{\text{blanket}}$	specific conductivity of the blanket layer [m/s]	Lognormal	2.00E-08	2.00E-08
$c_{\text{blanket}}$	cohesion of blanket material [kN/m <sup>2</sup> ]	Deterministic	0	0
$\varphi_{\text{blanket}}$	Friction angle of blanket material [deg]	Normal	28	4.5

**Table A1.3** Standard parameters of the aquifer layer for the dikes in the hypothetical case-study

Symbol	Description	Distribution	Parameters	
			$\mu$	$\sigma$
$d_{\text{aquifer}}$	Aquifer layer thickness [m]	Deterministic	30	
$\gamma_{\text{sat,aquifer}}$	saturated volumetric weight of the aquifer layer [kN/m <sup>3</sup> ]	Normal	18	0.1
$\eta$	drag factor/White's coefficient [-]	Deterministic	0.25	
$\theta$	bedding angle [rad]	Deterministic	0.61	
$d_{70}$	70%-percentile of the grain size distribution [m]	Lognormal	3.07E-04	4.61E-05
$k_{\text{aquifer}}$	specific conductivity aquifer [m/s]	Lognormal	4.86E-04	2.82E-04
$ch_{\text{aquifer}}$	cohesion of aquifer material [kN/m <sup>2</sup> ]	Deterministic	0	0
$\varphi_{\text{aquifer}}$	Friction angle of aquifer material [deg]	Deterministic	31.3	4.5

**Table A1.4** Standard parameters for the dike soil material for the dikes in the hypothetical case-study

Symbol	Description	Distribution	Parameters	
			$\mu$	$\sigma$
$\gamma_{\text{sat,core}}$	saturated volumetric weight of the dike core [kN/m <sup>3</sup> ]	Normal	18.2	0.1
$\gamma_{\text{dry,core}}$	dry volumetric weight of the core[kN/m <sup>3</sup> ]	Normal	13.1	0.1
$ch_{\text{core}}$	cohesion of core material [kN/m <sup>2</sup> ]	Deterministic	0	0
$\varphi_{\text{core}}$	Friction angle of core material [deg]	Normal	33	4.5

Hydraulic load parameters are given in Table A1.5. Representative water and wind characteristics were estimated from the hydraulic loads database of the upper Rhine area in the Netherlands which is available as part of the WBI software. For simplification the wind direction is only considered in the direction perpendicular to the dike.

**Table A1.5** Standard hydraulic load and resistance parameters for the dikes in the hypothetical case-study

Symbol	Description	Distribution	Parameters		Source
			$\mu$	$\sigma$	
$\rho_w$	density of water [kg/m <sup>3</sup> ]	Normal	1000	1	Known constant
$h$	water level [m] above REF	Generalized extreme value	-2.5	$\sigma = 1.5$ , $\xi = -0.17$	Assumed
$\gamma_{break}$	breaker index of waves [-]	Normal	0.425	0.075	Estimated (TAW, 2002; van der Meer <i>et al.</i> , 2016)
$\gamma_f$	roughness factor for an outer slope with grass [-]	Deterministic	1	-	(TAW, 2002; van der Meer <i>et al.</i> , 2016)
$u_v$	hourly wind speed at 10 m above the surface [m/s]	Gumbel	16.8	1.6	Assumed
$F_{max}$	fetch [m]	Deterministic	1800		Assumed (van Hoven, 2015)
$q_c$	critical overtopping discharge [l/m/s]				
	No house (closed grass cover)	Lognormal	100	120	
	Intact house (open grass cover)	Lognormal	70	80	
	Collapsed house (no major overtopping allowed)	Lognormal	0.1	-	

## A.2 Overflow and overtopping limit state function

Overflow is calculated directly from the water level ( $h$ ) and crest height ( $z_{crest}$ ) by the formula for a broad crested weir:

$$q_{overflow} = \sqrt{2g} * \frac{2\sqrt{3}}{9} (h - z_{crest})^{\frac{3}{2}} \quad (A.2.1)$$

To calculate the overtopping discharge first the significant wave height ( $H_s$ ) and period ( $T_s$ ) perpendicular to the dike are estimated from the water depth ( $h$ ), fetch length ( $F$ ), and wind speed ( $u_{wind}$ ) with the equations of Bretschneider as presented by Holthuijsen (1980):

$$F_x = \frac{gF}{u_{wind}^2} \quad (A.2.2)$$

$$h_x = \frac{gh}{u_{wind}^2} \quad (A.2.3)$$

$$p_1 = \tanh(0.53 * h_x^{0.75}) \quad (A.2.4)$$

$$p_2 = \tanh(0.833 * h_x^{0.375}) \quad (A.2.5)$$

$$H_s = 0.283 * \frac{u_{wind}^2}{g} * p_1 * \tanh\left(0.0125 * \frac{F_x^{0.42}}{p_1}\right) * m_{Bret,H} \quad (A.2.6)$$

$$T_s = 7.54 * \frac{u_{wind}}{g} * p_2 * \tanh\left(0.077 * \frac{F_x^{0.25}}{p_2}\right) * m_{Bret,T} \quad (A.2.7)$$

With the wave characteristics the average overtopping discharge is calculated following the formulas by TAW (2002) and van der Meer *et al.* (2016). Since no berm is present on the dike of the case-study and waves are assumed perpendicular factors related to these aspects are omitted.

$$\xi_0 = \frac{\tan(\alpha_{out})}{\sqrt{\frac{2\pi H_s}{gT_s^2}}} \quad (A.2.8)$$

$$q_1 = \min\left(\frac{0.067}{\sqrt{\tan \alpha_{out}}} * \xi_0 * \exp\left(c_1 * \frac{z_{crest} - h}{H_s} * \frac{1}{\xi_0 * \gamma_f}\right), 0.2 * \exp\left(-2.6 * \frac{z_{crest} - h}{H_s} * \frac{1}{\gamma_f}\right) * \sqrt{g * H_s^3}\right) \quad (A.2.9)$$

$$q_2 = 10^{c_2} * \exp\left(-\frac{z_{crest} - h}{\gamma_f * H_s * (0.33 + 0.022 * \xi_0)}\right) * \sqrt{g * H_s^3} \quad (A.2.10)$$

$$q_{overtopping} = \begin{cases} q_1 & \xi_0 < 5 \\ 10^{\frac{\log(q_1) + \log(q_2)}{2}} & 5 \geq \xi_0 \geq 7 \\ q_2 & \xi_0 > 7 \end{cases} \quad (A.2.11)$$

A description and values for the variables are presented in Table A.2.1.

**Table A.2.1** Description and values of variables in the overtopping and overflow limit state function

Variable	Description	Note
$\alpha_{out}$	Outer slope angle [-]	-
$\gamma_f$	Friction factor for the outer slope [-]	1 (TAW, 2002)

$H_s$	Significant wave height [m]	See Eq. (A.2.6)
$\xi_0$	Iribaren number [-]	See Eq. (A.2.8)
$c_1$	Factor for overtopping [-]	Normally distributed with $\mu=4.75$ and $\sigma=0.5$ (TAW, 2002)
$c_2$	Factor for overtopping [-]	Normally distributed with $\mu=-0.92$ and $\sigma=0.24$ (TAW, 2002)
$m_{\text{Bret,H}}$	Model factor for Bretschneider equation	Lognormally distributed with $\mu=1$ and $\sigma=0.27$ (Diermanse, 2016)
$m_{\text{Bret,T}}$	Model factor for Bretschneider equation	Lognormally distributed with $\mu=1$ and $\sigma=0.13$ (Diermanse, 2016)

The limit state function is then evaluated as:

$$Z_{\text{overflow and overtopping}} = q_c - q_{\text{overflow}} - q_{\text{overtop}} \quad (\text{A.2.12})$$

### A.3 Piping limit state function

Piping is evaluated with the piping erosion formulae of Sellmeijer *et al.* (2011).

The critical head difference ( $H_c$ ) is calculated as:

$$F_R = \frac{\gamma_p - \gamma_w}{\gamma_w} * \eta * \tan \theta * \left( \frac{RD}{RD_m} \right)^{0.35} \quad (\text{A.3.1})$$

$$F_S = \frac{d_{70}}{\sqrt[3]{\kappa L}} * \left( \frac{d_{70m}}{d_{70}} \right)^{0.6} \quad (\text{A.3.2})$$

$$F_G = 0.91 * \left( \frac{d_{\text{aquifer}}}{L} \right)^{\frac{0.28}{\left( \frac{d_{\text{aquifer}}}{L} \right)^{2.8} - 1} + 0.04} \quad (\text{A.3.3})$$

$$H_c = F_R * F_S * F_G * L \quad (\text{A.3.4})$$

Failure occurs when the critical head level ( $H_c$ ) is exceeded by the head difference ( $H$ ) and the resistance of the blanket layer:

$$Z_{\text{piping}} = m_p * H_c - (H - 0.3 * d_{\text{blanket}}) \quad (\text{A.3.5})$$

The variables introduced by Eq. A.3.1 to Eq. A.3.5 are given in Table A.3.1. and are based on estimates used in Dutch dike assessments. The intrinsic

permeability ( $\kappa$ ) which is directly converted from the permeability of the aquifer ( $\kappa_{\text{aquifer}}$ ).

**Table A.3.1** Description and values of variables in the piping limit state function

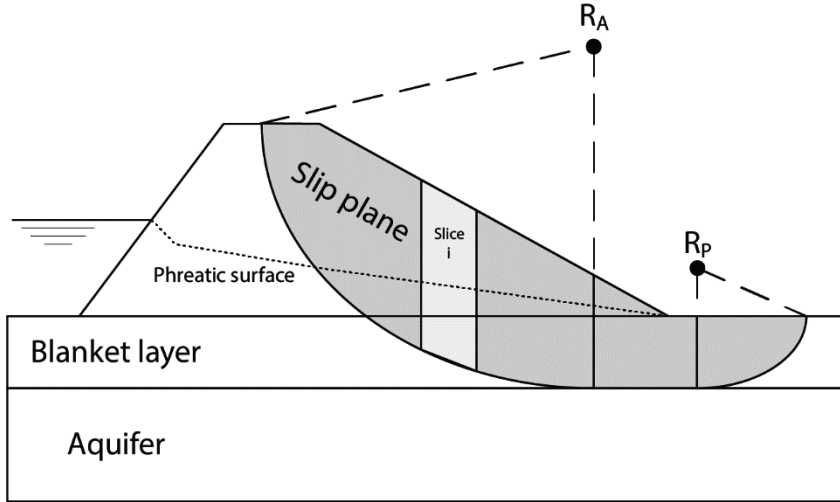
Variable	Description	Distribution	Parameters	Unit
$\gamma_p$	specific weight of sand particles	Deterministic	26	$\frac{kN}{m^3}$
$\gamma_w$	specific weight of water	Deterministic	10	$\frac{kN}{m^3}$
$\eta$	drag factor	Deterministic	0.25	-
$\theta$	bedding angle [°]	Deterministic	35	-
$\frac{RD}{RD_m}$	Relative density of the material compared to small-scale piping experiments	Deterministic	1	-
$d_{70m}$	Reference $d_{70}$ of the material used in small-scale piping experiments	Deterministic	$2 \cdot 10^{-4}$	$m$
$m_p$	Model factor for piping	Lognormal	$\mu = 1, \sigma = 0.12$	-

## A.4 Macro stability limit state function

The macro stability of the dike is evaluated using the schematisation of the phreatic surface of a clay dike from the TAW (2004) following the official Dutch guidelines (see Fig. A.4.1). The TAW (2004) schematisation assumes a drop in the phreatic surface on the interface of the dike with the outside water (1 m as by default) and a linear drop towards the inner toe. The water head in the aquifer was calculated using the equations by TAW (2004) as implemented in the D-stability software (Brinkman & Nuttall, 2018).

The stability of the slope is calculated with the method by Van (2001) for the slip plane and works on the same principle as the method by Bishop (1955). The main difference between the methods is the separation of the slip plane in an active circle connected by a straight section followed by a passive circle. The centres of these circles of the critical slip plane ( $R_A$  and  $R_P$ ) are found iteratively using the D-stability software (Brinkman & Nuttall, 2018).

The slip plane is divided into slices and the net force induced by each slice is calculated. If the moment induced by the active slices ( $\Sigma M_S$ ) is greater than the combination of friction forces and moments induced by the passive slices ( $\Sigma M_R$ ) the slope is unstable. This is both expressed in a factor of safety ( $F_S$ ) and Z-function.



**Figure A.4.1.** Schematisation of the slip plane and phreatic surface used for the macro stability calculation

$$F_S = \frac{\Sigma M_R}{\Sigma M_S} \quad (\text{A.4.1})$$

$$Z_{\text{macrostability}} = F_S - 1 \quad (\text{A.4.2})$$

To calculate the probability of failure with FORM the factor of safety needs to be evaluated during each iteration with D-stability. An experimental version of D-stability with an additional piece of software from the same developers called the probabilistic toolkit (PTK) was utilised to automatically execute D-stability with updated parameters calculated by the FORM algorithm in the PTK.

The iterative procedure of finding the critical slip plane is both computationally demanding and complicates conversion in the probabilistic FORM algorithm. To speed up the procedure in the computation first a test run is performed using average soil strength parameters at a fixed critical slip plane with a water level halfway at the crest. With the results of the first indicative run, stochastic variables with little to no influence ( $|\alpha| < 0.001$ ) are set as constants. Then the entire model was run for each discretised water level.

After the run the fragility curve was checked for points where no convergence was achieved with FORM or a non-critical slip circle must have been evaluated. To this end points where the maximum number of iterations was

reached or the probability of failure decreased with ascending water level were removed to obtain a monotonically increasing fragility curve.

## A.5 FORM algorithm

The first order reliability method (FORM) is a method to iteratively calculate the probability of a limit state function  $(Z(\mathbf{X}) \leq 0)$  being exceeded given a set of independent random variables  $(\mathbf{X})$  (Hasofer & Lind, 1974). The starting point for the iteration is arbitrary, but usually the mean of the variables is taken as the first point to evaluate  $(\mathbf{x}^*)$ . The problem is first simplified by converting the random variables before each iteration into realisations of equivalent normally distributed variables  $(\mathbf{x}')$  with an equivalent normal transformation (Rackwitz & Flessler, 1978).

$$\mu'_{x_i} = x_i^* - \sigma'_{x_i} * \Phi^{-1}[F(x_i^*)] \quad (\text{A.5.1})$$

$$\sigma'_{x_i} = \frac{\varphi\{\Phi^{-1}[F(x_i^*)]\}}{f(x_i^*)} \quad (\text{A.5.2})$$

Where  $\mu'_{x_i}$  and  $\sigma'_{x_i}$  are the mean and standard deviation of the equivalent normal distribution of variable  $x_i$  in the point  $\mathbf{x}^*$ . Also  $f$  and  $F$  are the probability density function (PDF) and cumulative distribution function (CDF) of variable  $x_i$  while  $\varphi$  and  $\Phi$  are the standard normal PDF and CDF. The mean and standard deviation of the limit state function are evaluated by:

$$\mu_Z = Z(\mathbf{x}^*) + \sum_{i=1}^n \frac{\partial Z}{\partial X_i} (\mu'_{x_i} - x_i^*) \quad (\text{A.5.3})$$

$$\sigma_Z = \sqrt{\sum_{i=1}^n \left( \frac{\partial Z}{\partial X_i} \right)^2 \sigma'^2_{x_i}} \quad (\text{A.5.4})$$

With the mean and standard deviation calculated from the design point  $(\mathbf{x}^*)$  the reliability index  $(\beta)$  and influence factor of each variable  $(\alpha_{x_i})$  are calculated.

$$\beta = \frac{\mu_Z}{\sigma_Z} \quad (\text{A.5.5})$$

$$\alpha_{x_i} = \frac{\partial Z}{\partial X_i} * \frac{\sigma'_{x_i}}{\sigma_Z} \quad (\text{A.5.6})$$

The point is updated by adjusting each variable based on the overall safety level ( $\beta$ ) and the sensitivity of the limit state to the variable ( $\alpha_{x_i}$ ):

$$x_i^* = \mu'_{x_i} - \alpha_{x_i} \beta \sigma'_{x_i} \quad (\text{A.5.7})$$

The process is repeated until the reliability index has converged and no longer changes significantly after an iteration.

While the method is effective there are limitations. It is not guaranteed FORM finds the design point with the highest probability but rather converges to a local design point. Furthermore for FORM to converge the limit state function should be smooth without jumps or discontinuities. This complicated the implementation of for example macro stability as when a different slip circle becomes critical there can be a sudden jump in the evaluation of the limit state function.

## Appendix B: Appendices belonging to Chapter 3

### B.1 List of Symbols

**Table B.1.1** List of symbols used in Chapter 3

Symbol	Variable	Unit
Universal:		
$g$	Gravitational acceleration	$ms^{-2}$
$t$	Time	$s$
$x$	x-coordinate	$m$
$y$	y-coordinate	$m$
Culvert:		
$H$	Culvert height	$m$
$L$	Culvert length	$m$
$Q$	Culvert discharge	$m^3s^{-1}$
$S_0$	Culvert slope	—
$S_c$	Critical slope	—
$W$	Culvert width	$m$
$z_{culvert}$	Culvert bottom elevation	$m + NAP$
$c_D$	Discharge coefficient	—
$n$	Manning's roughness coefficient	$m^{1/3}s^{-1}$
$\alpha$	Energy loss correction coefficient	—
$\zeta_{in}$	Water level relative to the culvert bottom at the intake	$m$
$\zeta_{out}$	Water level relative the culvert bottom at the outlet	$m$
$\mu$	Flow contraction coefficient	—
Dike profile		
$F_{sand}$	Sand fraction within clay	—
$d_{clay}$	Clay thickness	$m$
$z_{crest}$	Dike crest elevation	$m + NAP$
$z_{foreshore}$	Foreshore elevation	$m + NAP$
$z_{stone}$	Elevation of transition between stone and grass revetment	$m + NAP$
$\alpha$	Dike slope	—
$\gamma_f$	Roughness factor for overtopping	—
$\gamma_\beta$	Wave direction factor for overtopping	—
Wave Erosion		
$B_t$	Terrace width of the erosion profile	$m$
$D$	Cumulative overload. Subscript c for critical overload	$m^2s^{-2}$
$U$	Wave run-up velocity. Subscript c, for critical velocity	$ms^{-1}$
$a$	Constant in relation between wave height and grass strength duration	$m$
$b$	Constant in relation between wave height And grass strength duration	$hr^{-1}$

$c$	Constant in relation between wave height and strength duration	$m$
$c_e$	Clay erosion coefficient	—
$t_{damage}$	Maximum duration the revetment can withstand wave impacts	$hr$
$t_{RS,grass}$	Maximum duration the root zone beneath the surface can withstand wave impacts	$hr$
$V_e$	Erosion volume per unit width of dike	$m^3m^{-1}$
$\alpha_M$	Factor for increased load at transitions and objects	—
$\alpha_S$	Factor for decreased strength at transitions and objects	—
<b>Hydraulic parameters</b>		
$H_s$	Significant wave height	$m$
$s_{op}$	Wave steepness $[H_s / (1.56 \cdot T_p^2)]$	—
$T_{offset}$	Time lag between the peak of the storm surge and high tide	$hr$
$T_p$	Spectral wave peak period	$s$
$T_{peak}$	Duration of the peak of the storm	$hr$
$T_{storm}$	Storm duration	$hr$
$h$	Water level	$m + NAP$
$q$	Overtopping discharge	$m^3m^{-1}s^{-1}$
$\beta_{wave}$	Wave direction	—
$\gamma_{break}$	Wave breaker index	—

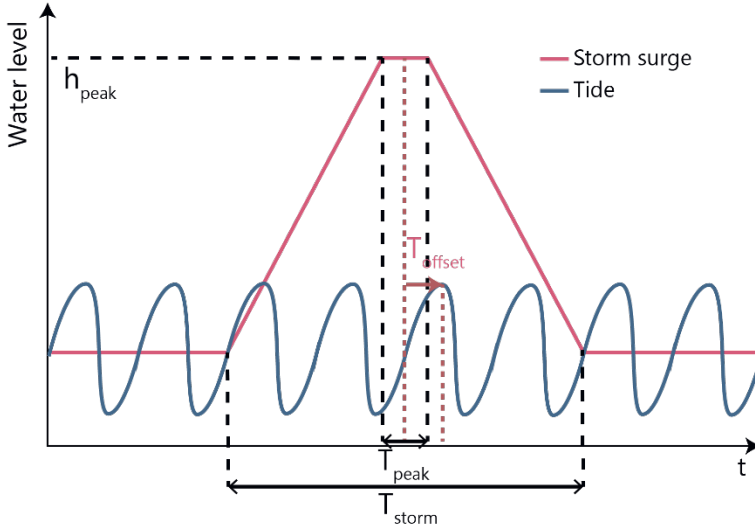
## B.2 Modelling storm surges

Storms are modelled following the conventional Dutch dike assessment tools in the (WTI-2017). For the case-study area the regular tide at Delfzijl was combined with the storm surge model by Chab (2015). The storm surge is modelled as a trapezoidal timeseries (see Figure B.2.1) characterized by a storm duration ( $T_{storm}$ ), peak duration ( $T_{peak}$ ), peak water level ( $h_{peak}$ ), and the time lag between the peak of the storm surge and the next high tide ( $T_{offset}$ ). For the eastern Waddensea where the double dike case-study is located, Chab (2015) suggests a schematization with  $T_{storm} = 45$  hours,  $T_{peak} = 2$  hours, and  $T_{offset} = 6$  hours.

The off-shore wave heights are assumed to remain constant for the duration of the storm. A simple correction for wave breaking on the foreshore was made as follows:

$$H_{s,dike}(t) = \min (H_{s,offshore} ; \gamma_{break} * (h(t) - z_{foreshore})) \quad B.2.1$$

where  $H_s$  is the wave height,  $\gamma_{break}$  is the breaker index set at 0.5,  $h$  is the water level, and  $z_{foreshore}$  is the foreshore elevation.



**Figure B.2.1** Schematization of a storm by combining a regular tide with a synthetic storm surge

### B.3 Modelling culvert discharge

This entire section was adapted from Deltares (2020) (p. 301 to 303). To simplify the formulas, first some notation is introduced. The up- and downstream water depths at the culvert are defined as:

$$\zeta_u = \max(0; \zeta_{in}) \quad (\text{B.3.1})$$

$$\zeta_d = \max(0; \zeta_{out}) \quad (\text{B.3.2})$$

The critical water depth in the culvert is calculated as:

$$H_c = \sqrt[3]{\frac{Q^2}{gW^2}} \quad (\text{B.3.3})$$

The flow rate through the culvert depends on the flow regime. Six flow regimes are distinguished following the classification by French (1985), with different discharge formulas for each.

**Table B.3.1** The different flow regimes through a culvert with associated conditions

Type	Flow regime	Conditions			
		$\zeta_u$	$\zeta_d$	$\zeta_d$	Other
1	Supercritical flow at intake	$< 1.5H$	$\leq H$	$\leq H_c$	$S_0 > S_c$
2	Supercritical flow at outlet	$< 1.5H$	$\leq H$	$\leq H_c$	$S_0 \leq S_c$
3	Tranquil flow	$< 1.5H$	$\leq H$	$> H_c$	
4	Submerged flow	$> H$	$> H$		
5	Rapid flow at inlet	$\geq 1.5H$	$\leq H$	$\leq H_c$	
6	Full flow free outlet	$\geq 1.5H$	$\leq H$	$> H_c$	

The general formula for the discharge can be written as:

$$Q = \mu H_{flow} W * \sqrt{2g\Delta H}, \quad (B.3.4)$$

where:

$$\mu = f(\text{Flow type}, H, W, L, n, c_D, \alpha) \quad (B.3.5)$$

$$H_{flow} = \begin{cases} H_c, & \text{Flow type} = 1, 2 \\ \zeta_d, & \text{Flow type} = 3 \\ H, & \text{Flow type} = 4, 5, 6 \end{cases} \quad (B.3.6)$$

$$\Delta H = \begin{cases} \zeta_u - H_c, & \text{Flow type} = 1, 2 \\ \zeta_u - \zeta_d, & \text{Flow type} = 3, 4 \\ \zeta_u, & \text{Flow type} = 5 \\ \zeta_u - H, & \text{Flow type} = 6 \end{cases} \quad (B.3.7)$$

For the full discharge formulas with the calculation of the flow contraction coefficient see Deltares (2020) (p. 301 to 303).

## B.4 Wave erosion and overtopping formulas

This section only describes the main components of the prototype dike erosion model that was used for the study. The full documentation of the model and the integration between failures is described by Kaste and Klein Breteler (2015) and Rongen *et al.* (2018). The values of all parameters used within this study are presented in the supplement to the online article.

### B.4.1 Erosion of the grass revetment:

The grass can fail by wave-run and wave impacts in the impact zone. The run-up part is calculated with the method by de Waal and van Hoven (2015b). For

the duration of the storm, the expected number of waves with a run-up velocity greater than the resistance of the grass ( $U_{max} > U_c$ ) is calculated across the slope of the dike weighted into a damage number ( $D$ ). When the critical amount of damage ( $D_c$ ) is computed the grass layer is considered failed and the layer beneath it is subjected to wave loads. This process is described by the equations:

$$D = \sum_{i=1}^{n_{waves}} \max(\alpha_M U_{max,i}^2 - \alpha_S U_c^2; 0), \quad (B.4.1)$$

$$U_{max} = c_u \cdot \sqrt{g \cdot z_{2\%} \sqrt{\frac{\ln p}{\ln 0.02'}}} \quad (B.4.2)$$

where  $\alpha_M$  and  $\alpha_S$  are calibration constants for discontinuities on the dike slope (assumed to be 1 for the case-study),  $z_{2\%}$  is the 2% wave run-up,  $c_u$  is a constant (1.1), and  $p$  is the probability of a wave. Failure of the grass is assumed when  $D > D_c$ , at  $7000 \text{ m}^2\text{s}^{-2}$  (de Waal & van Hoven, 2015b).

The failure from wave impact is calculated with the method of de Waal and van Hoven (2015a). Failure of the grass by wave impact is calculated with wave impact resistance curves described by the equation:

$$t_{damage} = \begin{cases} \max\left(\frac{1}{b} \ln\left(\frac{H_s - c}{a}\right); 0\right), & H_s > c \\ 1000, & H_s \leq c \end{cases} \quad (B.4.3)$$

When during a storm the critical duration for wave loads ( $t_{damage}$ ) at a section of the revetment is exceeded, that grass section is considered damaged and the root zone beneath can erode. Erosion of the root zone below is calculated in a similar way:

$$t_{RS,grass} = \begin{cases} \frac{\min(d_{clay}; 0.5) - 0.2}{c_d \tan \alpha^{1.5} \max(H_s - 0.5; 0.001)}, & H_s > 0.5 \\ 1000, & H_s \leq 0.5 \end{cases} \quad (B.4.4)$$

Where:

$$c_d = 1.1 + \max(0; 8 * (F_{sand} - 0.7)) \quad (B.4.5)$$

To combine damage by run-up and impact after time step  $j$  with a duration  $\Delta t$ , the failure fractions for both mechanisms per vertical dike segment are added and failure is defined as:

$$\sum_{i=1}^j \left( \frac{D_i}{D_c} + \frac{\Delta t}{t_{damage,i} + t_{RS,grass,i}} \right) > 1 \quad (B.4.6)$$

#### B.4.2 Erosion of clay:

The erosion rate of the clay layers inside the dike when subjected to waves is calculated with the formula by Mourik (2015):

$$\frac{\partial V_e}{\partial t} = \begin{cases} c_e \cdot [1.32 - 0.079 \frac{V_{e0}}{H_s^2}] \cdot [16.4 (\tan \alpha)^2] \cdot \\ \left[ \min \left( 3.6; \frac{0.0061}{s_{op}^{1.5}} \right) \right] \cdot [1.7 \cdot (H_s - 0.4)^2], & H_s > 0.4 \\ 0, & H_s \leq 0.4 \end{cases} \quad (B.4.7)$$

When clay is eroded from the profile, a cliff (slope 1:1) is formed around the water level and a terrace (slope 1:8) is formed below the water line.

#### B.4.3 Erosion of sand:

The erosion of sand is computed with the model by Klein Breteler *et al.* (2012a):

$$\frac{\partial V_e}{\partial t} = \frac{H_s^2}{T_p} \left( \frac{0.15}{s_{op}^{1.3}} \tan \alpha^{0.8} (135 - 1500 \cdot s_{op}) \cdot \exp \left( -0.0091 \cdot \left( \frac{B_t}{H_s} \right)^2 \right) \right) \quad (B.4.8)$$

Here,  $B_t$  is the terrace width of the eroded profile. The erosion profile again consists of a steep cliff (slope 1:1) and a shallow terrace (slope 1:8) around the water line.

A small change was made to the model to better represent the erosion around the sand and clay around clay core of the dike in the case-study of this paper. Originally, the equation of the weakest material in the wave impact zone was used to calculate the erosion volume per time step (Kaste & Klein Breteler, 2015; Rongen *et al.*, 2018). This caused an unrealistically high erosion rate of the clay core when the top of the wave impact zone happened to extend just above the core into the

sand above. An additional requirement was implemented that equation B.4.8 is used only if at least 25% of the material in the impact zone is sand.

#### B.4.4 Erosion of other materials:

The erosion of other materials like stone is not implemented yet. Instead, it is simply assumed these sections will not fail when exposed to wave impacts. The revetment will still fail, however, by erosion propagating from a section directly above or below the revetment as the revetment is literally being undermined.

### B.5 Overtopping

After erosion of the dike profile has been accounted for, overtopping is calculated with the EurOtop formulas (van der Meer *et al.*, 2016):

$$q = \min \left( \frac{0.067}{\sqrt{\tan \alpha}} * \xi_0 * \exp \left( -4.75 * \frac{z_{\text{crest}} - h}{H_s} * \frac{1}{\xi_0 * \gamma_f * \gamma_\beta} \right), 0.2 * \exp \left( -2.6 * \frac{z_{\text{crest}} - h}{H_s} * \frac{1}{\gamma_f * \gamma_\beta} \right) \right) * \sqrt{g * H_s^3} \quad (\text{B.5.1})$$

$$\xi_0 = \frac{\tan(\alpha)}{\sqrt{\frac{2\pi H_s}{g T_p^2}}} \quad (\text{B.5.2})$$

and,

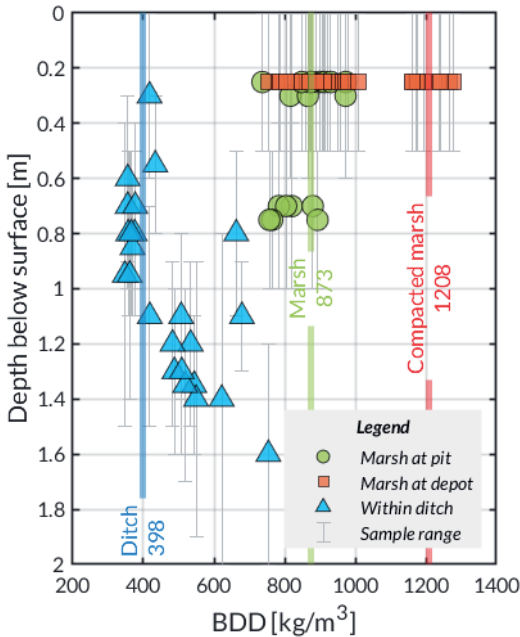
$$\gamma_\beta = 1 - 0.0033 * \min(|\beta_{\text{wave}}|, 80^\circ) \quad (\text{B.5.3})$$

## Appendix C: Appendices belonging to Chapter 4

### C.1 Marsh soil investigations

As part of preparatory work for the pilot project of the wide green dike soil investigations have been carried out by private companies within the marsh to measure potential contamination and suitability of the clay for direct application in dike construction (Raadgevend Ingenieursbureau Wiertsema & Partners, 2016; Sweco Nederland B.V., 2018). These reports have been shared confidentially for this study. The moisture content, dry matter content, fraction of organic matter content, and the depth below the surface from which the sample were taken were recorded. Additionally the locations of the samples were recorded: at the marsh at the location of the pit, at the marsh near the clay depot (closer to the dike toe) or within one the ditches in the marsh.

Bulk dry density (BDD) of the samples was not measured and direct measurements of BDD within the Dollard marsh are limited. Esselink *et al.* (2019) measured BDD from 10 marsh samples. The values ranged between 744 and 1085



**Figure C.1.1** Bulk dry density estimations of the marsh soil in the Dollard at three locations/ The triangles were samples from a ditch, the sampled represented by circles were taken around the centre of the marsh before the borrow pit was excavated and the squares were samples close to the dike toe.

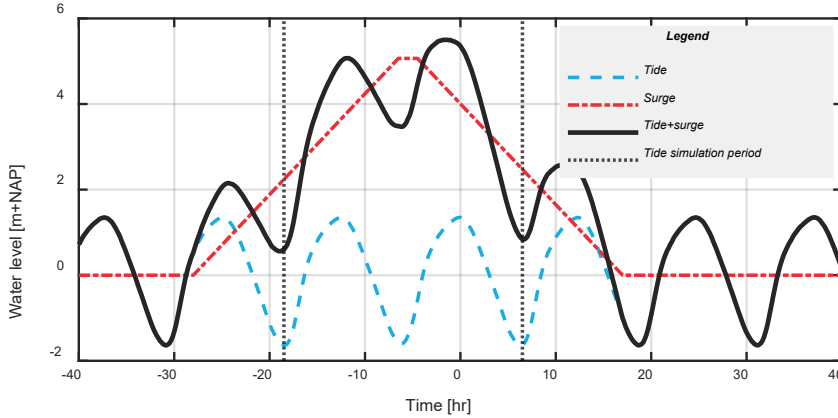
kg/m<sup>3</sup> with an average of 873 kg/m<sup>3</sup>. Assuming the average BDD of the marsh of both Esselink *et al.* (2019)'s measurements and the soil investigations is the same, the properties measured in the soil investigations can be converted to BDD estimations assuming a saturation of 0.94. This allowed for an expansion of the BDD data-set as shown by figure A1. BDD within the marsh varies between 737 and 1008 kg/m<sup>3</sup>. A distinct class with higher values around 1208 kg/m<sup>3</sup> was found. These high values indicate clay has compacted from grazing cattle on the marsh (Esselink, 1998; Karle & Bartholomä, 2008).

Three measurements of BDD within the infilling borrow pit were taken by Esselink *et al.* (2019) measuring BDD's of 342, 367 and 407 kg/m<sup>3</sup>. These values are comparable to the estimated BDD within ditches of the marsh. It was therefore assumed the BDD within the borrow pit will follow a similar density distribution over depth as shown in Figure C.1.1.

## C.2 Simulating storm surges

The progression of the water level during a high water event was determined the tool called “waterstandsverloop” used for Dutch dike safety assessments based on the schematisation of Chab (2015). The tool generates a storm surge using the tide at the location and the maximum water level during the storm as inputs. A trapezium-shape is added to the tidal signal such that the maximum water level matches the highest water level of the storm (see Figure C.2.1). The storm duration and phase of the tide for the Dollard area were adopted directly from the report by Chab (2015).

To shorten the simulation time, the time series was restricted to only the two tidal cycles with the highest water levels. For the deposition model this section contains the fast rise in water level where sediment can enter the marsh and the period during high water where it settles. This extended peak of the storm is also the critical period for wave impacts at the dike as high waves are dependent on the high water level.



**Figure C.2.1** Progression of a simulated high water event of 5.5 m+NAP, composed of a tidal signal in the Dollard and an artificial storm surge. The two vertical lines denote the two tidal cycles of the time series used for computations.

### C.3 Simulating the water level within the borrow pit

The borrow pit in the Dollard is connected to the tidal network by a ditch. A weir was installed between the pit and the ditch to keep water around the bird island at the centre of the pit. This weir affects the flow of water in and out of the pit. In particular the weir prevents the pit from draining completely at low tide, allowing sediment to settle even during low tide.

Modelling the weir was achieved by incorporating the Bernoulli equation. Since the flow of the tide is orders of magnitude smaller than the flow over the weir, the flow velocity in and out of the pit over the weir is calculated as:

$$u = \sqrt{2g * (\hat{h}_{tide} - \hat{h}_{pit})} \quad (C.3.1)$$

Where  $\hat{h}_{tide}$  and  $\hat{h}_{pit}$  are the water depths at the sea and pit side of the weir above the level of the weir. The discharge ( $Q$ ) in and out of the pit is computed as follows:

$$Q = (\max(h_{tide}; z_{weir}) - h_{pit}) * R * u \quad (C.3.2)$$

Where  $h_{tide}$  is the water level of the tide,  $h_{pit}$  is the water level within the pit,  $z_{weir}$  is the elevation of the weir crest, and  $R$  is an inverse resistance term accounting for both the width of and friction induced by the weir. The change in

water level within the pit is the result of discharge in and out of the pit spread out over the area of the pit:

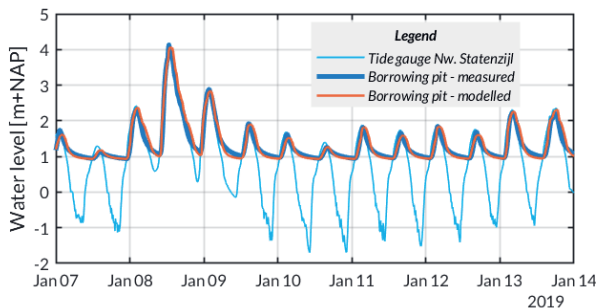
$$\frac{dh_{pit}}{dt} = \frac{(\max(h_{tide}; z_{weir}) - h_{pit}) * R * u}{A_{pit}} \quad (C.3.3)$$

The resistance term  $R$  was calibrated for three situations: during inflow when the tide enters the pit at flood tide, during outflow when the pit drains at ebb tide, and during overflow when the tide is higher than the edges of the pit. Calibration was performed with direct measurements of the water level within the pit at the Dollard between September of 2018 and March 2019 and the local tide gauge at Nieuwe Statenzijl.

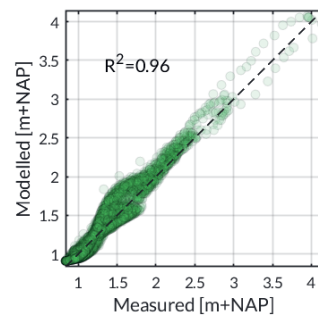
With the calibrated parameter  $R$  (Table C.3.1) an excellent fit ( $R^2=0.96$ ) was achieved between the measured water levels within the pit and the water levels converted from the tidal signal at Nieuwe Statenzijl (Figure C.3.1).

**Table C3.1** The parameters used to convert water levels from the tide gauge at Nieuwe Statenzijl to water levels within the pit

Symbol	Description	Value	Unit
$A_{pit}$	Pit surface area	3.5	ha
$z_{crest}$	Weir crest elevation	0.9	m+NAP
$R$	Weir flow resistance term	$R_{in} = 3.5$ $R_{out} = 2.7$ $R_{over} = 13.5$	m



(a)



(b)

**Figure C.3.1** (a) comparison of the tide at Nieuwe Statenzijl (light blue) measured tide at the borrow pit (dark blue), and the modelled water level in the borrow pit over 1 week. (b) comparison of the measured and modelled water levels in the borrow pit over a three month period.

## C.4 Modelling auto-compaction within the pit

Allen (2000a) presented a formula to model compaction as follows:

$$T = (T_0 - T_{min}) * e^{-kH} + T_{min} \quad (C.4.1)$$

Where  $T$  is the layer thickness,  $T_0$  is the layer thickness during deposition,  $T_{min}$  the minimum thickness after compaction,  $H$  is the overburden height and  $k$  is a compaction constant. For this study it is more convenient to reformulate the formula in terms of bulk dry density ( $\rho$ ) and mass of sediment within the pit ( $m$ ):

$$\frac{1}{\rho_{sed}} = \left( \frac{1}{\rho_0} - \frac{1}{\rho_{inf}} \right) * e^{-km} + \frac{1}{\rho_{inf}} \quad (C.4.2)$$

Where  $\rho_{sed}$  is the BDD of the sediment layer,  $\rho_0$  is the BDD before compaction and  $\rho_{inf}$  is the BDD after compaction. Constant  $k$  can be computed from the known profile within the ditch, the BDD of unconsolidated clay in the ditch and the consolidated clay in the marsh:

$$k = -\frac{1}{m_t} \ln \left( \frac{\frac{\rho_{inf}}{\rho_t} - 1}{\frac{\rho_{inf}}{\rho_0} - 1} \right) \quad (C.4.3)$$

From the measurements the  $\rho_{inf}$  is taken as the BDD of the marsh and  $\rho_0$  as the BDD at the surface of the ditch where (mostly) unconsolidated deposits are present. From the ditch measurements a BDD over depth profile was fitted:

$$\rho_{sed,ditch} = 45.53 * D^{4.284} + \rho_0 - 4.4 \quad (C.4.4)$$

Where ( $D$ ) is the depth below the surface. The mass below the surface can be found by the integral:

$$m = \int \rho(D) * dD \quad (C.4.5)$$

The deepest sample from the ditch was at 1.6 m below the surface and using expected BDD values for the marsh and ditch samples (873 kg/m<sup>3</sup> and 398 kg/m<sup>3</sup> respectively, see Appendix C.1), the compaction constant  $k$  can thus be estimated to be  $4.6*10^{-4} \text{ kg}^{-1}$  with uncertainty around this value. A new BDD accounting for compaction in the lower layers is computed for each time step of the model with the compaction constant  $k$  and the mass within the pit  $m$  using eq. C.4.3.

## C.5 Failure of a grass on clay revetment

### C.5.1 Wave impact

Failure by wave impact is considered in three stages: a) failure of the grass cover, b) failure of the roots within the clay and c) failure of the entire clay layer. In terms of a limit state approach, the failure is described by:

$$Z_{wave\ impact} = t_{grass} + t_{root} + t_{clay} - t_{wave\ impact} \quad (C.5.1)$$

A recent study suggests adding a reduction factor for wave heights in wave impact calculations to account for lower pressures exerted by oblique waves (Klein Breteler & Mourik, 2019). However, this has not yet been implemented in Dutch dike assessment calculations and was therefore not yet considered to keep the results of this study comparable to previous designs of the wide green dike.

### Failure of the grass cover

Within the WBI 2017 the time required for initial damage of the top layer with grass ( $t_{grass}$ ) is calculated with an empirically fitted formula (Klerk & Jongejan, 2016):

$$t_{grass} = \frac{1}{C_b} \ln \left( \frac{H_s - C_c}{C_a} \right) \quad (C.5.2)$$

Where:	$C_a$	= Constant in resistance duration curve, Lognormal ( $\mu=1.82$ , $\sigma=0.62$ )	$[m^{-1}]$
	$C_b$	= Constant in resistance duration curve, Constant (-0.035)	$[hr^{-1}]$
	$C_c$	= Constant in resistance duration curve, Constant (0.25)	$[m]$
	$H_s$	= Significant wave height	$[m]$

### Failure of the grass and root zone

The subsequent time required to erode the clay layer reinforced by the roots of grass until 0.5 m below the surface ( $t_{grass}$ ) is also determined from an empirically fitted formula (Klein Breteler, 2015):

$$t_{root} = \frac{0.5 - d_{top}}{C_d(H_s - 0.5) * (\tan \alpha)^{1.5}} \quad (C.5.3)$$

With  $C_d$ :  $Normal (\mu_{C_d} = 0.59 + \max(0; 8(f_{sand} - 0.7)),$   
 $\sigma_{C_d} = 0.32)$

Where:

$d_{top}$	=	Thickness of the top-layer of grass, (0.2 m)	[m]
$H_s$	=	Significant wave height	[m]
$\alpha$	=	Slope angle	[°]
$f_{sand}$	=	Sand fraction within the clay, For clay from the pit $f_{sand} < 70\%$	[%]

### Failure of the deeper clay layer

The time required for the remaining clay below the 0.5 m is calculated with the model by (Mourik, 2015):

$$t_{clay} = -12.66 * H_s^2 \ln \left( 1 - \frac{V_e}{466 * C_e * H_s^2 * (H_s - 0.4)^2 * (\tan \alpha)^2 * \min \left( 3.6; \frac{0.0061}{s_{op}^{1.5}} \right)} \right) \quad (C.5.4)$$

$V_e$	=	the total erosion volume	[m <sup>2</sup> ]
$C_e$	=	erosion coefficient for clay, Normal ( $\mu=0.55, \sigma=0.1375$ )	[-]
$s_{op}$	=	Wave steepness	[-]

The erosion profile forming within the dike changes as erosion progresses. To greatly simplify the calculation a worst case erosion profile is assumed where the cliff side has a 1:1 (=45°) slope while the terrace is horizontal. With these assumptions the required erosion volume to erode the entire thickness of the clay layer ( $d$ ) follows as:

$$V_e = \frac{1}{2} d_{clay}^2 * \left( \frac{1}{\tan \alpha} + \frac{1}{\tan(45^\circ - \alpha)} \right) \quad (C.5.5)$$

## Wave impact duration

The zone where waves can impact the slope extends from the water line to half a wave height below the water line. The maximum duration of wave impact along any point on the slope is thus the time the water level is within a range of half a wave height of that point.

For calculations the slope is discretised in sections of wave impact zones, each with a height of  $0.5 H_s$ . The erosion of each section is calculated using eq. C.5.5. When the erosion profile starts expanding into the next section, the erosion volume extending in the section above must be added to the erosion volume of the section above. From the geometry of the erosion profile the erosion volume in the next section is calculated as:

$$\Delta V_{e,i+1} = \max \left( 0; 1 - \frac{1}{2} H_s * \frac{\tan(45^\circ - \alpha)}{d_i} \right) * V_{e,i} \quad (C.5.6)$$

Here  $d_i$  is the erosion depth of section  $i$  resulting in additional erosion in the next section ( $\Delta V_{e,i+1}$ ). Using eq. A.4 the additional erosion is converted in additional time of wave impact exposure ( $\Delta t_{wave\ impact}$ ) because of erosion propagating from the section below.

## C.5.2 Overtopping

Failure of a dike by overtopping is induced by an excessive amount of waves overtopping the crest of the dike resulting in erosion of the inner slope from water flowing down the inner slope. In the limit state approach this is expressed as:

$$Z_{overtopping} = q_c - q \quad (C.5.7)$$

Here  $q$  is the average discharge along the inner slope of the dike induced by overtopping waves while  $q_c$  is the critical discharge before erosion of the inner slope is induced. The formulas by TAW (2002) and van der Meer *et al.* (2016) are used to compute the discharge.

$$q_{overtopping} = \begin{cases} q_1 & \xi_0 < 5 \\ 10^{\frac{\log(q_1) + \log(q_2)}{2}} & 5 \leq \xi_0 \leq 7 \\ q_2 & \xi_0 > 7 \end{cases} \quad (C.5.8)$$

Of which the parameters  $q_1$ ,  $q_2$  and  $\xi_0$  are calculated with the formulas:

$$q_1 = \min \left( \frac{0.067}{\sqrt{\tan \alpha}} * \xi_0 * \exp \left( c_1 * \frac{z_{\text{crest}} - h}{H_s} * \frac{1}{\xi_0 * \gamma_f * \gamma_\beta} \right), 0.2 * \exp \left( -2.6 * \frac{z_{\text{crest}} - h}{H_s} * \frac{1}{\gamma_f * \gamma_\beta} \right) \right) * \sqrt{g * H_s^3} \quad (\text{C.5.9})$$

$$q_2 = 10^{c_2} * \exp \left( -\frac{z_{\text{crest}} - h}{\gamma_f * \gamma_\beta * H_s * (0.33 + 0.022 * \xi_0)} \right) * \sqrt{g * H_s^3} \quad (\text{C.5.10})$$

$$\xi_0 = \frac{\tan(\alpha)}{\sqrt{\frac{2\pi H_s}{g T_p^2}}} \quad (\text{C.5.11})$$

And the influence factor for the wave direction ( $\gamma_\beta$ ):

$$\gamma_\beta = 1 - 0.0033 * \min(|\alpha_{\text{wave}}|, 80^\circ) \quad (\text{C.5.12})$$

The parameters used as input are in the table below.

**Table C.5.1** The input variables for the overtopping calculations

Symbol		Description	Unit
$q_c$	=	Critical overtopping discharge: Lognormal( $\mu=70$ , $\sigma=80$ )	$l^{-1}m^{-1}s^{-1}$
$\alpha$	=	Angle of the outer slope	$^\circ$
$c_1$	=	Overtopping model coefficient: Normal( $\mu=-4.75$ , $\sigma=0.5$ )	—
$z_{\text{crest}}$	=	Dike crest elevation	$m + NAP$
$h$	=	Water level	$m + NAP$
$H_s$	=	Significant wave height	$m$
$\gamma_f$	=	Slope roughness factor: 1 for grass	—
$g$	=	Gravitational acceleration: 9.81	$m s^{-2}$
$c_2$	=	Overtopping model coefficient: Normal( $\mu=-0.92$ , $\sigma=0.24$ )	—
$T_p$	=	Wave peak period	$s$
$\alpha_{\text{wave}}$	=	Wave direction relative to the dike normal	$^\circ$

## Appendix D: Appendices belonging to Chapter 5

### D.1 Model parameters

This appendix presents the parameter values and distributions in chapter 5.

**Table D.1.1** Marsh accretion parameters

Variable	Description	Value	Unit
$h_{HW}$	Distribution of the water level at high tide	GEV( $\mu = 1.3$ , $\sigma = 0.4$ , $\xi = -0.1$ )	$m + NAP$
$C_{flood}$	Suspended sediment concentration	See Table 1	$\frac{kg}{m^3}$
$f_d$	Fraction of suspended sediment retained per tidal cycle	0.8	—
$\rho_{deposit}$	Bulk dry density of the marsh	See Table 1	$\frac{kg}{m^3}$
$S_{subsidence}$	Subsidence rate	2.7	$\frac{mm}{yr}$

**Table D.1.2** Marsh profile parameters

Variable	Description	Value	Unit
$z_{marsh}$	Initial marsh elevation	1.86	$m + NAP$
$B_{marsh}$	Initial marsh width	750	$m$
$\tan \alpha_{marsh}$	Slope of the marsh elevation	1/4000	-

**Table D.1.3** Parameters used in the dike reinforcement calculation. Distributions are GEV= generalized extreme value distribution, W=Weibull distribution, C=constant, L=lognormal, V= variable is adjusted between computations

Variable	Description	Distribution type	Value(s)			Unit
Hydraulic						
$h$	Combined high water + storm surge (excluding SLR)	GEV	$\mu = 3.70$	$\sigma = 0.44$	$\xi = 0$	$m + NAP$
$H_s$	Significant wave height	W	$A = 0.75$	$B = 1.66$		$m$
$T_p$	Wave peak period	W	$A = 3.15$	$B = 3.40$		$s$
$u_{10}$	Wind speed 10 m above the water	GEV	$\mu = 23.2$	$\sigma = 2.00$	$\xi = -0.02$	$\frac{m}{s}$

<i>Dike</i>						
$\tan \alpha_{dike}$	Dike slope	C	1/7			-
$z_{crest}$	Dike crest height	V				$m + NAP$
$q_c$	Critical overtopping discharge	L	$\mu = 70$	$\sigma = 80$		$l^{-1}m^{-1}s^{-1}$
<i>Modelling factors</i>						
$m_o$	Overtopping factor	N	$\mu = 4.5$	$\sigma = 0.5$		-
$c_o$	Shallowness factor	L	$\mu = 0.92$	$\sigma = 0.24$		-

**Table D.1.4** The correlation matrix between hydraulic parameters fitted from Hydra-NL

	$h$	$H_s$	$T_p$	$u_{10}$
$h$	1	0.77	0.56	0.71
$H_s$	0.77	1	0.94	0.62
$T_p$	0.56	0.94	1	0.39
$u_{10}$	0.71	0.62	0.39	1

## D.2 Dike reinforcement formulas

### D.2.1 The overtopping calculation

Before the amount of overtopping can be determined the wave conditions at the dike toe need to be known. The SWAN wave model was used to transform offshore wave and wind conditions into a significant wave height ( $H_s$ ) and spectral wave period ( $T_{m-1}$ ) at the dike toe. From the database of computed SWAN transformations new offshore conditions could be readily transformed to conditions at the dike (see section 5.3.4).

The following section summarizes the procedure to calculate the average discharge of water over a dike during storm conditions following the EurOtop manual (van der Meer *et al.*, 2016). First the type of wave breaking is determined with the breaker index ( $\xi$ ), a ratio between the slope steepness and wave steepness.

$$\xi_{m-1,0} = \frac{\tan(\alpha_{dike}) * \sqrt{gT_{m-1}^2}}{\sqrt{2\pi H_s}} \quad (D.2.1)$$

Since the spectral wave period  $T_{m-1}$  is used in this variation, the breaker index has the subscript  $m-1$ . For  $\xi_{m-1,0} < 5$  the average overtopping discharge ( $q$ ) is calculated with the formula:

$$\frac{q}{\sqrt{gH_s^3}} = \frac{0.067}{\sqrt{\tan(\alpha_{dike})}} * \gamma_b * \xi_{m-1,0} * \exp\left(-m_o * \frac{R_c}{\xi_{m-1,0} * H_s * \gamma_b * \gamma_f * \gamma_\beta}\right) \quad (D.2.2)$$

with a maximum of:  $\frac{q}{\sqrt{gH_s^3}} = 0.2 * \exp\left(-2.6 * \frac{R_c}{H_s * \gamma_f * \gamma_\beta}\right)$

When  $\xi_{m-1,0} > 7$  the average overtopping discharge ( $q$ ) is calculated as:

$$\frac{q}{\sqrt{gH_s^3}} = 10^{c_o} * \exp\left(-\frac{R_c}{\gamma_f * \gamma_\beta * H_s * (0.33 + 0.022 * \xi_{m-1,0})}\right) \quad (D.2.3)$$

For cases where  $5 \leq \xi_{m-1,0} \leq 7$  the overtopping discharge is interpolated between the two equations.

In the equations  $g$  is the gravitational acceleration constant,  $R_c$  is the crest height above the average water level and the  $\gamma$ 's are various influence factors. The other input variables are explained in Table D.1.3.

Because the dike was schematised as a smooth grass dike with no berm,  $\gamma_b$  and  $\gamma_f$  are both set to 1. The influence of wave angle ( $\beta_{wave}$ ) is calculated with the equation:

$$\gamma_\beta = 1 - 0.0033 * \min(|\beta_{wave}|, 80^\circ) \quad (D.2.4)$$

The procedure so far describes the amount of overtopping, but not whether the dike fails. Failure of the dike was assumed when the overtopping discharge ( $q$ ) exceeds a critical threshold ( $q_c$ ). This was described by the limit state function ( $Z$ ) where dike failure is induced when  $Z > 0$ .

$$Z = q - q_c \quad (D.2.5)$$

### D.2.2 First order reliability method (FORM)

The first order reliability method is an approach to approximate the probability of failure of a system. The type of failure considered in this study is excessive overtopping during a storm. Mathematically failure is described by the limit state function (Eq. D.2.5) and the other equations of section D.2.1.

Combining the values of all parameters into one single vector ( $\mathbf{x}$ ), in the FORM algorithm the values in  $\mathbf{x}$  are iterative varied until  $Z(\mathbf{x}) = 0$ . However many combinations of values in  $\mathbf{x}$  satisfy this condition. The probability of failure is determined by the combination of values in  $\mathbf{x}$  with the highest probability of occurring given the probability distributions in Table D.1.3 and correlations

specified in table D.1.4. Following the FORM-method presented by Low and Tang (2007) the probability of failure is approximated by first solving:

$$\beta_{Z(x)=0} = \min \left( \sqrt{\mathbf{n}^T R^{-1} \mathbf{n}} \right) \quad (D.2.6)$$

Here  $\beta$  is the reliability index and  $R$  is the correlation matrix. The vector  $\mathbf{n}$  is a normalization of the elements in  $\mathbf{x}$  as:

$$n_i = \Phi^{-1}(F_i(x_i)) \quad (D.2.7)$$

Where  $F_i$  is the cumulative distribution function from the  $i^{\text{th}}$  parameter in  $\mathbf{x}$ , and  $\Phi^{-1}$  is the inverse standard normal distribution. The probability of failure ( $P_f$ ) is computed from the reliability index  $\beta$  as:

$$P_f = \Phi(-\beta) \quad (D.2.7)$$

The mathematical problem stated in Eq. B.6 is an example of a constrained non-linear optimization problem. The numerical solver called fmincon in the program MATLAB was used to numerically solve the system of equations in this appendix. This way the probability of failure of different crest heights was computed until an optimal height was found meeting the safety standard.

# Acknowledgements

It is strange to think the PhD journey has ended. During the four years of research I have had the pleasure to share the experience with many people. Without them, I would have not been able to complete this thesis.

Thank you Jantsje, for being there as my supervisors and co-promotor very step of the journey. As a matter of fact, the journey towards this PhD started with our meeting in Delft on marshes in Canada. While that PhD proposal was not granted, I was glad to find you had a position for this PhD. After coming to Wageningen I was amazed to find someone with connections all across the field whether it is about flood protection, climate adaptation, the delta program. You must have scratched your head many times when I was rambling about model codes, probabilistic algorithms and computational methods. Yet all the while you have been there to connect the numbers to the flood protection strategies. For that, I am grateful.

I also want to thank my two promotors, Carolien Kroeze and Matthijs Kok. I dare say this research would not have been possible without your discussions and different perspectives. Indeed, intertwining discussions on the global issues of climate adaption with regional safety frameworks of Dutch Dikes and back again has been challenge, yet it would not have been possible with your guidance and advice.

Of course, I am grateful to the many researchers in the All-Risk program who have supported me during my thesis. A special thanks to Wim Kanning, who helped me get started with the many probabilistic calculations that would later follow. Also a large thanks to the fellow researchers I met and discussed with along the way: Yuka, Wouter-Jan, Luca, Mark, Joost, Guido, Chris, Beatriz, Vera, Matthijs, Monica, Willemijn and Martijn as well as the many other researchers.

This research would also not have been possible without the active participation from the users of All-Risk. In particular I want to thank Eric Jolink from waterboard Hunze & Aas, as well as Kees de Jong, Jan Willem Nieuwenhuis and Marco Veendorp from waterboard Noorderzijlvest for the discussions and feedback on the case-studies within the program. Furthermore I want to thank

## Acknowledgements

---

Henk van Hemert, Richard Jorissen, and Marieke Visser and Judith Klöstermann who helped as users with their insights. I also want to thank Peter Esselink who shared his many years of experience and knowledge of the Wadden Sea marshes during the project.

I was lucky to be part of such a great group as the Water-Systems and Global Change group in Wageningen. It was a blast getting to know you through your work across many topics spanning different fields and cultures. But above all, I will never forget the many social events we had like the beer tasting contest or staying in the office to watch Game of Thrones. A thanks to the many wonderful PhDs and postdocs of the WSG group: Bram, Kim, Emmanuel, Wouter, Spyros, Nancy, Joreen, Maria, Talardia, Annette, Dianneke, Uthpal, Kirina, Chen, Coco, Ang, Mengru, and many others.

I also want to thank my good friends Joep and Roel. Ever since our studies and Vietnamese adventure abroad, we continued to have many good conversations our work alongside beers in Den Bosch or a Limburgse vlaai. Without your support, the thesis would not have been the same.

Als allerlaatste wil ik mijn familie bedanken. Pap, mam, Rick en Leonie, jullie zijn er altijd voor me geweest en hebben me altijd gesteund en ik kan me geen beter gezin voorstellen. Hetzelfde geldt ook voor mijn opa, oma en schoonzus Femke. Ik weet zeker dat jullie niet kunnen wachten om mijn verhalen over zandzakken en dijken nog eens uitgebreid na te lezen ;). Ook een klein dankje voor mijn lachende nichtje Myla, die al bijna anderhalf jaar geleden bij de familie is gekomen.

## About the author

Richard J.C. Marijnissen was born in the south of the Netherlands, Breda, in 1993. After finishing high school at the Stedelijk Gymnasium Breda he moved to Delft to study Civil Engineering at Delft University of Technology. Here he obtained both his bachelor and master's degree in Civil Engineering. During his studies he specialised in coastal engineering with a special interest in Building with Nature solutions through an additional thesis at Deltares on the intertidal area of San Francisco Bay, a multidisciplinary student project in Vietnam, and a study into the restoration of wetlands on Sturgeon Bank near Vancouver, Canada at Boskalis. After graduation he continued his study into the marshes of Sturgeon Bank as a junior researcher at TU Delft, before moving on as a PhD within the NWO-TTW project All-Risk at Wageningen University and Research in 2017. Within the All-Risk subproject A2, he focussed on developing a framework for the assessment and design of multifunctional flood defences within the Dutch Flood Protection Program.



### Journal publications:

- Marijnissen, R. J. C., Kok, M., Kroeze, C., & van Loon-Steensma, J. M. (2019). Re-evaluating safety risks of multifunctional dikes with a probabilistic risk framework. *Natural Hazards & Earth System Sciences*, **19**(4), 737-756. <https://doi.org/10.5194/nhess-19-737-2019>
- Marijnissen, R. J. C., Kok, M., Kroeze, C., & van Loon-Steensma, J. M. (2020). The Sensitivity of a Dike-Marsh System to Sea-Level Rise—A Model-Based Exploration. *Journal of Marine Science and Engineering*, **8**(1), 42. <https://doi.org/10.3390/jmse8010042>
- Marijnissen, R. J. C., Esselink, P., Kok, M., Kroeze, C., & van Loon-Steensma, J. M. (2020). How natural processes contribute to flood protection - A sustainable adaptation scheme for a wide green dike. *Science of The Total Environment*, **739**, 139698. <https://doi.org/10.1016/j.scitotenv.2020.139698>
- Marijnissen, R. J. C., Kok, M., Kroeze, C., & van Loon-Steensma, J. M. (2021). Flood risk reduction by parallel flood defences – case-study of a coastal multifunctional flood protection zone. *Coastal Engineering*, **167**, 103903. <https://doi.org/10.1016/j.coastaleng.2021.103903>
- Baaij, B.M., Kooijman, J., Limpens, J., Marijnissen, R.J.C., van Loon-Steensma, J.M. (2021). Monitoring Impact of Salt-Marsh Vegetation Characteristics on Sedimentation: an Outlook for Nature-Based Flood Protection. *Wetlands*, **41**, 76. <https://doi.org/10.1007/s13157-021-01467-w>

## Other publications

- Fila, J., Kampen, M., Knulst, K., Marijnissen, R.J.C., van Noort, R. (2016). *Coastal erosion along Cua Dai beach in Hoi An, Vietnam - Multidisciplinary Project Report*. Delft University of Technology, Delft, Netherlands. <http://resolver.tudelft.nl/uuid:d7e9a5c7-bfbc-406f-aaee-b7f1bc71b3d2>
- Marijnissen, R.J.C. (2017). *Potential mechanisms for the salt marsh recession on Sturgeon Bank*, (MSc.). Delft University of Technology, Delft, Netherlands. <http://resolver.tudelft.nl/uuid:4fb116d6-39d4-46f9-ba4c-ac8f59e74549>
- Marijnissen, R.J.C., Aarninkhof, S.G.J. (2017). *Marsh Recession and Erosion study of the Fraser Delta, B.C., Canada from Historic Satellite Imagery*. (Communications on Hydraulic and Geotechnical Engineering, **2017-1**, 1). Delft University of Technology, Delft, Netherlands. <http://resolver.tudelft.nl/uuid:719daaa9-6c9e-4c44-9608-b58f3c614d94>
- Marijnissen, R.J.C., Kok, M. Kroeze, C., van Loon-Steensma, J.M. (2021) . The four components to combine flood protection with other functions. Paper presented as part of the proceedings of the online *FLOODRisk2020 conference* (June 2021). [https://floodrisk2020.net/uploads/papers/12\\_3/12\\_3FLOODrisk2020\\_full%20paper\\_RM\\_5Jan-1610016805.pdf](https://floodrisk2020.net/uploads/papers/12_3/12_3FLOODrisk2020_full%20paper_RM_5Jan-1610016805.pdf)

# SENSE training and education diploma



*Netherlands Research School for the  
Socio-Economic and Natural Sciences of the Environment*

## D I P L O M A

*for specialised PhD training*

The Netherlands research school for the  
Socio-Economic and Natural Sciences of the Environment  
(SENSE) declares that

***Richard Johannes Cornelis Marijnissen***

born on 29<sup>th</sup> July 1993, Breda, Netherlands

has successfully fulfilled all requirements of the  
educational PhD programme of SENSE.

Wageningen, 6<sup>th</sup> October 2021

Chair of the SENSE board



Prof. dr. Martin Wassen

The SENSE Director



Prof. Philipp Pattberg

*The SENSE Research School has been accredited by the Royal Netherlands Academy of Arts and Sciences (KNAW)*



K O N I N K L I J K E N E D E R L A N D S E  
A K A D E M I E V A N W E T E N S C H A P P E N



The SENSE Research School declares that **Richard Johannes Cornelis Marijnissen** has successfully fulfilled all requirements of the educational PhD programme of SENSE with a work load of 41.3 EC, including the following activities:

#### SENSE PhD Courses

- o Environmental research in context (2018)
- o Research in context activity: 'Communicating PhD research on the "Shared-use of Flood Defences" with story lines'(2021)

#### Other PhD and Advanced MSc Courses

- o Reliability and risk in geotechnical engineering practice, Delft University of Technology (2017)
- o The essentials of scientific writing and presenting, Wageningen Graduate Schools (2018)
- o Competence assessment, Wageningen Graduate Schools (2018)
- o Practical modelling for marine biologists, University of Groningen (2019)
- o DAT275x: Principles of machine learning: Python Edition, edX (2020)

#### Management and Didactic Skills Training

- o Coaching in the BSc course 'Introduction To Global Change' (2018)
- o Technical assistance of three MSc students with their thesis on Nature based flood protection (2018-2020)
- o Supervising three MSc students with thesis (2019-2021)
- o Teaching in the BSc course 'Disaster Risk Management' (2021)
- o Coaching in the MSc course 'Academic Consultancy Training' (2020)

#### Oral Presentations

- o *Multifunctional flood defences as climate adaptation measures for the Netherlands: Putting Potential into Practise.* Water Science for Impact, 16-18 October 2018, Wageningen, The Netherlands
- o *How natural processes contribute to flood protection – A sustainable adaptation scheme for a wide green dike system.* Coastal Ecology workshop, 11-15 November 2019, Antwerp, Belgium

SENSE coordinator PhD education

Dr. ir. Peter Vermeulen



The research described in this thesis was financially supported by NWO Domain Applied and Engineering Sciences.

Financial support from Wageningen University for printing this thesis is gratefully acknowledged.

